

Raytheon

APOGR-TR. 89-1673

(2)

Final Report

AD-A217 507

**Experimental Testing of
Corpuscular Radiation
Detectors**

DTIC
ELECTE
JAN 12 1990
S & D D

Submitted to:

**Defense Advanced Research
Project Agency (DARPA)**

**DARPA Order No. 5271
Contract No. F49620-87-C-0050**

**Monitored by Air Force Office of
Scientific Research (AFOSR)**

**DARPA Program Director:
U.S. Army Lt. Col. G. P. Lasche', Ph.D**

7 September 1989

DISTRIBUTION STATEMENT
Approved for public release
Distribution Unlimited

90 01 11 110

**Raytheon Company
Submarine Signal Division
1847 West Main Road
Portsmouth, RI 02871-1087 U.S.A.
Telephone (401) 847-8000**

CN-RA-064

Raytheon

Final Report

Experimental Testing of Corpuscular Radiation Detectors

Submitted to:

**Defense Advanced Research
Project Agency (DARPA)**

DARPA Order No. 5271

Contract No. F49620-87-C-0050

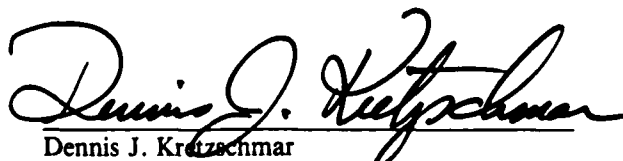
Monitored by Air Force Office of
Scientific Research (AFOSR)

DARPA Program Director:
U.S. Army Lt. Col. G. P. Lasche', Ph.D

7 September 1989

The views and conclusions contained in this document are those of the authors and should not be interpreted as necessarily representing the official policies, either expressed or implied, of the Defense Advanced Research Projects Agency or the U.S. Government.

Approved:


Dennis J. Kretzschmar
Program Manager,
Raytheon Company

Raytheon Company
Submarine Signal Division
1847 West Main Road
Portsmouth, RI 02871-1087 U.S.A.
Telephone (401) 847-8000

AIR FORCE OFFICE OF SCIENTIFIC RESEARCH (AFOSR)
 NOTICE OF TRANSFER TO DTIC
 This technical report has been reviewed and is
 approved for release under AFR 190-12.
 DTIC Form 100-2, 1-78
 MATN 1979-10-12
 Chief, Technical Information Division

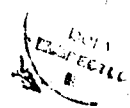
VOLUME II

TABLE OF CONTENTS

Section

Approved for public release;
 distribution unlimited. Page

Acknowledgements	ii
Executive Summary	iii
FIRST QUARTERLY REPORT, Contract F49620-87-C-0050, dated 15 August 1987	
SECOND QUARTERLY REPORT, Contract F49620-87-C-0050, dated 16 November 1987	
THIRD QUARTERLY REPORT, Contract F49620-87 C-0050, dated 15 February 1988	
FOURTH QUARTERLY REPORT, Contract F49620-87-C-0050, dated 15 May 1988	
FIFTH QUARTERLY REPORT, Contract F49620-87-C-0050, dated 15 August 1988	



Accession For	
NTIS CRA&I	<input checked="" type="checkbox"/>
DTIC TAB	<input type="checkbox"/>
Unannounced	<input type="checkbox"/>
Justification	
By	
Distribution/	
Availability Codes	
Dist	Avail and/or Special
A-1	

ACKNOWLEDGEMENTS

This Final Report has been prepared by Mario D. Grossi, Principal Investigator, with inputs from all members of the program team. For each Section, credit is given to the writer who contributed it.

Raytheon Company, Submarine Signal Division, Portsmouth, RI, was the Prime Contractor for this program. Raytheon PMO wishes to acknowledge the contributions of two major Subcontractors :Smithsonian Astrophysical Observatory (SAO), Cambridge, Massachusetts, and University of Maryland, Department of Physics, College Park, Maryland. In addition, we wish to express our appreciation to LANL-WX5, Los Alamos, NM, for having provided to the project laboratory space in Technical Area TA-33, and for having manufactured the tritium-filled source and the deuterium-filled reference, used in the tests illustrated in this Report. Special thanks to H. Richard Maltrud for the competent technical assistance and for the hospitality extended to Program personnel at TA-33.

EXECUTIVE SUMMARY

This Final Report, issued in two Volumes, is a self-contained documentation of the overall activity that Raytheon has performed under the terms of Contract F49620-87-C-0050. Volume I illustrates the program accomplishments in the most important, conclusive period of contract performance, from August 1988 through January 1989. Volume II is a collection of five Quarterly Reports, published by Raytheon to illustrate project activity between August 1987 and August 1988.

These past six months have been of great importance for the project, because of the availability of tritium sources of neutrinos at LANL, Los Alamos, NM. This has made it possible to acquire data of scientific value, and to answer some of the questions that had motivated the conduct of the investigation. These data were processed and analyzed at LANL, in real time, making it possible to draw immediate conclusions about the meaning of the measurements. The observations were performed by using Prof. Joe Weber's torsion balance, a room-temperature instrument that was constructed by University of Maryland under a subcontract from Raytheon, and was installed at LANL in Summer 1988. The torsion balance was mounted at a fixed location, close to the edge of a rotating table (1 RPM rotational speed) that Raytheon had constructed and moved to Los Alamos, NM. As the table rotated, the tritium-filled container (neutrino source) and the deuterium-filled container (that provided a "newtonian force" reference) were sensed by the instrument. At the time of writing of this Report, the results of the measurements are not fully conclusive. A six-month Contract extension, expected to last until 31 December 1989, will provide the final answer whether or not we could observe repulsion forces, attributable to neutrino pressure, with the torsion balance.

The experiment consisted, basically, of a comparison between the following two functions: (1) output of the torsion balance, integrated for 168 hours, with a deuterium-filled sphere mounted on the table (deuterium is non-radioactive, and the only forces applied to the torsion balance were newtonian attractions); and, (2) output of the same instrument, again integrated for 168 hours, with a tritium-filled sphere now mounted on the table (providing a newtonian attraction force because of its mass, with this force decreased by a repulsion force due to the hypothesized neutrino radiation pressure). The quality of the measurements was affected negatively by the following causes:

(1) The torsion balance is characterized by a very small damping factor (about 6%), while it would be advisable to operate with critical damping (a factor of 100%). As a consequence, once excited, the oscillation train lasts well beyond the 60-second period of table rotation, and interferes with the signal of the next table rotation.

(2) The torsion balance has an oscillation period (about 14 seconds) dependent upon room temperature. We noticed changes of about 5% from Summer to Winter 1988-1989. Fortunately, these changes in period were slow enough that the effect could be minimized by applying a numerical correction to the recorded outputs, after computer integration.

(3) The output of the torsion balance exhibits a DC drift from -10 V to + 10V (a full cycle in about two months). The required signal, characterized by a very small amplitude \pm (10 microVolt-to-100 microVolt), is on top of this slowly varying drift. By using a 16 bit resolution in the digitization process (instead of the 12 bit resolution of Prof. Weber's earlier tests), we were able to detect the signal most of the time.

Once the relevance of these torsion balance difficulties was fully appreciated, Raytheon (with the concurrence of Prof. Joe Weber) submitted a recommendation to DARPA to extend the present phase of the project for three-to-six months. This would at least, provide a new damper (characterized by critical, or near-critical, damping) and a thermal control subsystem for the instrumentation. Then the data collection could be resumed with 26 source-replicas mounted on the top of the 1 RPM table. LANL is already proceeding, under direct DARPA funding, to fabricate these 26 replicas and to mount them around the rim of the 1 RPM rotating table, in order to maximize the ratio "repulsion force/attractive force". The repulsion force represents the desired signal, and the attractive force, due to gravity-gradient background, the undesired one. Computer simulations, carried out at SAO under a Raytheon subcontract, have shown that, with this arrangement, we could expect an improvement in the ratio "repulsive force/attractive force" of 500-1000.

Thus far, data have been collected by Raytheon without using the 26 replicas. With all applicable caveats, we could draw the following tentative conclusions (we cannot stress strongly enough how tentative our current results are):

(1) There is a difference between the recordings (obtained with 168 hours integration time) performed with tritium and with deuterium. This difference would be consistent with a repulsion force which is present when experimenting with the tritium. The intensity of this repulsion force appears to be of a few microdynes. This tracks closely Prof. Weber's observations at U. of Maryland in 1986;

(2) If a 1/4" lead shield is wrapped around the 8" diameter cylinder that houses the torsion balance, this repulsion force seems to disappear;

(3) Observations (1) and (2) above have been performed only once, and the SNR was rather limited. That is why we say that the experimental evidence is, thus far, most tentative. Should these results be confirmed by the forthcoming tests during the contract extension, the question will arise as to the origin of a radiation pressure that produces a torsion balance force that disappears when a lead shield is interposed between source and sensor. We do not expect that this question will be easy to answer. A first candidate radiation that comes to mind is X-ray radiation. However, where do these X-rays come from? They cannot come from the inside of the tritium container: the thickness of its wall is too large to allow even the smallest leak. Another possible mechanism has been proposed that would generate 14.1 MeV neutrons, that, in turn, could produce secondary radiation affecting the torsion balance. Clearly, we need to add new sensors to our instrumentation at LANL such as a proportional counter, a X-ray detector, a gamma-ray detector, a neutron spectrometer, etc. Dependent upon the results of the measurements above, we could interpose shields between source and torsion balance, such as: (a) IR shield made of several layers of gold-coated mylar, each with 95% reflection coefficient in the IR band, or an equivalent shield; (b) Magnetic shield (several layers of flexible Permag metglass); (c) 1/4" lead shield, against X-rays; (d) Cadmium/boron/lead shield against 14 MeV neutrons.

* * *

In addition to the experimental activity that Raytheon has carried out at LANL with the torsion balance, we have constructed and tested in Portsmouth, RI (without using tritium sources of neutrinos, thus far) a cryogenic force sensor that has exhibited a sensitivity of about 10^{-9} dyne in 10^4 seconds integration time. Testing this cryogenic instrument (that operates at 4°K, is tuned at 100 Hz, and is suspended from a tripod equipped with a 2-stage vibration isolator) at

LANL requires a 2000 RPM rotating table, with three tritium sources mounted on the table top, 120° apart, to modulate the neutrino flux amplitude at 100 Hz. This table has not yet been built, although an analysis of its feasibility and a preliminary design have been completed by Raytheon and SAO.

Should the tests with the torsion balance, to be completed by December 1989, provide support to Prof. Weber's expectation of an abnormally large coherent scattering cross-section using tritium-radiated neutrinos, we would then have a simpler and cheaper alternative for the 100 Hz modulation of neutrino flux. This would consist of a modified Weber chopper, rotating at 100/n RPS, where n is the number of sapphire crystals mounted at the periphery of the rotating disk. The chopper could be used at LANL with a tritium source kept at a fixed station, on a stand. By replacing the tritium source with a deuterium-filled container, we could verify whether a tritium-induced signal would continue to be present, or would disappear, when using the deuterium.

The cryogenic force sensor that Raytheon has constructed provides a sensitivity improvement of more than 4 orders of magnitude with respect to the room-temperature torsion balance, thus reaching a threshold of less than 10^{-10} dynes, with a 168-hour integration time. The instrument has the potential of achieving a sensitivity of the order of a picodyne (10^{-12} dynes), by adding cryostat dilution refrigeration provisions, which would bring the operating temperature down to 4 milli°K.

* * *

Finally, concerning the laboratory tests on the feasibility of the magnetic interaction sensor, Raytheon has constructed a SQUID magnetometer under the 1988 Independent Development

Program (IDP), and has performed the following measurements, as contractually required:

(1) Determination of the SQUID system noise (this is called intrinsic noise, when the SQUID is unloaded): for frequencies larger than 10 Hz, our SQUID has an intrinsic noise of about $10^{-6} \phi_0 \text{ Hz}^{-1/2}$ (where $\phi_0 = 2.07 \cdot 10^{-15} \text{ Wb}$). This is a factor of 10 better than commercially available SQUIDs. However, we need a noise level less than, or equal to, $10^{-7} \phi_0 \text{ Hz}^{-1/2}$, when the SQUID is loaded by the target. Therefore, we have still a long way to go. JASON estimated that a loaded SQUID would have, at best, a system noise of $10^{-6} \phi_0 \text{ Hz}^{-1/2}$.

(2) Determination of the maximum achievable relative permeability for the interaction target. We have measured a $\mu_r = 10^6$, when operating on the steep side of the hysteresis cycle. We require $\mu_r = 10^8$. We have still a factor of 100 to gain. JASON had estimated that at best we could achieve a $\mu_r = 10^3$.

(3) Determination of the maximum achievable collecting area. We need 10^3 cm^2 . Our SQUID stopped operating with a 15 cm^2 area. JASON had estimated that at best we could achieve 1 cm^2 . Here also, we have a factor of 100 to gain. The use of a superconducting transformer offers great promise.

Our estimate of the effort that is required to complete the preliminary laboratory tests on the three basic JASON questions concerning magnetic sensor feasibility is as follows: (a) Laboratory work on SQUID improvement and on target testing, still using a 1 Kg mass for the high-permeability interaction target, will require about 3 man-years effort over a 1 year period. (This work does not require tritium sources and can be carried out at Raytheon, Portsmouth, RI);

(b) Completion of the SQUID improvement program, and laboratory work with a 25 Kg interaction target, will require about 4 man-years effort over a 1 year period (work still to be done in Portsmouth, RI).

Should the answers to the three JASON questions provide support for sensor feasibility, we could then move toward a program phase that includes construction of the actual sensor. This would be used at LANL/TA-33 with tritium sources of neutrinos (this instrument would use a 250 Kg interaction target, housed in a custom-made 4°K cryostat) for the conduct of fully-probative detection experiments.

Concerning an assessment of the likelihood of success, we must distinguish between two goals. Achieving the three goals in the instrumentation subsystem performance identified by JASON, could be characterized, in Raytheon's opinion, as better than 50%, while the probability of detecting neutrinos with the magnetic sensor cannot yet be assessed at this time. Notwithstanding this uncertainty, our strong recommendation is that support be provided by DARPA to build up, item by item, the technology basis that is a pre-requisite to fully develop this novel detector of low-energy neutrinos.

SECOND CONTRACT

FIRST QUARTERLY REPORT

15 AUGUST 1987

EXPERIMENTAL TESTING OF CORPUSCULAR RADIATION DETECTORS

SUBMITTED TO

DEFENSE ADVANCED RESEARCH PROJECT AGENCY (DARPA)

DARPA ORDER #5271

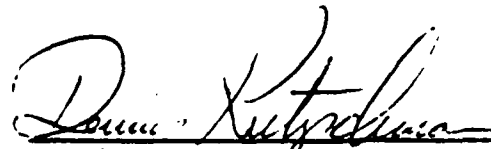
CONTRACT #F49620-87-C-0050

MONITORED BY AIR FORCE OFFICE OF SCIENTIFIC RESEARCH

(AFOSR)

DARPA PROGRAM DIRECTOR: US ARMY LT. COLONEL G. P. LASCHE', Ph.D

The views and conclusions contained in this document are those of the authors and should not be interpreted as necessarily representing the official policies, either expressed or implied, of the Defense Advanced Research Projects Agency or the U.S. Government.



Approved by: Dennis Kretzschmar
Program Manager, Raytheon Co.

RAYTHEON COMPANY
SUBMARINE SIGNAL DIVISION
PORTSMOUTH, RHODE ISLAND 02871

TABLE OF CONTENTS

<u>SECTION</u>	<u>PAGE</u>
ACKNOWLEDGEMENTS	ii
EXECUTIVE SUMMARY	iii
APPENDIX A - THE PROGRAM PLAN FOR THE ADDED SCOPE EFFORT, AS PRESENTED TO JASON ON 7/10/87 AT LA JOLLA, CALIFORNIA.	

ACKNOWLEDGEMENTS

This quarterly report has been prepared by Mario D. Grossi, Principal Investigator, with inputs from all members of the program team. For each section, credit is given to the writer who contributed it.

EXECUTIVE SUMMARY

In the first two months of program performance, Raytheon's effort concentrated in planning the added-scope activity, which will consist of constructing instruments and performing detection tests using a tritium source. The tritium is expected to be provided as a government furnished unit by Lawrence Livermore National Laboratory (LLNL). An initial draft of the program plan has been reviewed by DARPA and the JASON Study Group. Raytheon expects to receive instructions from DARPA as to redirections of activity priorities, as formulated in the above reviews. At that point, the final version of the plan will be issued, and the project activity will begin in earnest.

APPENDIX A, attached to this report, reproduces the plan as submitted to DARPA and JASON. We expect that any changes and redirection will affect only a minor portion of the plan, and will be limited to the calibration of the sensors used in the forthcoming experiments, and the modalities of the data collection. To compensate for the increase in scope of some of the tasks, there might be a decrease in the amount of work done for the magnetic interaction sensor. This would also be in deference to the concerns expressed in JASON Report JSR-84-105, entitled "Neutrino Detection Primer", dated June 1987, that has been critical of Raytheon's magnetic approach to neutrino detection.

At this point, our expectations about the content of the final program plan are that most of the effort will be spent in constructing a high-sensitivity cryogenic force sensor (essentially a gravity gradiometer with one of the proof masses replaced by sapphire crystals, operated at 4°K), and a replica of Prof. Weber's torsion balance and tuning-fork instruments (both working at room temperature); in collecting data with the LLNL tritium source of neutrinos (a 3.5" sphere with a 100 Kilocurie source intensity); and in reducing, processing and analyzing the data. The source will be rotated on a revolving round-table, capable of variable

angular velocities as high as 6000 RPM. We also expect that the final program plan will include the construction of a scaled-down magnetic interaction sensor, with a target of only 25 Kg, instead of the full-scale target of 250 Kg. It will use a standard-size 4°K cryostat, instead of the custom-made large-size cryostat that was designed as a part of the previous contract. The scaled-down magnetic sensor would be used in laboratory tests of such fundamental performance parameters as the maximum achievable relative permeability of the high- μ target material, and the minimum achievable system noise, when the squid pick-up loop is loaded by the target itself. These laboratory tests would directly address the concerns expressed by JASON of the magnetic sensor's ability to detect neutrinos, and would resolve the disagreement between JASON/Raytheon on the topic of the required integration time: JASON states that 10^{24} seconds are necessary, Raytheon that 10^4 seconds are enough. A ratio 10^{20} between the two estimates translates in a ratio of 10^{10} between the estimates in Signal-to-Noise ratio expected to be achieved in the proposed experiment. Specific items of disagreement are:

- relative permeability of magnetic material

JASON 10^3

Raytheon 10^8 (by the Bozorth treatment consisting of applying
thermal processes and mechanical stresses)

- SQUID pick-up coil area

JASON 1 cm^2

Raytheon 10^3 cm^2 (by the use of a superconducting transformer)

- SQUID noise density

JASON $10^{-4} \text{ } \oint_0 / \sqrt{\text{Hz}}$

Raytheon $10^{-6} \text{ } \oint_0 / \sqrt{\text{Hz}}$

It can be seen from the above that these three areas, by themselves, account for the 10^{10} discrepancy ($10^5 \times 10^3 \times 10^2 = 10^{10}$). The laboratory tests with the scaled-down instrument would provide values for each of the above parameters and would serve as a realistic estimate for the performance of the final, full-scale instrument.

APPENDIX A

THE PROGRAM PLAN FOR THE ADDED SCOPE EFFORT, AS PRESENTED
TO JASON ON 7/10/1987, AT LA JOLLA, CA.

This Appendix contains the copy of the viewgraphs used
by Raytheon in the presentation to JASON.

EXPERIMENTAL TESTING OF CORPUSCULAR RADIATION DETECTORS

DARPA/NFOSR CONTRACT # F 49620-87-C-0050, PROJECT FO 86671-8700644

DARPA PROGRAM MANAGER :LT.COL. GEORGE P.LASCHE', DARPA/DSO/GSD

A PRESENTATION

TO

JASON - MITRE

10 JULY 1987

RAYTHEON PROGRAM MANAGER : D.J.KRETZSCHMAR
RAYTHEON PRINCIPAL INVESTIGATOR:M.D.GROSSI

RAYTHEON COMPANY

SUBMARINE SIGNAL DIVISION
PORTSMOUTH, R.I. 02871

OUTLINE OF RAYTHEON PRESENTATION

1. PROGRAMMATIC ASPECTS - RAYTHEON NEUTRINO DETECTORS PROJECT

MR. DENNIS J. KRETZSCHMAR

2. THE INSTRUMENTATION SYSTEM

DR. MARIO D. GROSSI

3. THEORETICAL ASPECTS

PROF. ROBERT R. LEWIS, U. OF MICHIGAN

4. MEASUREMENT DIFFICULTIES AND SOME WAYS OF COPING WITH THEM UNDER CONSIDERATION

DR. MARIO D. GROSSI

5. THE CONDUCT OF THE VERIFICATION EXPERIMENT

DR. MARIO D. GROSSI

6. CONCLUSIONS

MR. DENNIS J. KRETZSCHMAR

PROGRAMMATIC ASPECTS OF RAYTHEON NEUTRINO DETECTORS PROJECT

WORK STATEMENT

DARPA/AFOSR CONTRACT # F 49620-87-C-0050

- a. Fabricate a cryogenic force detector using Weber's sapphire crystals mounted on one segment of a gravity gradiometer. This force detector will be suspended in a liquid helium dewar so that it will be at 4.2 degrees K. The suspension system will have acoustic decoupling to minimize noise.
- b. Using a tritium source, test the cryogenic force detector, Weber's torsion balance sensor, Weber's tuning fork sensor and Raytheon's magnetic interaction sensor.
- c. Take data 24 hours a day when the tritium source is available and analyze the data.

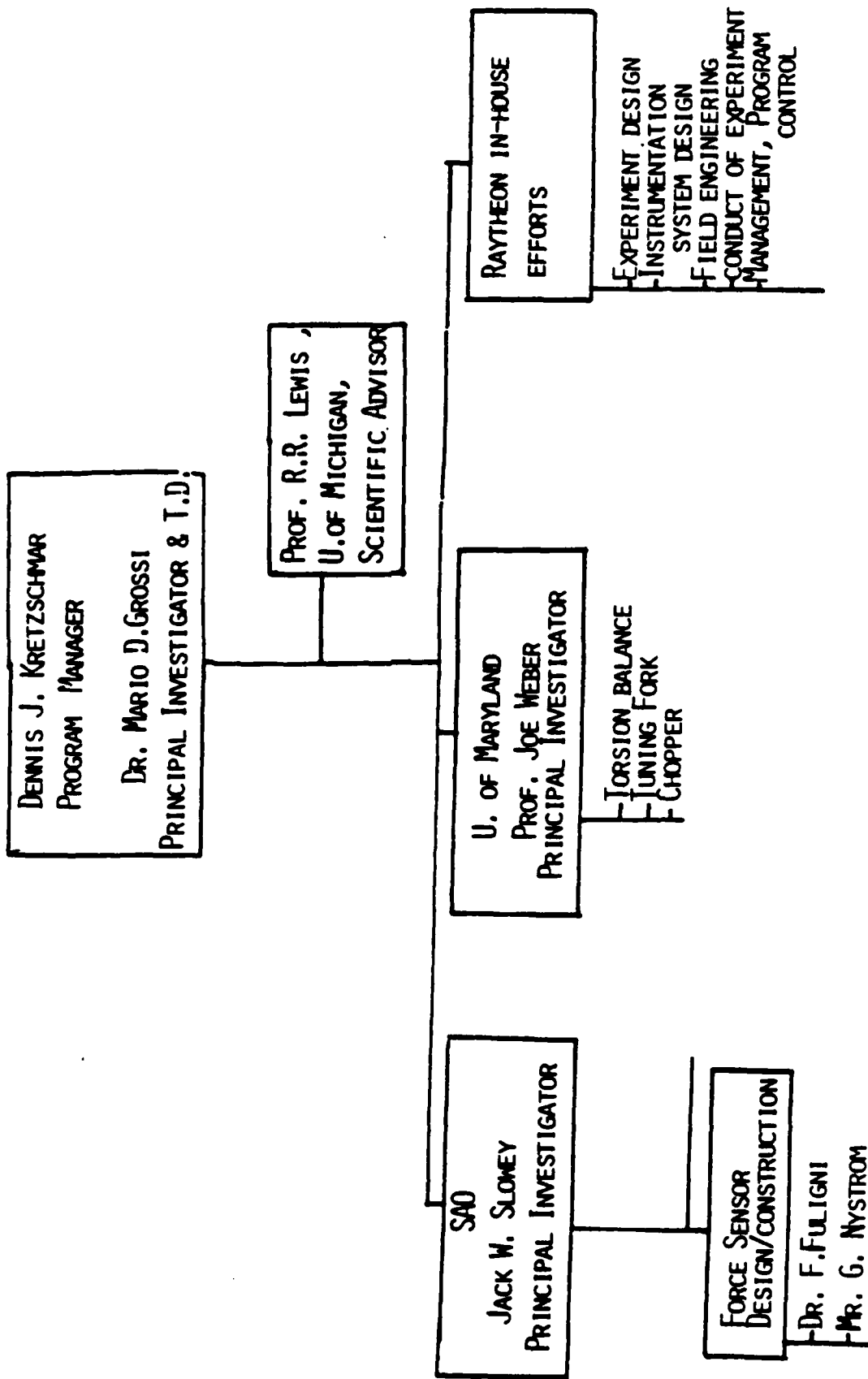
NOTE: THE MAGNETIC INTERACTION SENSOR IS NOT A PART OF WEBER VERIFICATION EFFORT

MAIN OBJECTIVE OF THE RAYTHEON NEUTRINO DETECTORS PROGRAM

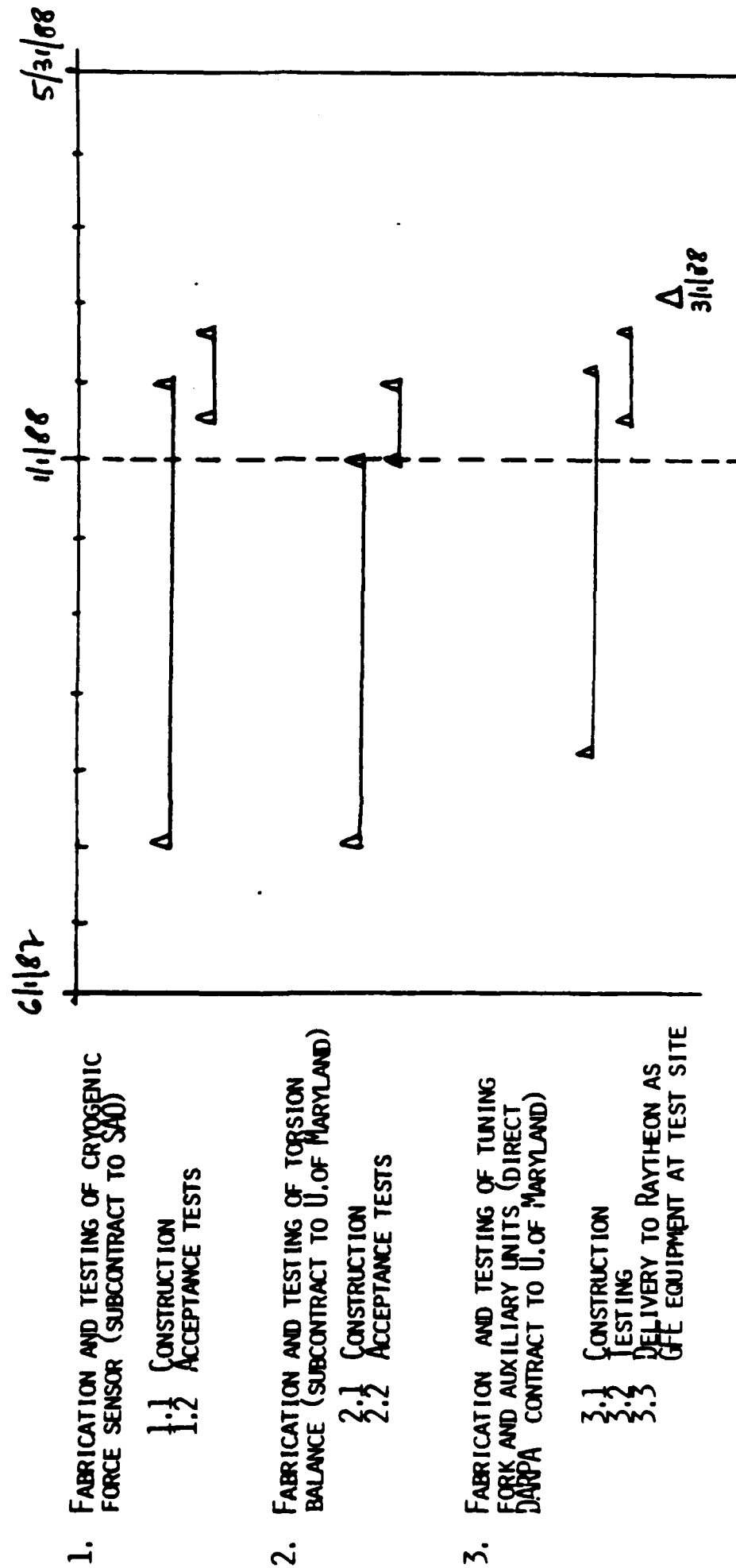
- 0 RAYTHEON HAS BEEN TASKED BY DARPA TO ATTEMPT TO INDEPENDENTLY REPRODUCE THE EXPERIMENTAL RESULTS REPORTED BY PROF. JOE WEBER : I.E. THAT HE HAS DETECTED THE RADIATION PRESSURE OF NEUTRINOS WITH ROOM-TEMPERATURE INSTRUMENTATION
- 0 THIS ASSIGNMENT WILL BE FULFILLED BY USING A ROOM-TEMPERATURE TORSION BALANCE AND A NEUTRINO CHOPPER-AND-TUNING FORK CONSTRUCTED UNDER PROF. WEBER'S GUIDANCE BY UNIVERSITY OF MARYLAND
- 0 CURRENT PLANS CALL FOR REPEATING WEBER'S MEASUREMENTS BY USING A 100 KILOCURIE TRITIUM SOURCE CONTAINED IN A 3.5" SPHERE, MADE AVAILABLE COURTESY OF LAWRENCE LIVERMORE NATIONAL LABORATORY
- 0 FURTHER MEASUREMENTS WILL BE PERFORMED BY USING A CRYOGENIC FORCE SENSOR AT 4° K WITH A BETTER EXPECTED SENSITIVITY THAN WEBER'S TWO ROOM-TEMPERATURE INSTRUMENTS.

RAYTHEON NEUTRINO DETECTORS PROGRAM ORGANIZATION

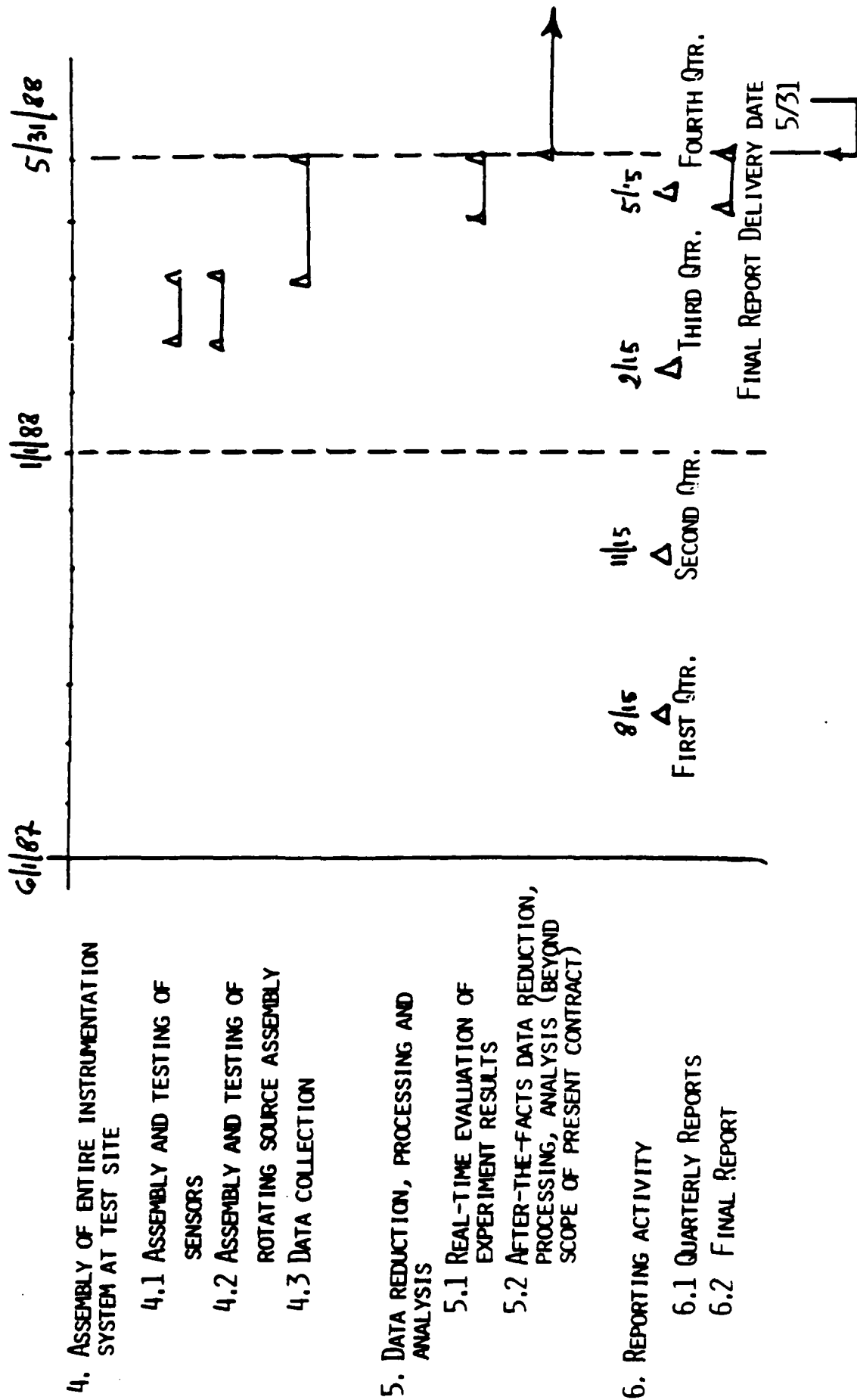
WEBER VERIFICATION EFFORT



RAYTHEON NEUTRINO DETECTORS PROGRAM- TASK DESCRIPTION AND SCHEDULE



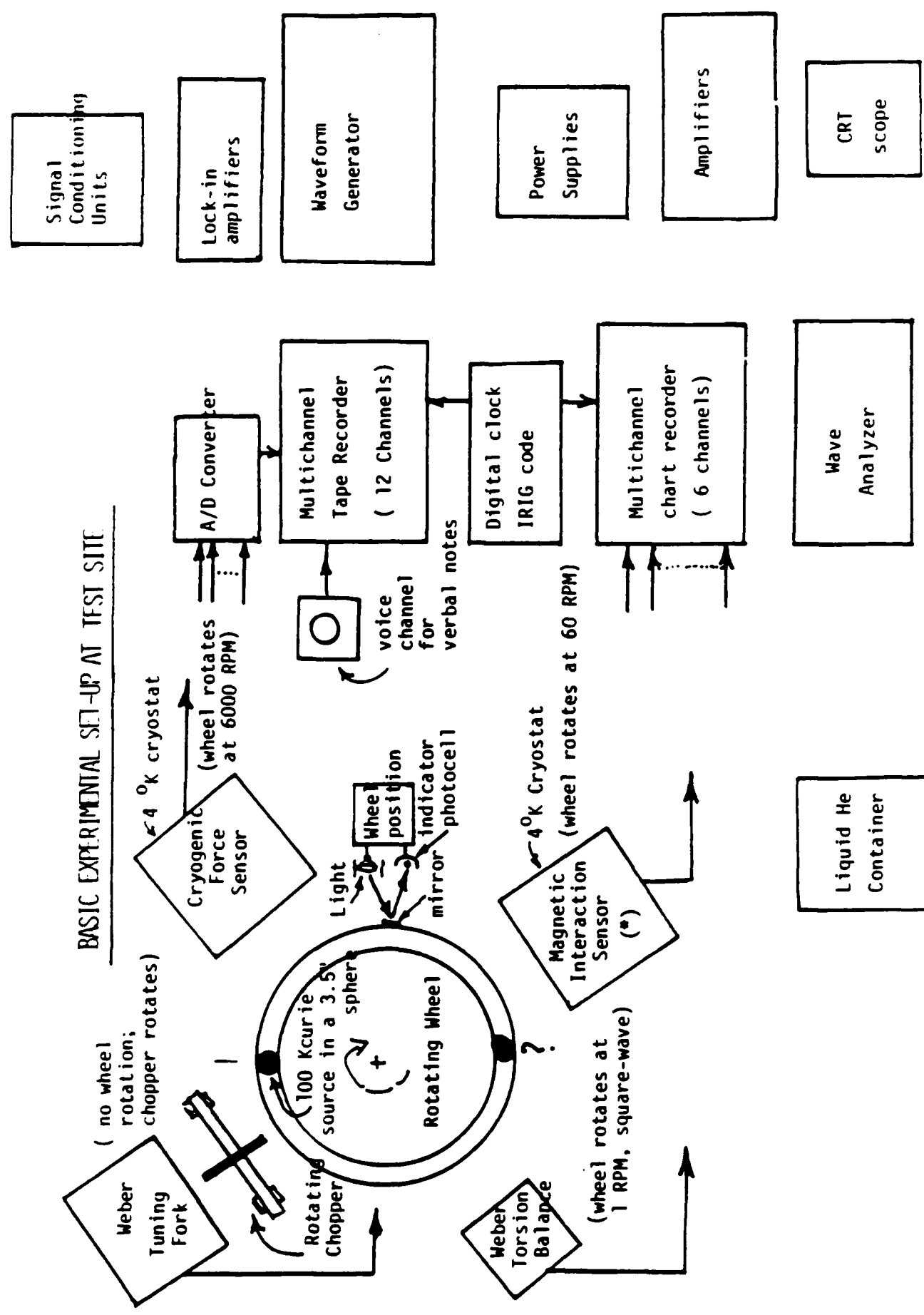
RAYTHEON NEUTRINO DETECTORS PROGRAM - TASK DESCRIPTION AND SCHEDULE (Continued)



POSSIBLE SOURCES OF MEASUREMENT ERRORS THAT HAVE BEEN IDENTIFIED
AND THAT REQUIRE SPECIAL ATTENTION

1. ISOLATION OF INSTRUMENTS FROM MECHANICAL VIBRATIONS, SEISMIC OSCILLATIONS,
GRAVITY GRADIENT NOISE, TO A DEGREE COMPATIBLE WITH REQUIRED SENSITIVITY
2. ABATEMENT OF VIBRATIONS PRODUCED BY ROTATING SOURCE ASSEMBLY AND CHOICE OF
SIGNAL FREQUENCY TO MINIMIZE EFFECTS OF RESIDUAL VIBRATIONS THAT REACH SENSORS
3. OTHER SOURCES OF SPURIOUS SIGNALS THAT HAVE BEEN IDENTIFIED : TIME-VARIABLE
GRAVITY GRADIENTS, MAGNETIC FIELDS, THERMAL SOURCES- SPECIAL ATTENTION REQUIRED
TO MINIMIZE THEIR EFFECTS ON SENSORS, TO ISOLATE SENSORS FROM RESIDUAL EFFECTS,
TO ASSESS QUANTITATIVELY THEIR REMAINING INFLUENCE

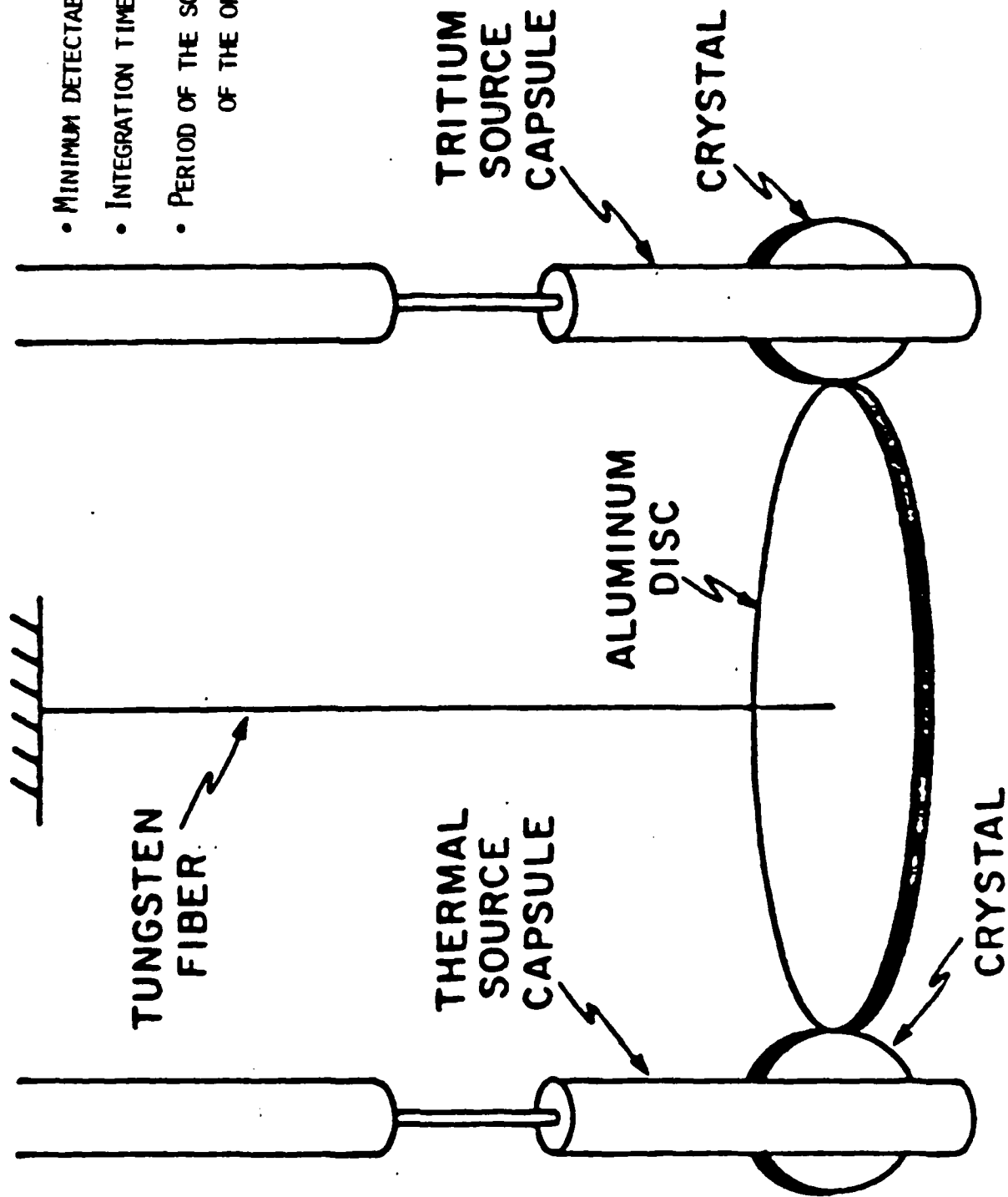
BASIC EXPERIMENTAL SET-UP AT TEST SITE



(*) NOT PART OF WEBER VERIFICATION EFFORT

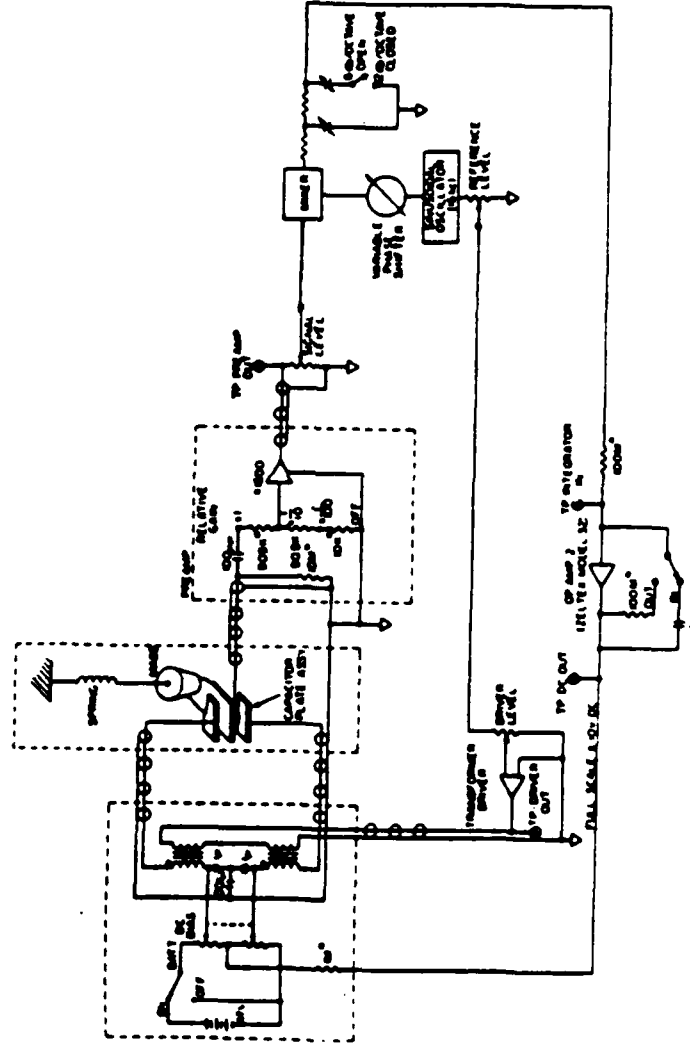
THE INSTRUMENTATION SYSTEM

WEBER TORSION BALANCE WITH SOURCE



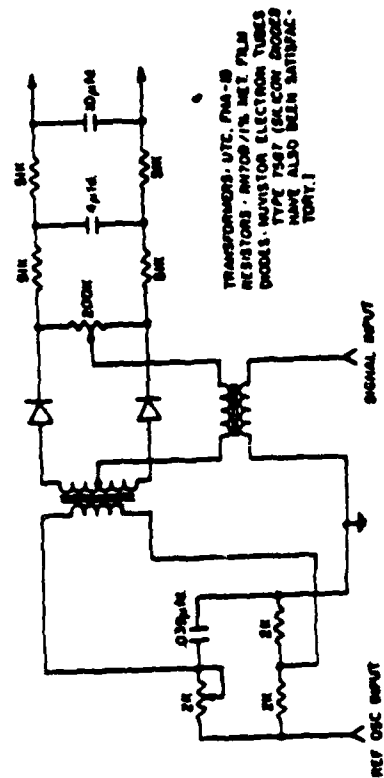
- MINIMUM DETECTABLE FORCE: 10^{-7} DYNES
- INTEGRATION TIME : ABOUT 10^6 SEC
- PERIOD OF THE SOURCE OSCILLATION:
OF THE ORDER OF ONE MINUTE

WEBER TORSION BALANCE - ELECTRONICS



SCHEMATIC DIAGRAM OF OVERALL INSTRUMENT

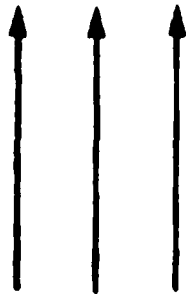
SCHEMATIC DIAGRAM OF PREAMPLIFIER



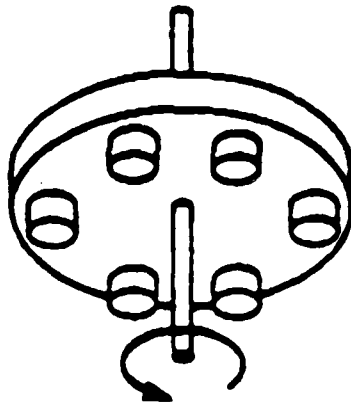
SCHEMATIC DIAGRAM OF PHASE-SENSITIVE DETECTOR

WEBER TUNING FORK AND ROTATING CHOPPER

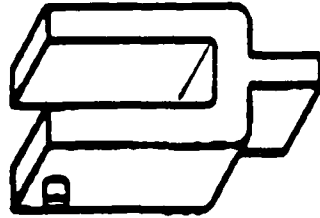
**Neutrinos
From
Reactor**



**Wheel
With
Crystals**



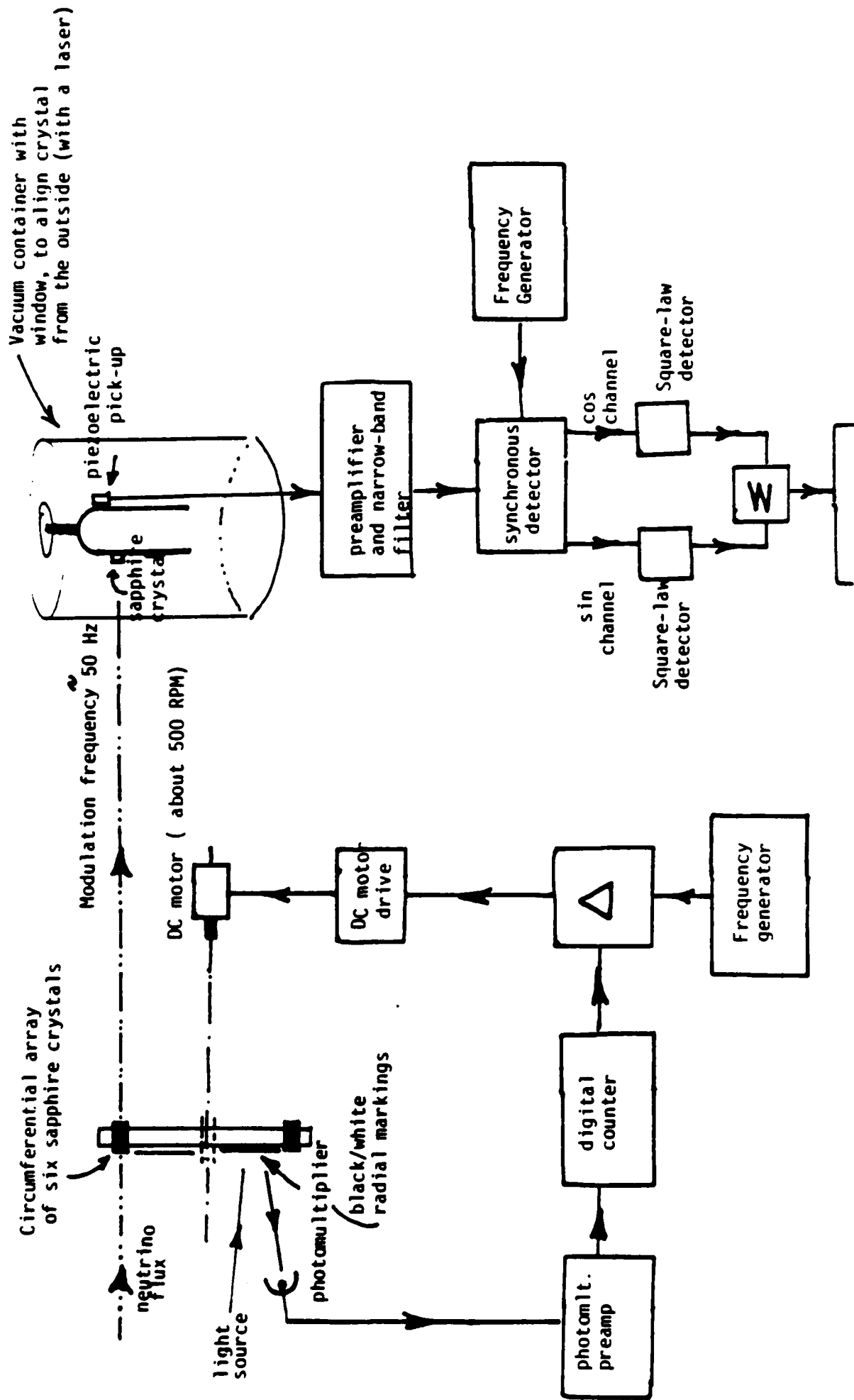
**Tuning Fork
With
Crystal**



**Tuning Fork Vibrates at Resonance Due to
Chopper-Modulated Neutrino Flux**

- MINIMUM DETECTABLE FORCE 10^{-7} DYNES
- INTEGRATION TIME $\sim 10^2$ SEC

WEBER TUNING FORK INSTRUMENTATION SYSTEM SIMPLIFIED BLOCK DIAGRAM



THE CRYOGENIC FORCE SENSOR (IN A 4°K CRYOSTAT)

BASIC PERFORMANCE PARAMETERS

- MASS 250 GR
- TEMPERATURE 4° K
- RESONANCE FREQUENCY 100 Hz
- Q FACTOR 10^4
- REQUIRED INTEGRATION TIME 10^4 SECONDS
- MINIMUM DETECTABLE FORCE 10^{-8} DYNES
- OSCILLATION DECAY TIME 32 SECONDS
- REQUIRED ABATEMENT OF VIBRATION NOISE ≥ 150 DB

THE STARTING POINT FOR THE DEVELOPMENT OF THE CRYOGENIC FORCE SENSOR

WHAT EXISTS NOW ?

- WHAT EXISTS IS AN IFSI/SAO ROOM-TEMPERATURE GRAVITY GRADIMETER WITH THE FOLLOWING PERFORMANCE SPECIFICATIONS :

0 MASS	200 GRAMS
0 TEMPERATURE	ABOUT 300 °K (ROOM TEMPERATURE)
0 RESONANCE FREQUENCY	ABOUT 22 Hz WITHOUT NEGATIVE SPRING " 15 " WITH "
0 Q FACTOR	1.5 10 ³
0 WEAKEST FORCE ACTUALLY DETECTED	4 · 10 ⁻⁷ DYNES (WITHOUT VIBRATION ABATEMENT; WITH 10 ⁻⁴ COMMON MODE REJECTION)

- CHANGING THE RESONANCE TO 100 Hz MAKES THE MECHANIZATION OF THE CRYOGENIC FORCE SENSOR EASIER.

NUMERICAL ESTIMATE OF MINIMUM DETECTABLE FORCE SIGNAL

- o MINIMUM DETECTABLE FORCE SIGNAL, AT RESONANCE,
BY EACH ONE OF THE SENSING CELLS, IN ABSENCE OF
VIBRATIONS

$$F \geq \sqrt{\frac{2 \kappa T M \omega_0}{Q T_{INT}}}$$

WHERE:

$$\kappa = 1.38 \cdot 10^{-23} \text{ JOULES (DEG K)}^{-1}$$

$$M = 0.250 \text{ KG}$$

$$T = 400 \text{ K}$$

$$\omega_0 = 2\pi \cdot 10^7$$

$$Q = 10^4 \quad ; \quad T_{INT} = 10^4 \text{ SECONDS}$$

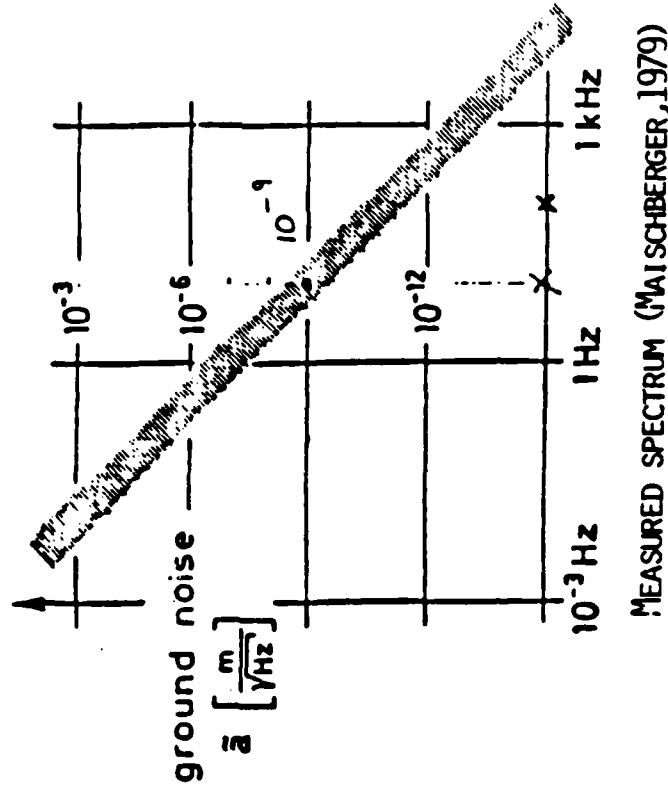
$$\text{THEREFORE } F \geq \frac{1.3 \cdot 10^{-14} \text{ NEWTON}}{1.3 \cdot 10^{-9} \text{ DYNES}} = 10^{-8} \text{ DYNES}$$

- o ADOPTED SENSITIVITY SPECIFICATION

- o MINIMUM DETECTABLE GRADIENT (BASELINE = 20 CM) $2.83 \cdot 10^{-3} \text{ E6TVGS UNITS}$

ESTIMATE OF VIBRATION NOISE

o DISPLACEMENT NOISE DENSITY (MAX PLANCK INSTITUTE)



o ADOPTED VALUES , IN OUR SYSTEM STUDIES (CONSERVATIVE ASSUMPTION)

AN ORDER OF MAGNITUDE WORSE THAN ABOVE SPECTRUM
(AT 100 Hz, $\tilde{a} = 10^{-8} \text{ cm}/\sqrt{\text{Hz}}$)

o ACCELERATION NOISE AT 100 Hz

ACCELERATION NOISE DENSITY :

$$(2\pi 100)^2 \cdot 10^{-8} \approx 4 \cdot 10^{-3} \text{ GAL}/\sqrt{\text{Hz}}$$

WITH A 10⁴ SECONDS INTEGRATION TIME, ACCELERATION
NOISE AT EACH CELL IS $4 \cdot 10^{-3}$ GAL

A BACK-OF-AN ENVELOPE ESTIMATE OF SIGNAL-TO-NOISE RATIO

0 ACCELERATION SIGNAL INTENSITY

A MINIMUM DETECTABLE FORCE OF 10^{-8} DYNES
APPLIED TO A 250 GR MASS PRODUCES AN ACCELERATION
OF $10^{-8} / 250 = 4 \cdot 10^{-11}$ GAL.

0 REQUIRED EXTENT OF VIBRATION ABATEMENT

BECAUSE THE ACCELERATION NOISE IN THE LABORATORY
IS $4 \cdot 10^{-5}$ GAL (SEE PREVIOUS SLIDE), WE REQUIRE
AN ABATEMENT OF AT LEAST

$$\frac{4 \cdot 10^{-11}}{4 \cdot 10^{-5}} = 10^{-6} \text{ OR } -120 \text{ DB}$$

0 ADOPTED VALUE FOR MINIMUM ACCEPTABLE VIBRATION ABATEMENT (CONSERVATIVE)

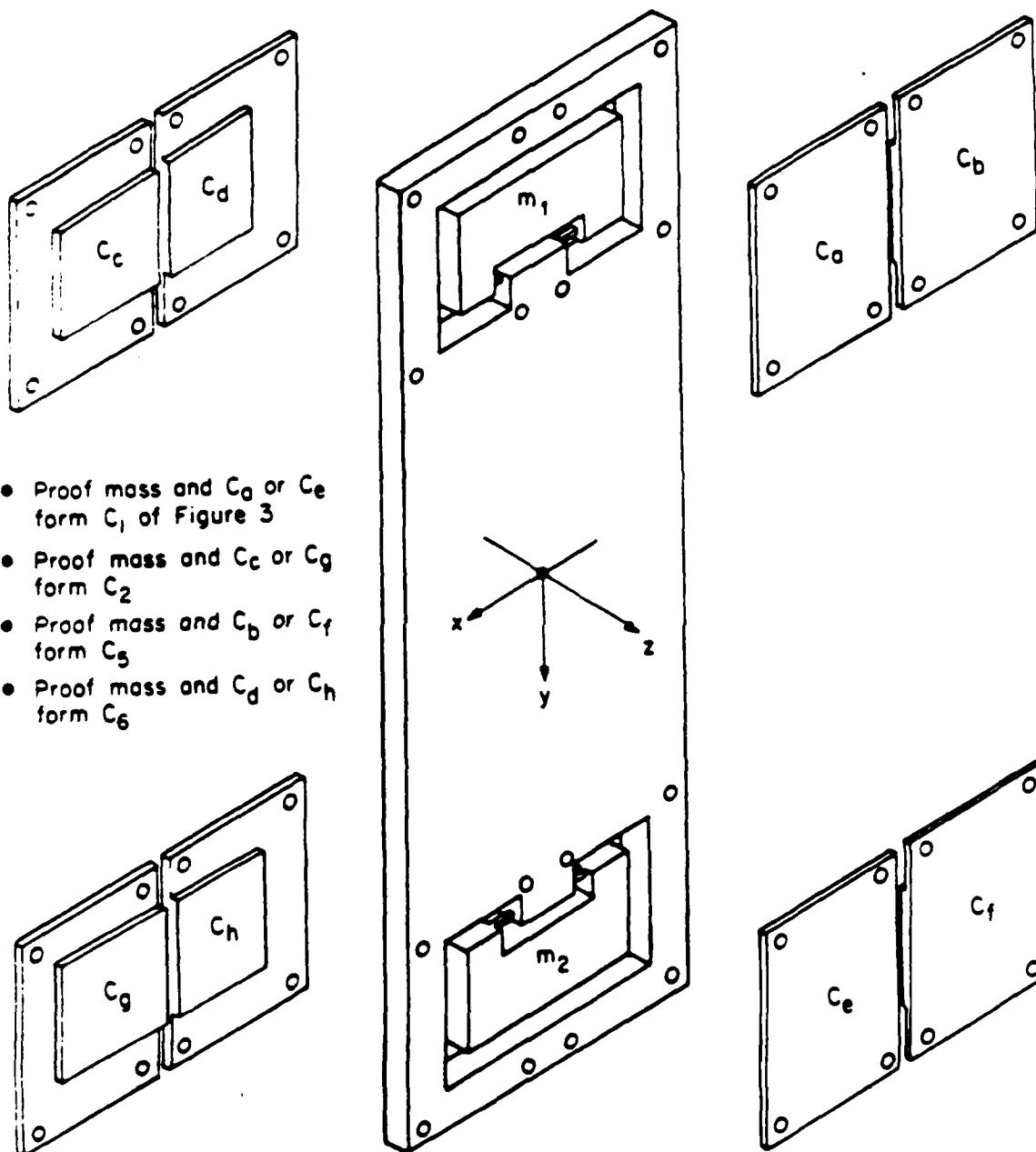
- 150 DB

0 WHAT DO WE EXPECT TO ACHIEVE ?

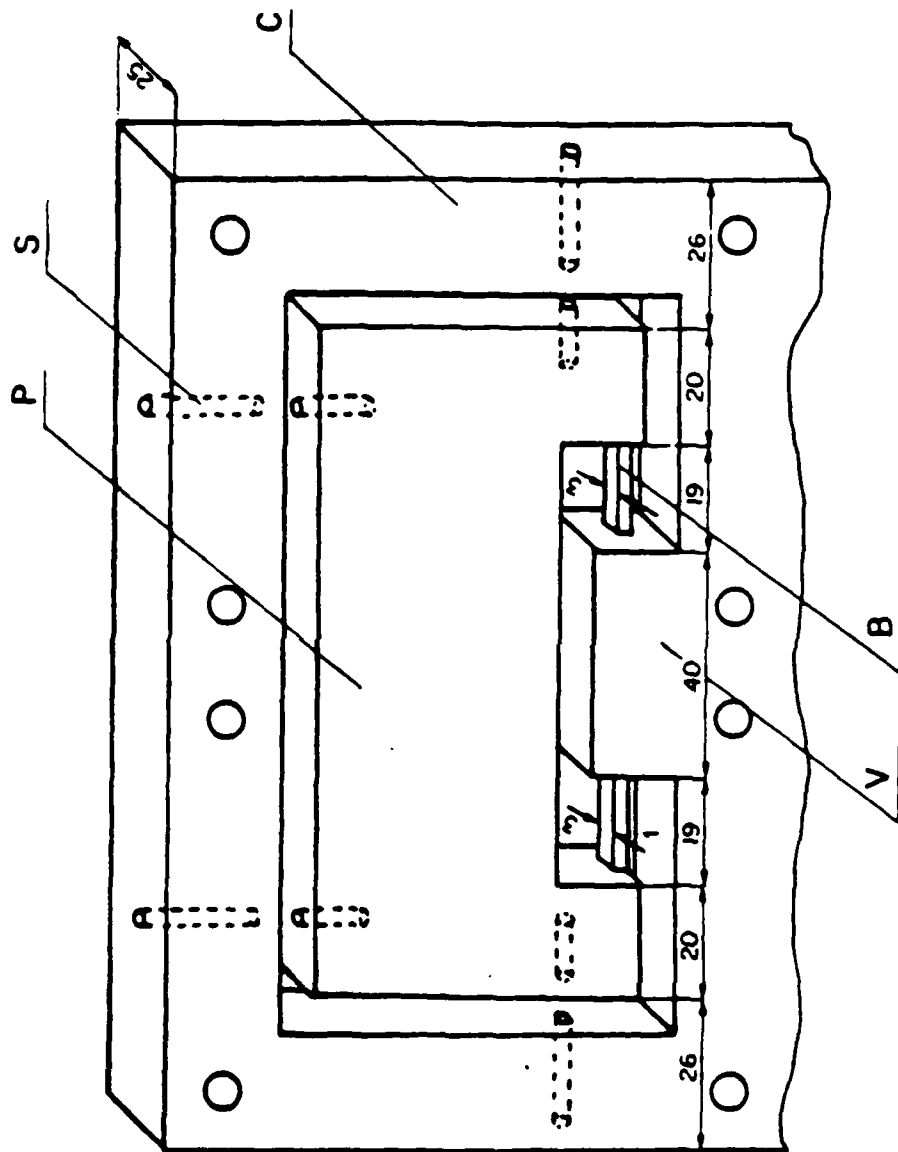
COMMON MODE REJECTION WILL PROVIDE AN ISOLATION
OF AT LEAST 10^{-4} OR 80 DB.

BY USING A SUSPENSION WITH RESONANCE FREQUENCY
OF 1 HZ, EASY TO MECHANIZE, WE ACHIEVE AN ISOLATION
(AT 100 HZ) OF 10^{-4} OR 80 DB. THIS PROVIDES A
TOTAL ISOLATION OF -160 DB, 10 DB MORE THAN
REQUIRED.

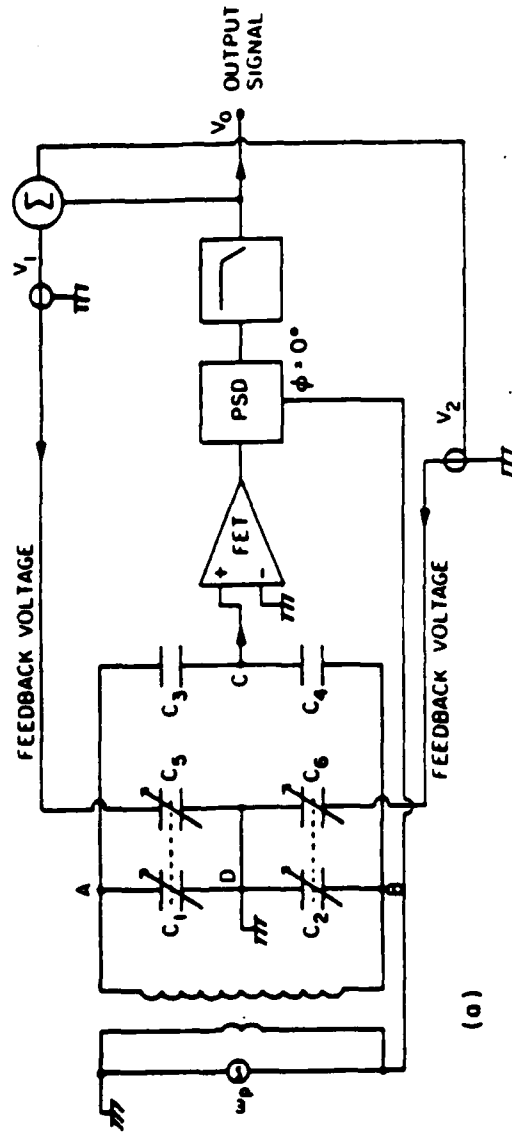
MECHANICAL STRUCTURE OF GRAVITY GRADIOMETER



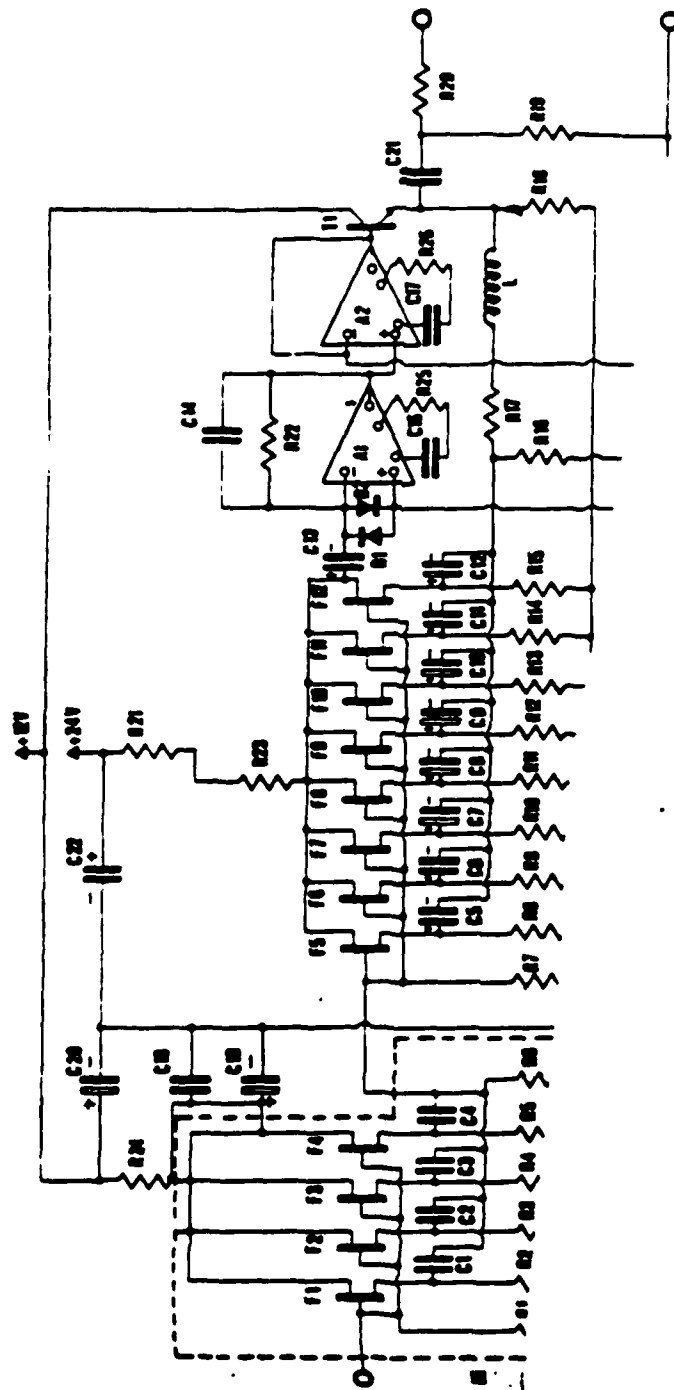
STRUCTURE OF SINGLE CELL



SIMPLIFIED BLOCK DIAGRAM OF ELECTRONICS USED IN SENSOR

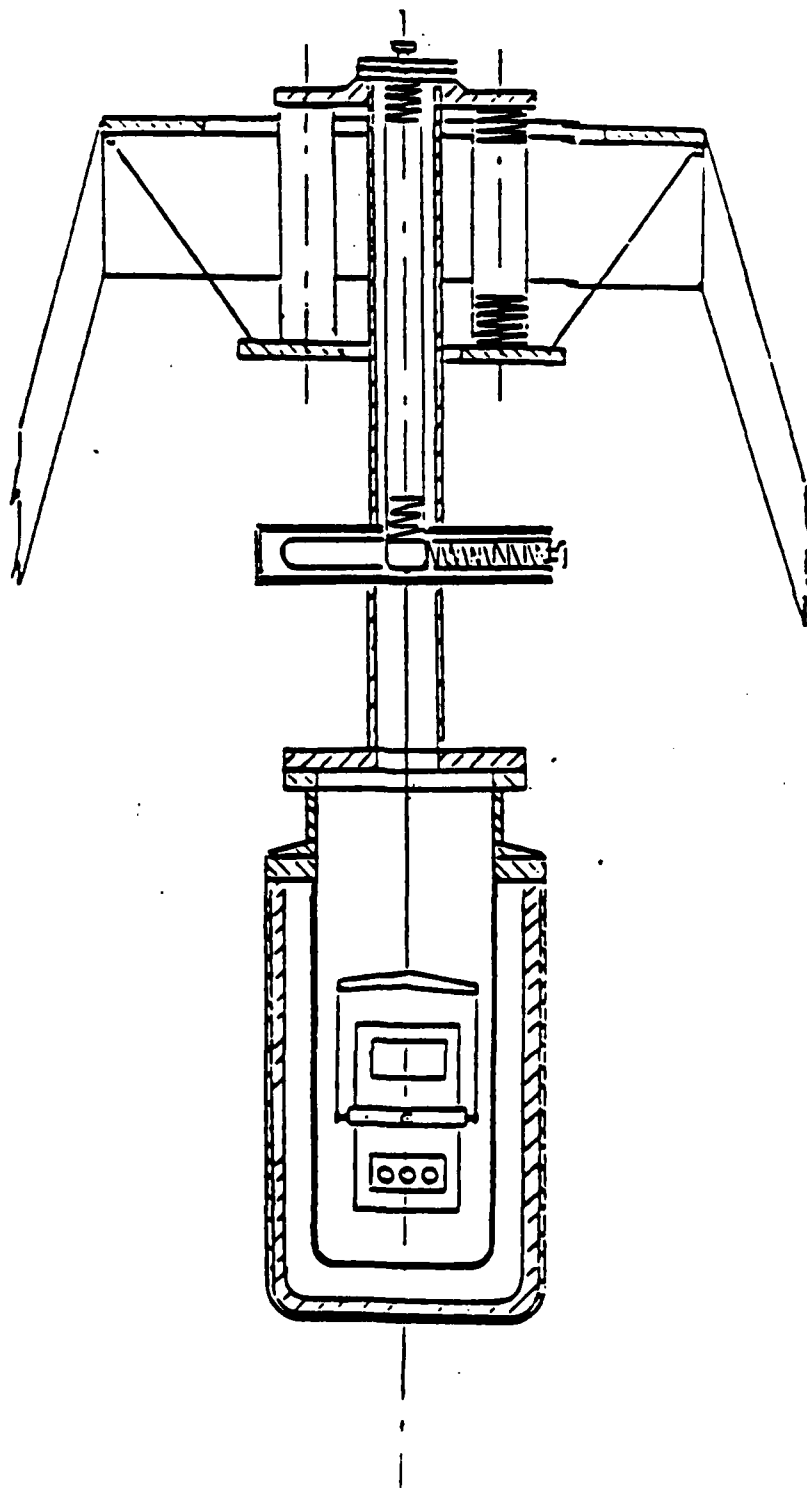


SCHEMATIC DIAGRAM OF LOW-NOISE FET PREAMPLIFIER



0 MEASURED EFFECTIVE TEMPERATURE (WHEN COOLED DOWN TO 4°K) : 0.2 °K
SENSING CELL IS

CRYOGENIC FORCE SENSOR COMPLETE WITH CRYOSTAT
AND SUSPENSION SYSTEM



THEORETICAL ASPECTS (*)

(*) Contributed by Prof. R.R. Lewis

MAXIMUM

EXPECTED INTENSITY OF FORCE SIGNAL GENERATED BY A

100 KILOCURIE TRITIUM SOURCE

- 0 F_{SIG} CANNOT EXCEED THE FORCE THAT WOULD RESULT FROM THE TRANSFER TO THE TARGET OF THE TOTAL MOMENTUM OF THE NEUTRINOS INTERSECTED BY THE TARGET'S AREA.

- 0 THEREFORE, WE HAVE :

$$F_{SIG} \leq j \left(\frac{E_\nu}{c} \right) \cdot A$$

WHERE

$$j = \text{FLUX} = 1.2 \cdot 10^{12} \overline{\nu} \text{ cm}^{-2} \text{ sec}^{-1} \quad (\text{THIS IS THE FLUX FROM A 100 KILO- CURIE SOURCE AT A DISTANCE OF 15 CM; } 1 \text{ CURIE} \rightarrow 3.4 \cdot 10^{10} \overline{\nu} \text{ sec}^{-1})$$

$$E_\nu \approx 10 \text{ KeV } (= 10^4 \cdot 1.6 \cdot 10^{-12} \text{ ERG})$$

$$A \approx 50 \text{ cm}^2 \quad (\text{AREA OF THE TARGET, A SAPPHIRE CRYSTAL})$$

$$c = \text{VELOCITY OF LIGHT} = 3 \cdot 10^{10} \text{ CM SEC}^{-1}$$

AND , NUMERICALLY:

$$F_{SIG} \leq 3.2 \cdot 10^{-5} \text{ DYNES}$$

- 0 IT IS PRUDENT TO DESIGN A SENSOR WITH A SENSITIVITY MARGIN OF 10^3 . UNDER THESE CIRCUMSTANCES, THE THRESHOLD SENSITIVITY OF THE INSTRUMENT SHOULD BE $3.2 \cdot 10^{-8}$ DYNES.

MEASUREMENT DIFFICULTIES AND SOME WAYS OF COPING WITH THEM

UNDER CONSIDERATION

VIBRATIONS CAUSED BY THE ROTATING SOURCE ASSEMBLY

- 0 THE DESIGN AND THE CONSTRUCTION OF THE ROTATING SOURCE ASSEMBLY REPRESENT A DIFFICULT PROBLEM OF MECHANICAL ENGINEERING, IN VIEW OF THE REQUIREMENT TO MINIMIZE VIBRATIONS RESULTING FROM ITS HIGH-SPEED ROTATION, TO AN UNUSUAL DEGREE. WHEEL MUST ALSO BE WELL ISOLATED FROM THE FLOOR, BY THE USE OF SUITABLE FILTERS. POSSIBILITY OF ENCLOSING WHEEL IN VACUUM CONTAINER MUST BE CONSIDERED.
- 0 BALANCING OF THE WHEEL IS EXPECTED TO REQUIRE SUBSTANTIAL EFFORT. WE MUST MEASURE LEVELS OF VIBRATIONS AT SENSOR STATIONS, TO PROVIDE GUIDANCE IN DEBUGGING AND ADJUSTING SYSTEM. WE PLAN TO USE ACCELEROMETERS TO ACHIEVE THIS OBJECTIVE.
- 0 SPECTRAL DENSITY AS A FUNCTION OF FREQUENCY OF INDUCED VIBRATIONS MUST BE DETERMINED THEORETICALLY FIRST AND LATER BY MEASUREMENTS, SO THAT A COMPETENT SELECTION COULD BE MADE (AMONG POSSIBLE VALUES) OF DESIRABLE SIGNAL FREQUENCY (FOR INSTANCE, MOUNTING TWO SOURCES IN THE RIM OF THE WHEEL INSTEAD OF A SINGLE ONE, THUS MULTIPLYING $\times 2$ SIGNAL FREQUENCY).

OTHER AREAS FOR SPECIAL ATTENTION THAT HAVE BEEN IDENTIFIED

1. TIME-VARIABLE NEWTONIAN GRADIENTS PRODUCED BY THE SOURCE MOTION, AT THE SIGNAL FREQUENCY OF 100 Hz
2. TIME-VARIABLE THERMAL RADIATION, ALSO ASSOCIATED WITH THE ROTATING SOURCE
3. TIME-VARIABLE MAGNETIC FIELDS AND ELECTROSTATIC FIELDS, OF POSSIBLE EXTERNAL AS WELL AS INTERNAL ORIGIN
4. EFFECTS DUE TO EXPERIMENT OPERATORS MOVING IN THE VICINITY OF SENSORS

TIME-VARIABLE GRAVITY GRADIENTS PRODUCED BY

ROTATING SOURCE ASSEMBLY

- 0 THE ROTATING SOURCE ASSEMBLY REVOLVES AT 6000 RPM AROUND ITS VERTICAL AXIS. WE WILL EXERT OUR BEST CARE TO ACHIEVE A GOOD CYLINDRICAL SYMMETRY, THUS REDUCING THE NEWTONIAN GRADIENTS AT 100 Hz , AS MUCH AS PRACTICAL
- 0 THE DENSITY OF THE RIM OF THE ROTATING TABLE WILL BE MADE AS MUCH AS POSSIBLE EQUAL TO THE DENSITY OF THE SOURCE
- 0 AN INITIAL SET OF MEASUREMENTS WILL BE PERFORMED, WITH THE CRYOGENIC FORCE SENSOR, BY REPLACING THE 3.5" SPHERE TRITIUM SOURCE WITH AN IDENTICAL DUMMY, HAVING SAME VOLUME AND SAME MASS AS THE TRITIUM SOURCE. THE DUMMY WILL ALSO REPRODUCE THE DENSITY PROFILE, INSIDE THE CONTAINER, OF THE REAL SOURCE.
- 0 INTEGRATION TIME NECESSARY TO DETECT RESIDUAL NEWTONIAN GRADIENTS WILL BE MAXIMIZED BY MAKING ADJUSTMENTS IN ROTATING WHEEL, AIMED AT IMPROVING ITS CYLINDRICAL SYMMETRY
- 0 DUMMY SPHERE WILL THEN BE REPLACED BY REAL SOURCE; INTEGRATION TIME NECESSARY TO ACHIEVE DETECTION WILL BE DETERMINED. IF THIS INTEGRATION TIME IS MUCH SHORTER THAN THE PREVIOUS ONE (WITH THE DUMMY), WE WILL HAVE A CANDIDATE SIGNAL.
- 0 ANALYTICAL TASK PRESENTLY UNDERWAY : QUANTITATIVE ESTIMATE OF THE EXPECTED RESIDUAL NEWTONIAN GRADIENTS DUE TO THE IMPERFECT CYLINDRICAL SYMMETRY OF THE ROTATING WHEEL ASSEMBLY.

HEAT RADIATION BY THE TRITIUM SOURCE

- 0 THE CRYOGENIC FORCE SENSOR IS CONTAINED IN A THICK-WALL CRYOSTAT, EXPECTED TO PROVIDE SUFFICIENT THERMAL SHIELDING
- 0 RESIDUAL SENSITIVITY TO THERMAL EFFECTS WILL BE DETERMINED BY REPLACING THE 3.5" TRITIUM SOURCE IN THE RIM OF THE ROTATING WHEEL WITH AN EQUAL 3.5" CONTAINER EQUIPPED WITH A BATTERY-OPERATED HEATER RAISING DUMMY BODY'S TEMPERATURE TO TRITIUM SOURCE TEMPERATURE, OR HIGHER. THE INTEGRATION TIME NECESSARY TO OBTAIN A DETECTABLE OUTPUT WILL BE DETERMINED.
- 0 IF NECESSARY, THERMAL SHIELDING OF SENSOR WILL BE INCREASED, UNTIL REQUIRED INTEGRATION TIME IS MUCH LONGER THAN INTEGRATION TIME NECESSARY TO DETECT TRITIUM SOURCE. SHOULD THIS BE HAPPENING, WE WILL HAVE A CANDIDATE SIGNAL, WHEN MAKING MEASUREMENTS WITH THE TRITIUM SOURCE.
- 0 ANALYTICAL TASK UNDERWAY AT PRESENT : PERFORM A QUANTITATIVE ESTIMATE OF THE RESIDUAL SENSITIVITY OF THE INSTRUMENT TO THERMAL EFFECTS OF THE SOURCE.

POSSIBLE MAGNETIC FIELDS PRODUCED BY ROTATING

SOURCE ASSEMBLY

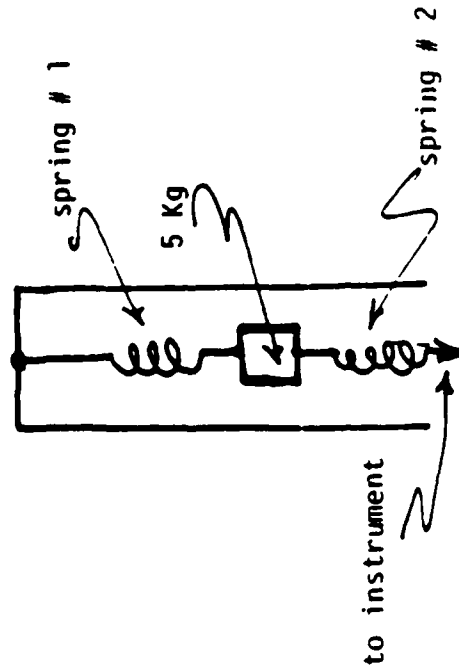
- o THE ROTATING WHEEL ASSEMBLY WILL BE DE-GAUSSSED
- o THE SUBSYSTEMS USED INSIDE THE CRYOSTAT WILL BE ALSO DE-GAUSSSED
- o THE CRYOGENIC FORCE SENSOR WILL BE SHIELDED WITH METGLASS LAMINATION ENVELOPING THE CRYOSTAT
- o RESIDUAL SENSITIVITY TO TIME-VARIABLE MAGNETIC EFFECTS WILL BE MEASURED BY REPLACING TRITIUM SOURCE IN THE RIM OF THE ROTATING WHEEL WITH A DUMMY CONTAINER EQUIPPED WITH A PERMANENT MAGNET. THE INTEGRATION TIME NECESSARY TO OBTAIN A DETECTABLE OUTPUT WILL BE DETERMINED.
- o IF NECESSARY, MAGNETIC SHIELDING WILL BE IMPROVED, UNTIL NECESSARY INTEGRATION TIME BECOMES MUCH LONGER THAN INTEGRATION TIME REQUIRED TO DETECT TRITIUM SOURCE. SHOULD THIS HAPPEN, WE WOULD HAVE A CANDIDATE OBSERVATION OF NEUTRINOS.
- o ANALYTICAL TASK PRESENTLY UNDERWAY : THE QUANTITATIVE ESTIMATE OF THE RESIDUAL SENSITIVITY TO MAGNETIC SIGNALS (EXTERNAL AS WELL AS INTERNAL).

AN APPROACH TO ABATE MECHANICAL VIBRATIONS AND SEISMIC OSCILLATIONS

o REQUIRED OVERALL VIBRATION ATTENUATION

150 DB

o PASSIVE, SIMPLE, TWO-SPRING, SYSTEM



o INSTRUMENT ATTACHMENT TO SECOND VERTICAL SPRING

EACH VERTICAL SPRING RESONATES AT 1 Hz
AND PROVIDES AN ATTENUATION OF 80 DB AT
THE FREQUENCY OF THE SIGNAL (100 Hz).

TOTAL ATTENUATION PROVIDED BY THE SPRING
PAIR 160 DB

BY ADDING THE CONTRIBUTION TO THE ATTENUATION
DUE TO THE COMMON-MODE REJECTION (80 DB), WE
ACHIEVE A GRAND TOTAL ATTENUATION OF.....240 DB
(WITH A 90 DB MARGIN WITH RESPECT TO REQUIREMEN

BY FRICTION-LESS GIMBALS, THE CENTER OF MASS OF
THE INSTRUMENT BEING THE ACTUAL SUSPENSION POIN

o CHECKING THE ANGULAR POSITION OF THE INSTRUMENT
INSIDE THE CRYOSTAT

BY FIBER OPTICS VISUAL OBSERVATIONS FROM THE
OUTSIDE

THE CONDUCT OF THE VERIFICATION EXPERIMENT

CALIBRATION OF INSTRUMENTATION AT TEST SITE

PRIOR TO TESTS WITH TRITIUM SOURCE

- 0 THE SENSITIVITY OF THE CRYOGENIC FORCE SENSOR AND OF WEBER TORSION BALANCE WILL BE CALIBRATED WITH A PREDETERMINED GRAVITY GRADIENT, GENERATED BY A KNOWN MASS (1 KG AT A DISTANCE OF 1 M PRODUCES A GRADIENT OF 1.334×10^{-1} E.U.)
- 0 FOR ALL OTHER SENSORS, WE WILL DETERMINE LEVEL OF OUTPUT NOISE WITH VARIOUS INTEGRATION TIMES, WITH THE TRITIUM SOURCE REMOVED FROM THE ROOM

PLAN OF OBSERVATIONS AT TEST SITE

A. PRELIMINARY TESTS, EXCLUSIVE OF USE OF TRITIUM SOURCE

A.1 SOURCE IS REPLACED BY A 3.5" SPHERE, A DUMMY THAT IS EQUAL IN MASS AND SIZE TO TRITIUM SOURCE

A.1.1	WEBER TUNING FORK	0 MEASUREMENT OF NOISE OUTPUT WITHOUT TURNING-ON CHOPPER, ROTATING WHEEL OFF (DUMMY AT CORRECT POSITION WITH RESPECT TO CHOPPER/FORK)	12 Hours
		0 REPETITION OF MEASUREMENTS ABOVE, BY TURNING ON CHOPPER	12 H
		0 REPETITION OF MEASUREMENTS ABOVE, BY TURNING ON BOTH CHOPPER AND ROTATING WHEEL	12 H
A.1.2	WEBER TORSION BALANCE	0 MEASUREMENT OF NOISE OUTPUT WITH ROTATING WHEEL TURNED OFF	48 H
		0 MEASUREMENT OF NOISE OUTPUT WITH ROTATING WHEEL TURNED ON	48 H
A.1.3	CRYOGENIC FORCE SENSOR	0 MEASUREMENT OF NOISE OUTPUT WITH ROTATING WHEEL TURNED OFF	12 H
		0 MEASUREMENT OF NOISE OUTPUT WITH ROTATING WHEEL TURNED ON	12 H
A.1.4	MAGNETIC INTERACTION SENSOR (*)	0 MEASUREMENT OF NOISE OUTPUT WITH ROTATING WHEEL TURNED OFF	12 H
		0 MEASUREMENT OF NOISE OUTPUT WITH ROTATING WHEEL ON	12 H

PLAN OF OBSERVATIONS AT TEST SITE (CONTINUED)

A.2 SOURCE IS REPLACED BY A 3.5", A DUMMY WITH EQUAL MASS AND SIZE THAT CONTAINS A BATTERY-OPERATED HEATER

A.2.1	WEBER TUNING FORK	0 MEASUREMENT OF NOISE OUTPUT WITHOUT TURNING ON CHOPPER (DUMMY IS IN THE CORRECT POSITION WITH RESPECT TO CHOPPER/FORK)	12 H
		0 REPETITION OF MEASUREMENT ABOVE, BY TURNING ON CHOPPER ROTATION	12 H
A.2.2	WEBER TORSION BALANCE	0 MEASUREMENT OF NOISE OUTPUT BY TURNING ON THE ROTATING WHEEL	48 H
A.2.3	CRYOGENIC FORCE SENSOR	0 MEASUREMENT OF NOISE OUTPUT BY TURNING ON ROTATING WHEEL	12 H
A.2.4	MAGNETIC INTERACTION SENSOR (*)	0 MEASUREMENT OF NOISE OUTPUT BY TURNING ON ROTATING WHEEL	12 H

A.3 SOURCE IS REPLACED BY A 3.5" SPHERE, A DUMMY OF EQUAL MASS AND SIZE THAT CONTAINS A PERMANENT MAGNET

A.3.1	WEBER TUNING FORK	0 MEASUREMENT OF NOISE OUTPUT WITHOUT TURNING ON CHOPPER (DUMMY IS IN THE CORRECT POSITION WITH RESPECT TO CHOPPER/FORK)	12 H
		0 REPETITION, AS FOR A.2.1 ABOVE	12 H
A.3.2	WEBER TORSION BALANCE	0 MEASUREMENTS AS PER A.2.2, ABOVE	48 H
A.3.3	CRYOGENIC FORCE SENSOR	0 MEASUREMENTS AS PER A.2.3 ABOVE	12 H
A.3.4	MAGNETIC INTERACTION SENSOR (*)	0 MEASUREMENTS AS PER A.2.4 ABOVE	12 H

PLAN OF OBSERVATIONS AT TEST SITE (CONTINUED)

B. MEASUREMENT WITH THE TRITIUM SOURCE (3.5" SPHERE) MOUNTED ON THE RIM OF ROTATING WHEEL

B.1	WEBER TUNING FORK	0	INTEGRATION OF SENSOR OUTPUT, BY TURNING ON CHOPPER, AND BY POSITIONING SOURCE AS REQUIRED, WITH RESPECT TO CHOPPER/FORK (ROTATING WHEEL IS OFF)	12	H
B.2	WEBER TORSION BALANCE	0	INTEGRATION OF SENSOR OUTPUT, BY TURNING ON THE ROTATING WHEEL	48	H
B.3	CRYOGENIC FORCE SENSOR	0	INTEGRATION OF SENSOR OUTPUT BY TURNING ON ROTATING WHEEL	12	H
B.4	MAGNETIC INTERACTION SENSOR (*)	0	INTEGRATION OF SENSOR OUTPUT BY TURNING ON ROTATING WHEEL	12	H

TOTAL TIME SEGMENTS 456 HOURS

(*) NOT PART OF WEBER VERIFICATION EFFORT

PLAN OF OBSERVATIONS AT TEST SITE (CONTINUED)

ADVISABLE SEQUENCE OF OBSERVATIONS, WITH REPETITIONS

0 WEBER TUNING FORK

A.1.1	36 HOURS
A.2.1	24 H
A.3.1	24 H
B.1	12 H
A.1.1	36 H

132 HOURS

0 WEBER TORSION BALANCE

A.1.2	96 HOURS
A.2.2	48 H
A.3.2	48 H
B.2	48 H
A.1.2	96 H

336 HOURS

0 CRYOGENIC FORCE SENSOR

A.1.3	24 HOURS
A.2.3	12 H
A.3.3	12 H
B.3	12 H
A.1.3	24 H

84 HOURS

PLAN OF OBSERVATIONS AT TEST SITE (CONTINUED)

O	MAGNETIC INTERACTION SENSOR(*)		
	A.1.4	24	HOURS
	A.2.4	12	H
	A.3.4	12	H
	B.4	12	H
	A.1.4	24	H
<hr/>			
		84	HOURS
GRAND TOTAL OBSERVATIONS TIME.....		636	HOURS

(*) NOT PART OF WEBER VERIFICATION EFFORT

CONCLUSIONS

- 0 RAYTHEON WILL ATTEMPT TO INDEPENDENTLY REPRODUCE THE EXPERIMENTAL RESULTS REPORTED BY PROF. J. WEBER IN DETECTION OF NEUTRINOS
- 0 OUR APPROACH WILL BE CHARACTERIZED BY IMPARTIALITY, SCIENTIFIC AND TECHNICAL SOUNDNESS, AND STRICT ADHERENCE TO THE PRINCIPLES OF GOOD EXPERIMENTAL METHOD
- 0 OUR PRELIMINARY PLAN HAS BEEN PRESENTED IN THE HOPE THAT ANY IMPROVEMENTS TO ACHIEVE THE MOST RELIABLE CONCLUSIONS CAN BE IDENTIFIED IN TIME TO IMPLEMENT THEM, WITHIN THE CONSTRAINTS OF THE PROJECT BUDGET AND SCHEDULE

SECOND CONTRACT
SECOND QUARTERLY REPORT

16 NOVEMBER 1987

EXPERIMENTAL TESTING OF CORPUSCULAR RADIATION DETECTORS

SUBMITTED TO

DEFENSE ADVANCED RESEARCH PROJECT AGENCY (DARPA)

DARPA ORDER #5271

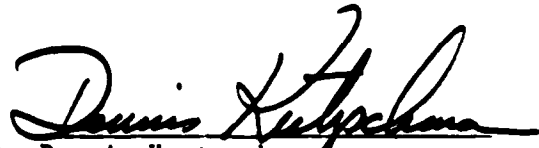
CONTRACT #F49620-87-C-0050

MONITORED BY AIR FORCE OFFICE OF SCIENTIFIC RESEARCH

(AFOSR)

DARPA PROGRAM DIRECTOR: US ARMY LT. COLONEL G. P. LASCHE', Ph.D

The views and conclusions contained in this document are those of the authors and should not be interpreted as necessarily representing the official policies, either expressed or implied, of the Defense Advanced Research Projects Agency or the U.S. Government.


Approved by: Dennis Kretzschmar
Program Manager, Raytheon Co.

RAYTHEON COMPANY
SUBMARINE SIGNAL DIVISION
PORTSMOUTH, RHODE ISLAND 02871

TABLE OF CONTENTS

<u>SECTION</u>	<u>PAGE</u>
ACKNOWLEDGEMENTS	ii
EXECUTIVE SUMMARY	iii
1. INTRODUCTION	1
2. ANALYTICAL DEVELOPMENTS	4
2.1 SIGNAL SHAPE FOR DIFFERENT NUMBERS OF NEUTRINO SOURCES ON A ROTATING WHEEL	4
2.2 RESPONSE OF MAGNETIC SENSOR TO NEUTRONS	17
3. INSTRUMENTATION HARDWARE EFFORTS	21
3.1 CONCEPTUAL DESIGN OF THE ROTATING SOURCE ASSEMBLY	21
3.2 A FIRST EXAMPLE OF A FEASIBLE MECHANIZATION OF THE ROTATING SOURCE ASSEMBLY	23
3.3 STATUS REPORT ON THE DEVELOPMENT OF THE ROOM TEMPERATURE GRAVITY GRADIOMETER AT IFSI-CNR	27
4. CONCLUSIONS AND RECOMMENDATIONS	34

ACKNOWLEDGEMENTS

This quarterly report has been prepared by Mario D. Grossi, Principal Investigator, with inputs from all members of the program team. For each section, credit is given to the writer who contributed it.

EXECUTIVE SUMMARY

In the past quarter, activity for most of the project proceeded close to the pre-established schedule, although we are experiencing delays in some areas.

Progress was substantial for the cryogenic force sensor. The construction of the room-temperature gravity gradiometer at IFSI-CNR (to be used, after modification, by SAO and Raytheon) was completed in early October 1987. The PMO witnessed a laboratory demonstration of its functionality on October 13, 1987. Sapphire crystals (being procured from Union Carbide by Raytheon) will be embedded in one of the two proof-masses at IFSI-CNR prior to shipment of the modified instrument to SAO. This shipment is scheduled to take place on or before 4/30/88. In the meantime, SAO is scheduled to procure the 4°K cryostat, the tripod for the support of the instrument, the related suspension, etc., so that a fully integrated measurement system will be made available to Raytheon by 5/31/88. This will enable initiation of the feasibility tests with a neutrino source of 100 Kilocurie, in an area suitably licensed by the Nuclear Regulatory Commission (NRC). These tests are expected to last four months, until 9/30/88.

There was also progress in the SAO design of the rotating source assembly, although this design could not be completed, as planned, in this last quarter. LLNL has not yet provided Raytheon with drawings of the 3.5" tritium source sphere, including information on its mass. The rotating table, with vertical axis of rotation, will turn at 3000 RPM and will be characterized by a rotational stability of 1 part in 10^4 . At 3000 RPM, two sources, mounted at diametrically opposite points on the rim of the round table, will generate a signal at 100 Hz, which is the resonance frequency of the cryogenic gravity gradiometer. If three sources were available, the rotational speed could be 2000 RPM, still providing a signal at 100 Hz. The reason for multiple sources is to obtain a signal frequency different than the frequency of mechanical rotation of the table (50 Hz for 3000

RPM), the latter being the frequency at which the mechanical vibration noise produced by the table is expected to be at its maximum. An adaptive servomechanism speed control will make it possible to choose other values of rotational speed, such as 30 RPM (1 Hz signal frequency for 2 sources) for experimenting with the magnetic interaction sensor, or 0.05 RPM to 0.5 RPM (1/600 and 1/60 Hz signal frequency respectively, again with two sources), for experimenting with Prof. Weber's torsion balance. The rotating source assembly is expected to be ready for feasibility tests at Raytheon on or before 29 February 1988, if the missing information from LLNL is available no later than 30 November 1988. On 15 March 1988, we expect to start experimenting with Prof. Weber's torsion balance (about three months prior to the availability of Raytheon's cryogenic force sensor).

In this past quarter, the University of Maryland received from Raytheon the subcontract to construct a replica of Weber's torsion balance-expected delivery to Raytheon on 15 March 1988.

Concerning the tuning fork and the rotating shutter, work proceeds on schedule at University of Maryland, under a direct contract from DARPA/AFOSR. We also understand that the feasibility tests with this sensor will be carried out directly by University of Maryland, without Raytheon's involvement.

Initiation of work for the reduced-scope magnetic interaction sensor, to be used in the laboratory measurements of fundamental instrument parameters, has experienced a delay of about one month, with respect to the schedule worked out at the planning meeting at IESS-CNR on 12 October 1987. The completion of the design of the 25 Kg high-permeability interaction target is now expected

31 December 1987. The impact of this delay on the overall project schedule is minor, because the laboratory tests on the magnetic sensor represent an activity that is outside the main focus of our present work, which is the verification of Prof. Weber's findings.

At the time of this writing, two issues are of some concern to the project:

- (a) the lack of information, thus far, on the LLNL tritium source (this prevents the completion of SAO's design work for the rotating source assembly);
- (b) the unresolved issue of the location of feasibility tests. Although, at this point, site selection does not hold back progress in other areas of project activity, it is a necessary input for the detailed planning of data collection. Since the data collection is expected to begin in March 1988, the effort with the NRC to upgrade a lab facility presently cleared to handle radioactive sources will have to begin 3 months earlier - no later than 15 December 1987. The site selection is a Raytheon responsibility, and Raytheon will concentrate on it in the weeks ahead. At present, potentially available sites are Raytheon Sudbury, University of Rhode Island, and LLNL (the latter is a solution of last resort, considering the distances involved).

1. INTRODUCTION

The project has entered a new and more pressing phase of activity: the construction of the instrumentation for conducting the feasibility tests. In performing the design of this instrumentation, Raytheon is taking into account, under DARPA direction, the recommendations formulated by JASON at the project review meeting of July 10, 1987. The consequence is that the original design must be modified in several areas, with a substantial upgrading in the quality of the hardware and the rigor of the experimental methodology to be adopted.

The most significant changes are introduced in the design of the rotating source assembly (also called the rotating table, or the rotating wheel):

(a) housing the rotating table in a vacuum container, to prevent airborne mechanical vibrations from reaching the sensors;

(b) choosing number of sources N (to be mounted on the rim of the rotating table) such that the frequency (Hz) of the signal ($\frac{\text{RPM}}{60} \times N$) falls on a local minimum of the spectrum of the mechanical vibration noise generated at the sensors' input by the rotating table (this noise is expected to have a maximum at the fundamental frequency (RPM/60));

(c) reducing to the lowest possible value the time-variable gravity gradient forces produced by the rotation of the table, and determine the residuals by replacing the N sources mounted on the rim of the wheel with empty dummies (utilizing 36 dummies, instead of $(36-N)$ dummies and N sources);

(d) replacing the N sources in the rotating table with dummies containing heat sources to verify the extent of the sensor's response to thermal effects (the cryogenic force sensor will be immune from this effect, because of the thick wall of the cryostat. The torsion balance, on the contrary, might be affected);

(e) as above, but with the dummies containing a permanent magnet, to verify the extent of the sensor's response to time-variable magnetic fields that are at the rotational signal frequency. The changes in the design of the cryogenic force sensor are more limited and consist of the following:

(a) embedding, into the aluminum block of one of the so-called "proof-masses", sapphire crystals (to prevent X-ray induced electrostatic charging these crystals are totally encapsulated in the aluminum); the crystals will be in the form of ten rods, with a 1 cm diameter and 5.2 cm length. They will be inserted in ten cylindrical wells drilled in the aluminum block of the proof-mass.

(b) modifying the feedback circuit of the null-servo that keeps the proof-mass at equilibrium, to make it possible to apply an external electrical signal for sensor calibration;

(c) providing a signal for fine tuning the resonance frequency of the cryogenic force sensor. This will be derived from the measurement of the rotational speed of the rotating table.

The changes in the magnetic interaction sensor represent a reduction in scope of the work planned for this instrument. This work now consists of laboratory measurements of fundamental sensor parameters, exclusive of attempts to detect magnetization induced in a high-permeability target by low-energy neutrinos. We have already started the design of a 25 Kg interaction target (instead of the contemplated 250 Kg version) and we will measure the following system parameters with a high-sensitivity SQUID (provided to SAO by IESS-CNR, Roma, Italy):

(1) thermal noise of the SQUID when its input is loaded, via a superconducting transformer, by the 25 Kg target;

(2) maximum achievable relative permeability of the target material, when operating on the steep ascending side of the hysteresis cycle;

(3) maximum achievable target cross-sectional area.

In FY 88, analytical work has been limited to the computer simulation of the expected performance of the instrumentation being designed. At the JASON review of 7/10/87, Raytheon illustrated its plans to analyze the expected response of the cryogenic gravity gradiometer to forces expected to be generated by the rotation of the table. This work has started, and a first account of what we have done is provided in Section 2.1 of this Quarterly Report: the expected neutrino-induced signal shape is illustrated for different numbers of neutrino sources (1 through 7). Next step will consist of computing the forces produced by gravity gradients due to realistically-estimated non-idealities in the rotating table's cylindrical symmetry. For the magnetic interaction sensor, an analysis of the response of this instrument to neutrons was performed. Section 2.2 illustrates our findings on this topic. This analysis is useful in understanding the response of the sensor to neutrinos and in exploring the possibility of a sensitivity calibration of the instrument by the interaction of particles with the target.

The progress achieved in this past quarter in instrumentation design and construction is illustrated in Section 3, which documents what was accomplished in the design of the rotating source assembly, and provides the status on the development of the room-temperature gravity gradiometer at IFSI-CNR, Frascati, Italy (instrument functionality was demonstrated to Raytheon on 13 October 1987).

2.0 ANALYTICAL DEVELOPMENTS

2.1 Signal Shape For Different Numbers Of Neutrino Sources On A Rotating Wheel(*)

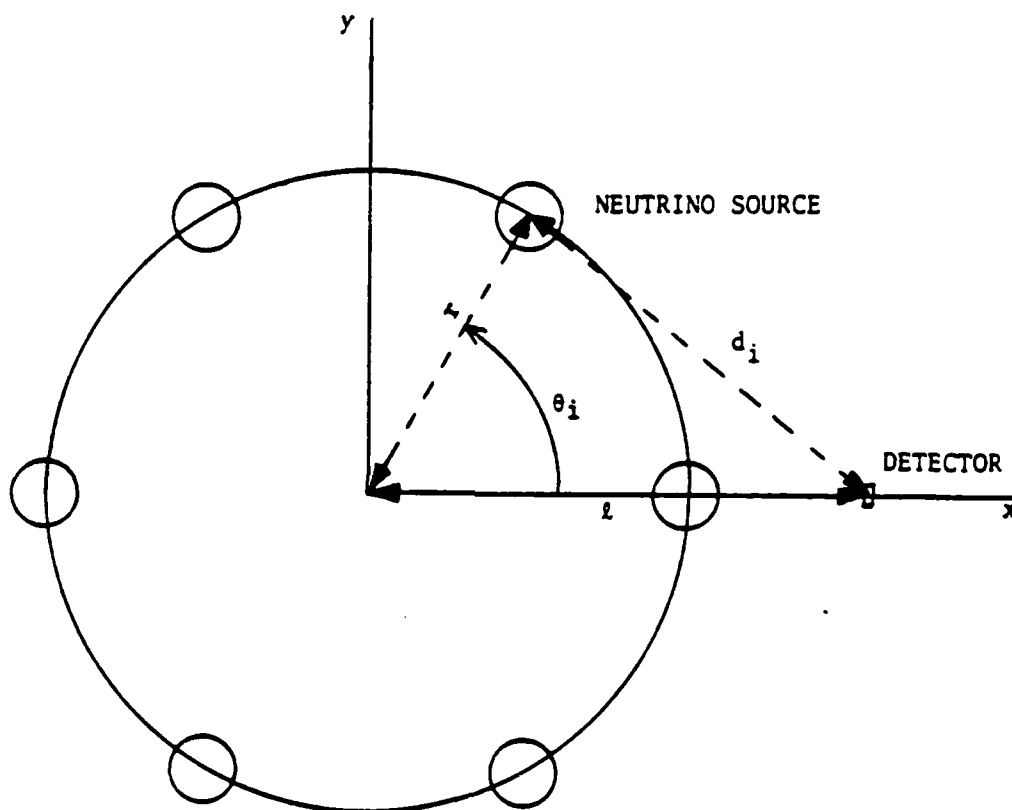


Figure 1. Neutrino Sources on a Rotating Wheel

Figure 1 shows a set of neutrino sources equally spaced around a circle of radius r . There is a detector located at a distance ℓ from the center of the wheel on the x -axis which measures the x -component of the neutrino flux from the n sources on the wheel. We wish to calculate the shape of the signal

*Contributed by David A. Arnold, SAO

measured by the detector as a function of the rotation angle of the wheel. The positions of the neutrino sources as a function of time are given by the equations

$$x_i = r \cos \theta_i \quad (1)$$

$$y_i = r \sin \theta_i \quad (2)$$

where

$$\theta_i = (i-1) \Delta\theta + \omega t \quad (3)$$

and

$$\Delta\theta = 2\pi/n \quad (4)$$

The source on the x axis closest to the detector is labelled $i = 1$, and the sources are numbered counterclockwise. The wheel rotates with angular velocity ω . The distance of the i^{th} source from the detector is

$$d_i = \sqrt{\Delta x_i^2 + y_i^2} \quad (5)$$

where

$$\Delta x_i = \ell - x_i \quad (6)$$

The intensity of the neutrino flux at the detector from the i^{th} source is

$$F_i = C / d_i^2 \quad (7)$$

where C is a constant and d_i is the distance. The sum of the x - components of the fluxes from all the sources is

$$F_z = \sum_{i=1}^n F_i \frac{\Delta x_i}{d_i} \quad (8)$$

A computer program called *FLYWHEEL* has been written to calculate the value of F_z vs. the rotation angle of the wheel. A set of runs has been done for $i = 1$ to 7 with F_z plotted at 3 degree intervals, using $C = 100.$, $r = 45$ cm and $\ell = 70$ cm. The value of C was chosen arbitrarily to give numbers close to unity. The flywheel is expected to be one meter in diameter with spherical sources 9 cm in diameter. The container for the detector is expected to be about 14 inches (35.56 cm) in diameter.

Figure 2 shows the shape of the signal for a single neutrino source. At the closest approach the distance is 25 cm and the signal from equation (7) is .16000 in arbitrary units. At the furthest point from the source ($\omega t = 180$ deg) the signal is .00756. The difference is .15244 units. At $\omega t = 90$ deg the magnitude of the signal (with $d = 83.216$ cm) is .01444 and the x - component is .01215. Figure 2a shows the flux F_z vs. rotation angle of the wheel at 3 deg intervals from 0 to 360 deg. Figure 2b shows the signal from -180 to +180 deg. Figures 3 to 8 show the signal for $n = 2$ to 7. The pulse width for $n = 1$ is about 40 deg. at half amplitude. At this width, several sources could be used before there would be significant overlap of the signals. As more sources are added the signal becomes more sinusoidal.

Table 1 lists the maximum signal F_{\max} , the minimum signal F_{\min} , and the difference ΔF between the maximum and minimum signals for each of the seven cases.

Table 1

n	F_{\max}	F_{\min}	ΔF
1	.16000	.00756	.15244
2	.16756	.02429	.14327
3	.17829	.04852	.12977
4	.19185	.07897	.11288
5	.20808	.11359	.09449
6	.22681	.15033	.07648
7	.24780	.18762	.06018

Table 1. Amplitude of the signal vs. number of sources n .

Table 2 gives some of the details of the calculations of F_s for $n = 6$ and $\omega t = 0$. The geometry for this case is given in Figure 1.

Table 2

i	θ	x	y	d	F	F_s	$\sum F_s$
1	0	45	0.00	25.00	.16000	.16000	.16000
2	60	22.5	38.97	61.44	.02649	.02048	.18048
3	120	-22.5	38.97	100.37	.00993	.00915	.18963
4	180	-45.	0.	115.00	.00756	.00756	.19719
5	240	-22.5	-38.97	100.37	.00993	.00915	.20633
6	300	+22.5	-38.97	61.44	.02649	.02048	.22681

Table 2. Calculation of the signal for $n = 6$ and $\omega t = 0$.

The neutrino sources to be used in this experiment have a strength of 100 Kilocurie. Since 1 Curie translates into $3.4 \cdot 10^{10}$ neutrinos/sec, we have an intensity of $3.4 \cdot 10^{15}$ neutrinos/sec with each source. The constant C in equation (7) can be evaluated from the equation

$$C = \frac{3.4 \cdot 10^{15}}{4 \pi} = 2.7 \cdot 10^{14}.$$

In the calculations, a value of 100 was used to produce numbers on the order of unity. The flux values can be converted to absolute units for this source strength by multiplying by $2.7 \cdot 10^{12}$. For example, with one source at a distance of 25 cm, the flux in arbitrary units was 0.16 and the absolute value is $4.3 \cdot 10^{11}$ neutrinos $\text{sec}^{-1} \text{cm}^{-2}$.

The momentum per second passing through the target is given by the formula

$$j \frac{E_p}{c} A$$

where j is the flux in neutrinos $\text{sec}^{-1} \text{cm}^{-2}$, E_p is the average energy per particle, c is the velocity of light and A is the area of the target. If the average energy of the neutrinos is 10 keV, the energy per particle is $1.6 \cdot 10^{-8}$ ergs (with $1 \text{ eV} = 1.6 \cdot 10^{-12}$ ergs). Using a target area of 52 cm^2 gives

$$j \frac{E_p}{c} A = 1.2 \cdot 10^{-5} \text{ dynes.}$$

This is the force on the target if all the momentum of the incident beam is transferred to the target. In the arbitrary units used in the signal strength calculations, the signal was 0.16 for the case of one source at 25 cm. The arbitrary units can be converted to dynes by multiplying by

$$\frac{1.2 \cdot 10^{-5}}{0.16} = 7.5 \cdot 10^{-5}.$$

The neutrino flux is incident upon a target which is a high-Q mechanical oscillator. The behaviour of the detector can be computed from the mass, restoring stiffness, and damping of the target. The force as a function of time is given by curves such as Figures 2 through 8. A computer program has been written to calculate the response of the detector for various input signal shapes. Calculations are also being done to evaluate the gravity force on the detector from the rotating masses. The results of these studies will be presented in the next quarterly report.

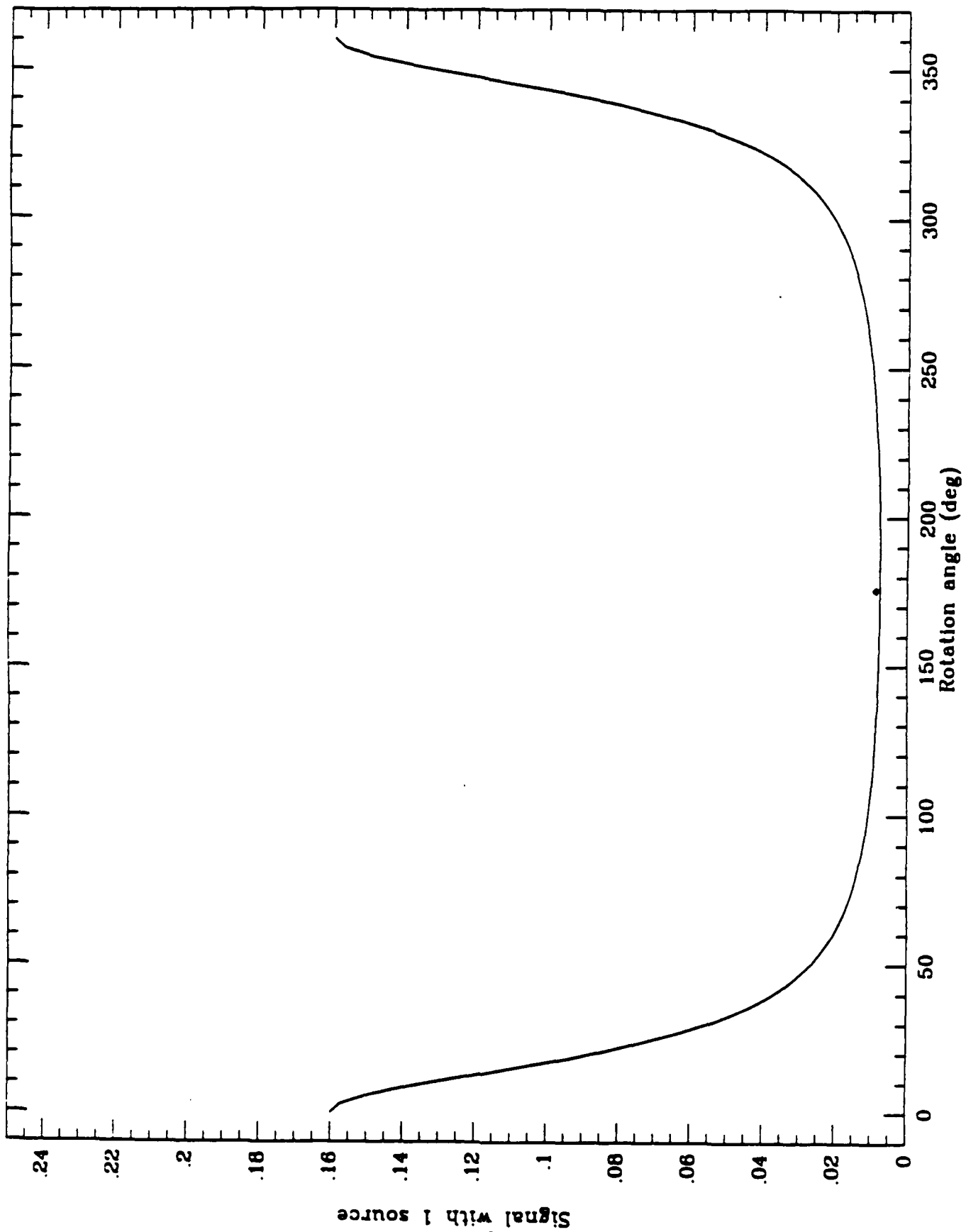


Figure 2a

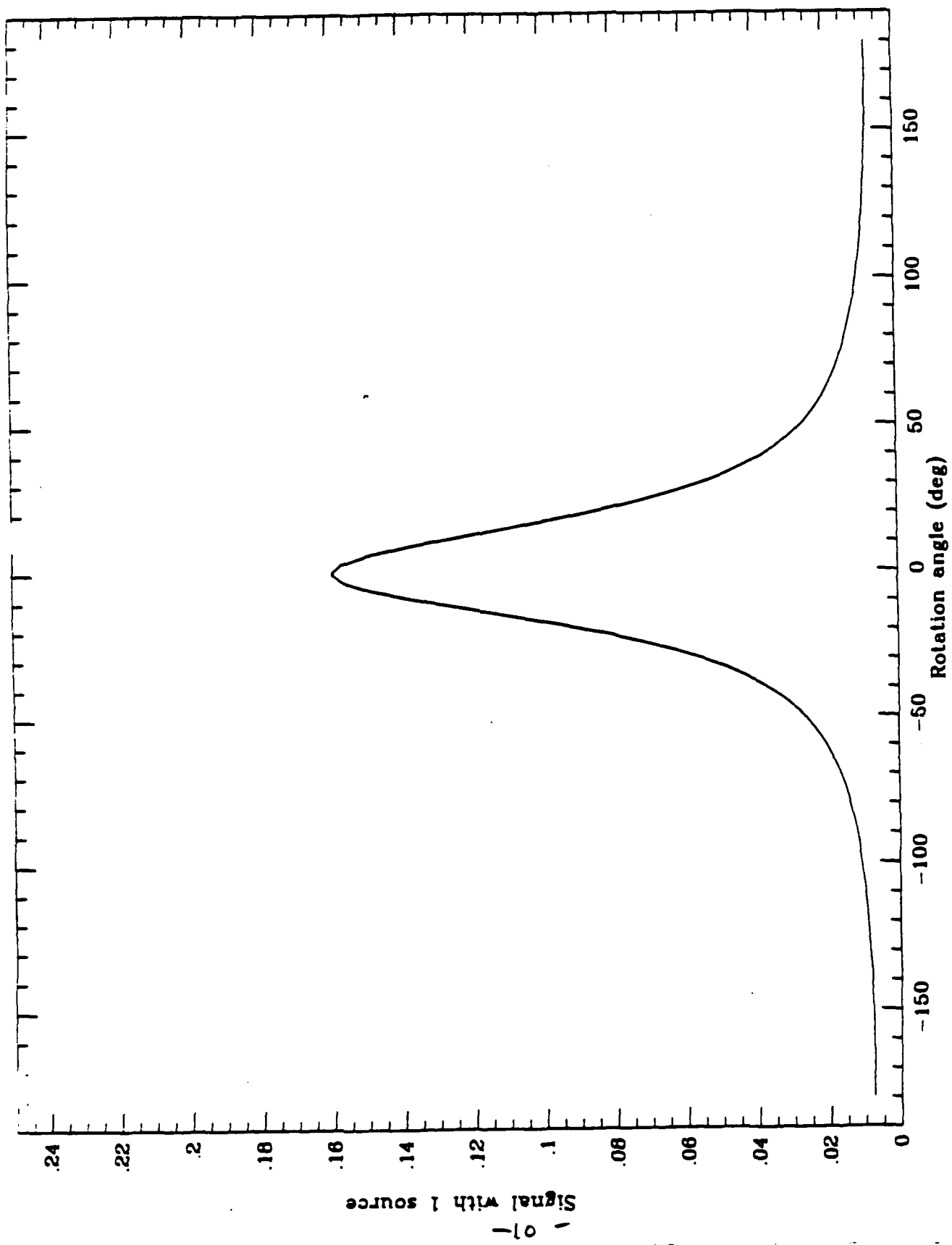


Figure 2b

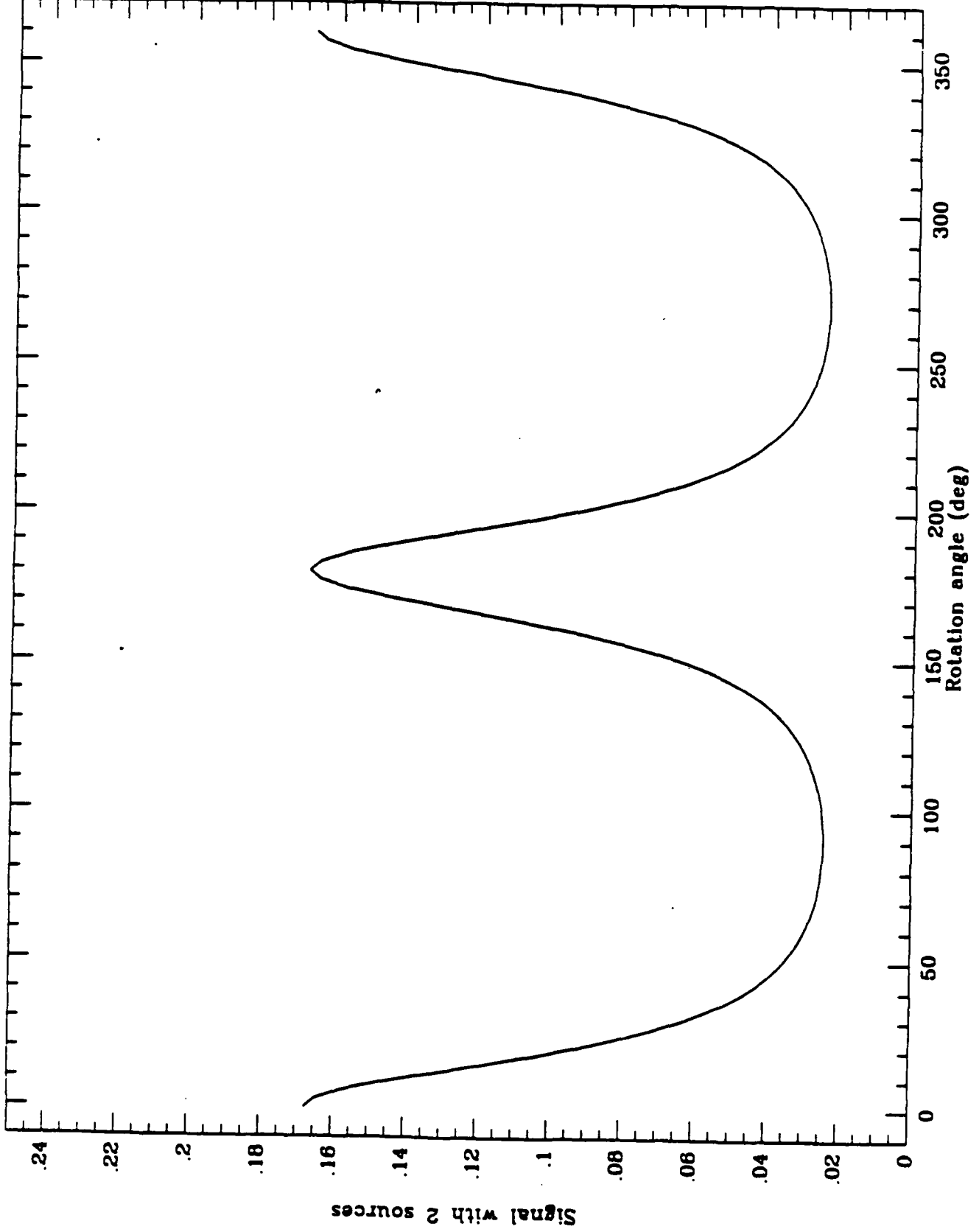


Figure 3

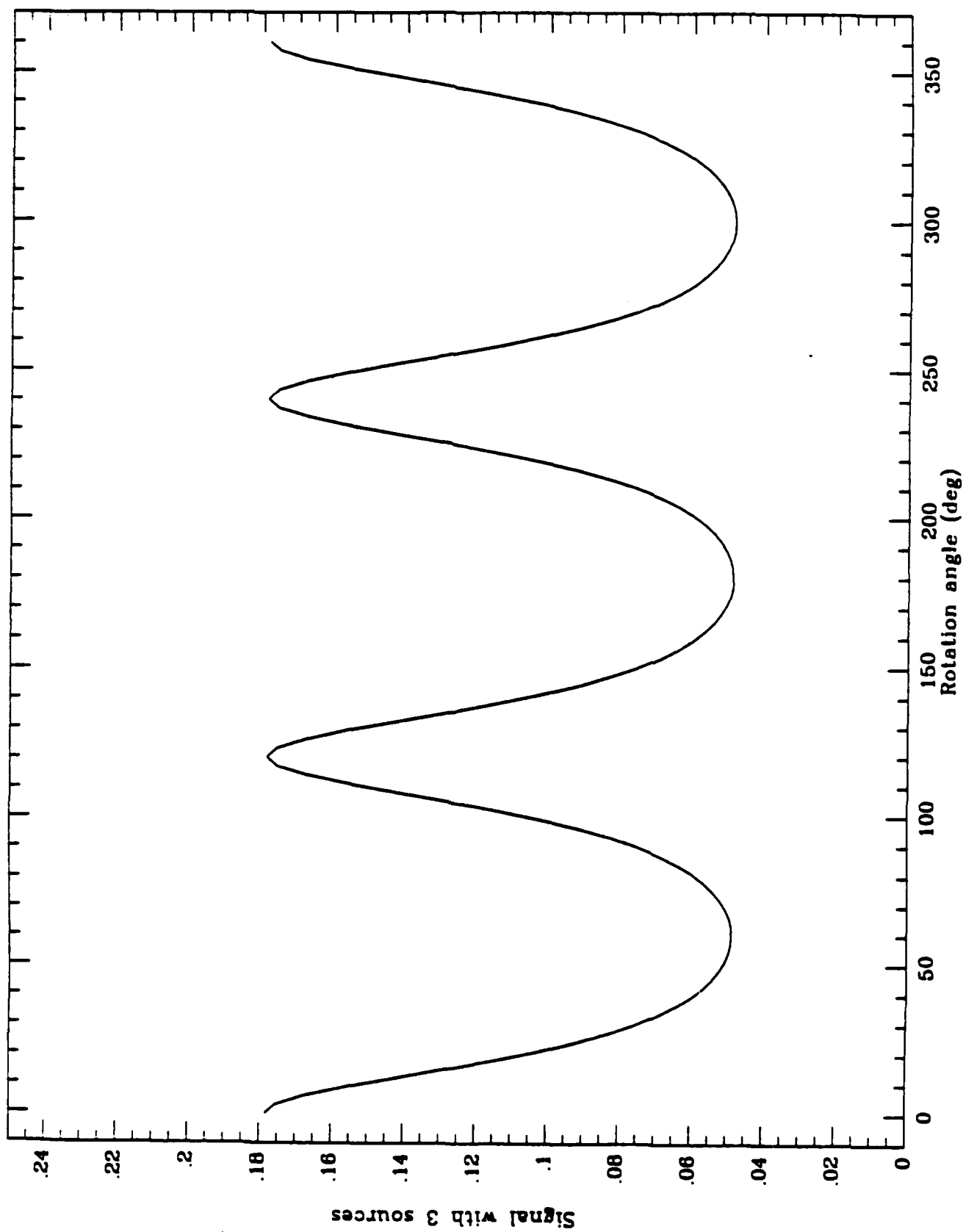


Figure 4

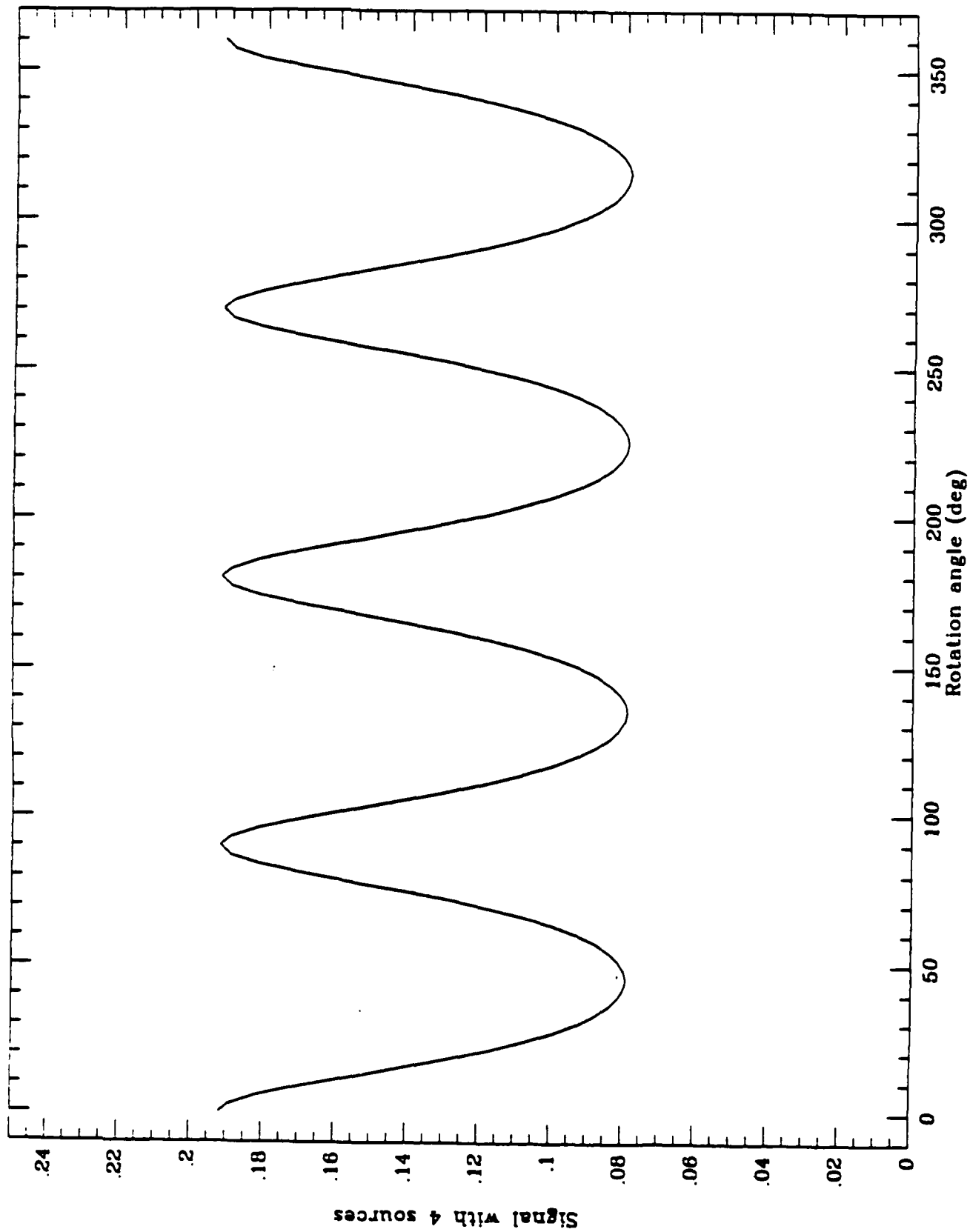


Figure 5

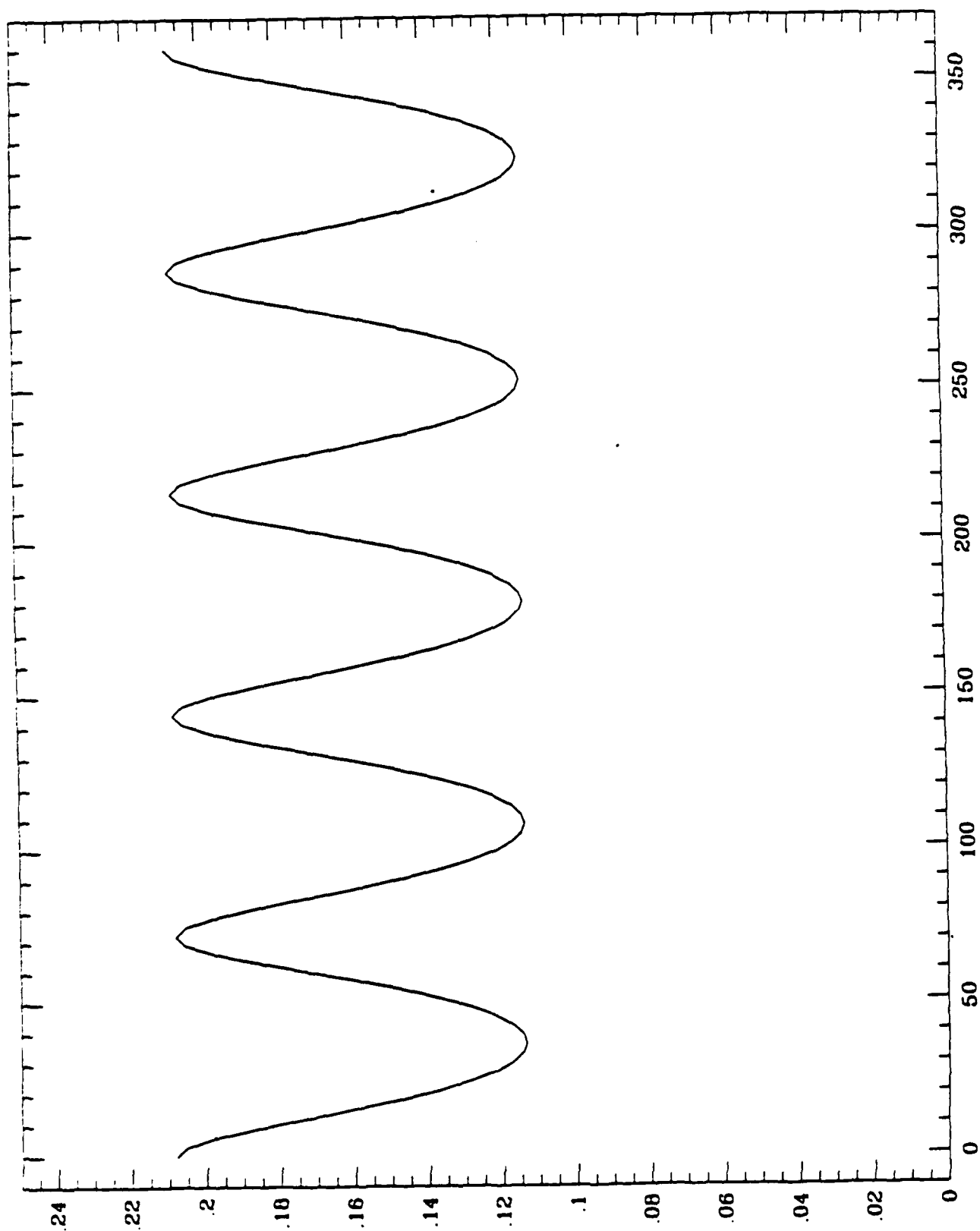


Figure 6

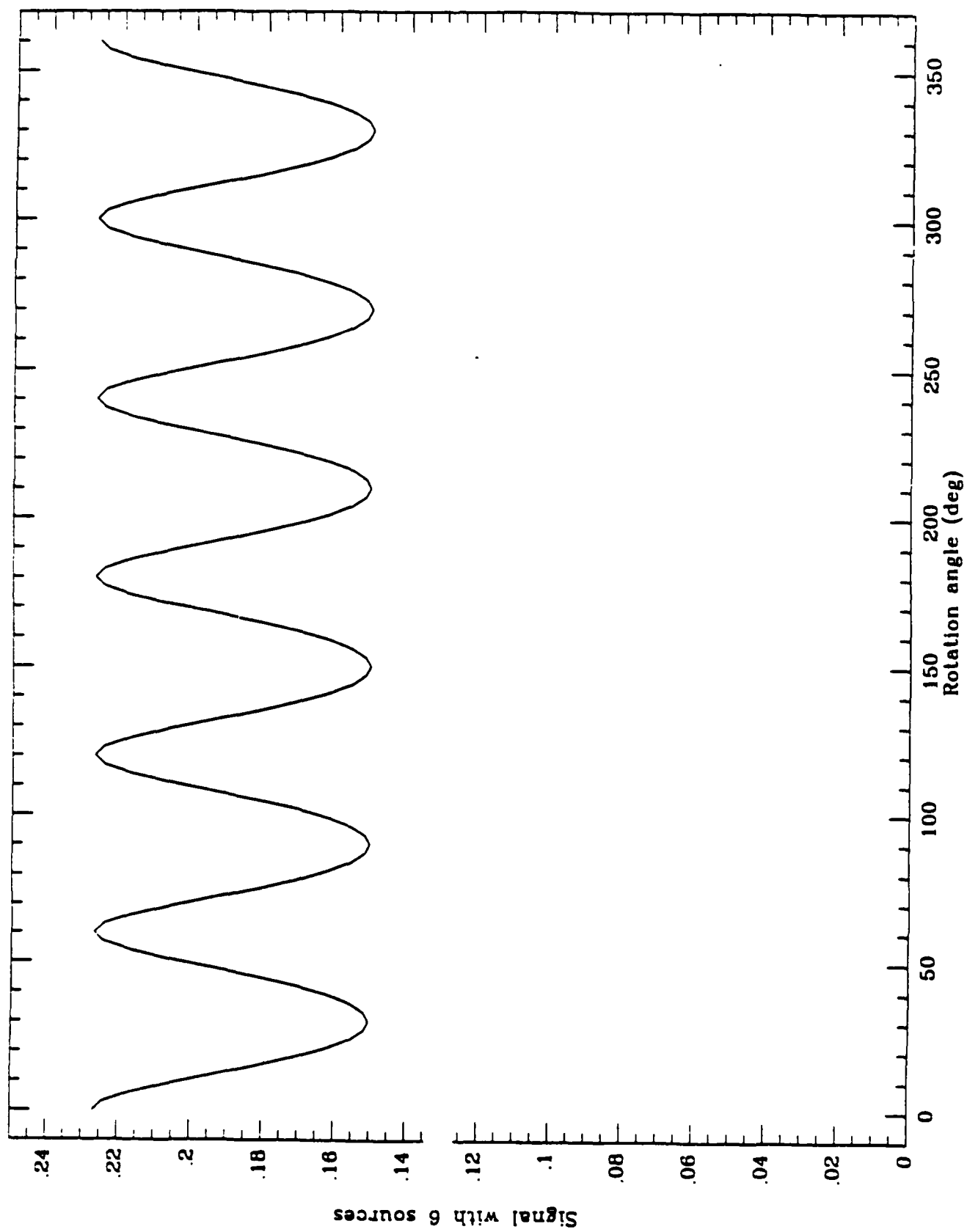


Figure 7

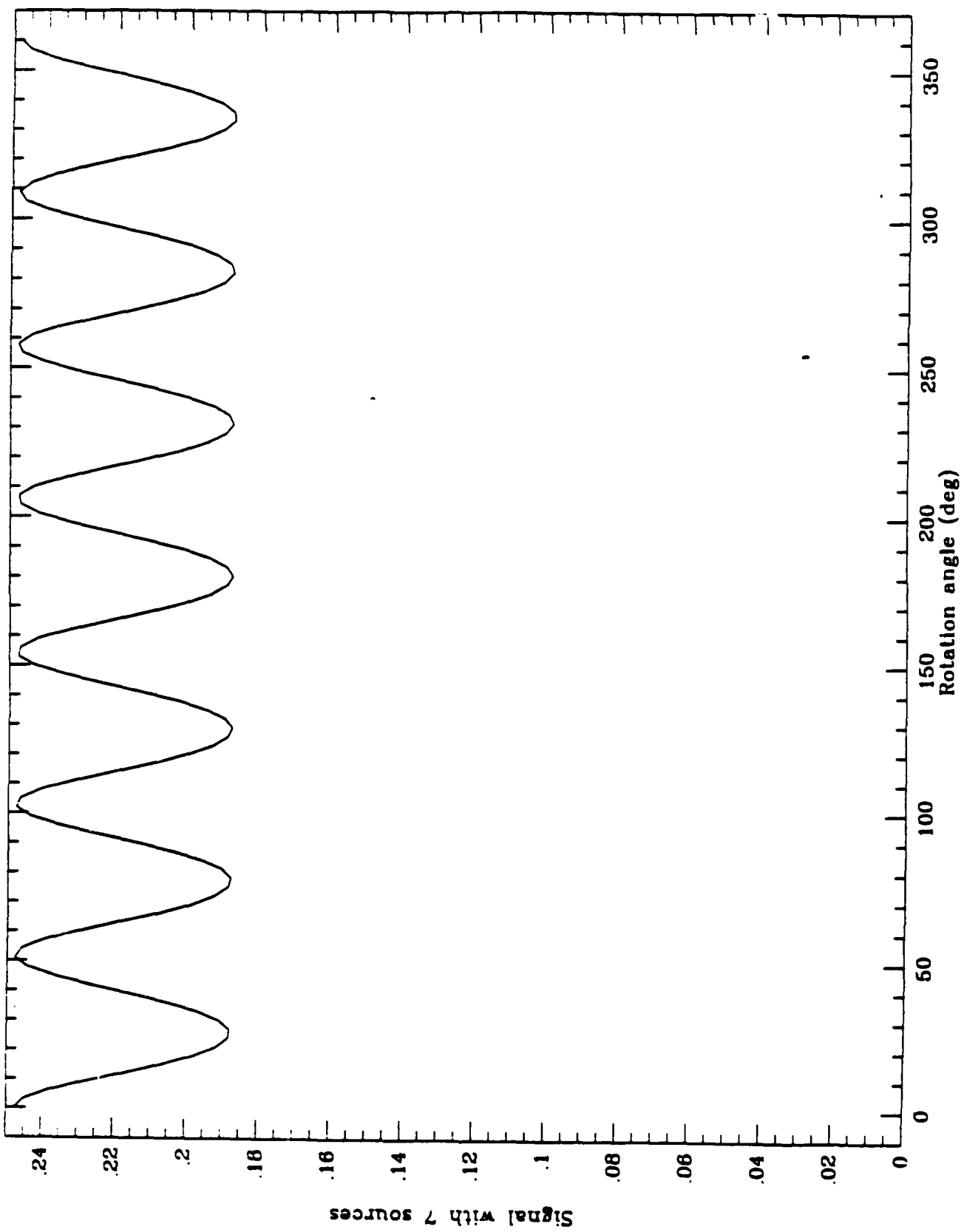


Figure 8

2.2 Responses of Magnetic Sensor to Neutrons

(*)

We have based our design of the magnetic sensor on the detection of the "Stodolsky effect" for neutrinos. But there should be a similar effect for polarized neutrons...much larger and easier to detect. It is unlikely that our magnetic sensor would be useful as a detector for neutron polarization, but there may be some interesting physics in the measurement of both the mechanical torque and the magnetic signal produced by neutrons in a variety of solid targets.

Direct Magnetization

The magnetic sensor will respond in two different ways to an incident beam: one is a magnetization of the target by the magnetic moment of the incident particles; the other is the magnetization by the torque exerted on the magnetic moment of the target particles. These responses are independent since the first mechanism is linear in the neutron magnetic moment and the second is independent of it; both depend on the magnetic moment of the target particles. We will show that the first mechanism, which we will call "direct magnetization" is much smaller than the second "indirect magnetization". This is due primarily to the small size of the neutron magnetic moment when compared with atomic moments.

A single neutron has a magnetic moment of magnitude

$$\mu_n = 1.813 \text{ (n.u.)} \mu_p = 0.984 \cdot 10^{-23} \text{ erg./Gauss}$$

oriented in the direction opposite to its spin. A dilute sample of polarized neutrons with number density N and polarization P has a magnetic moment per unit volume

$$\vec{M} = -\mu_n N \vec{P}$$

This magnetization is the source of a field in vacuum with magnitude

$$\vec{B} = 4\pi \vec{M} = -4\pi \mu_n N \vec{P}$$

Inside our target, it produces a magnetic field given by

$$\vec{B} = \mu \vec{M} = -4\pi \mu \mu_n N \vec{P}$$

where μ is the magnetic permeability of the target.

We have not included the effect of any motion of the neutrons, which are considered to be at rest. In an similar calculation of the response to neutrinos, we had to include a factor $1/\gamma$ due to the transformation of fields from the rest frame of the neutrinos to the rest frame of the target. This suppresses the response to ultra-relativistic particles of light mass. Neutrons are more massive, and have velocities $v \ll c$. They do not suffer any corresponding suppression.

(*) Contributed by Prof. R.R. Lewis, U. of Michigan, Program Advisor

A sample calculation indicates how small this field might be for a typical case. In cgs units, keeping only the orders of magnitude

$$\mu_n \approx 10^{-23} \text{ erg/Gauss}$$

$$n \approx 10^{23}$$

$$r \approx 1$$

$$V \approx 10^{-2} \text{ cm}^3$$

giving a field

$$B \approx 10^{-17} \text{ Gauss}$$

We will show that the "indirect magnetization" of the sample is larger than this.

Mechanical Torque of Polarized Neutrons

Stodolsky was originally concerned with rather exotic questions of the mechanical effects of "relativistic neutrinos" in matter¹. Neutrinos have a spin polarization along their direction of motion, and this polarization influences their scattering in polarized matter. Stodolsky showed that the neutrinos exerted a torque on the target, proportional to the neutrino flux and to the strength of the weak interaction, in the direction of motion of the beam.

For neutrons, there is no such correlation of polarization and propagation vectors: we can polarize a beam of neutrons in any direction. The strong forces which govern the scattering of neutrons from nuclei include spin dependent forces which will make the scattering depend on both the spin polarization of the neutron and the nuclear polarization of the target. There is also some scattering of neutrons from the electrons in the target, and a possible dependence on the electronic polarization as well. Therefore, we can expect a "Stodolsky effect" for neutrons as well as for neutrinos, but with the torque along the polarization of the neutron beam, not along its direction. Since the scattering amplitudes of neutrons are much larger than the scattering amplitudes of neutrinos, the resulting torque on the target should be much larger.

We can provide a rough estimate of the magnitude of the torque exerted by neutrons by comparison with Stodolsky's result for neutrinos. If we consider a single electron in a beam of neutrinos, then the weak interaction energy (Fermi interaction) is

$$\mathcal{H}_V = \sqrt{2} G_F \vec{S}_e \cdot \vec{J}_\nu / c$$

where \vec{S}_e is the electron spin and \vec{J}_ν / c is the neutrino density, where G_F is the weak interaction coupling constant (Fermi constant). An interaction energy of this form implies a torque on the electron in the direction of the neutrino flux,

$$\vec{\tau}_e = \sqrt{2} G_F \vec{J}_\nu / c$$

or equivalently, a "pseudomagnetic" field

$$\vec{H}_n = \gamma \vec{S}_n / \mu_N$$

where μ_N is the Bohr magneton.

The interaction energy of a neutron beam with a single atomic nucleus can be written in a similar form using the pseudopotential, also due to Fermi:

$$X_n = (2\pi\hbar^2 a / m_n) \vec{S}_n \cdot \vec{S}_N \delta(\vec{r} - \vec{r}_N)$$

where a is the scattering length, typically of order 10^{-13} cm (also called the Fermi). Here the subscript n refers to the neutron and N to the nucleus. We are considering only that part of the interaction between neutron and nucleus which depends on the directions of the neutron and nuclear spins. If we take the expectation of this energy for a plane wave neutron normalized to give flux ϕ_n , then we find for the interaction energy

$$X_n = (2\pi\hbar a \phi_n / k_n) \vec{S}_n \cdot \vec{S}_N$$

This represents a torque on the nucleus of

$$\vec{\tau}_n = (2\pi\hbar a \phi_n / k_n) \vec{S}_n$$

or a "pseudomagnetic" field

$$\vec{H}_n = (2\pi\hbar a \phi_n / k_n) \vec{S}_n / \mu_N$$

where μ_N is the nuclear magneton.

Putting in some typical numbers, we see that for equal fluxes the torque exerted by the neutron beam is larger than for the neutrino beam by a factor

$$\tau_n / \tau_\nu \approx (\hbar a / \hbar a_\nu) \approx 10^{11}$$

This is roughly the ratio of the strength of the nuclear interaction to the strength of the weak interaction. The "pseudomagnetic" field due to the beam of neutrons is also larger than for the neutrino beam by an additional factor of the ratio of the Bohr magneton to the nuclear magneton,

$$H_n / H_\nu \approx 10^{14}$$

We can also express these results in absolute terms. Rather than relative to the response to neutrinos, the "pseudomagnetic" field can be estimated for the following conditions:

$$a \approx 10^{-13} \text{ cm}$$

$$\phi_n = 10^{17} \text{ cm}^2\text{-sec}$$

$$\kappa_n \approx 10^{-8} \text{ /cm}$$

$$\mu_n = 10^{-23} \text{ erg/gauss}$$

giving, for a sample with permeability $\mu = 10^{-3}$

$$B_n = 10^{-17} \text{ gauss}$$

$$B_n = \mu \mu_n = 10^{-14} \text{ gauss}$$

This is substantially larger than our estimate of the direct magnetization, indicating that the magnetic signal will be dominated by the "indirect mechanism" of a torque on the nuclei in the sample.

These numbers make it clear that the magnetic sensor is potentially much more sensitive to neutrons than to neutrinos, and that we should consider the possible consequences of calibrating the sensor with neutrons.

3. INSTRUMENTATION HARDWARE EFFORTS

3.1 Conceptual Design of the Rotating Source Assembly (*)

The rotating source assembly is a circular table, having a diameter of about 1 meter, that revolves around a vertical axis at a speed variable from 0.05 RPM to 3000 RPM. The speed is adjustable by external control and is stabilized within 1 part in 10^4 by an active servo-loop mechanism. Figure 9 shows that the rim of the table accommodates the neutrino sources, in number that can be chosen from 2 to 4. The source is a sphere with about 9 cm diameter. If there are two sources in the rim, they are diametrically opposite and the space in between is filled with identical spheres that, however, are dummies and do not contain tritium in their interior. We expect to use a number of dummies from a minimum of 22 to a maximum of 34 (assuming to use two sources, which makes for a total number of spheres in the rim from 24 to 36). The objective that we expect to achieve with the arrangement above is as follows :

(a) We can have, as signal frequency, a value as high as 100 Hz (for instance rotating two sources at 3000 RPM, or three sources at 2000 RPM). By doing so, we simplify tremendously the protection of the sensor from vibration noise, because a rather simple suspension that resonate at 1 Hz, can immediately provide an attenuation of $(100/1)^2$, or 80 dB (two in series will give 160 dB attenuation). We would lose totally this attenuation, if the signal frequency would be 1 Hz instead. This is an advantage that can be hardly overemphasized, as it is well known to every scientist who works with force sensors at frequency in the vicinity of, or below, 1 Hz;

(b) By filling the rim with dummies identical in all respects to the source, but devoid of tritium, we minimize the time-variable gravity gradient forces produced by the rotation of the table. The residual time-variable component will have a spectrum centered at a frequency $\frac{\text{RPM}}{60} \times (\text{Number of dummies} + \text{Number of sources})$, therefore well outside the passband of the receiver (tuned at 100 Hz, and with a bandwidth of 10^{-4} Hz).

(c) The rotating table, with the rim suitable for accommodating sources and dummies can be utilized to carry out measurement of the sensitivity of the instrumentation under test to heat sources and to magnetic sources. This can be done by placing into a dummy a heat generator (for instance a resistor fed by a battery) or a permanent magnet. By rotating the table, we can vary the frequency of these spurious signals and check the response to them of each sensor.

(*) Contributed by Dr. M.D. Grossi, P.I., Raytheon Co.

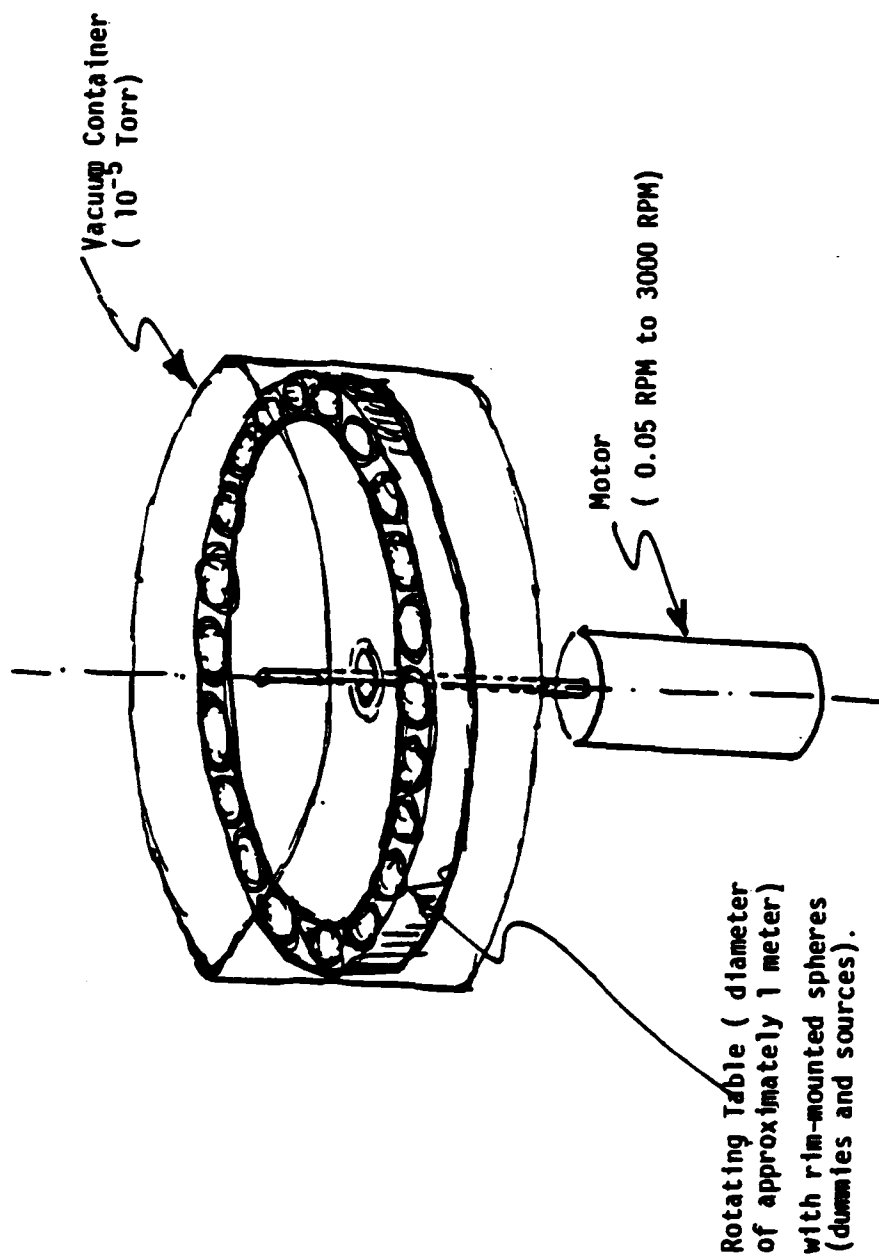


Figure 9 - Sketch of rotating source assembly

3.2 A first example of a possible mechanization of the rotating source assembly (*)

The requirements for the rotating source assembly can be recapitulated as follows :

- 1) Speed must be variable from an upper limit of 3000 RPM (if at all possible, 6000 RPM) to a lower limit that is close to zero (something like 0.05 RPM);
- 2) We need the ability to set the speed of the table to match the resonant frequency, or the most suitable frequency, of one or more detectors used in the feasibility tests. The cryogenic force sensor (gravity gradiometer) has its resonance at approximately 100 Hz, and this determines the maximum frequency of operation. The resonance is fairly sharp-- a Q of about 10,000-- so the turntable frequency must have a stability of about 0.001 Hz p-p variation if it is not to jitter in and out of resonance;
- 3) At least one of the detectors requires a frequency reference signal for locking its internal wheel to the source rotation frequency;

A system to meet all these requirements can be shown in Figure 10. In the Figure, the turntable is phase-locked to a precision variable frequency generator, which also drives a frequency synthesizer, which in turn provides a reference signal for any sensor system that requires it.

A literature search was done among all the product literature pertaining ^{to} high-torque variable speed motors. Motors in the 6000 RPM range seem to have insufficient torque. The only off-the-shelf motor that could be identified was MAVILOR Model M010,000, with rated torque of 375 lb-in at a speed of 3000 RPM. Figures 11a and 11b are catalog pages describing this motor. The manufacturer also provides a driver module for the motor, capable of supplying 200 V DC, at 60 A. This driver has some digital control capability, so it may be feasible to design in a small single-board computer to handle all the loop control and frequency compensation.

When we know more about the number of sources that we will utilize in the rim of the rotating table, we will be able to formulate a more complete set of design requirements and do a more thorough study of the motor market before we can make a hardware selection.

(*) Contributed by Larry Coyle, SAO Central Engineering.

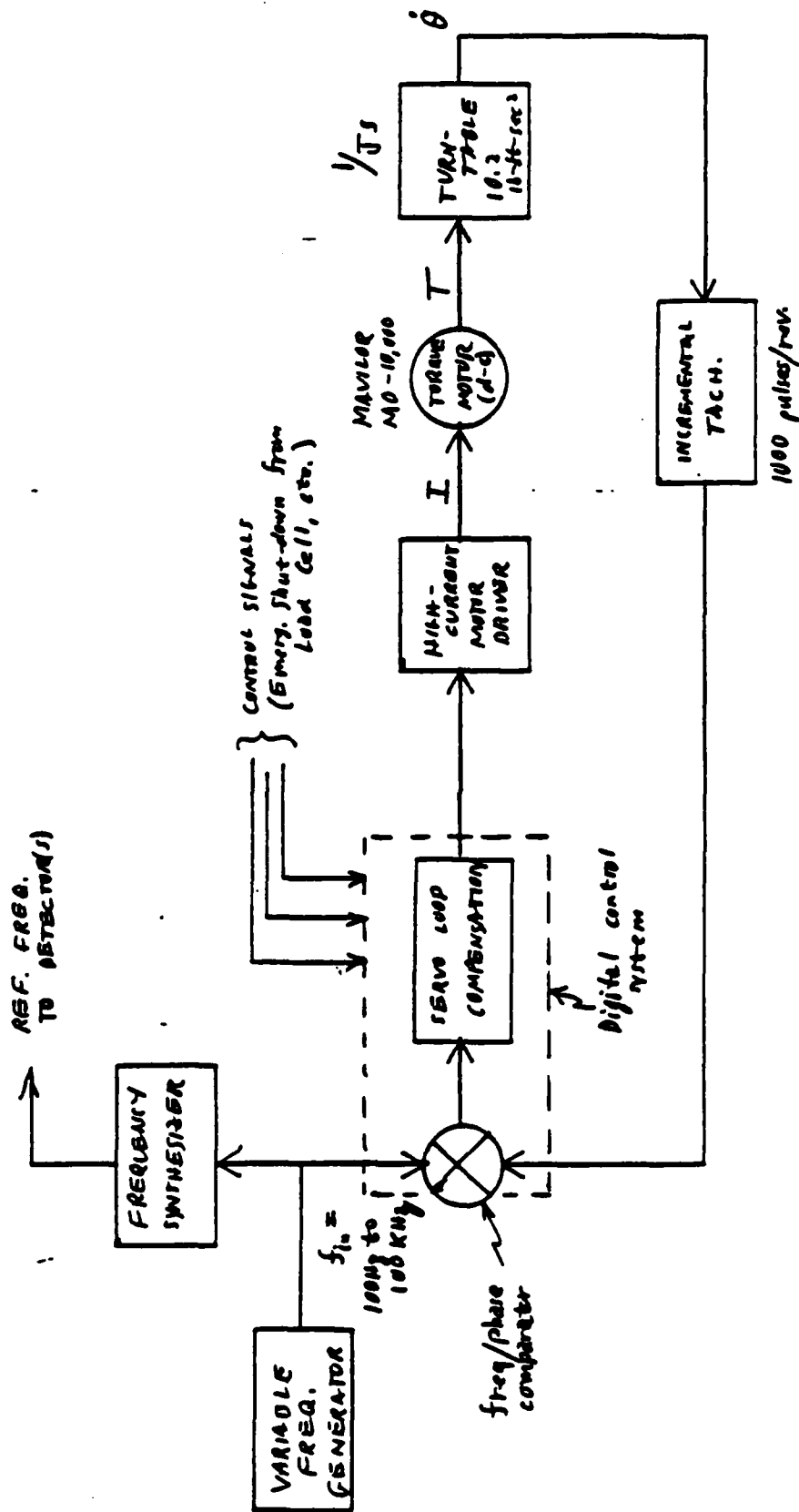


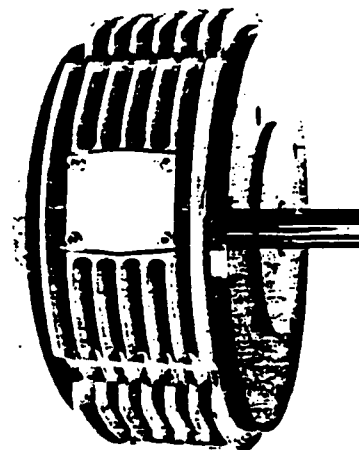
Figure 10 - Block Diagram, Rotating Table Concept, Servo-loop Control and compensation

MAVILOR Motors

Model MO10,000

Compact "flat-style" construction permits Mavilor Series 10,000 DC servo-motor to produce up to 18 hp in less than 8.8 in. of motor length. Rated for continuous duty at 3,000 rpm with a maximum speed of 3,500 rpm, they will run as slowly as 0.1 rpm under load without cogging, and with infinitely variable control of all speeds in between.

The ironless dish-shaped armature limits inertia to 1/10th that of a conventional motor and holds inductance to less than 200 μ H. Low inertia and high instantaneous torque make the Mavilor motor ideal for applications that require high acceleration and deceleration and fast reversals. Low inductance and planar commutation prevent arcing, extending brush life to over 10,000 hr. Copper wire windings embedded in epoxy form a strong, rigid armature for long life in demanding service.



Specifications

Model	MO10,000		
	Fan Cooled (105 cfm)		
Cont. Torque Rating	Tc	oz-in.	5897
		lb-in.	375
Output Power ¹	Po	hp	17.8
Rated Voltage ($\pm 5\%$)	Vr	Vdc	237
Rated Current	Ir	amps	81
Rated Speed	Nr	rpm	3000
Max. Power Rate	\dot{P}	kW/sec	2300
Efficiency		%	92
Peak Torque Rating ²	Tp	oz-in.	48144
		lb-in.	3009
Maximum Speed ³	Nm	rpm	3500
Torque Sensitivity ($\pm 5\%$)	Kt	oz in./amp	102
Volts Back EMF ($\pm 5\%$)	Ke	Volts/krpm	78
Friction Torque	Tf	oz-in.	42.6
Viscous Friction	Ff	oz-in./krpm	56.6
Terminal Resistance	Ra	ohms	.14
Armature Inductance	La	μ H	196
Moment of Inertia	Jm	oz-in.-sec ²	7.08
Mechanical Time Constant	tm	ms	20

Notes:

¹ With a 27.6 x 27.6 x 0.6 inch metal heat sink.

² For maximum 2.0 seconds at a 1% duty cycle.

³ Maximum speed in continuous service.

At no load can run at 4000 rpm for 5 minutes.

Continuous Service Characteristics

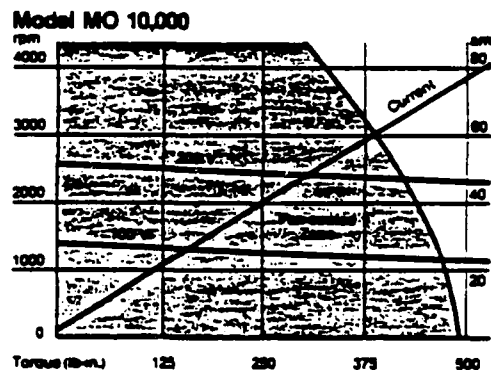
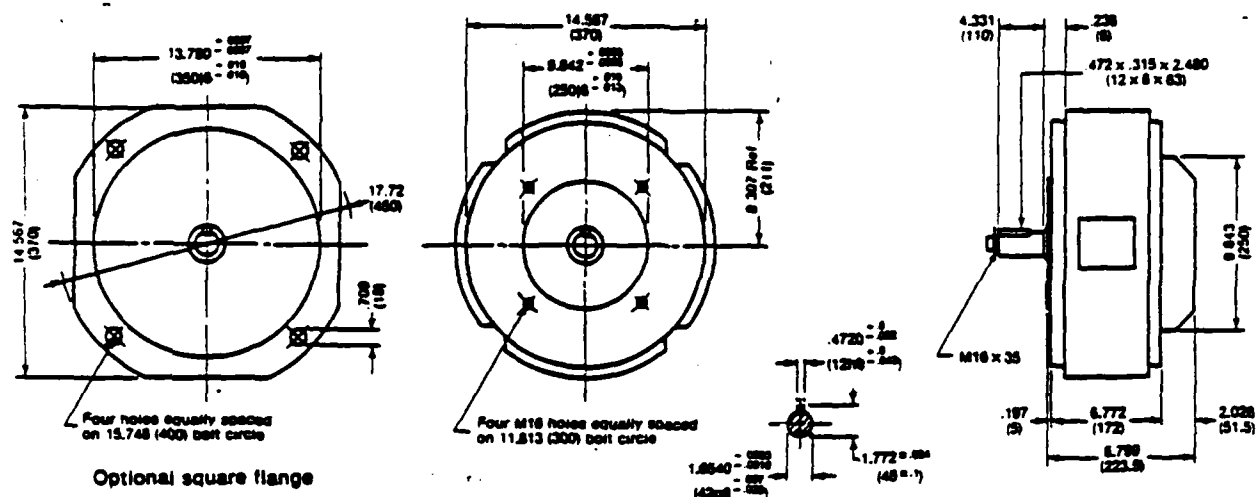
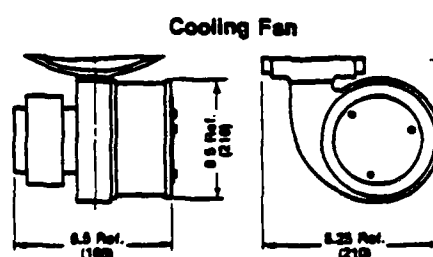


Figure 11 a
MAVILOR Motors, Model MO10,000
(Specifications)

Dimensions in inches (millimeters)

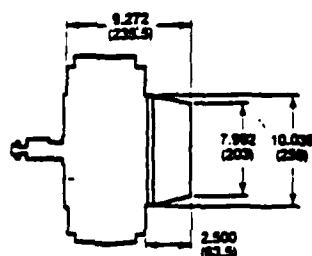


	Fan-cooled	All Models
Thermal time constant, sec		Radial load ¹ , lb 242
—armature to case	390	Axial load, lb 185
—case to ambient	2250	Weight, lb 187
Thermal resistance, °C/Watt		
—armature to case	.11	¹ Radial load applied
—case to ambient	.03	at midlength of shaft



Tachometer Option

This tachometer, specifically designed for integration into Mavilor Motors, has a very low inertia and low ripple assuring optimum performance.



Characteristics

Voltage constant, V/krpm	10
Voltage ripple, %	1.5
Voltage linearity at 3600 rpm, %	0.15
Bidirectional tolerance, %	0.10
Temperature coefficient, %/°C	-0.02
Inertia, oz-in.-sec ²	3.77×10^{-3}
Armature resistance, ohms	98.4
Inductance, mH	30
Current, mA	5
Maximum current, mA	30
Maximum velocity, rpm	6000
Armature weight, oz	4.8
Stator weight, oz	8.3

Accessories and Options

To fulfill broad design requirements, the Mavilor Motors can incorporate integrally mounted and industrially housed accessories:

- Tachometer
- Encoder
- Brake
- Gearhead

Other options include dual shaft, special shaft, hollow shaft, mounted speed reducer and brush monitoring.

INFRANOR Drive Systems

Infranor supplies complete servo systems comprising appropriate Mavilor motors with wide-band PWM amplifiers and other controls and components incorporating any available options and accessories appropriate to specific applications.

INFRANOR

285 Murphy Road • Hartford, CT 06114
Telephone: (203) 525-7743 • Telex: 96-6469

Figure 11 b
MAVILOR Motors, Model M010,000
(Dimensions and options)

3.3 Status Report on the development of the room-temperature gravity gradiometer at IFSI-CNR (*)

On October 13, 1987, the PMO attended a project review at IFSI-CNR, Frascati, Italy, and witnessed laboratory tests on the room-temperature gravity gradiometer developed by Prof. F. Fuligni for use at SAO and at Raytheon in the neutrino detector feasibility tests. The performance parameters were as follows:

- Mass 250 grams
- Temperature Room-temperature
- Resonance Freq. About 22 Hz without negative spring
" 15 " with " "
- Q factor $1.5 \cdot 10^3$
- Weakest detectable force $4 \cdot 10^{-7}$ dynes (without vibration abatement, and with 10^{-4} common mode rejection)

The gradiometer above is now undergoing modifications to become suitable for use in our program. We must add sapphire crystals to one of the two proof-masses and Figure 12 shows a possible way of doing this. The Figure illustrates how ten rods of sapphire could be embedded inside the aluminum block of the proof mass, with no parts of the rods being exposed outside the aluminum. This is to prevent electrostatic charging of the rods due to possible X-ray illumination. Each rod is a cylinder with 5.2 length and 1 cm diameter. The mounting of the rods into the proof-mass will be done in such a way that the Q of the mechanical oscillator will not be affected by this addition. The resonance frequency will be increased to 100 Hz.

At SAO, this gravity gradiometer will be mounted inside a 4°K cryostat for use in the feasibility tests. We expect that, by cooling the instrument to liquid Helium temperature, the Q will improve and become 10^4 , so that, with a 10^4 seconds integration time, we will be able to detect at threshold a force of $1.3 \cdot 10^{-9}$ dynes (DARPA requirement is to achieve the design goal of 10^{-8} dynes).

Figures 13 through 16 show several views of the instrument that was tested at IFSI-CNR on 10/13/87. Figure 13 depicts the gradiometer baseline, with the two sensing cells at its ends. Figure 14 shows the electronic subsystem with its cover removed; it contains the bridge, the feedback system, the preamplifier, low-pass filter, etc. In

(*) Contributed by M.D.Grossi, with inputs from F. Fuligni, IFSI-CNR.

the cryogenic version of the instrument, to be implemented at SAO, the electronics will be housed external to the cryostat. The reason is that the system noise is determined only by the temperature of the proof-mass, that is at 4°K . In fact, the sensor is a mechanical oscillator that works at resonance: under these conditions, the contribution of the preamplifier noise is negligible. This is also the reason why the utilization of quantum non-demolition approaches is not required here (QND is useful when the preamplifier noise predominates and we want to avoid the back-action on the oscillating mass). Figure 15 gives further details of the electronics package, while Figure 16 shows the specular quality of the surface finishing by high-precision machine tools.

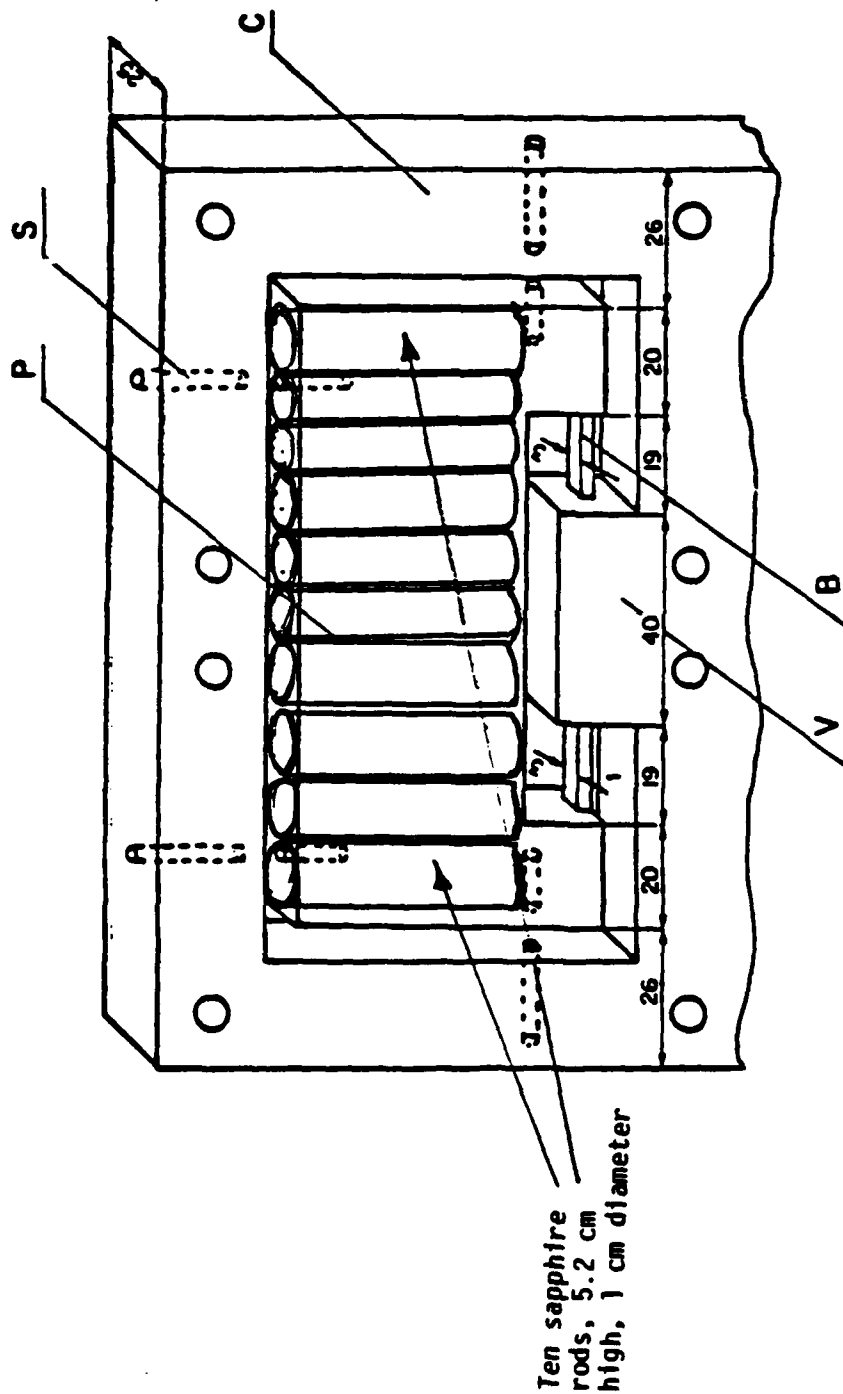


Figure 12
Modified single cell of the gravity gradiometer
to add the ten sapphire rods required for the
neutrino detection tests

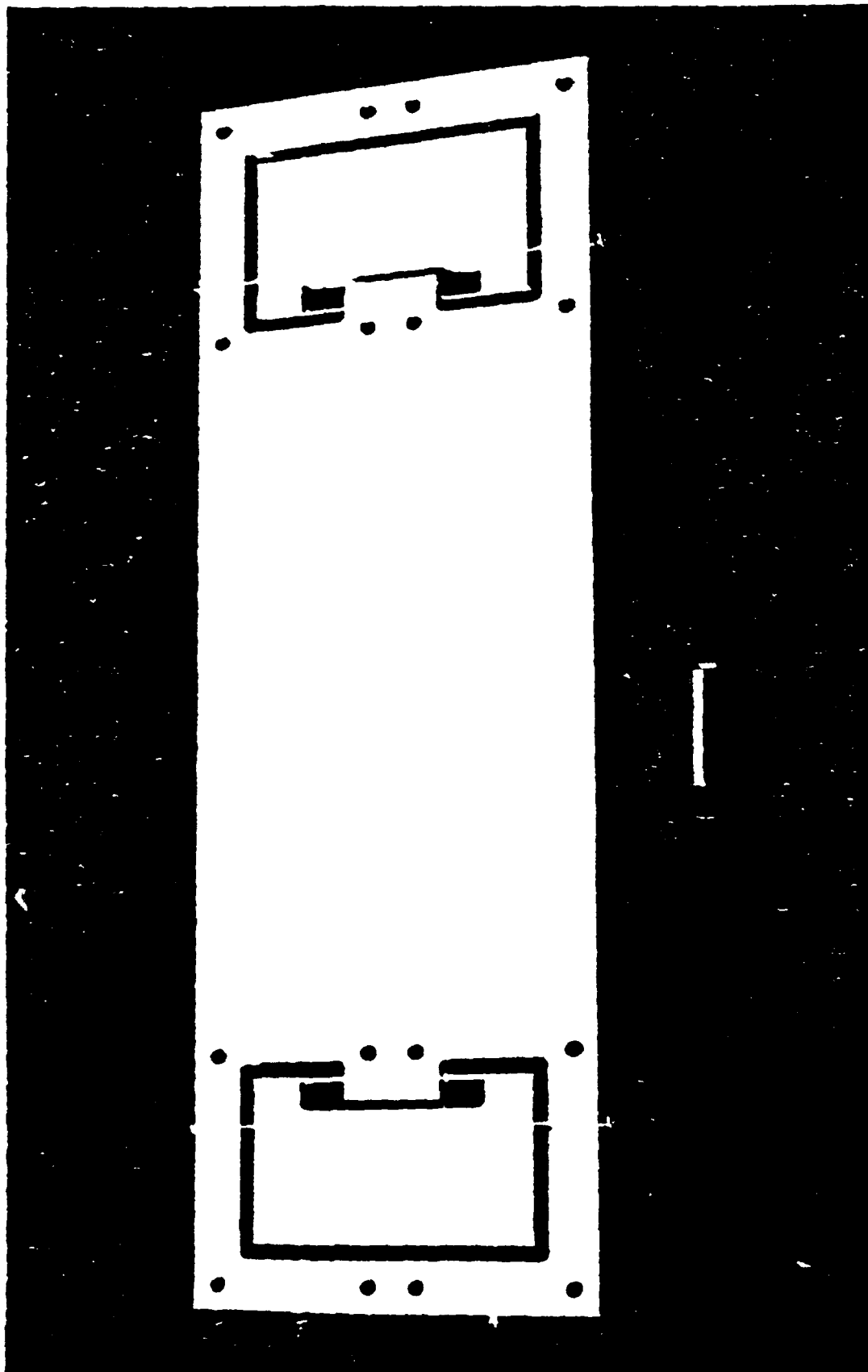


Figure 13 - The gradiometer baseline, with the sensing cells at its two ends

100-1100112

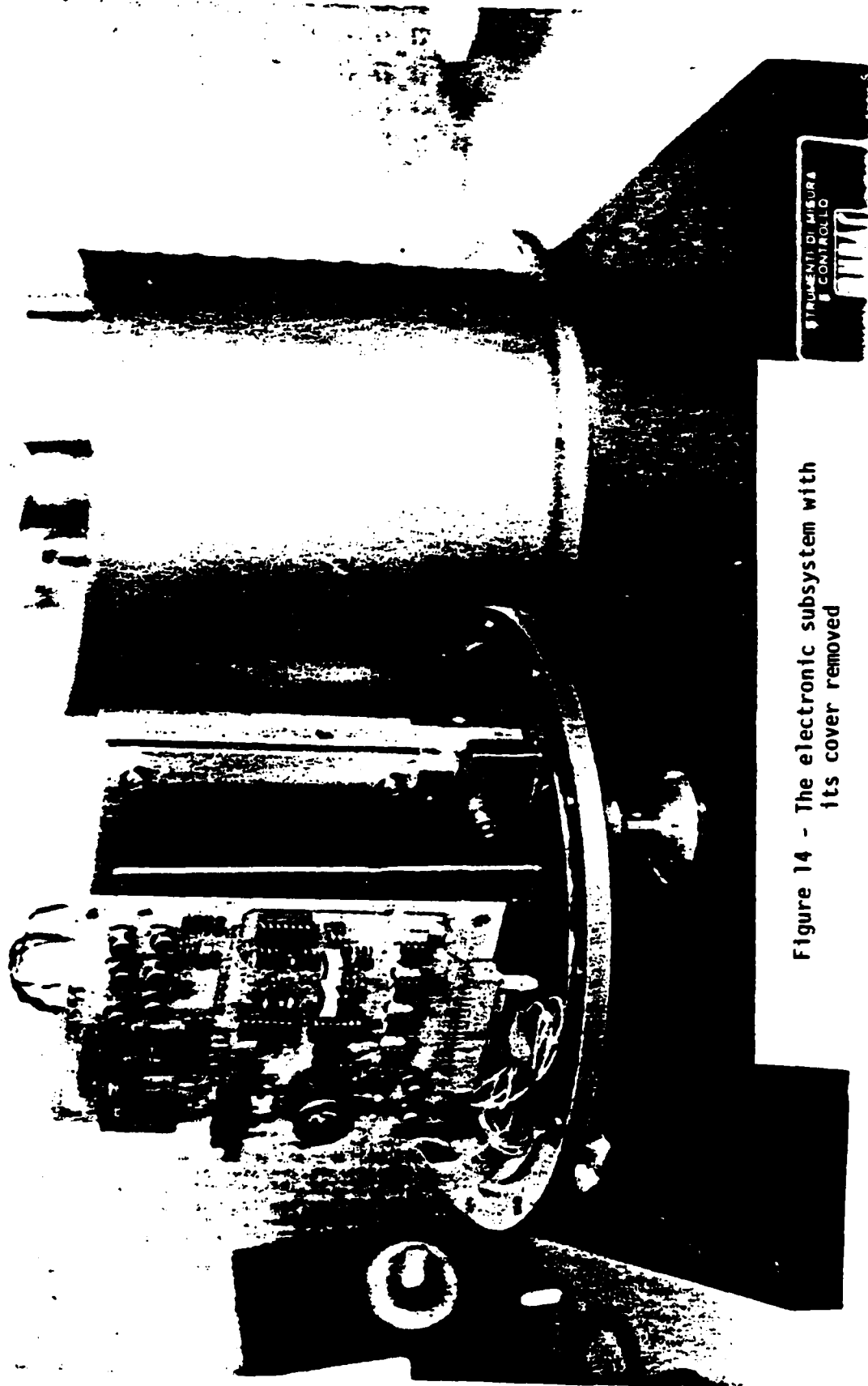


Figure 14 - The electronic subsystem with
its cover removed

SM-4951

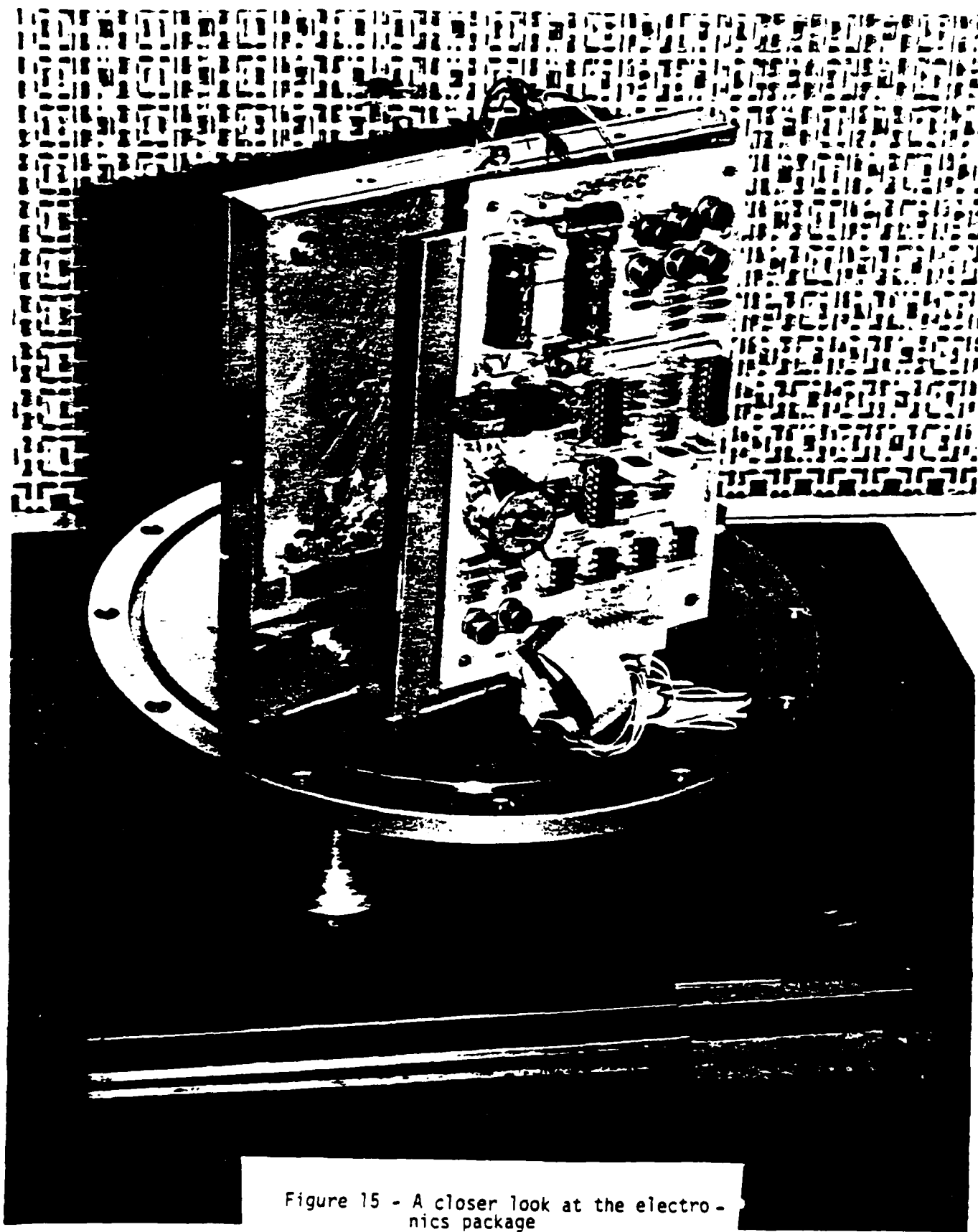


Figure 15 - A closer look at the electro-
nics package

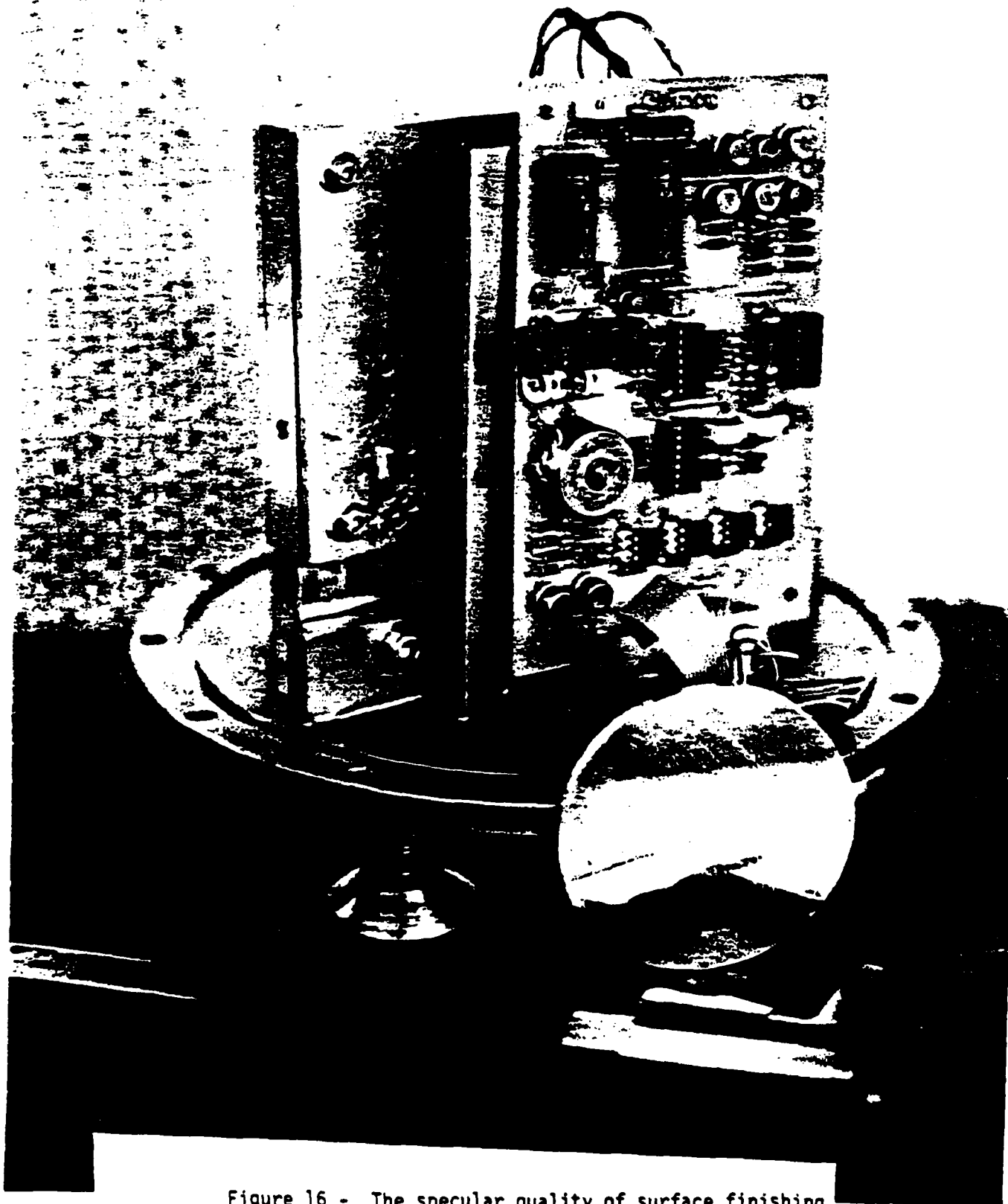


Figure 16 - The specular quality of surface finishing by high-precision machine tools is clearly visible in the picture

4. CONCLUSIONS AND RECOMMENDATIONS

The project has entered a hardware fabrication phase, where a significant coordination effort is necessary to integrate hardware from institutions as IFSI-CNR, IESS-CNR (both in Italy), University of Maryland, SAO, LLNL, Meyer Tool Mfg. Co., Union Carbide, Arnold Engineering, etc. We feel that we are closely tracking the critical paths, with the expectation of soon resolving two present causes of concern; the availability of the tritium source drawings (and the source itself), and selection of a NRC-licensed test site. Of great encouragement was witnessing the demonstration of the room-temperature gravity gradiometer in October, at IFSI-CNR, by Prof. Fuligni and Dr. Bordoni and to see the enthusiasm and the competence by Prof. Carelli and his assistants at IESS-CNR. They are preparing themselves to arrive at SAO with a SQUID that is at least two orders of magnitude better than any commercially available SQUID.

With some help from DARPA to break the administrative logjam to obtain the 3.5" tritium source, we are confident that we will recover the current one-month delay in this task.

SECOND CONTRACT

THIRD QUARTERLY REPORT

15 FEBRUARY 1988

EXPERIMENTAL TESTING OF CORPUSCULAR RADIATION DETECTORS

SUBMITTED TO

DEFENSE ADVANCED RESEARCH PROJECT AGENCY (DARPA)

DARPA ORDER #5271

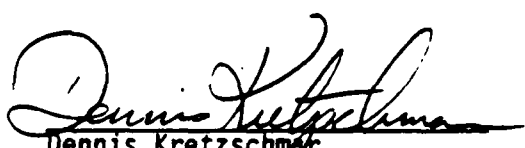
CONTRACT #F49620-87-C-0050

MONITORED BY AIR FORCE OFFICE OF SCIENTIFIC RESEARCH

(AFOSR)

DARPA PROGRAM DIRECTOR: US ARMY LT. COLONEL G. P. LASCHE', Ph.D

The views and conclusions contained in this document are those of the authors and should not be interpreted as necessarily representing the official policies, either expressed or implied, of the Defense Advanced Research Projects Agency or the U.S. Government.

Approved by: 
Dennis Kretzschmar
Program Manager, Raytheon Co.

RAYTHEON COMPANY
SUBMARINE SIGNAL DIVISION
PORTSMOUTH, RHODE ISLAND 02871

TABLE OF CONTENTS

<u>Section</u>	<u>Page</u>
Acknowledgements	ii
Executive Summary	iii
1.0 Introduction	1
2.0 Response of the Detector for Various Signal Inputs	4
3.0 Signal from 3 Rotating Sources vs. Wheel Diameter ...	28
4.0 Gravity Signal vs. Radius of the Rotating Wheel	29
5.0 Two Mass Model of the Neutrino Detector	31
6.0 Numerical Integration of the Two Mass Model	51
7.0 Conclusions and Recommendations	64

ACKNOWLEDGEMENTS

This quarterly report has been prepared by Mario D. Grossi, Principal Investigator, with inputs from all members of the program team. For each section, credit is given to the writer who contributed it.

EXECUTIVE SUMMARY

The program activity in the quarter reported herewith has been truly substantial and the definition of the feasibility experiment has progressed significantly. Also visible progress has been made in the construction of the sensors to be used in the experiment.

The torsion balance has been constructed at the University of Maryland and is now undergoing tests there, under the direction of Prof. Joe Weber, by him and his associates. This sensor is expected to be delivered to Raytheon, Portsmouth, Rhode Island, sometime during April 1988.

The cryogenic force sensor is also under construction at IFSI-CNR, Italy and the sapphire rods have been already mounted in one of the proof masses. This sensor is expected to arrive in Portsmouth, R.I. in mid June 1988, after system tests at IFSI-CNR inside a 4°K cryostat, to be procured by IFSI-CNR in Europe, and to be then shipped to Portsmouth, R.I., together with the 2-cell force sensor.

Concerning the tuning fork, that Prof. Weber is constructing under a direct contract from DARPA, we understand that it is in advanced stage of construction. Raytheon is preparing the test area, ready to accommodate also the tuning fork, disregard of the final disposition by DARPA of this sensor.

Raytheon is also setting-up, with in-house funds, a SQUID magnetometer to be added to the array of sensor in the test area, and to be used to fulfill the assignment consisting of measurement three basic parameters of the magnetic interaction sensor (highest achievable relative permeability in the interaction target, largest achievable pick-up area, and lowest achievable intrinsic noise density when the SQUID is loaded by the large-mass, high-permeability target).

Should DARPA, in early May, provide Raytheon with a suitable tritium source (now expected to be of cylindrical shape), Raytheon would be able to start experimenting in mid May 1988, with the following set-up:

- (a) Torsion Balance, with the cylindrical source mounted on a very simple, 1 RPM rotating table, equipped with an optical sensor of its angular position and rotational speed. For this initial test, Raytheon needs a tritium-filled cylinder and 2 dummy cylinders. We understand that these three items would be available.
- (b) Tuning Fork, with the cylindrical source kept in a fixed position, mounted on a pedestal (replaceable with a dummy, in verification tests), to be used in association with a sapphire-crystal-equipped, high-speed rotating shutter (to be built by Prof. Weber under direct contract from DARPA), interposed between the tritium source and the tuning fork, in order to function as the alleged modulator of the neutrino beam.

In mid June 1988, Raytheon would add to the two sensors in items (a) and (b) above, the cryogenic force sensor. This could be tested just by replacing the tuning fork with it, leaving everything else unchanged.

In mid July, then, Raytheon is expected to receive from SAO the high-speed (2000 RPM) rotating table, with air bearing and vacuum enclosure (subject to funding authorization by DARPA for the added scope), to be equipped with three spherical sources (3.5" spheres, or equivalent), and with 30 dummies for gravity gradient signal minimization. The rotating table will make it possible to test the cryogenic force sensor, as well as the tuning fork, by the variable neutrino flux, due to distance modulation. Initial funding for the construction of this high-speed rotating table is about to be awarded to SAO by Raytheon, while the full added-scope contract is still under negotiation, at this time.

Raytheon plans to carry out the feasibility experiments, inclusive of Weber verification tests, in its Laboratories in Portsmouth, R.I. The specific laboratory area is about to be selected among three possibilities. We are carrying out measurements, by use of accelerometers, of the intensity of mechanical vibrations on the floor of each candidate area and we will select the quietest location. We have also initiated discussions with the Rhode Island Nuclear Regulatory Agency, with the objective of obtaining from them the license to handle radioactive materials. Raytheon fully expects that this license will be obtained in time for the mid-May tests.

Still of some concern is the fact that Raytheon has not yet received from LLNL the needed information on the size, mass and precise characteristics of the tritium sources. This lack of information is preventing SAO from completing the design of the rotating table. We are proceeding here at a risk, with making assumptions that might not be confirmed, once that the sources arrive, and that might require extra work.

On the analytical side, we have completed, during the report period, the analysis of of the response of the cryogenic force sensor to various solicitations produced by the rotating table and its distribution of sources and dummies. This quarterly report is totally devoted to the illustration of the results of this analysis.

1.0 INTRODUCTION

We devote this quarterly report to the study performed at SAO by David A. Arnold on the subject of the performance of the high-speed rotating table (also called the rotating wheel), and concerning the design of the experiment to be carried out with the cryogenic force sensor installed in the vicinity of the wheel, near its edge.

In the last quarterly report, analyses were presented that gave the shape of the signal to be expected from a set of n sources symmetrically placed on the rotating wheel. The present report presents the results of analyses of the detector to various signal inputs.

The detector has been modelled both as a single oscillator and as a compound system, consisting of both a detector and a case which is free to move. The motion of the case is particularly significant for gravitational forces. Both analytic and numerical solutions have been obtained for the one and two mass models. Studies have also been done of the influence of the wheel diameter on both neutrino and gravity signals.

Several software codes have been worked out and have been used in connection with plotting subroutines. The results are displayed in Figures 1 through 20. The captions of these figures are as follows:

- Figure 1. Resonant response with 1 percent of critical damping.
- Figure 2. Resonant response with critical damping.
- Figure 3. Resonant response with no damping.
- Figure 4. Response with the driving frequency 1.5 times the resonant frequency.

- Figure 5. Response to a single rotating source with a fast risetime detector.
- Figure 6. Resonant response to a single rotating source with no damping.
- Figure 7. Resonant response to a sinusoidal input with amplitude .5.
- Figure 8. Resonant response with 2 sources.
- Figure 9. Resonant response with 3 sources.
- Figure 10. Resonant response with 4 sources.
- Figure 11. Resonant response with 5 sources.
- Figure 12. Resonant response to a cosine driving force of amplitude .5.
- Figure 13. Response with a driving frequency 1.5 times the resonant frequency and $z_0 = -.8$.
- Figure 14. Resonant response with 10 percent of critical damping.
- Figure 15. Response with $\omega = .5\omega_0$ and $z_0 = 4/3$.
- Figure 16. In text.
- Figure 17. Resonance curve for mass 2 with $F_1 = 0$, and $F_2 = m_2$.
 - a. Real part of A_2 vs. frequency.
 - b. Imaginary part of A_2 .
 - c. Magnitude of A_2 .
 - d. Phase of A_2 .
- Figure 18. Resonance curve for mass 2 with $F_1 = m_1$, and $F_2 = .86 m_2$.
 - a. Real part of A_2 vs. frequency.
 - b. Imaginary part of A_2 .
 - c. Magnitude of A_2 .
 - d. Phase of A_2 .

- Figure 19. Resonance curve for mass 2 with $F_1 = m_1$, and $F_2 = m_2$.
- Real part of A_2 vs. frequency.
 - Imaginary part of A_2 .
 - Magnitude of A_2 (638.5 to 639.0 hertz).
 - Magnitude of A_2 (637.8 to 639.8 hertz).
 - Phase of A_2 .

- Figure 20. Response of the system with equal masses, equal driving forces, and about 10% of critical damping.
- Position of mass 1 vs. time.
 - Position of mass 2 vs. time.

2.0 RESPONSE OF THE DETECTOR FOR VARIOUS SIGNAL INPUTS*

The neutrino flux from the rotating tritium sources is incident on a detector which is a high Q mechanical oscillator. The frequency of the oscillator is tuned to that of the input signal. The motion of the detector is described by the equation

$$m\ddot{x} + b\dot{x} + kx = f(t) \quad (1)$$

A program called *DETECT* has been written to solve equation (1) numerically using the Gear integration technique. The Gear integrator consists of a subroutine *DIFSUB* which calls the routines *PEDERV*, *SOLVE*, and *DIFFUN*. The last routine *DIFFUN* must be supplied by the user and computes the rate of change of the state vector as a function of time and the current values of the state vector. For the case of equation (1) the state vector consists of the variables x and \dot{x} . The rate of change of x is \dot{x} and the rate of change of \dot{x} is

$$\ddot{x} = \frac{1}{m} (f(t) - b\dot{x} - kx) \quad (2)$$

Equation (1) can be solved analytically if the function $f(t)$ is sinusoidal. Let us consider the case

$$f(t) = Fe^{i\omega t} \quad (3)$$

We can assume a solution of the form

*Contributed by David A. Arnold, SAO

$$z = Ae^{i\omega t} \quad (4)$$

which gives the characteristic equation

$$-A\omega^2 m + Ai\omega b + Ak = F \quad (5)$$

Solving equation (5) gives

$$A = \frac{F}{-m\omega^2 + i\omega b + k} \quad (6)$$

If there is no damping so that $b = 0$, we have the amplitude given by

$$A = \frac{F}{-m\omega^2 + k} \quad (7)$$

The amplitude goes to infinity for

$$\omega^2 = \frac{k}{m} = \omega_0^2 \quad (8)$$

where ω_0 is the resonant frequency. For very high frequencies k can be neglected and we have a free oscillation given by

$$A = -\frac{F}{m\omega^2} \quad (9)$$

For very low frequencies, $m\omega^2$ can be neglected giving

$$A = \frac{F}{k} \quad (10)$$

At the resonance frequency given by equation (8), equation (6) becomes

$$A = \frac{F}{i\omega b} \quad (11)$$

In this case the response is 90° out of phase with the driving force. In equation (9) the response is 180° out of phase, and in equation (10) the response is in phase. In addition to the forced oscillation given by equation (4) we can have an oscillation at the natural frequency given by

$$x = Be^{i\omega_b t} \quad (12)$$

In the case of small damping, ω_b is given by equation (8). In the presence of damping the motion given by equation (12) will decay with time if there is no continuing excitation of this frequency.

In the case of a few sources on a rotating wheel the function $f(t)$ is not a perfect sinusoid. As the number of sources is increased, the driving force becomes more sinusoidal but the amplitude becomes smaller since the distribution around the wheel becomes more uniform.

Various test runs have been done with program *DETECT* to verify that the computer code gives the correct answer to cases that can be solved analytically. In the initial version, the values of m , b , k and x_0 are input parameters. The damping b is specified as a fraction of the critical damping coefficient given by

$$b_c = 2 \sqrt{mk} \quad (13)$$

A test run with $m = k = x_0 = 1$ and $b = 0$ gave a sinusoidal oscillation with period 2π . With $m = k = x_0 = 1$ and $b = b_c$, the motion is a decaying exponential. The next test run was done with $m = k = 1$, $b = .01 b_c$, $x_0 = 0$, and

$$f(t) = F \sin \omega_b t \quad (14)$$

with $F = 1$, and $\omega_b = 1$ as computed from equation (8). The response as a function of time is shown in Figure 1. The minimums of the curve occur at $t = 2\pi, 4\pi, 6\pi$, etc. The zero crossings occur a quarter of a cycle later when equation (14) has its maximum value. This is the phasing required to pump the oscillation in the most effective manner.

The next run was done with $m = 1$, $b = k = x_0 = 0$, and $F = 1$ in equation (14). The x coordinate increased monotonically with the velocity oscillating between 0 and 2. In equation (9) the amplitude is 180° out of phase with the driving force. The value of \dot{x}_0 has been added to the input parameters and the run repeated with $\dot{x}_0 = -1$. This produced the results given by equation (9) with $A = -1$.

The next test run has been done with $m = k = F = 1$, $x_0 = \dot{x}_0 = 0$, and $b = b_c = 2$. Using these values in equation (6) with $\omega = 1$ gives

$$A = \frac{1}{2i} \quad (15)$$

Figure 2 shows the response as a function of time. The minimums of the curve are at 2π , 4π , 6π etc. and the amplitude after the initial transient is .5 in agreement with equation (15). The phasing is the same as in Figure 1. Pumping the oscillator at the resonant frequency results in a buildup of the response until the damping forces equal the pumping forces. From equation (4) we have the velocity given by

$$\dot{x} = A i \omega e^{i \omega t} \quad (16)$$

With A given by (15) and $\omega = 1$, we have $\dot{x} = 1/2$. Since $b = 2$, the damping force is $b\dot{x} = 2 \times .5 = 1$, which is equal to the driving force $F = 1$.

In the next run, the damping b is set to zero and the other parameters are kept the same ($m = k = F = \omega = 1$, and $x_0 = \dot{x}_0 = 0$). The results are shown in Figure 3. The amplitude is a little larger than in Figure 1 which had $b = .01$.

All the runs so far have had $\omega = \omega_0$. If ω is not equal to ω_0 then it is possible to have components at both frequencies. The parameter ω has been added to the input and set equal to 1.5 for the next run. The other parameters are the same and the natural frequency is $\omega_0 = 1$. The results are shown in Figure 4. The beats between ω and ω_0 can be seen. Since b is zero, the oscillation at frequency ω_0 is undamped.

At this point some tests were done to see if the integration speed could be increased by decreasing the accuracy requested from the numerical integrator. Reducing the accuracy from 13 to 6 decimal places increased the stepsize from .036 seconds to .28 seconds. With 9 decimal places the stepsize was .1 seconds.

With the test runs completed using a sinusoidal driving force for the detector, the program has been modified to use the signal input from sources on a rotating wheel. The mathematical part of program *FLYWHEEL* has been put into a subroutine called *WHEEL* which has been added to program *DETECT*. An input variable specifies the number of sources to be placed symmetrically around the wheel. As a first test of the program, a run has been done with $m = .0001$, $b = .1$, $k = \omega = 1$, $x_0 = \dot{x}_0 = 0$, one source, and the constant F in the equation

$$FLUX = F/r^2 \quad (17)$$

set equal to 625. The sources are rotating at a 45 cm radius with the detector at 70 cm from the center of the wheel. This gives 25 cm for the closest approach and 115 cm for the furthest distance. From equation (17) the corresponding fluxes are 1.00000 and .04726. The natural frequency ω_b from equation (8) with $k = 1$ and $m = .0001$ is 100 hertz. This gives a fast risetime for the detector so that it will record the instantaneous value of the flux for test purposes. Figure 5 shows the response of the detector to the rotating source. The maximum response is 1.00 and the minimum is .04726 in agreement with the calculated values of the flux. The curve shape looks the same as curve shapes generated by program *FLYWHEEL*.

In the actual experiment the rotating wheel will spin so as to produce a signal having the same frequency as the ω_b of the detector. The next run has been done with 1 source, and $k = m = 1$ to produce a natural frequency $\omega_b = 1$. The angular velocity of the wheel is $\omega = 1$, and carries one source. The damping b is set to zero. Figure 6 shows the response of the detector. The input signal is always positive so that the mean position has a slight positive base.

In order to compare the response of the detector to a rotating source with the response to a sinusoid of the same amplitude, a run has been done with a sinusoid of amplitude $F = .5$. The peak to peak driving force is 1 with the signal varying between $-.5$ and $+.5$. For the case of a single rotating source the peak to peak amplitude is $.95274$ and the signal varies between $.04726$ and 1.00000 . Figure 7 shows the response to a sinusoid of amplitude $F = .5$.

A series of runs have been done with 2, 3, 4, and 5 sources uniformly spaced around the wheel. The rotation frequency of the wheel is $1/n$ where n is the number of sources. The response of the detector is shown in Figures 8, 9, 10 and 11 respectively.

The phasing of the rotation of the wheel is such that the first source is at its closest approach to the detector at $t = 0$, thereby giving a maximum in the signal at $t = 0$. This is 90° out of phase with the signal given by equation (14). For the sake of easier comparison of results the program has been changed to use the equation

$$f(t) = F \sin (\omega_b t + \delta) \quad (18)$$

where δ is a phase angle. Setting $\delta = 90^\circ$ causes $f(t)$ to have a maximum at $t = 0$ the same as the signal from the rotating wheel. A run has been done to give the response of the detector using $F = .5$, $\delta = 90^\circ$, $m = k = \omega = 1$, and $x_0 = \dot{x}_0 = 0$. The result is shown in Figure 12.

Table 1 gives a summary of the response of the detector to various types of signals as shown in Figures 6 through 12.

Table 1

Figure	Signal	Time	$z(t)$	Δz
6	1 source	45.586	+5.895	11.687
		48.728	-5.792	
7	.5sin ωt	40.840	+10.210	21.206
		43.982	-10.996	
		47.124	+11.781	
8	2 sources	45.609	+8.390	16.448
		48.750	-8.058	
9	3 sources	45.635	+8.975	17.290
		48.774	-8.315	
10	4 sources	45.668	+8.541	16.021
		48.805	-7.480	
11	5 sources	45.715	7.670	13.836
		48.848	-6.166	
12	.5cos ωt	45.574	+11.391	23.567
		48.715	-12.176	

Table 1. Response of the detector to various input signals.

For all of the cases except Figure 7, there is a minimum at about 45.6 seconds and a maximum at around 48.8 seconds. The last column lists the difference between the peaks. Figures 7 and 12 which are sinusoidal signals give the largest response. For the case of n sources on a rotating wheel, the signal is more sinusoidal as the number of sources is increased, but the difference between the peaks of the driving signal decreases as the pulses from individual sources start to overlap. The largest output response in Table 1 occurs for 3 rotating sources.

As a measure of the efficiency of the various types of driving signals the ratio of the detector response to the signal amplitude has been computed for each of the signal types listed in Table 1 (except for Figure 7 which is difficult to compare because the phase is different). Table 2 lists the type of

source, the minimum value of the signal F_{\min} , the maximum value F_{\max} , the peak to peak amplitude ΔF , the peak to peak output response Δz taken from Table 1, the ratio of the output to the input $\Delta z/\Delta F$, and the efficiency relative to $.5 \cos \omega t$ computed by dividing the values of $\Delta z/\Delta F$ by the last entry in that column.

Table 2

<i>Signal</i>	F_{\min}	F_{\max}	ΔF	Δz	$\frac{\Delta z}{\Delta F}$	<i>Efficiency</i>
1 source	.047	1.000	.953	11.687	12.266	.52
2 sources	.152	1.047	.895	16.448	18.368	.78
3 sources	.303	1.114	.811	17.290	21.317	.90
4 sources	.494	1.199	.705	16.021	22.708	.96
5 sources	.710	1.300	.590	13.836	23.428	.994
.5cos ωt	-.500	.500	1.000	23.567	23.567	1.000

Table 2. Efficiency of various input signals in driving the detector

The detector response has been calculated after a fixed interval of time, since there is a resonant buildup in the amplitude. Since no damping was used, the buildup would continue indefinitely. Equation (6) gives the amplitude for any frequency and with damping in the system. Some runs have been done to test the program under other conditions. For example, for $m = k = \omega_b = F = 1$, $b = 0$, and $\omega = 1.5$ equation (6) gives $A = -.8$. The detector is being driven above its resonant frequency, and the response is 180° out of phase with the driving force. A run has been done with $z_0 = -.8$ and $\dot{z}_0 = 0$. The results are shown in Figure

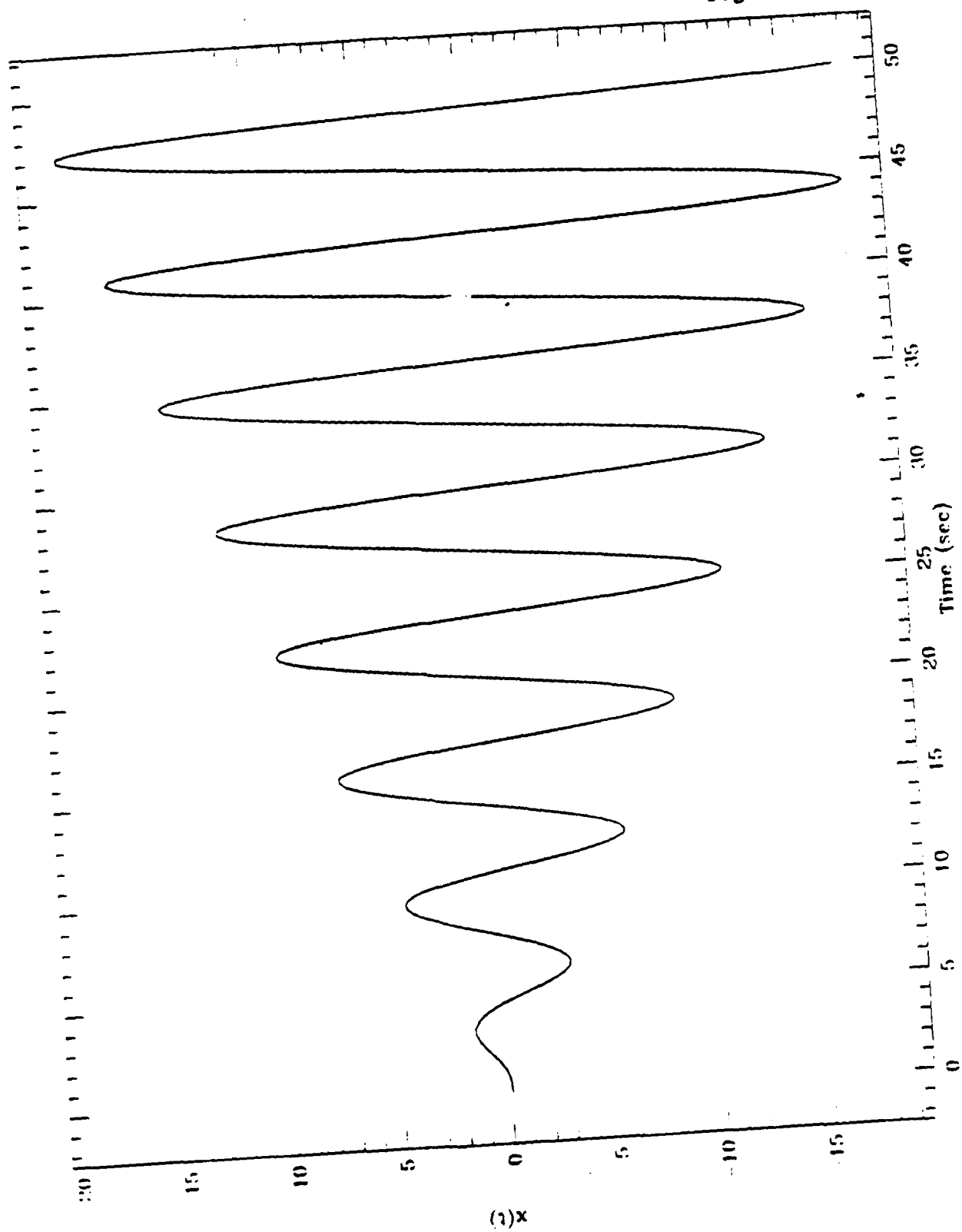


Figure 1.

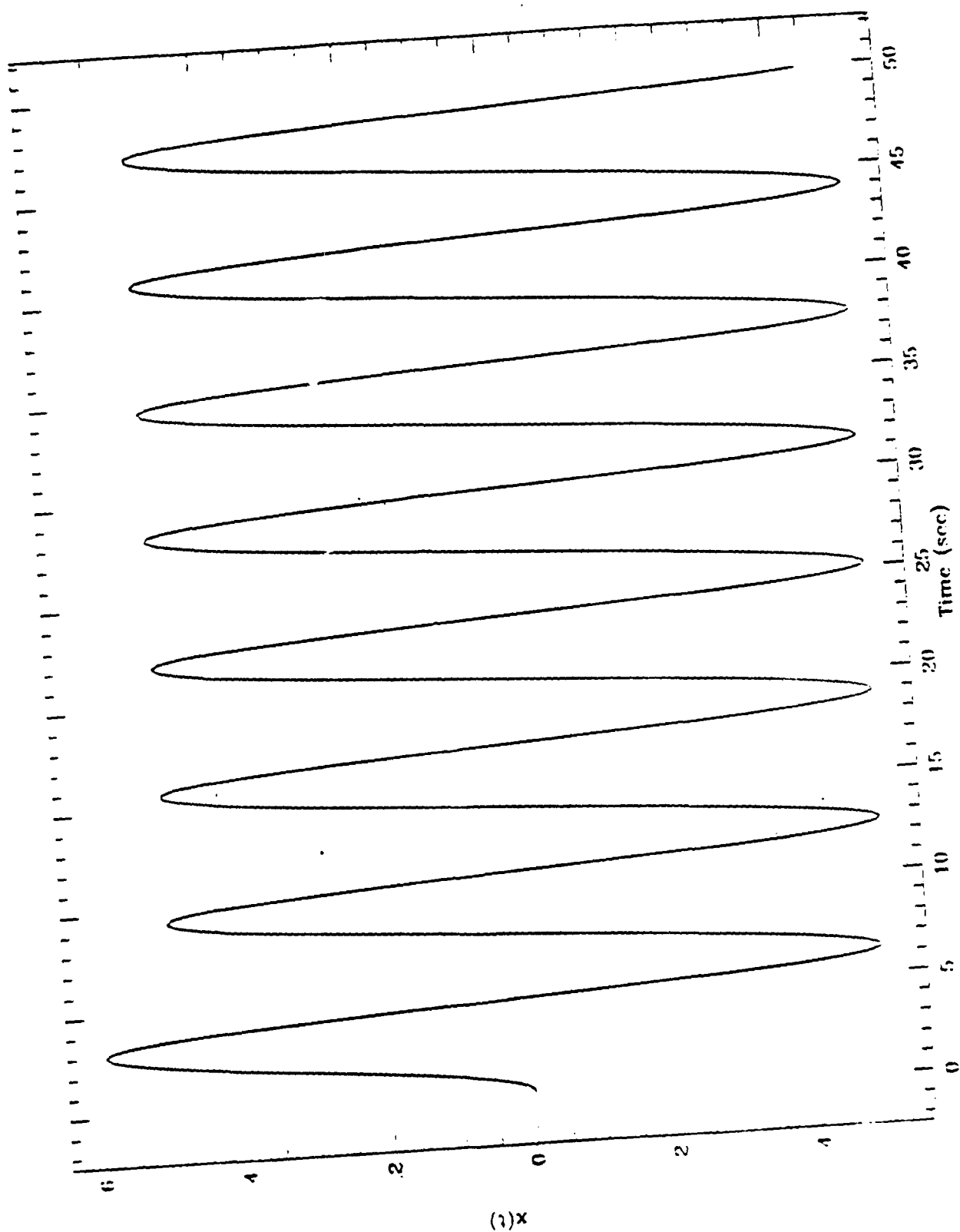


Figure 2.

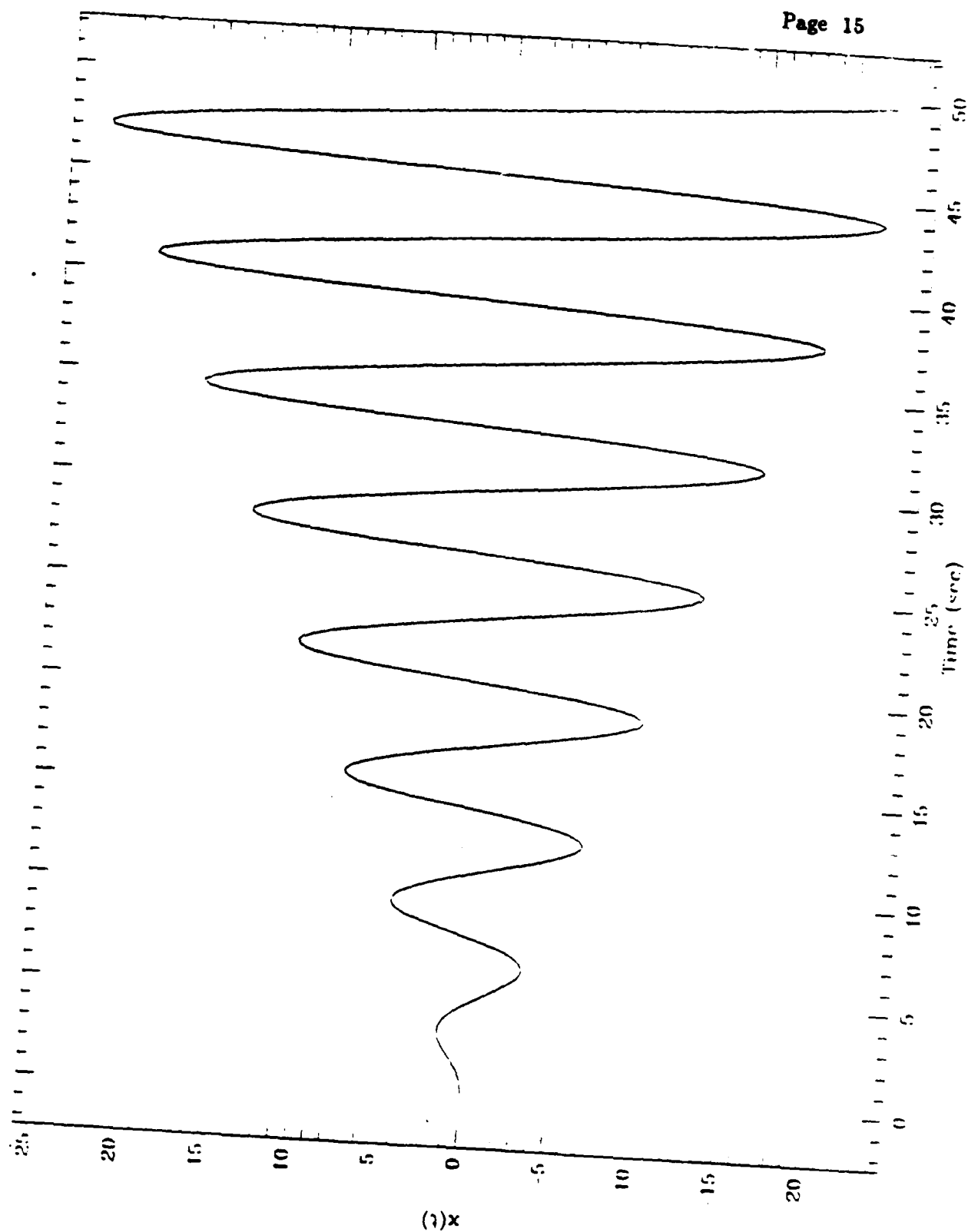


Figure 3.

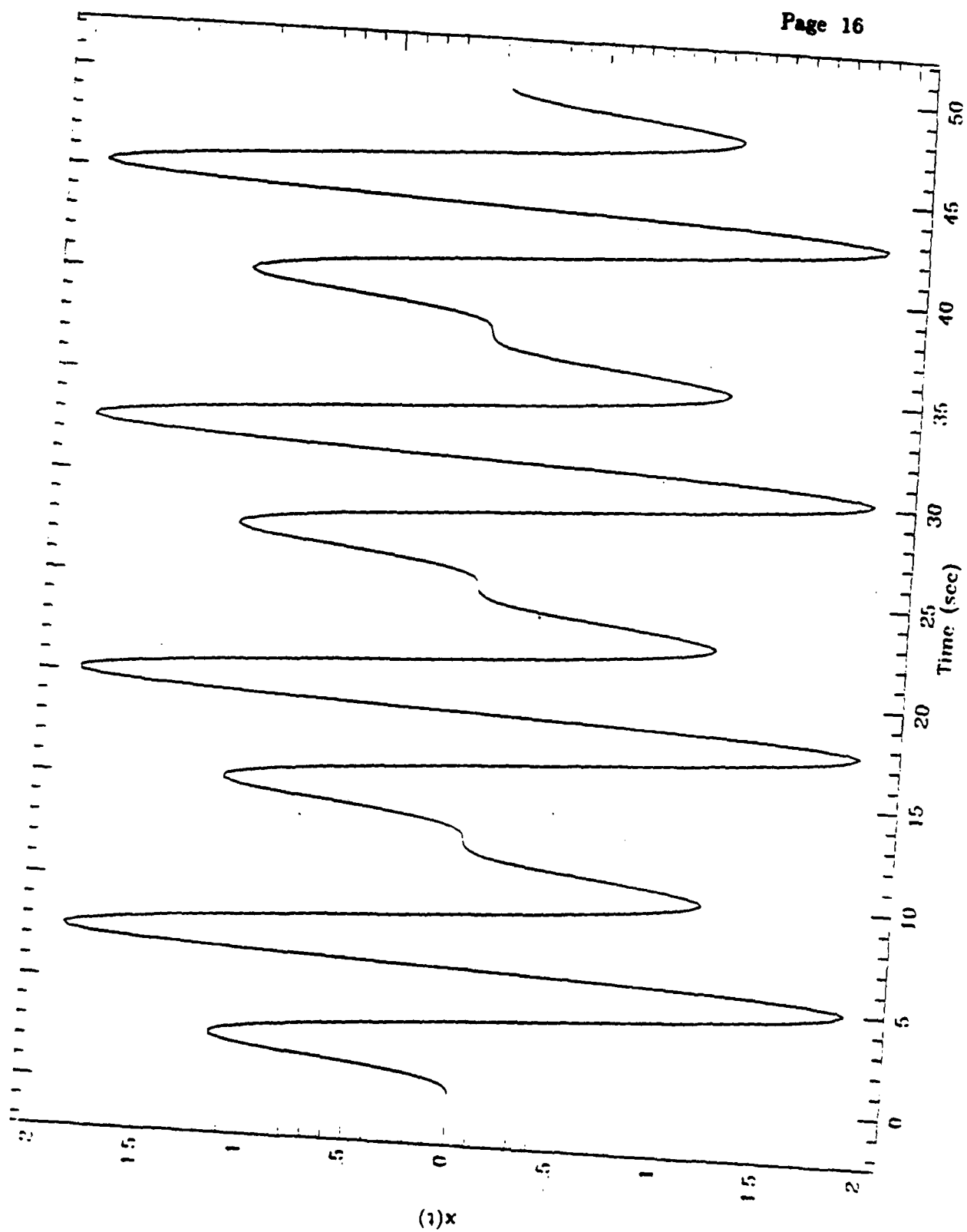


Figure 4.

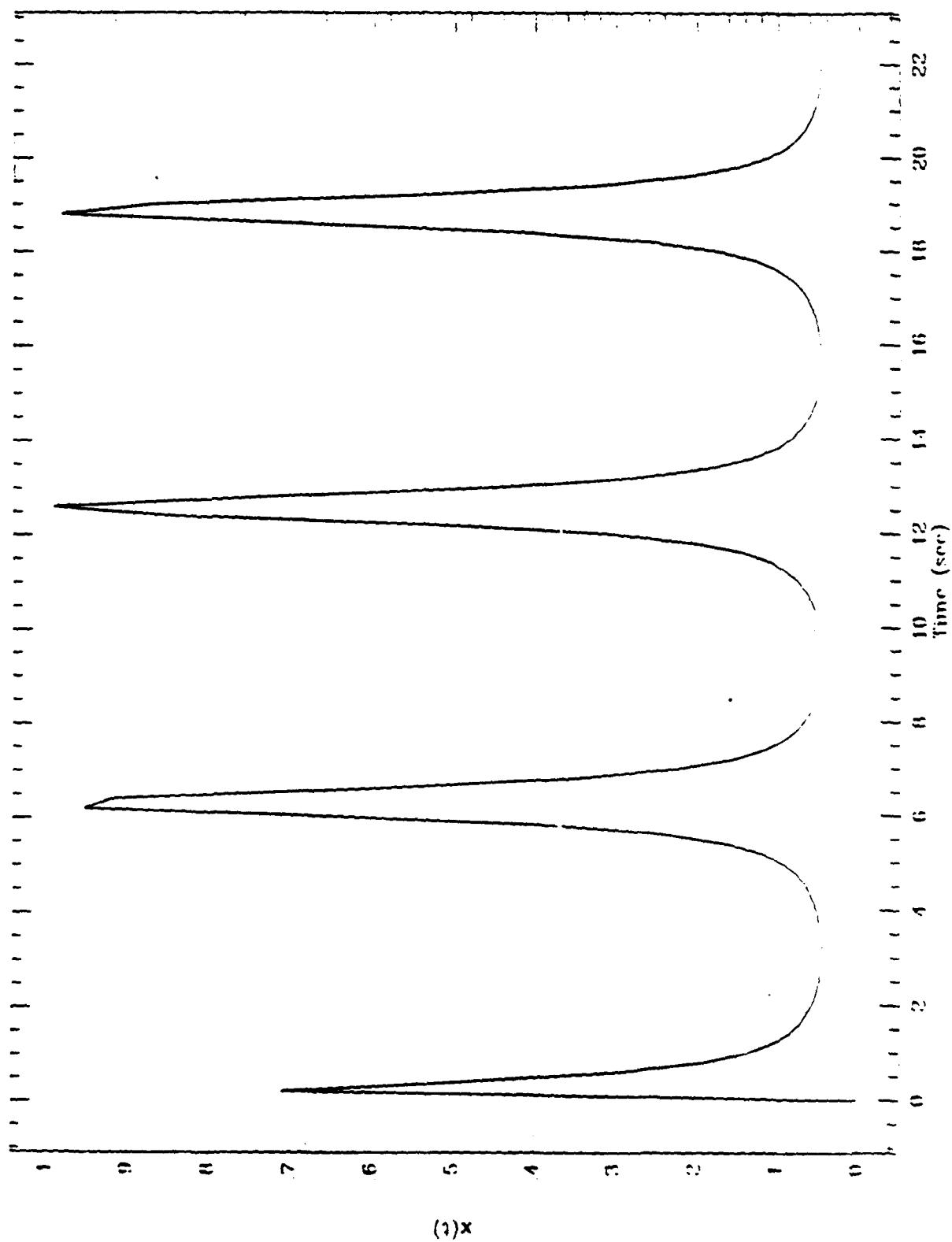


Figure 5.

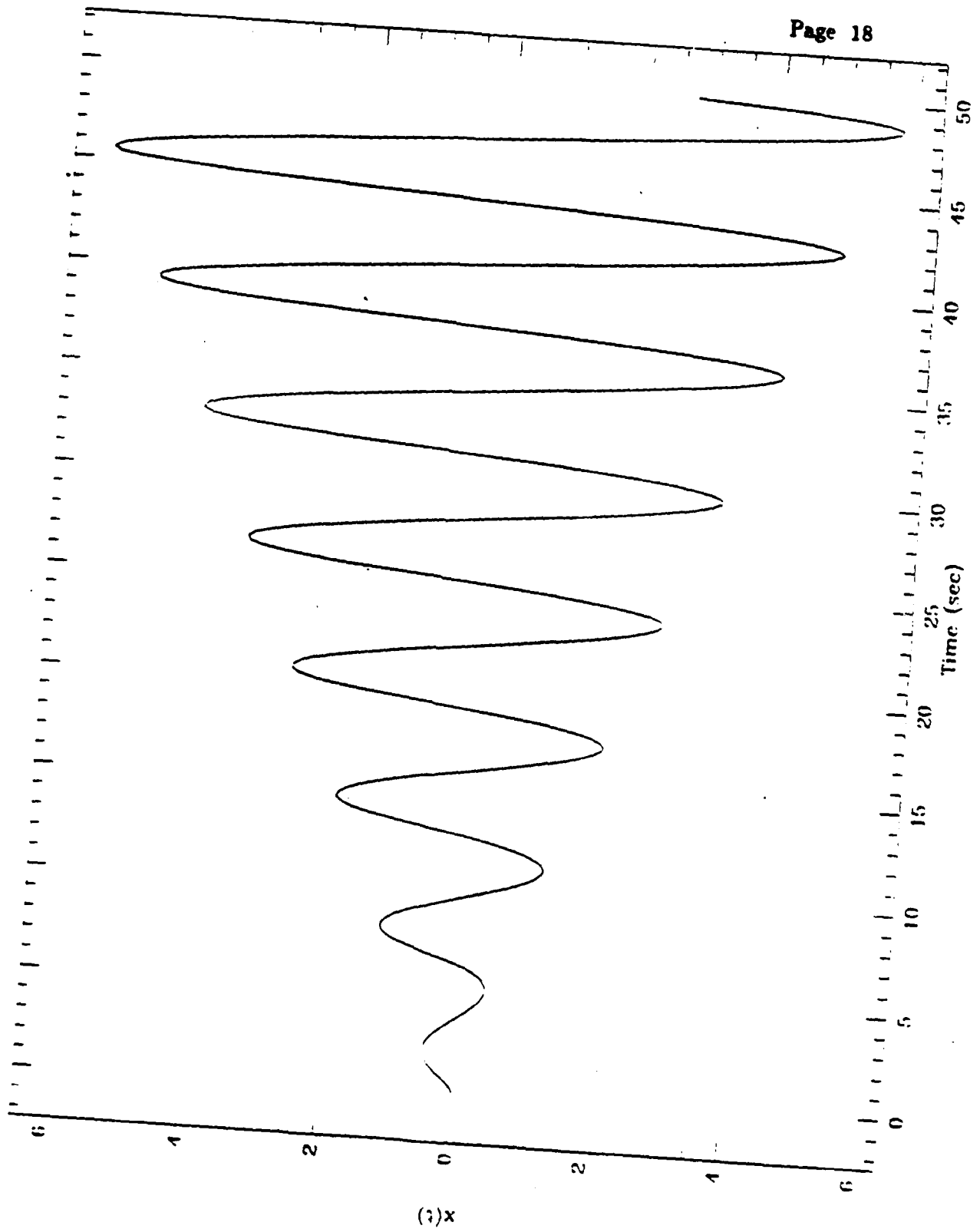


Figure 6.

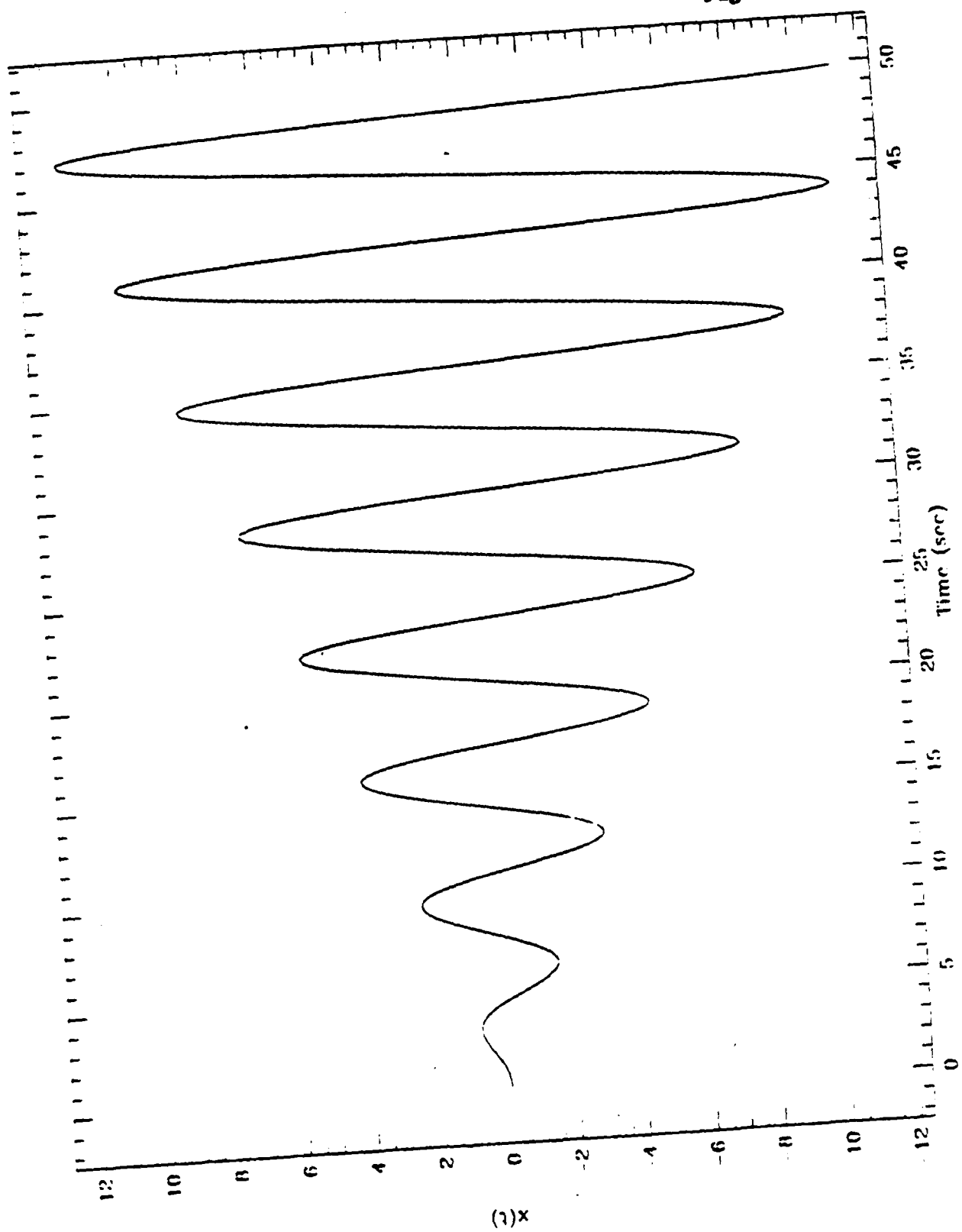


Figure 7.

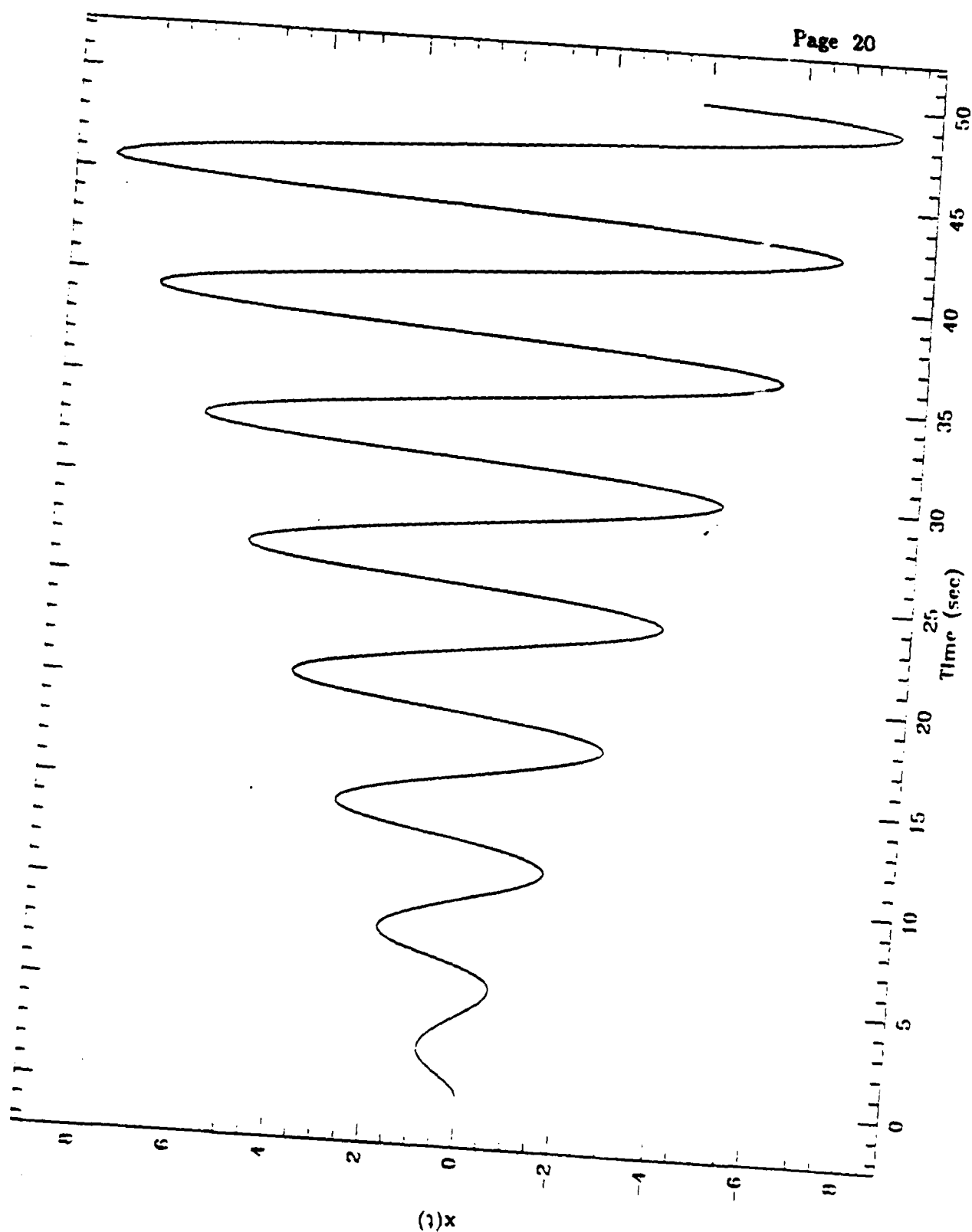


Figure 8.

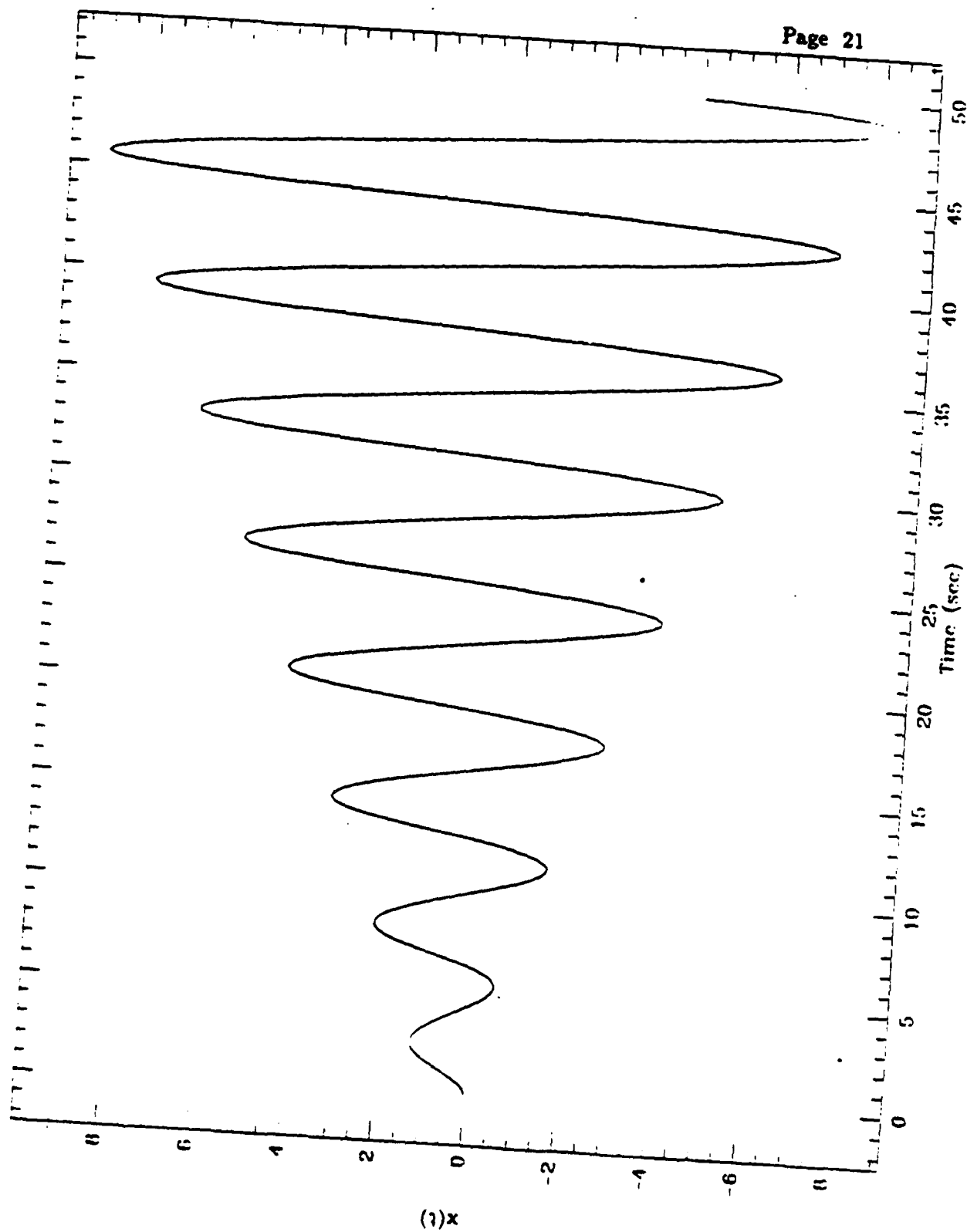


Figure 9.

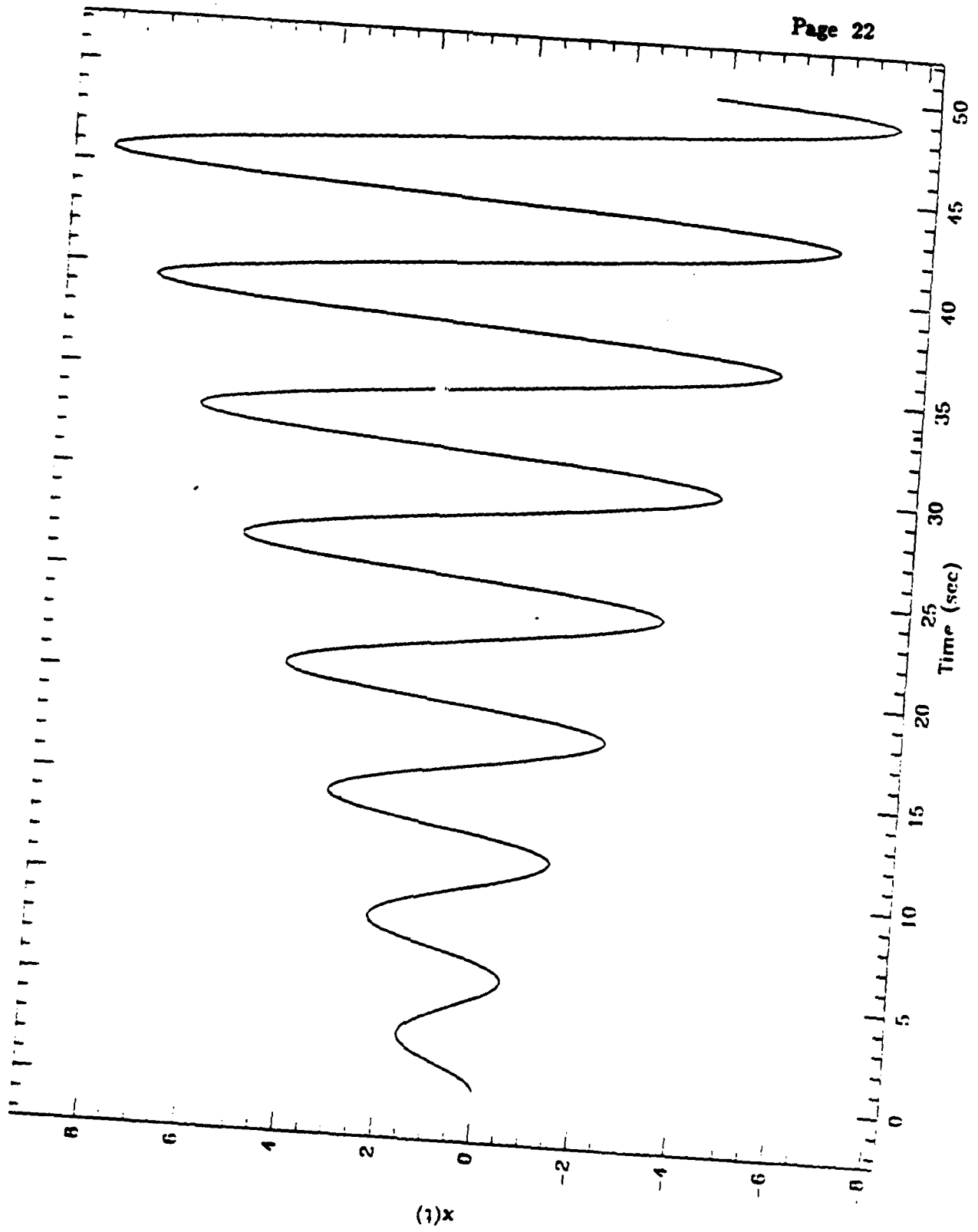


Figure 10.

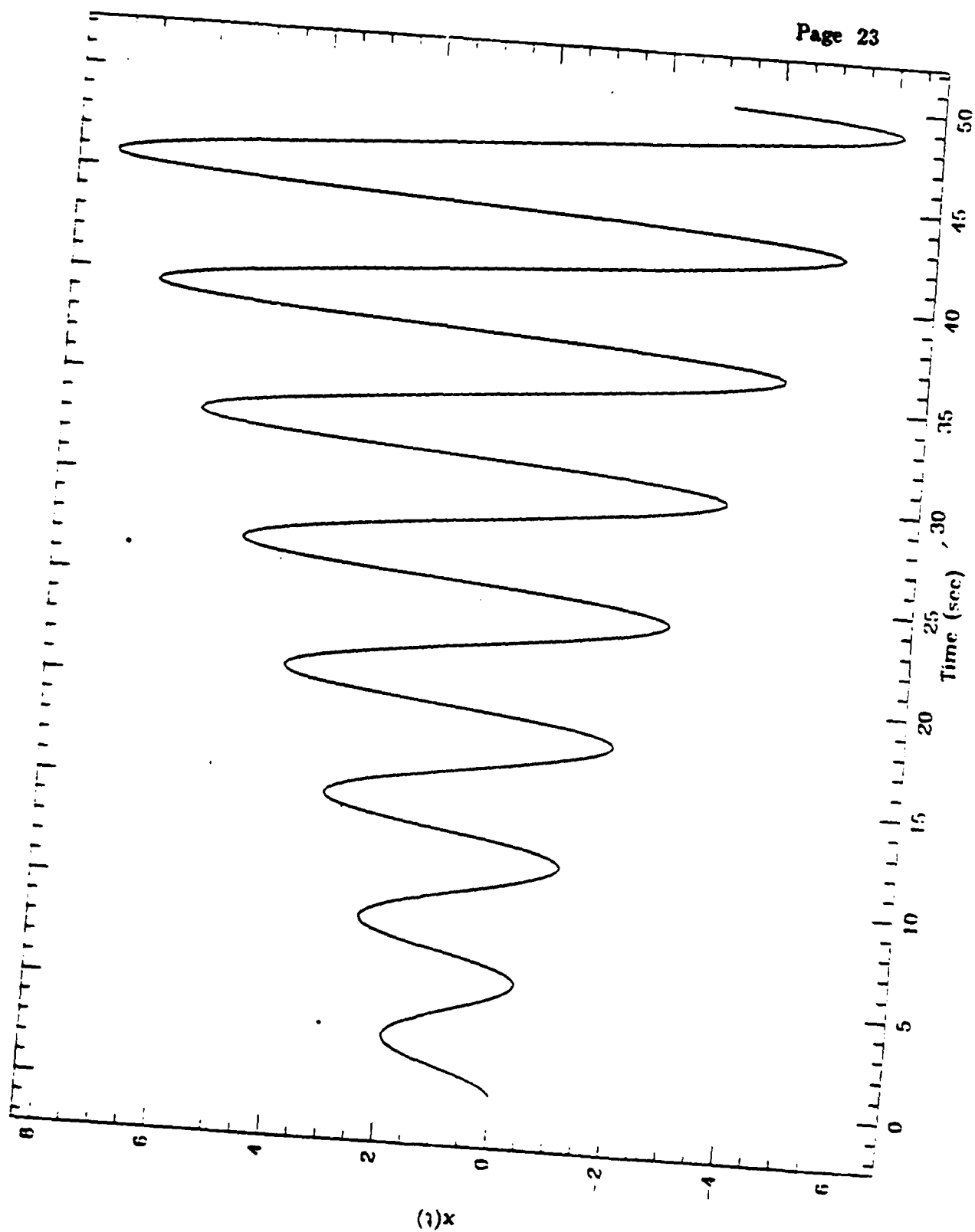


Figure 11.

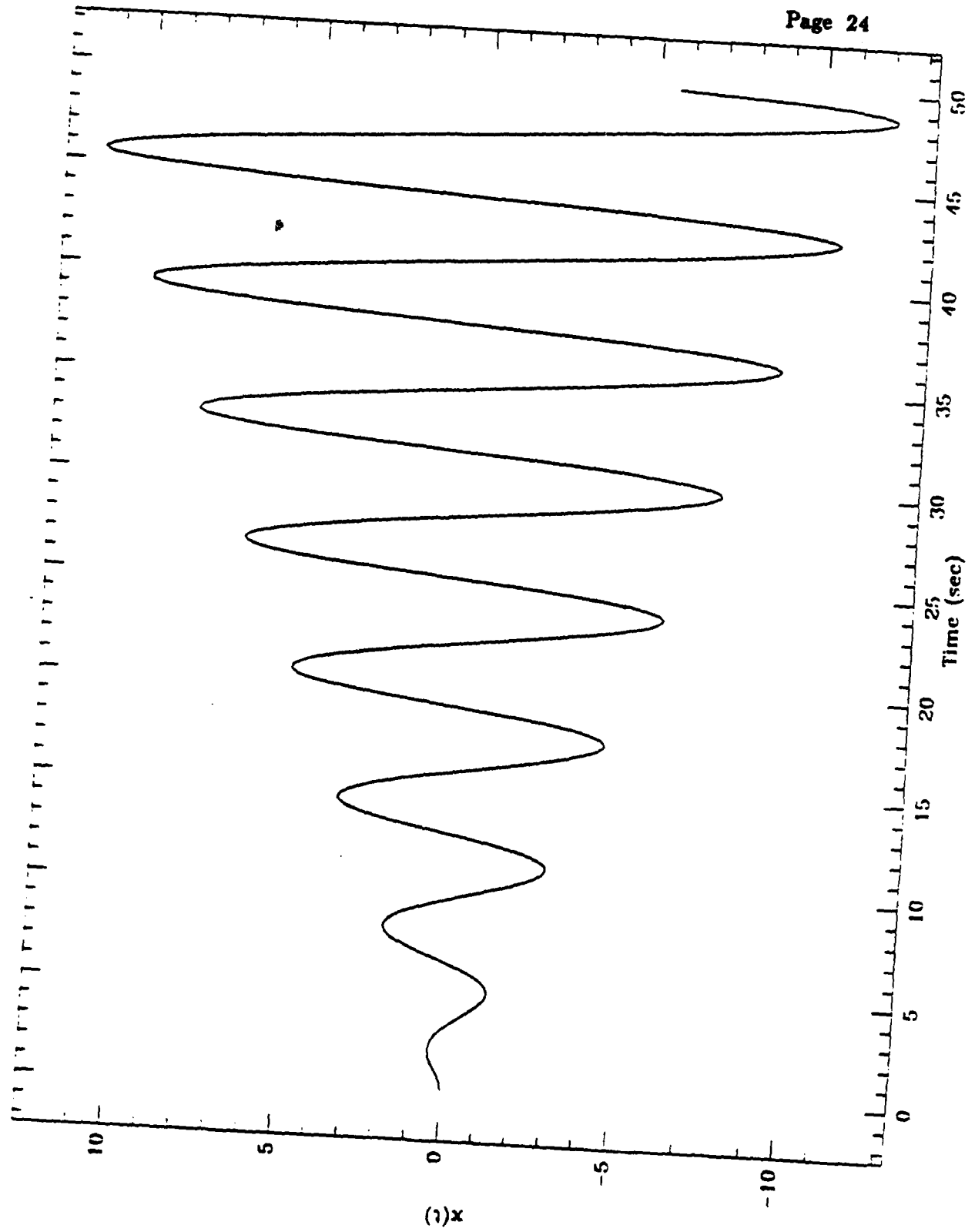


Figure 12.

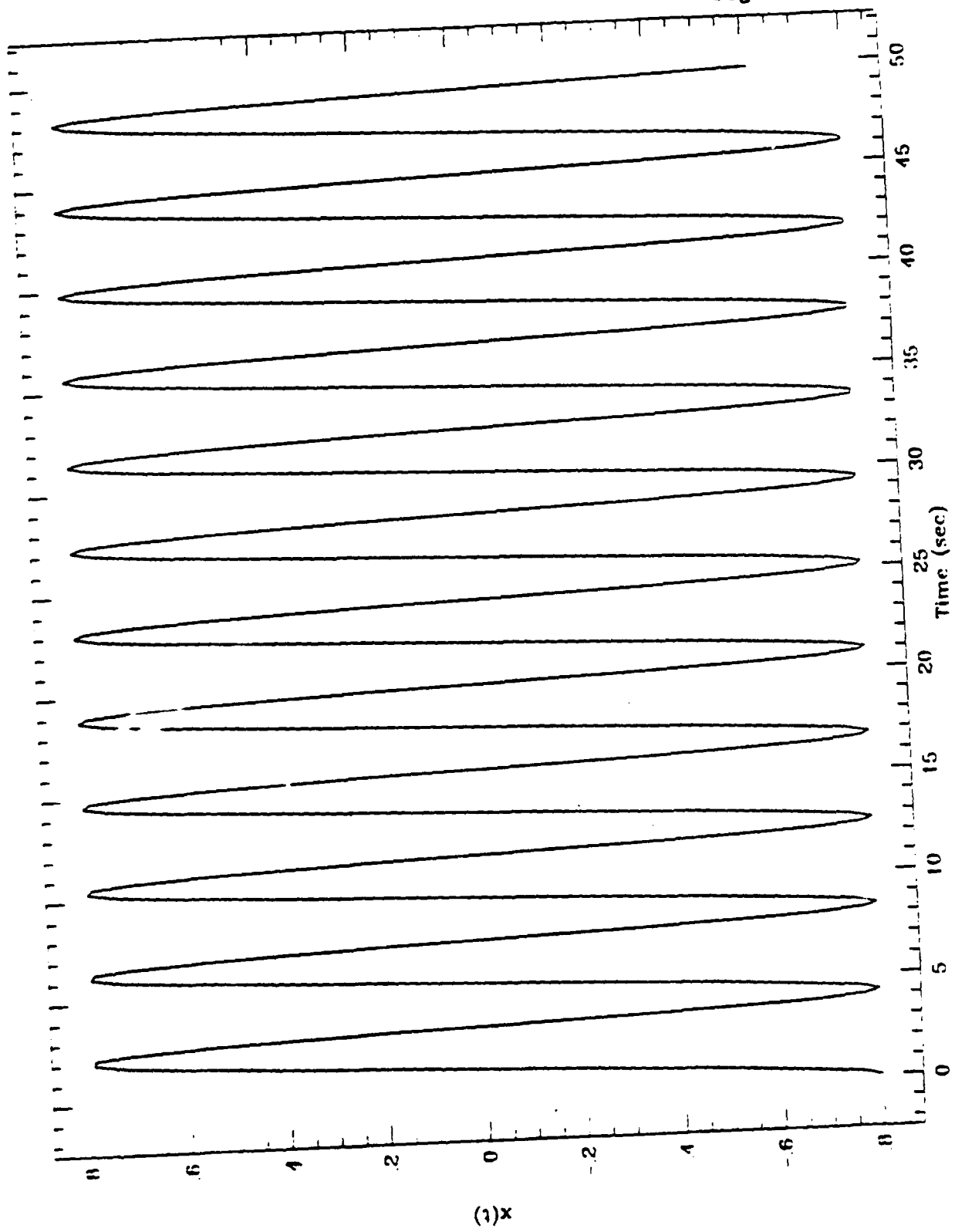


Figure 13.

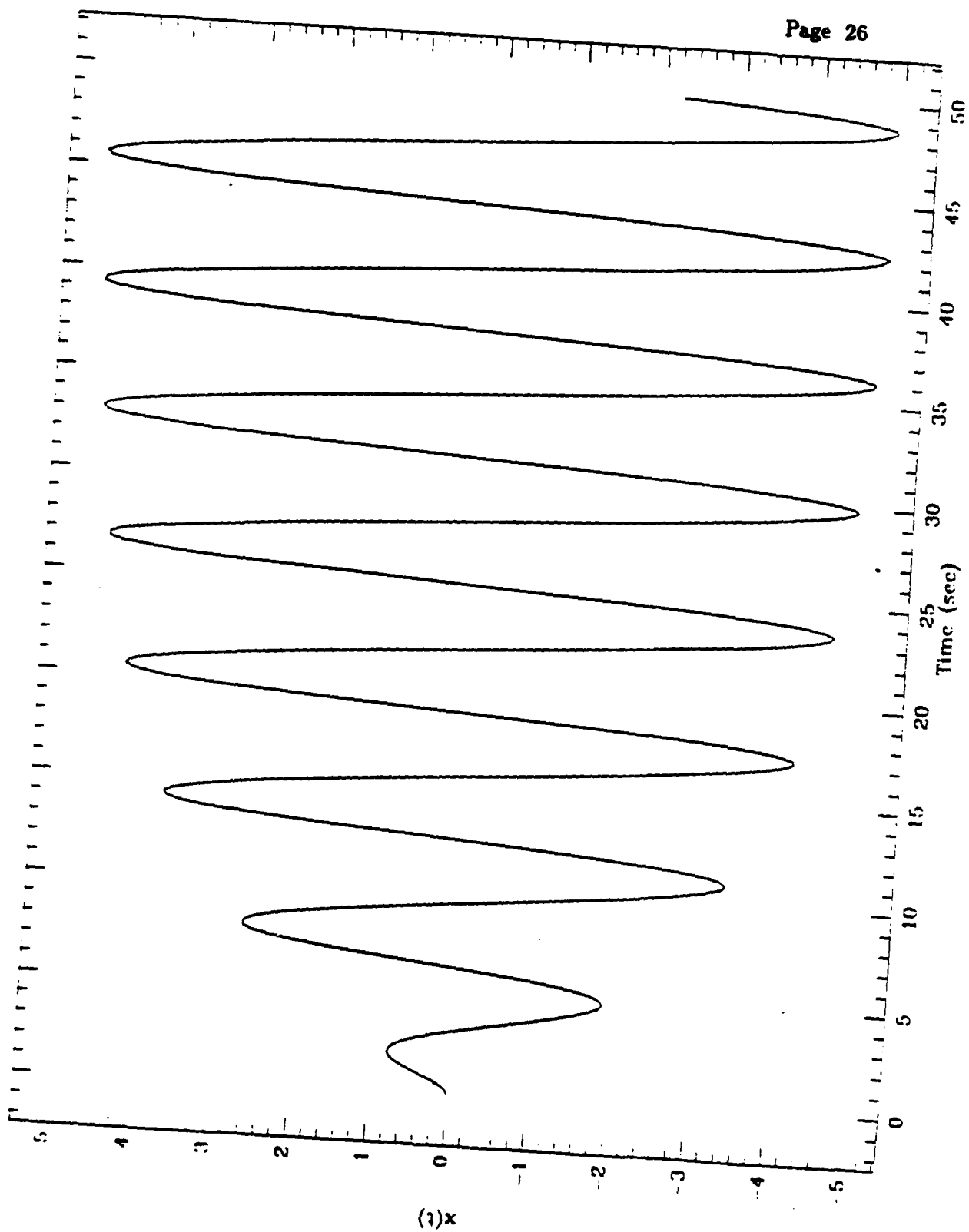


Figure 14.

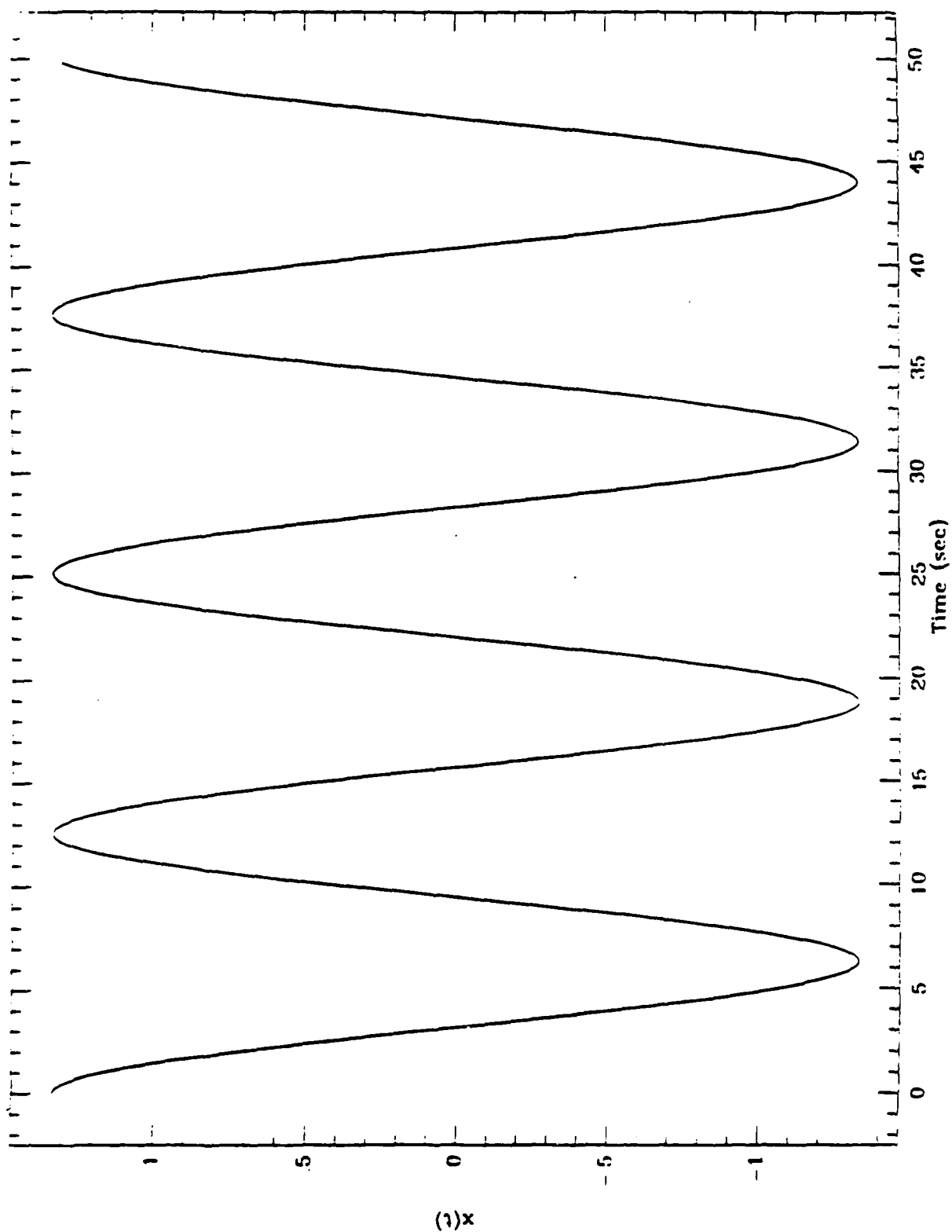


Figure 15.

13. The response is a steady state oscillation as described by equation (6).

If the damping is $b = .1k$ with $m = k = 1$, the value of b from equation (13) is .2. If $\omega = \omega_0 = F = 1$, the response from equation (11) is $A = 5/i$. A run has been done with $x_0 = \dot{x}_0 = 0$. The results are shown in Figure 14. After an initial transient phase, the amplitude approaches 5 asymmetrically. The last peak has an amplitude of -4.96. The driving force is a cosine function which has zero phase at 6.283, 12.566, 18.849, 25.133, 31.416, 37.699, and 43.982 seconds. Toward the end of the run, Figure 14 has maxima at 32.984, 39.267, and 45.551 seconds, which is $\pi/2$ seconds after the maxima of the driving function.

Finally a run has been done with $\omega = .5$, $m = k = \omega_0 = F = 1$, and $b = 0$. From equation (6) we have $A = 4/3$. The detector is being driven below its resonant frequency and the response is in phase with the driving force. A run has been done with $x_0 = 4/3$, and $\dot{x}_0 = 0$. The response is shown in Figure 15. The behavior is exactly as given by equation (6).

3.0 SIGNAL FROM 3 ROTATING SOURCES VS. WHEEL DIAMETER

From an engineering point of view, it is desirable to keep the rotating wheel carrying the neutrino sources smaller in order to minimize centrifugal effects. A series of runs have been done for different radii to see the effect on the signal from three evenly spaced sources. It is assumed the closest approach to the detector is 25 centimeters for all the cases. The flux is computed using equation (17) with $F = 625$. This gives unity at 25 cm. Table 3 gives the results of the calculations. The first column is the radius of the wheel, the second is the maximum signal, the third is the minimum signal, and the last column is the peak

to peak amplitude of the signal. As the wheel gets smaller, the peak to peak amplitude is reduced but the dependence is not severe over the range of values studied.

Table 3

$r(\text{cm})$	F_{max}	F_{min}	ΔF
34.5	1.1717	.4519	.7199
40.0	1.1374	.3638	.7736
43.0	1.1228	.3256	.7972
45.0	1.1143	.3033	.8111
51.5	1.0921	.2438	.8482

Table 3. Neutrino signal amplitude vs. wheel radius using three symmetrically placed sources.

4.0 GRAVITY SIGNAL VS. RADIUS OF THE ROTATING WHEEL

The previous section discusses the effect of wheel radius on the neutrino signal from three rotating sources. In order to minimize the gravity signals from the wheel, dummy sources consisting of empty 9 cm spheres are placed between the neutrino sources. As the wheel radius is decreased, fewer balls will fit on the rim and the gravity fluctuation increases as the wheel radius decreases. The gravity flux has been computed using equation (17) with a coefficient of 625 so that the signal is unity for one source at 25 cm. Table 4 gives the results of the

computations. The first column is the wheel radius, the second is the number of masses, the third is the maximum gravity signal, the fourth column is the minimum, and the fifth is the peak to peak amplitude. The absolute magnitude of the signal is listed (the actual force being negative). With a 45 cm radius, it is not possible to fit 36 nine centimeter diameter balls since the circumference is 282.7 cm and 324 cm is needed for 36 balls. For all the other cases, the balls should be just touching. For the 45 cm radius the balls would have to be 7.85 cm instead of 9 cm. This slightly closer spacing gives a significant reduction in the gravity ripple. However, the gravity ripple is a factor of 10^4 lower than the signal from a single ball for the first entry which is the largest one in the table. The magnitude of the signal from all the balls is equivalent to about 6 balls at the closest approach (25 cm from the detector).

Table 4

$r(cm)$	#masses	F_{max}	F_{min}	ΔF
34.5	24	5.8068743	5.8067482	.0001261
40	28	5.9817155	5.9816336	.0000819
43	30	6.0197642	6.0196919	.0000723
45	36	6.9407545	6.9407441	.0000104
51.5	36	6.1496537	6.1496060	.0000477

Table 4. Gravity signal vs. wheel radius and number of masses.

For the first entry, the signal is produced by 24 balls, three of which are neutrino sources. The frequency of the gravity signal is 8 times that of the

neutrino signal. Let us assume the detector is tuned to the frequency of the neutrino sources. If we neglect damping, we can use equation (7) to calculate the off-resonance response of the detector. For $k = m = F = 1$, and $\omega = 8$, equation (7) gives $A = .01587$. For $\omega = 0$, the amplitude from either equation (6) or (7) is 1. At resonance the amplitude is given by equation (11). If we have a high Q system the damping coefficient b given by $b = m\omega/Q$ will be small and the amplitude A will be large. For $\omega = 1$, and $Q = 10^4$, we have $b = 10^{-4}$. The amplitude from equation (11) is $A = -10^4 i$. The amplitude at $\omega = 8$ is about 2 orders of magnitude smaller than the response at $\omega = 0$, and about 6 orders of magnitude smaller than the response at resonance with $Q = 10^4$.

Up to this point, the detector has been modelled as a one degree of freedom harmonic oscillator. This is probably a reasonable approximation for the neutrino signal on the sapphire crystal. However, for the effect of gravity, the acceleration of the frame must be considered. In addition to translation, the frame can also rotate due to unequal force on the upper and lower sensing masses.

5.0 TWO MASS MODEL OF THE NEUTRINO DETECTOR

The neutrino detector consists of a sensor plate that is attached to a frame. The frame is suspended by a soft suspension system to minimize the transmission of seismic noise to the detector. An analysis has been done of the response of the system using the model shown in Figure 16. The equations of motion of the system are

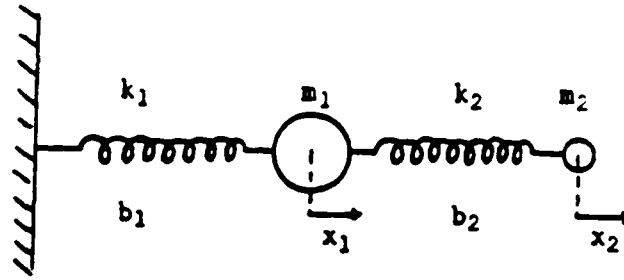


Figure 16. Two mass model of the neutrino detector with damping.

$$m_1 \ddot{x}_1 + b_1 \dot{x}_1 - b_2(\dot{x}_2 - \dot{x}_1) + (k_1 + k_2)x_1 - k_2 x_2 = F_1 e^{i\omega t} \quad (19)$$

$$m_2 \ddot{x}_2 + b_2(\dot{x}_2 - \dot{x}_1) + k_2 x_2 - k_2 x_1 = F_2 e^{i\omega t} \quad (20)$$

Assuming the solutions

$$x_1 = A_1 e^{i\omega t} \quad (21)$$

$$x_2 = A_2 e^{i\omega t} \quad (22)$$

gives the equations

$$-A_1 m_1 \omega^2 + A_1 i b_1 \omega - i b_2 \omega (A_2 - A_1) + (k_1 + k_2) A_1 - k_2 A_2 = F_1 \quad (23)$$

$$-A_2 m_2 \omega^2 + i b_2 \omega (A_2 - A_1) + k_2 A_2 - k_2 A_1 = F_2 \quad (24)$$

Equations (23) and (24) can be written in the form

$$A_1 B + A_2 C = F_1 \quad (25)$$

$$A_1 C + A_2 D = F_2 \quad (26)$$

where

$$B \equiv -m_1\omega^2 + k_1 + k_2 + i\omega(b_1 + b_2) \quad (27)$$

$$C \equiv -k_2 - ib_2\omega \quad (28)$$

$$D \equiv -m_2\omega^2 + k_2 + ib_2\omega \quad (29)$$

Equations (25) and (26) can be solved to give

$$A_1 = X_1/\Delta \quad (30)$$

$$A_2 = X_2/\Delta \quad (31)$$

where

$$X_1 = F_1D - F_2C \quad (32)$$

$$X_2 = F_2B - F_1C \quad (33)$$

$$\Delta = BD - C^2 \quad (34)$$

In order to evaluate equations (32), (33), and (34) let us write equations (27), (28) and (29) in the form

$$B = B_1 + i B_2 \quad (35)$$

$$C = C_1 + i C_2 \quad (36)$$

$$D = D_1 + i D_2 \quad (37)$$

where

$$B_1 = -m_1\omega^2 + k_1 + k_2 \quad (38)$$

$$B_2 = \omega(b_1 + b_2) \quad (39)$$

$$C_1 = -k_2 \quad (40)$$

$$C_2 = -b_2\omega = -D_2 \quad (41)$$

$$D_1 = -m_2\omega^2 + k_2 \quad (42)$$

$$D_2 = b_2\omega \quad (43)$$

Substituting equations (35) through (37) into equations (32) and (33) gives

$$X_1 = F_1D_1 - F_2C_1 + i(F_1D_2 - F_2C_2) \quad (44)$$

$$X_2 = F_2B_1 - F_1C_1 + i(F_2B_2 - F_1C_2) \quad (45)$$

Substituting equations (38) through (43) into (44) and (45) gives

$$X_1 = F_1(-m_2\omega^2 + k_2) + F_2k_2 + i(F_1 + F_2)b_2\omega \quad (46)$$

$$X_2 = F_2(-m_1\omega^2 + k_1 + k_2) + F_1k_2 + i\omega(F_2[b_1 + b_2] + F_1b_2) \quad (47)$$

Substituting equations (35) through (37) into equation (34) gives

$$\begin{aligned} \Delta &= (B_1 + iB_2)(D_1 + iD_2) - (C_1 + iC_2)^2 \\ &= B_1D_1 - B_2D_2 - C_1^2 + C_2^2 + i(B_2D_1 + B_1D_2 - 2C_1C_2) \end{aligned} \quad (48)$$

We can write equation (48) as

$$\Delta = \Delta_R + i \Delta_I \quad (49)$$

where

$$\Delta_R = B_1D_1 - B_2D_2 - C_1^2 + C_2^2 \quad (50)$$

$$\Delta_I = B_2D_1 + B_1D_2 - 2C_1C_2 \quad (51)$$

Evaluating the terms in equation (50) gives

$$B_1 D_1 = m_1 m_2 \omega^4 - \omega^2 (m_1 k_2 + m_2 k_1 + m_2 k_2) + k_1 k_2 + k_2^2 \quad (52)$$

$$- B_2 D_2 = - \omega^2 b_1 b_2 - \omega^2 b_2^2 \quad (53)$$

$$- C_1^2 = - k_2^2 \quad (54)$$

$$C_2^2 = \omega^2 b_2^2 \quad (55)$$

Substituting equations (52) through (55) into (50) gives

$$\Delta_R = m_1 m_2 \omega^4 - \omega^2 (m_1 k_2 + m_2 k_1 + m_2 k_2 + b_1 b_2) + k_1 k_2 \quad (56)$$

Evaluating the terms in equation (51) gives

$$B_2 D_1 = - \omega^3 (m_2 b_1 + m_2 b_2) + \omega (b_1 k_2 + b_2 k_2) \quad (57)$$

$$B_1 D_2 = - \omega^3 m_1 b_2 + \omega (b_2 k_1 + b_2 k_2) \quad (58)$$

$$- 2 C_1 C_2 = - 2 \omega b_2 k_2 \quad (59)$$

Substituting equations (57) through (59) into (51) gives

$$\Delta_I = - \omega^3 (m_1 b_2 + m_2 b_1 + m_2 b_2) + \omega (b_1 k_2 + b_2 k_1) \quad (60)$$

Combining equations (49), (56) and (60) gives

$$\Delta = m_1 m_2 \omega^4 - \omega^2 (m_1 k_2 + m_2 k_1 + m_2 k_2 + b_1 b_2) + k_1 k_2$$

$$+ i \left[-\omega^3 (m_1 b_2 + m_2 b_1 + m_2 b_2) + \omega (b_1 k_2 + b_2 k_1) \right] \quad (61)$$

Equations (46) and (47) can be written in the form

$$X_1 = X_{1R} + i X_{1I} \quad (62)$$

$$X_2 = X_{2R} + i X_{2I} \quad (63)$$

where

$$X_{1R} = F_1 (-m_2 \omega^2 + k_2) + F_2 k_2 \quad (64)$$

$$X_{1I} = (F_1 + F_2) b_2 \omega \quad (65)$$

$$X_{2R} = F_2 (-m_1 \omega^2 + k_1 + k_2) + F_1 k_2 \quad (66)$$

$$X_{2I} = \omega (F_2 [b_1 + b_2] + F_1 b_2) \quad (67)$$

Substituting equations (49), (62), and (63) into equation (30) and (31) gives

$$A_1 = \frac{X_{1R} + i X_{1I}}{\Delta_R + i \Delta_I} \quad (68)$$

$$A_2 = \frac{X_{2R} + i X_{2I}}{\Delta_R + i \Delta_I} \quad (69)$$

Equations (68) and (69) can be rationalized by multiplying numerator and denominator by

$$\Delta^* = \Delta_R - i \Delta_I \quad (70)$$

The denominator becomes

$$\Delta^2 = \Delta\Delta^* = \Delta_R^2 + \Delta_I^2 \quad (71)$$

Multiplying equations (62) and (63) by (70) gives

$$X_1\Delta^* = (X_{1R} + iX_{1I}) (\Delta_R - i\Delta_I) \quad (72)$$

$$X_2\Delta^* = (X_{2R} + iX_{2I}) (\Delta_R - i\Delta_I) \quad (73)$$

or

$$X_1\Delta^* = (X_{1R}\Delta_R + X_{1I}\Delta_I) + i(X_{1I}\Delta_R - X_{1R}\Delta_I) \quad (74)$$

$$X_2\Delta^* = (X_{2R}\Delta_R + X_{2I}\Delta_I) + i(X_{2I}\Delta_R - X_{2R}\Delta_I) \quad (75)$$

The final results are

$$A_1 = X_1\Delta^*/\Delta^2 \quad (76)$$

$$A_2 = X_2\Delta^*/\Delta^2 \quad (77)$$

with the terms defined by equations (71), (74) and (77).

If Δ_R is zero, equations (68) and (69) simplify to

$$A_1 = \frac{X_{1R} + iX_{1I}}{i\Delta_I} \quad (78)$$

$$A_2 = \frac{X_{2R} + iX_{2I}}{i\Delta_I} \quad (79)$$

or

$$A_1 = X_{1I}/\Delta_I - iX_{1R}/\Delta_I \quad (80)$$

$$A_2 = X_{2I}/\Delta_I - iX_{2R}/\Delta_I \quad (81)$$

In the special case of $b_1 = 0$, we see from equations (65) and (67) that $X_{1I} = X_{2I}$ so that A_1 and A_2 have the same real component and differ only in the imaginary part. In general the amplitudes are given by equations (76) and (77).

In the case of a high Q system, Δ_I will have a small value. The amplitude of the response will be very large when Δ_R goes to zero. In the case of zero damping we see from equation (60) that Δ_I is zero, and the amplitudes A_1 and A_2 will go to infinity when Δ_R is also zero. Setting equation (56) to zero gives two frequencies ω_1 and ω_2 where $\Delta_R = 0$. These are the resonant frequencies. For small damping (high Q) the maximums of A_1 and A_2 are nearly at ω_1 and ω_2 so equations (80) and (81) can be used to compute the maximum amplitudes.

Some case studies have been using the parameters

$$\begin{aligned} m_1 &= 12.5 \text{ kg} \\ m_2 &= .25 \text{ kg} \\ k_1 &= 500 \text{ newtons/meter} \\ k_2 &= 10^5 \text{ newtons/meter} \end{aligned} \quad (82)$$

For systems 1 and 2 individually the resonant frequencies given by

$$\omega' = \sqrt{\frac{k}{m}} \quad (83)$$

are $\omega_1' = 6.324555320 \text{ rad/sec}$ and $\omega_2' = 632.455320 \text{ rad/sec}$. Using a value of $b_2 = .016 \text{ newtons/(m/sec)}$ in the equation

$$Q = m\omega/b \quad (84)$$

gives a value of 9882 for Q_2 , or about 10^4 . Using a value of $b_1 = 4$ newtons/(m/sec) gives a value of 19.76 for Q_1 , or about 20. Using the parameters given by equation (82) with no damping the roots of equation (56) are $\omega_1 = 6.262236891$ rad/sec and $\omega_2 = 638.7493909$ rad/sec. The first frequency corresponds to masses m_1 and m_2 moving together. The frequency is somewhat lower than for system 1 alone because the mass is larger. The second frequency corresponds to masses m_1 and m_2 moving opposite to each other. The frequency is somewhat higher than for system 2 alone because the oscillation is about the center of mass and the effective spring constant is higher than k_2 .

Four cases have been run with the parameters given by equation (82) plus

$$\begin{aligned} b_1 &= 0 \\ b_2 &= .016 \end{aligned} \quad (85)$$

for the first 3 cases and $b_1 = 4$ for the fourth.

The cases differ in the type of applied forces F_1 and F_2 . All the cases are at the second resonance given by ω_2 .

Case	F_1	F_2	Amplitude
1	0 ($b_1=0$)	m_2	$A_1 = -.4806 \times 10^{-7} + .4703 \times 10^{-3}i$ $A_2 = -.4806 \times 10^{-7} - .2351 \times 10^{-1}i$
2	m_1	$.86m_2$	$A_1 = -.2444 \times 10^{-5} - .6589 \times 10^{-4}i$ $A_2 = -.2444 \times 10^{-5} + .3294 \times 10^{-2}i$
3	m_1	m_2	$A_1 = -.2451 \times 10^{-5} - .4611 \times 10^{-7}i$ $A_2 = -.2451 \times 10^{-5} + .2305 \times 10^{-5}i$
4	0 ($b_1=4$)	m_2	$A_1 = -.4385 \times 10^{-7} + .4290 \times 10^{-3}i$ $A_2 = -.1101 \times 10^{-4} - .2145 \times 10^{-1}i$

For cases 1, 2, and 3, the real parts of A_1 and A_2 are equal (see discussion following equations (80) and (81)). For all except case 3, the real part of the amplitude is small compared to the imaginary part. The amplitudes are limited by the damping and the response is 90° out of phase with the driving force. For case 3 the real and imaginary parts of A_2 are nearly equal and the phase angle is 134 degrees. For all 4 cases the ratio of the imaginary part of A_2 to the imaginary part of A_1 is -50 . The ratio of the masses is $12.5/.25 = 50$. The motions of m_1 and m_2 are inversely proportional to their masses and 180° out of phase (except for case 3). If we normalize the imaginary parts of A_2 to that of case 1, the relative amplitudes of the imaginary parts are

Case	Amplitude
1	1.00
2	.14
3	.0001
4	.91

The relative amplitudes of the 4 cases are determined primarily by the difference in the driving accelerations between the masses. In the first case, all the acceleration is applied to the second mass. This case gives the largest response of the system. In the second case the acceleration difference is 14 percent of the acceleration difference in case 1. The response is lower by 14 percent. In case 3 the applied accelerations are equal. This gives the smallest response. The difference $A_1 - A_2$ is not zero because of the effect of k_1 . For a single mass, the equation of motion is

$$m\ddot{x} + b\dot{x} + kx = Fe^{i\omega t} \quad (86)$$

Assuming a solution of the form

$$z = Ae^{i\omega t} \quad (87)$$

results in the solution

$$A = \frac{F}{-m\omega^2 + k + i\omega b} \quad (88)$$

At resonance, the real part of the denominator goes to zero and the response is 90° out of phase with the driving force F . Above the resonant frequency, the term $-m\omega^2$ is much larger than k . For the 4 cases that have been studied the driving force is close to the natural frequency of m_2 but is about 100 times the resonant frequency of m_1 on spring k_1 . As free masses ($b = k = 0$) with an applied force $g_0 m$, the response of each mass using equation (88) is

$$A = \frac{g_0 m}{-m\omega^2} = -\frac{g_0}{\omega^2} \quad (89)$$

If k_2 is present but k_1 is zero, equation (89) still applies since $A_2 - A_1$ is always zero. Finally, adding spring k_1 causes a small force on A_1 which introduces a small difference between A_1 and A_2 . The approximate magnitude of the perturbation caused by k_1 can be calculated as follows. At the resonant frequency ω_1 of mass 1, we have

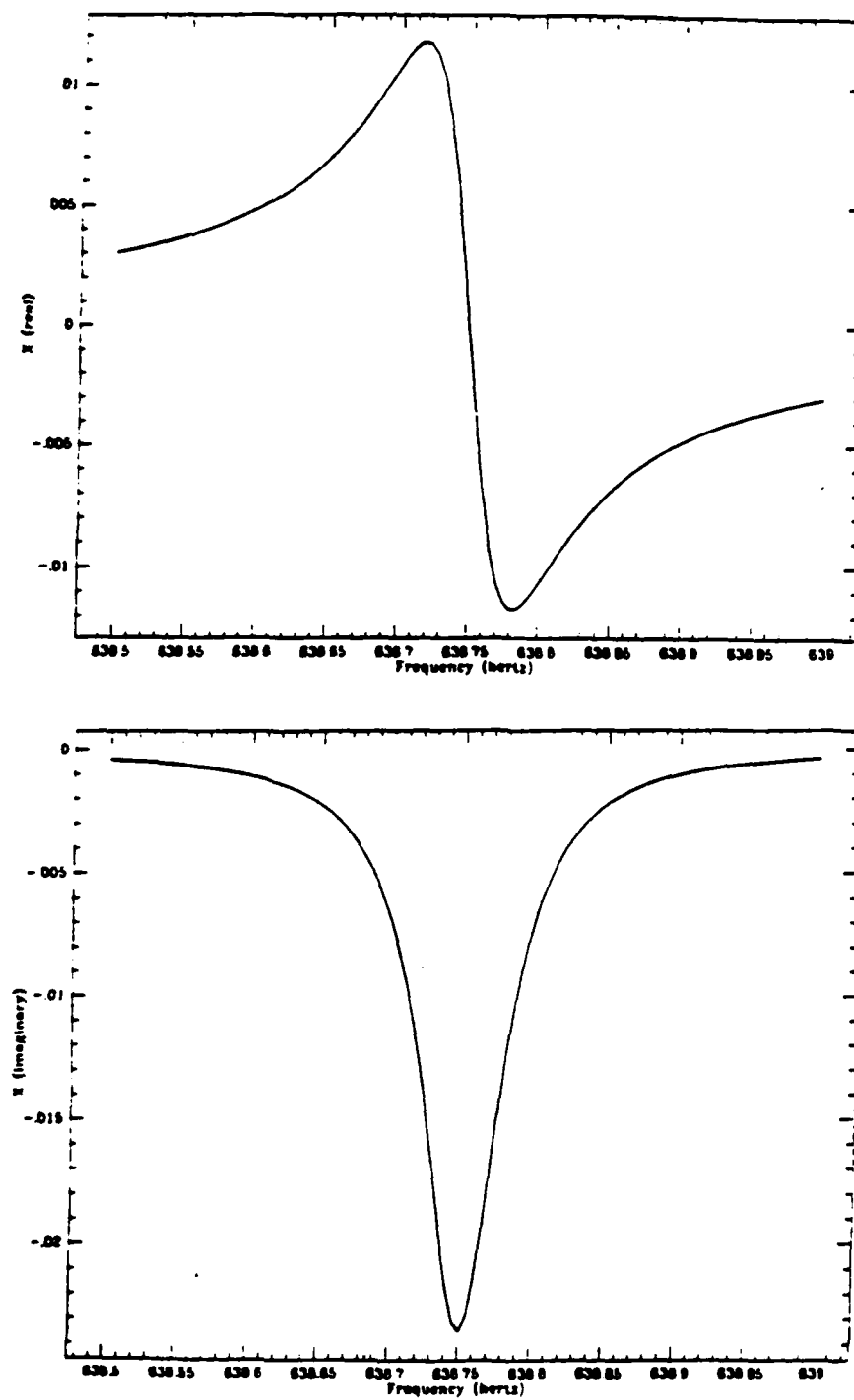
$$-m_1\omega_1^2 = k_1 \quad (90)$$

At frequency ω^2 where $\omega_2/\omega_1 = 10^2$, we have

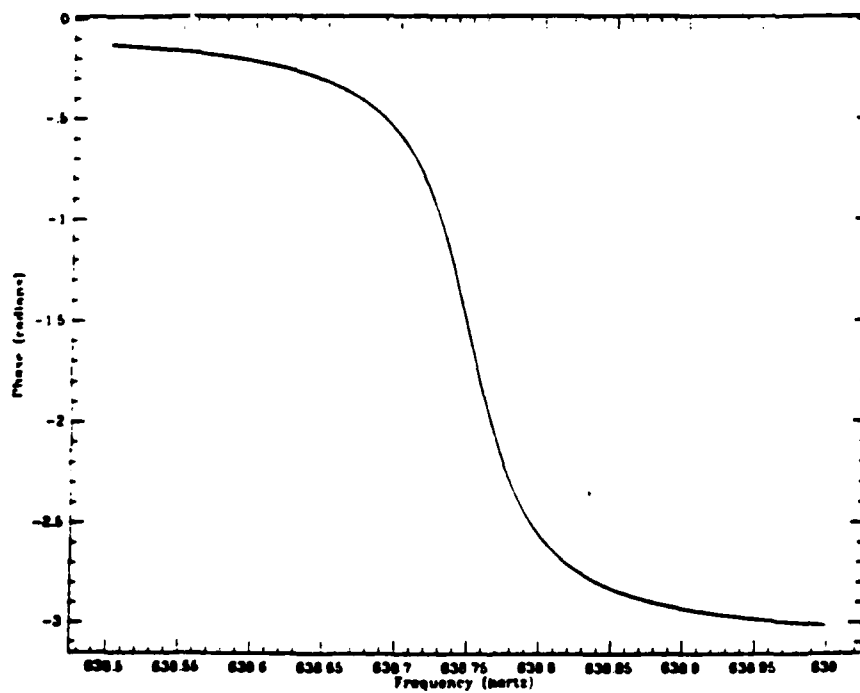
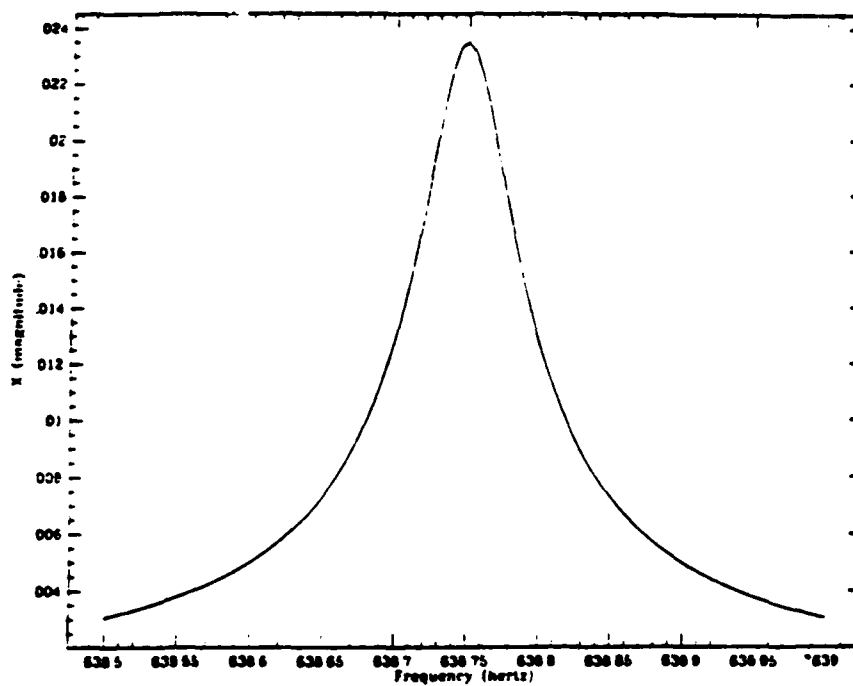
to the line width of about .1 rad/sec at half amplitude.

Figures 17, 18, and 19 show the resonance plots for cases 1, 2, and 3 respectively. The plots for case 4 look very similar to case 1 in Figure 17 and have been omitted. The quantities plotted in parts a), b), and c) are the real part of A_2 , the imaginary part of A_2 and the magnitude of A_2 . Because of the unusual behavior of Figure 19c, the magnitude has been plotted over a wider region in Figure 19d. The last part of each figure is the phase angle. Figures 17 and 18 for cases 1 and 2 look like standard resonance plots. For case 1 the real part is positive below resonance and negative above resonance. The imaginary part and the magnitude have their maximum values at resonance. The phase angle approaches 0° below resonance and approaches 180° above resonance. For case 2, the difference in applied force is of opposite sign and the displacements are reversed in sign and phase. Case 3 is unlike all the others. For the real part is always negative. The shape of the curve is similar to that of case 2. The imaginary part is also similar to case 2. The major difference is in the magnitude. There is no resonance peak. The shape is similar to the real part of the amplitude in case 1. The maximum amplitude occurs below resonance. The value at resonance is comparable to that on either side of the resonance. The phase angle approaches 180° on either side and decreases by about 46° to around 134° at resonance.

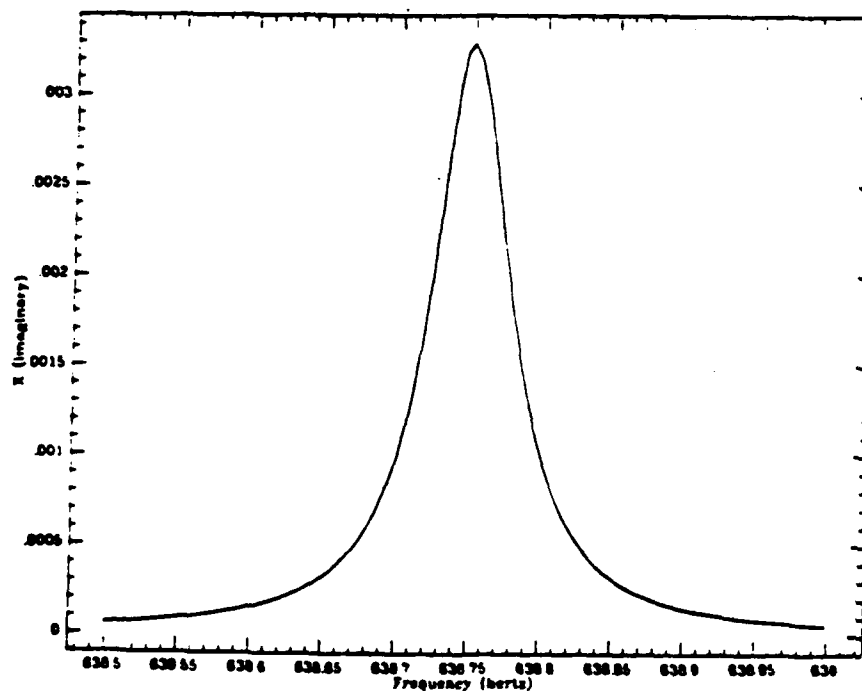
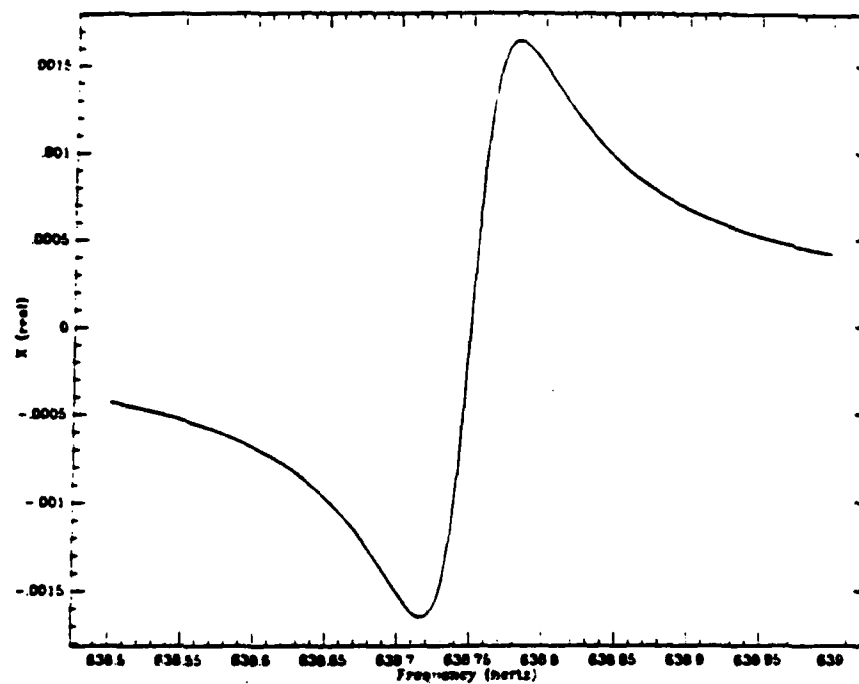
In summary the study of the two mass model shows that the response at the ω_2 resonance is proportional to the difference in acceleration applied to the two masses. The response for equal accelerations is very small but does not go to zero because of the effect of the spring k_1 .



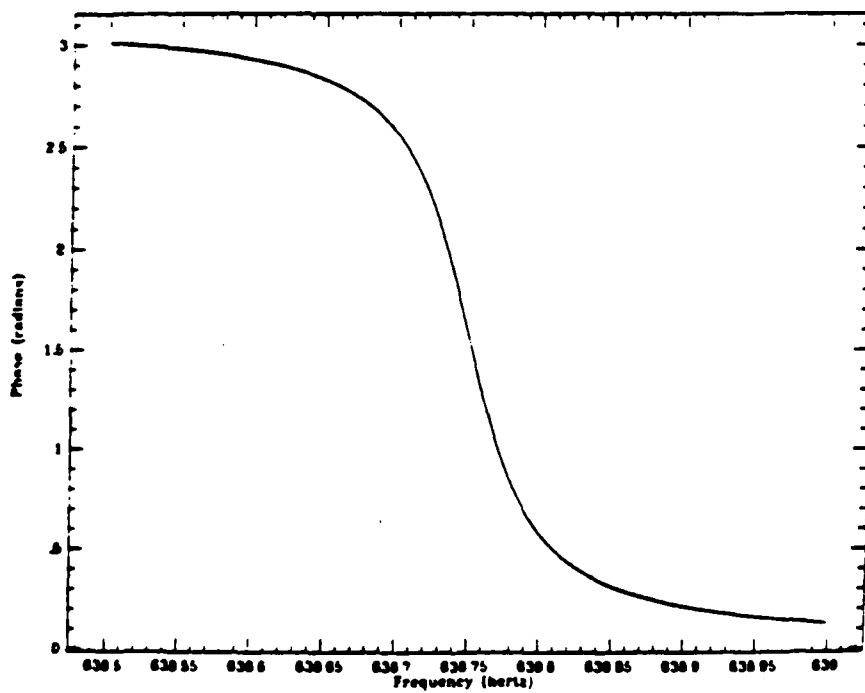
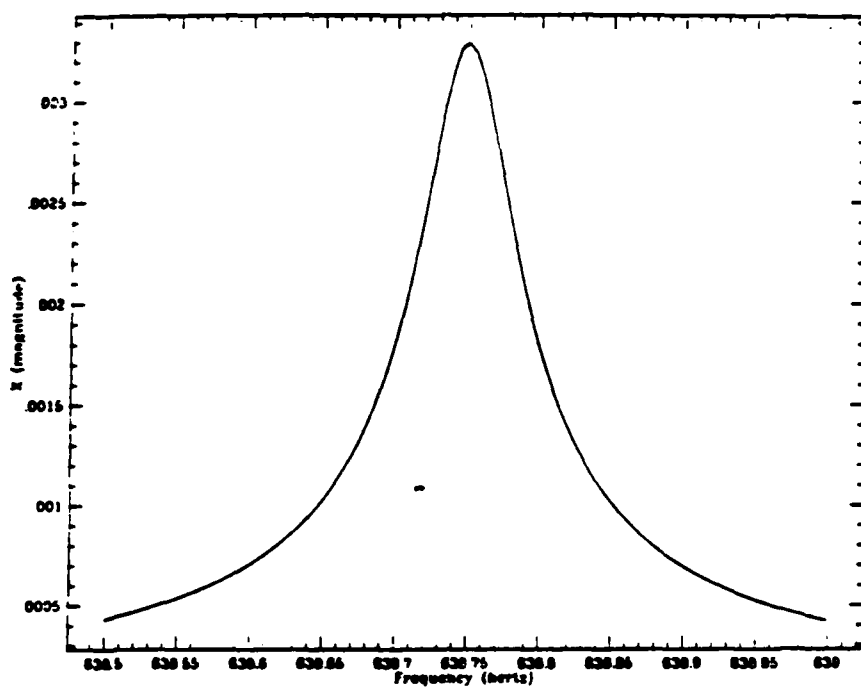
Figures 17(a) and 17(b).



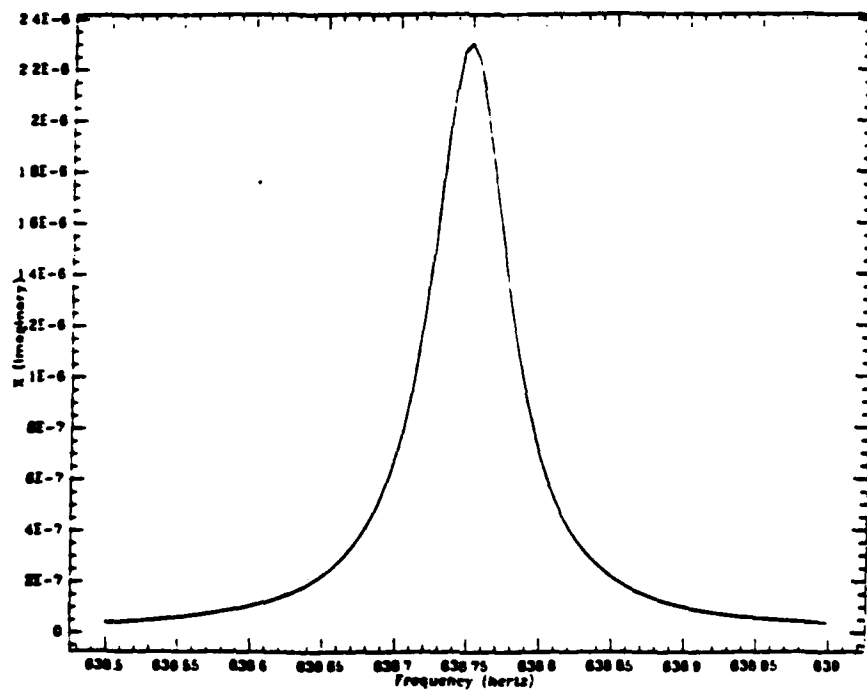
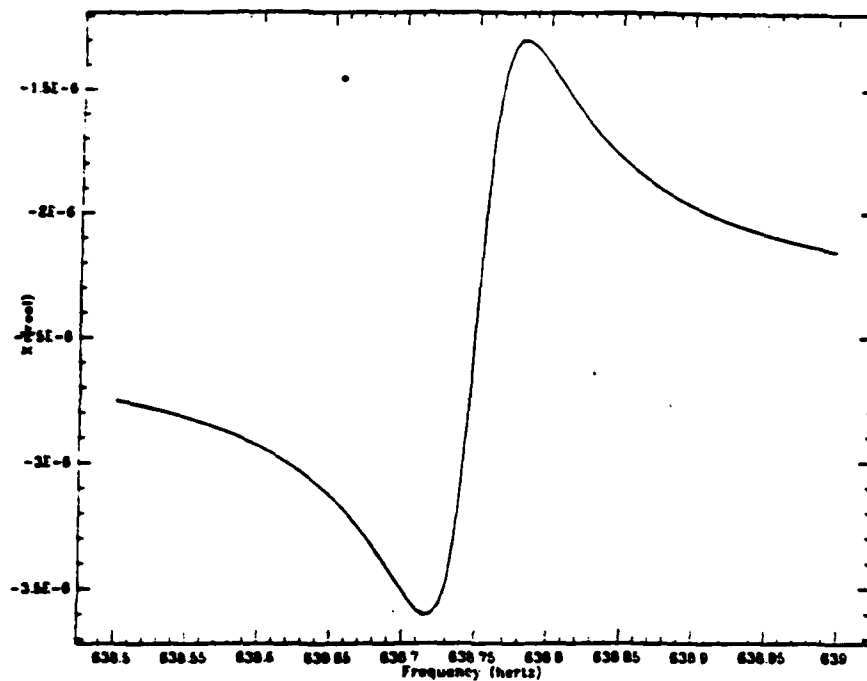
Figures 17(c) and 17(d).



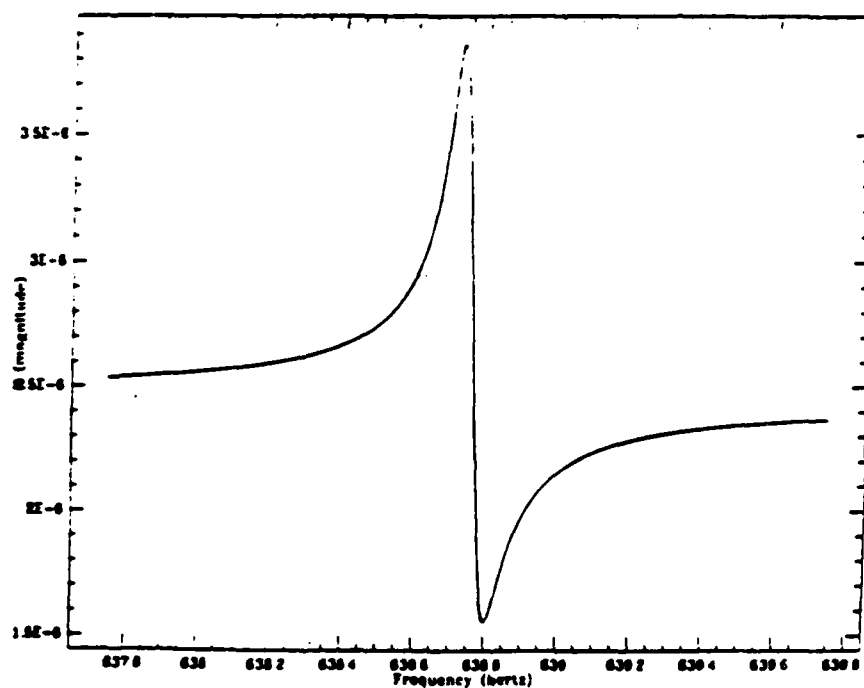
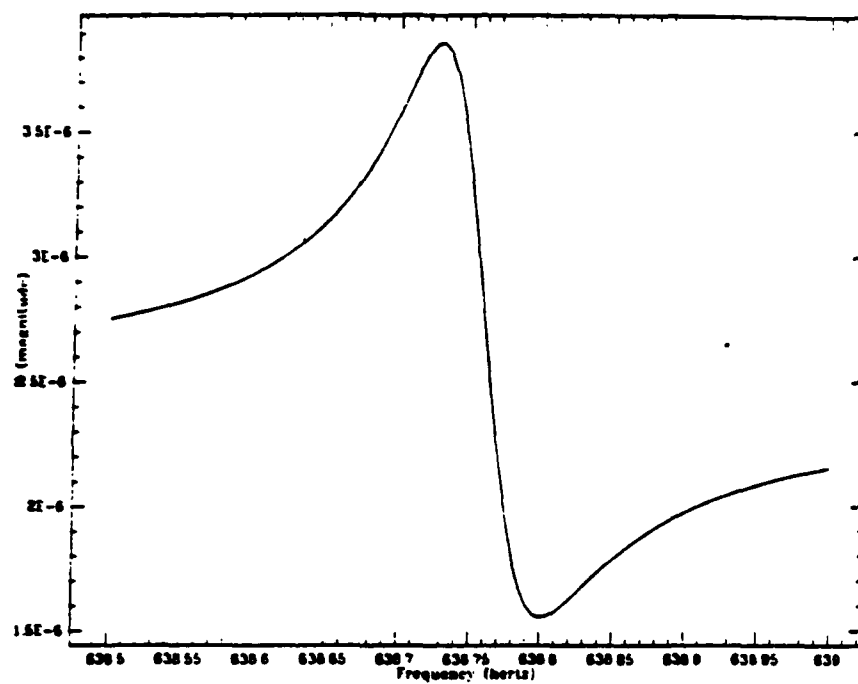
Figures 18(a) and 18(b).



Figures 18(c) and 18(d).



Figures 19(a) and 19(b).



Figures 19(c) and 19(d).

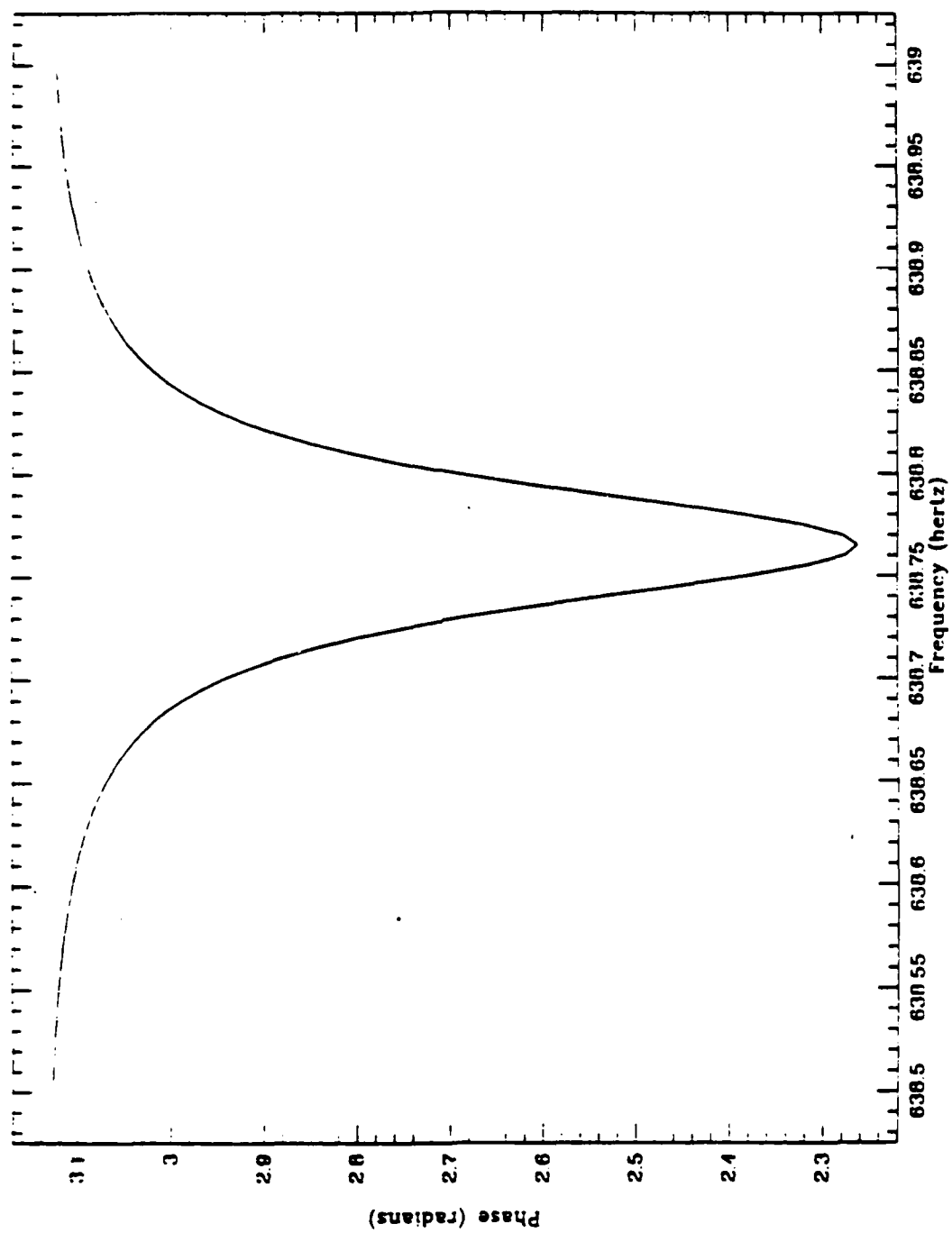


Figure 19(e).

6.0 NUMERICAL INTEGRATION OF THE TWO MASS MODEL

Section 2.0 describes a program called *DETECT* which integrates the motion of a single mass acted on by an elastic restoring force, a damping force and a driving force which may be sinusoidal or the signal from a rotating wheel carrying various numbers of rotating sources. Section 5.0 gives the equations of motion for a two mass system where one mass can represent the frame and the other mass can represent the detector attached to the frame. A new version of program *DETECT* called *DETECT2* has been written using the equations of motion in Section 5.0. The new program can handle either 1 or 2 masses. For one mass the program is identical to program *DETECT*. The equation of motion for mass 1 is

$$\begin{aligned} m_1 \ddot{x}_1 = & -b_1 \dot{x}_1 - k_1 x_1 + F_1 e^{i\omega t} \\ & + b_2 \dot{x}_2 - b_2 \dot{x}_1 - k_2 x_1 + k_2 x_2 \end{aligned} \quad (94)$$

If the single mass mode is selected the terms involving b_2 and k_2 are omitted. The equation of motion for mass 2 is

$$\begin{aligned} m_2 \ddot{x}_2 = & -b_2 \dot{x}_2 - k_2 x_2 + F_2 e^{i\omega t} \\ & + b_2 \dot{x}_1 + k_2 x_1 \end{aligned} \quad (95)$$

The steady state solution of equations (94) and (95) is given in Section 5.0 by equations (61) through (69). The solution for each of the masses is of the form

$$x = A e^{i\omega t} \quad (96)$$

where the amplitude A is a complex number

$$A = A_R + iA_I \quad (97)$$

The driving force is of the form

$$f = Fe^{i\omega t} = F \cos \omega t + iF \sin \omega t \quad (98)$$

Substituting equation (97) into equation (96) gives

$$x = (A_R + iA_I) (\cos \omega t + i \sin \omega t) \quad (99)$$

At $t = 0$, we have

$$x_0 = A_R + iA_I \quad (100)$$

The velocity obtained by differentiating equation (96) is

$$\dot{x} = i\omega A e^{i\omega t} \quad (101)$$

Substituting equation (97) into equation (101) gives

$$\dot{x} = i\omega (A_R + iA_I) (\cos \omega t + i \sin \omega t) \quad (102)$$

At $t = 0$, we have

$$\dot{z}_0 = -\omega A_I + i\omega A_R \quad (103)$$

Taking the real parts of equations (98), (100), and (103) we have

$$f = F \cos \omega t \quad (104)$$

$$z_0 = A_R \quad (105)$$

$$\dot{z}_0 = -\omega A_I \quad (106)$$

If A is real, the initial velocity is zero and the initial conditions consist of giving only the initial position. If A is pure imaginary the initial position is zero and there is only an initial velocity. If A is pure imaginary, it is possible to compute initial conditions involving only the position by means of the phase shift

$$\omega t = \omega t' + \frac{\pi}{2} \quad (107)$$

$$\cos \omega t = \sin \omega t' \quad (108)$$

$$\sin \omega t = -\cos \omega t' \quad (109)$$

Substituting equations (108) and (109) into equations (98), (99), and (102) gives

$$f = F \sin \omega t' - iF \cos \omega t' \quad (110)$$

$$z = (A_R + iA_I) (\sin \omega t' - i \cos \omega t') \quad (111)$$

$$\begin{aligned} \dot{z} &= i\omega(A_R + iA_I) (\sin \omega t' - i \cos \omega t') \\ &= (i\omega A_R - \omega A_I) (\sin \omega t' - i \cos \omega t') \end{aligned} \quad (112)$$

At $t = 0$, the real parts of equations (111) and (112) are

$$x_0 = A_I \quad (113)$$

$$\dot{x}_0 = \omega A_R \quad (114)$$

The real parts of equation (110) is

$$f = F \sin \omega t' \quad (115)$$

Equations (113) and (115) can be used in cases where A_R is zero.

Various test runs have been done to test the numerical integration program *DETECT2*. In the first test a case run of program *DETECT* was repeated on program *DETECT2* in the 1 mass mode with identical results.

For the two mass tests the parameters used are

$$m_1 = 12.5 \quad (116)$$

$$k_1 = 500 \quad (117)$$

$$m_2 = .25 \quad (118)$$

$$k_2 = 10^5 \quad (119)$$

If $b_1 = b_2 = k_1 = 0$, and $F_1 = -F_2$, the equations of motion are quite simple.

Equations (56), (64), (66) from Section 5.0 become

$$\begin{aligned} \Delta_R &= m_1 m_2 \omega^4 - \omega^2 (m_1 k_2 + m_2 k_2) \\ &= \omega^2 (m_1 m_2 \omega^2 - k_2 [m_1 + m_2]) \end{aligned} \quad (120)$$

$$\begin{aligned}
 X_{1R} &= -F_2(-m_2\omega^2 + k_2) + F_2k_2 \\
 &= F_2m_2\omega^2
 \end{aligned}
 \tag{121}$$

$$\begin{aligned}
 X_{2R} &= F_2(-m_1\omega^2 + k_2) - F_2k_2 \\
 &= -F_2m_1\omega^2
 \end{aligned}
 \tag{122}$$

The amplitudes are

$$\begin{aligned}
 A_1 &= \frac{X_{1R}}{\Delta_R} = \frac{m_2F_2}{m_1m_2\omega^2 - k_2(m_1 + m_2)} \\
 &= \frac{-F_2}{-m_1\omega^2 + k_2(m_1 + m_2)/m_2}
 \end{aligned}
 \tag{123}$$

$$\begin{aligned}
 A_2 &= \frac{X_{2R}}{\Delta_R} = \frac{-m_1F_2}{m_1m_2\omega^2 - k_2(m_1 + m_2)} \\
 &= \frac{F_2}{-m_2\omega^2 + k_2(m_1 + m_2)/m_1}
 \end{aligned}
 \tag{124}$$

The equation of motion for a single oscillation without damping given by equation (7) in Section 2.0 is

$$A = \frac{F}{-m\omega^2 + k}
 \tag{125}$$

Equations (123) and (124) can be written

$$A_1 = \frac{-F_2}{-m_1\omega^2 + k_1'}
 \tag{126}$$

$$A_2 = \frac{F_2}{-m_2\omega^2 + k_2'} \quad (127)$$

where

$$k_1' = k_2(m_1 + m_2)/m_2 \quad (128)$$

$$k_2' = k_2(m_1 + m_2)/m_1 \quad (129)$$

For the parameters given by equations (116), (118) and (119), we have

$$k_1' = 51 \quad k_2 = 51 \times 10^5 \quad (130)$$

$$k_2' = \frac{51}{50} \quad k_2 = 1.02 \times 10^5 \quad (131)$$

The natural frequency for equation (125) is

$$\omega_b = \sqrt{\frac{k}{m}} \quad (132)$$

The natural frequency for either equation (126) or (127) is

$$\begin{aligned} \omega_b &= \sqrt{\frac{k_2(m_1 + m_2)}{m_1 + m_2}} \\ &= 638.7487769 \text{ rad/sec} \end{aligned} \quad (133)$$

At ω_b , the amplitude is infinite. Program TWOMASS has been used to plot the response from 630 to 640 rad/sec. At 640 rad/sec, we have the particularly

simple response

$$A_1 = 5 \times 10^{-5} F_2 \quad (134)$$

$$A_2 = -2.5 \times 10^{-3} F_2 \quad (135)$$

A computer simulation has been done with program *DETECT2* using the initial conditions $x_1 = 5 \times 10^{-5}$, $\dot{x}_1 = 0$, $x_2 = -2.5 \times 10^{-3}$, $\dot{x}_2 = 0$, $F_1 = -1$, $F_2 = +1$, $k_1 = 10^5$, $b_1 = b_2 = 0$, $m_1 = 12.5$, $m_2 = .25$ and $\omega = 640$ rad/sec. The driving function was

$$f_1 = -\cos \omega t \quad (136)$$

$$f_2 = \cos \omega t \quad (137)$$

The maxima of x_1 were -5×10^{-5} at .00490874 sec and 5×10^{-5} at .00981747. With a period of .00981748, the maxima are at .5 and 1.0 cycles. The maxima of x_2 were 2.5×10^{-2} at .00490874 seconds and -2.5×10^{-2} at .00981747 seconds. The agreement with the theoretical calculations was essentially exact within the limits of the interpolation error between output points.

Program *TWOMASS* has been rerun with the same conditions as above but adding $b_2 = 32$. This gives about 10% of critical damping. The amplitudes computed by the program are

$$A_1 = 0 + 9.5928966 \times 10^{-7} i \quad (138)$$

$$A_2 = 0 - 4.7964483 \times 10^{-5} i \quad (139)$$

Program *DETECT2* has been run with the initial values of x_1 and x_2 set equal to

the imaginary parts of A_1 and A_2 . The initial velocities are zero and the driving function is

$$f_1 = -\sin \omega t \quad (140)$$

$$f_2 = \sin \omega t \quad (141)$$

The initial conditions and driving force are described by equations (113), (114), and (115). The driving frequency is the resonant frequency given by equation (133). The period is .009836708 seconds. The maxima of x_1 were $-9.5928960 \times 10^{-7}$ at .00491835 seconds and 9.5928943×10^{-7} at .00983670 seconds. The maxima of x_2 were 4.7964480×10^{-5} at .00491835 seconds and $-4.7964471 \times 10^{-5}$ at .00983670 seconds. The amplitude at resonance for a single oscillation with damping is

$$A = \frac{F}{ib\omega} \quad (142)$$

as shown in equation (11) of Section 2.0. For masses 1 and 2 the effective b is

$$b_1' = 51 \quad b_2 = 1632 \quad (143)$$

$$b_2' = 1.02 \quad b_2 = 32.64 \quad (144)$$

Equations (143) and (144) are similar to equations (130) and (131) for k . With ω given by equation (133), $F_1 = 1$, and $F_2 = +1$, equation (142) gives the amplitudes shown in equations (138) and (139) namely

$$\frac{-1}{1632 \times 638.7487769 i} = 9.5928966 \times 10^{-7} i$$

$$\frac{1}{32.64 \times 638.7487769 \text{ i}} = -4.7964483 \times 10^{-5} \text{ i}$$

Another test has been run with $b_1 = 0$, $b_2 = 32$, $F_1 = 12.5$, $F_2 = .25$, $k_1 = 500$ and $k_2 = 10^5$. Setting the force equal to the mass gives an equal acceleration to each body such as that caused by a gravity field variation. The presence of the spring k_1 causes the motions of m_1 and m_2 to be slightly different. The amplitudes computed by program *TWOMASS* at the second resonance $\omega = 638.7493909$ rad/sec are

$$A_1 = -2.45121128 \times 10^{-6} - 2.3055 \times 10^{-11} \text{ i} \quad (145)$$

$$A_2 = 2.45121128 \times 10^{-6} + 1.15265 \times 10^{-9} \text{ i} \quad (146)$$

The magnitudes of A_1 and A_2 are essentially the real component. The phases are

$$\theta_1 = -179.9994610 \text{ deg} \quad (147)$$

$$\theta_2 = +179.9730572 \text{ deg} \quad (148)$$

Numerical integration shows the phase of x_2 to be delayed by .027 deg as expected. The first maximum of x_1 is at .00491833 sec and the first maximum of x_2 is at .00491908 sec.

A number of other test runs have been done to check the agreement between the theoretical expressions and the numerical integration. In the next run $b_2 = 0.16$ which is a Q of 10^4 for mass 2. The other parameters are the same, namely $b_1 = 0$, $k_1 = 500$, $k_2 = 10^5$, $F_1 = 12.5$, and $F_2 = .25$. At the second resonance, $\omega_2 = 638.7493909$ rad/sec, the theoretically computed ampli-

tudes are

$$A_1 = -.245121128 \times 10^{-5} - .4611069 \times 10^{-7} i \quad (149)$$

$$A_2 = -.245121128 \times 10^{-5} + .2305308 \times 10^{-5} i \quad (150)$$

The phase angles are

$$\theta_1 = -178.9223137 \text{ deg} \quad (151)$$

$$\theta_2 = 136.7569631 \text{ deg} \quad (152)$$

The simulation uses the initial conditions

$$x_1 = x_2 = -.245121128 \times 10^{-5} \quad (153)$$

$$\dot{x}_1 = 2.94531779 \times 10^{-5} \quad (154)$$

$$\dot{x}_2 = -1.4725145 \times 10^{-3} \quad (155)$$

The computed magnitudes of A_1 and A_2 are $.24516449 \times 10^{-5}$ and $.3364949 \times 10^{-5}$. The values in the numerical simulation are $.245164 \times 10^{-5}$ and $.3364949 \times 10^{-5}$. The case was rerun with $b_2 = 0$ and the same initial conditions. The amplitude of A_1 remained at $.245164 \times 10^{-5}$ and the amplitude of A_2 showed values of $-.336501 \times 10^{-5}$, $+.336526 \times 10^{-5}$, $-.336551 \times 10^{-5}$, $+.336577 \times 10^{-5}$, $-.336602 \times 10^{-5}$, and $+.336627 \times 10^{-5}$ at times .00118165, .00610012, .01101859, .01593707, .2085555, and .02577403 seconds. Without damping, the amplitude builds up at resonance. The next test run was done with $b_1 = 16$ and $b_2 = 0$ with the other parameters kept the same. For this case the computed amplitudes are

$$A_1 = -.2237 \times 10^{-18} - .11991086 \times 10^{-6} i \quad (156)$$

$$A_2 = -.1249877 \times 10^{-3} + .5994955 \times 10^{-6} i \quad (157)$$

at the second resonance, $\omega = 638.74939091$ radians/sec. The numerical simulation agrees with the theoretical computation. In the last simulation, equal values of m , k , and b are used for both masses namely,

$$m_1 = m_2 = .25 \quad (158)$$

$$b_1 = b_2 = 32 \quad (159)$$

$$k_1 = k_2 = 10^5 \quad (160)$$

The value of b is approximately 10% of critical damping for a one mass system. The resonant frequencies are 387.3580658 and 1032.63630037 rad/sec. The amplitudes are

$$\begin{aligned} A_1 &= -.83367611 \times 10^{-6} - .83992923 \times 10^{-6} i \\ A_2 &= -.1250514 \times 10^{-5} + .4215206 \times 10^{-6} i \end{aligned} \quad (161)$$

at the second resonance. The magnitudes of A_1 and A_2 are $.1183459 \times 10^{-5}$ and $.13196459 \times 10^{-5}$. The phases are -134.7859257 and 161.3721777 deg. Figure 20(a) shows x_1 as a function of time and Figure 20(b) shows x_2 . The first peak of x_1 is $.1183425 \times 10^{-5}$ at .00227812 seconds. Since the period is .006084606 sec, the phase delay is -134.786 deg. The first positive peak of x_2 is $.1319643 \times 10^{-5}$ at .00335715 sec which is a phase lag of -198.628 deg or $+161.372$ deg. The phase is measured relative to the driving function which is $.25 \cos \omega t$.

The test runs with the numerical integration program confirm the analytical expressions derived in Section 5.0. The analytic expressions give only the final equilibrium state whereas the numerical integration allows the transient behavior to be studied also. In the case of a high Q system it would be time consuming to determine the equilibrium response by numerical integration. Plotting resonance curves is much more efficient with the analytic expressions.

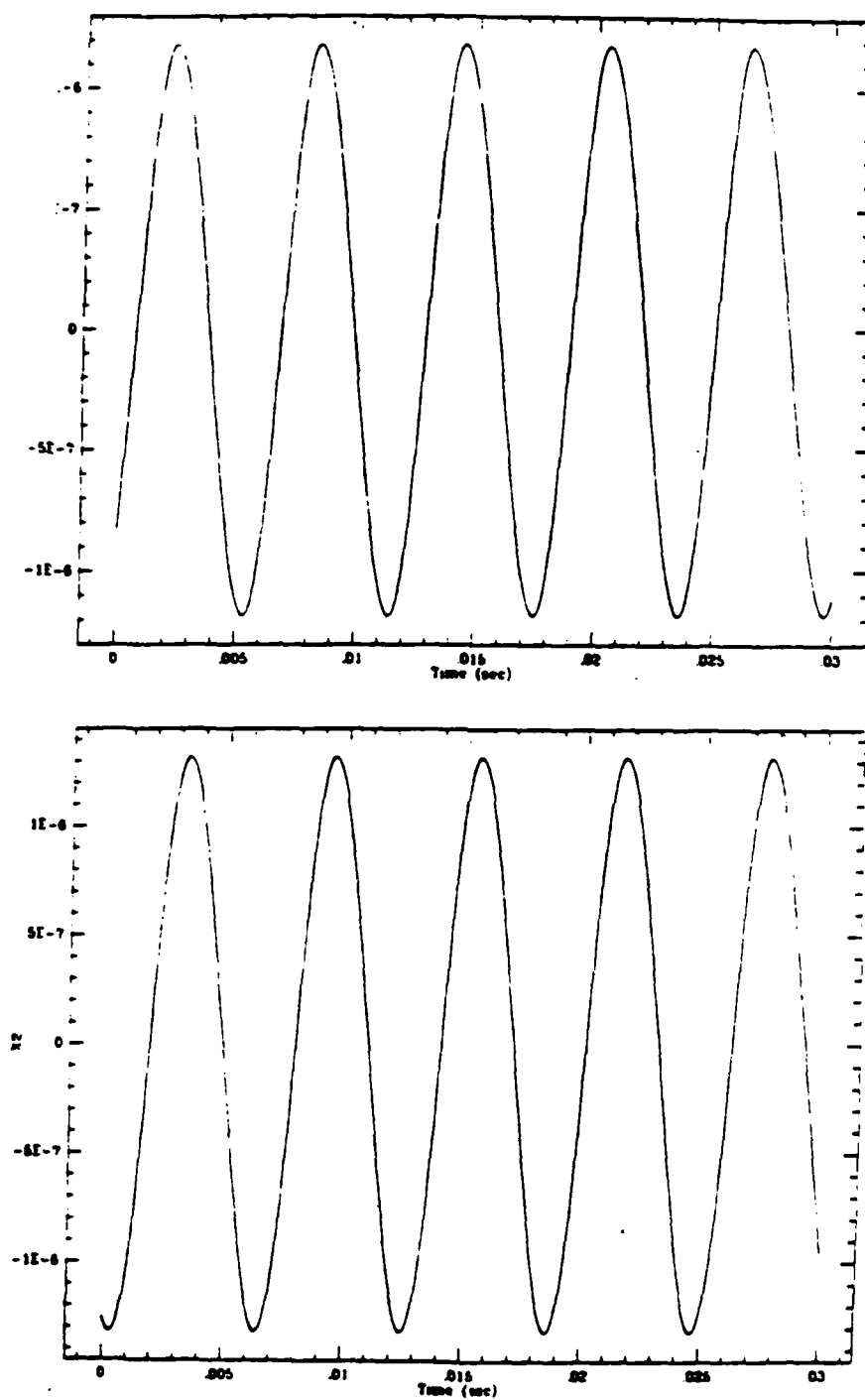


Figure 20(a) and 20(b).

7.0 CONCLUSIONS AND RECOMMENDATIONS

The experiment configuration is now nearly frozen and the measurement schedule approaches crystallization. The chances of substantial delay are reducing every week that goes by. We have to fear, still, administrative delays in subcontract award, such as contract for added scope to SAO, and the contract for the extra rotating shutter to University of Maryland. On the technical front, a possible delay might have to be faced in the procurement of the custom-made 4°K cryostat for the cryogenic force sensor. We still have to receive a quotation for it. Everything else is pretty much under control.

Of great help would be receiving from DARPA as soon as feasible the full data on the tritium source, so that the high-speed rotating table could be completed, design-wise, and SAO could proceed to the issuance of purchase orders for components and subsystems. This is particularly important because the SAO design team is scheduled to go to Australia on March 15, and if we do not have the rotating table fully defined by then, there will be a delay of about six weeks in the issuance by SAO of these purchase orders (the SAO team is scheduled to launch a balloon from down under, with a payload of their own design and mechanization).

Last but not least, we recommend that DARPA seriously consider funding expeditiously the added scope work.

SECOND CONTRACT
FOURTH QUARTERLY REPORT

15 MAY 1988

EXPERIMENTAL TESTING OF CORPUSCULAR RADIATION DETECTORS

SUBMITTED TO
DEFENSE ADVANCED RESEARCH PROJECT AGENCY (DARPA)
DARPA ORDER #5271

CONTRACT #F49620-87-C-0050

MONITORED BY AIR FORCE OFFICE OF SCIENTIFIC RESEARCH
(AFOSR)

DARPA PROGRAM DIRECTOR: US ARMY LT. COLONEL G. P. LASCHE', Ph.D.

The views and conclusions contained in this document are those of the authors and should not be interpreted as necessarily representing the official policies, either expressed or implied, of the Defense Advanced Research Projects Agency or the U.S. Government.


Approved by: Dennis J. Kretzschmar
Program Manager, Raytheon Co.

RAYTHEON COMPANY
SUBMARINE SIGNAL DIVISION
PORTSMOUTH, R HODE ISLAND 02871

TABLE OF CONTENTS

<u>SECTION</u>	<u>PAGE</u>
o Acknowledgements	ii
o Executive Summary	iii
o Development and Testing of Detectors of Low-Energy Neutrinos	1

ACKNOWLEDGEMENTS

This quarterly report has been prepared by Mario D. Grossi, Principal Investigator, with inputs from all members of the program team.

EXECUTIVE SUMMARY

During the report period, the project status has evolved substantially, areas of uncertainty have been cleared, and several milestones have been met. Specific accomplishments are:

(a) The torsion balance has been constructed and tested at University of Maryland. Prof. Weber is awaiting shipping instructions based on the experiment location;

(b) Same as above, for the tuning fork;

(c) The construction of the cryogenic force sensor has been completed in its room-temperature version, and the instrument is undergoing laboratory testing at IFSI-CNR, Frascati, Italy. It will be ready for shipment to Raytheon in late August 1988. In Portsmouth, the instrument will be housed in a 4°K cryostat, system tested and shipped to the test site;

(d) The 1 RPM rotating table for use in testing the torsion balance is now being assembled at Raytheon, Portsmouth, RI. It will be ready for shipment to the test site in early July 1988;

(e) A low-speed data acquisition system (suitable only for the torsion balance) has been identified as Raytheon available capital equipment and could be provisionally used at the test site, starting in early July;

(f) A high-speed data acquisition system (suitable for use with all three sensors) is now being procured by Raytheon and will be ready for shipment to the test site in late July 1988;

(g) The problems (of both security and safety nature) concerning the delivery to Raytheon of the 100 Kilocurie source, would be eliminated, should DARPA choose Los Alamos National Laboratory (LANL) as the experimental test site. Sources of adequate strength, contained in enclosures of acceptable size and shape, are already available at LANAL-WX-5.

(h) With the expectation that LANL will be chosen as the test site, Raytheon has already contacted LANL-WX-5, to explore the possibility of conducting the tests in a LANL lab area which would be assigned to the project. Also LANL was asked when they could provide Raytheon, on a loan basis, general-purpose laboratory instrumentation and supplies needed during testing. This includes the following items:

1. Multichannel digital tape recorder, with A/D converter (and a supply of blank tape reels);
2. Digital clock, IRIG-code time generator;
3. Multichannel chart recorder (and a supply of chart rolls);
4. Liquid helium container and refills;
5. Personal Computer PC-AT, for use with real-time data acquisition system.

(i) Concerning the 100 Hz modulator of the neutrino beam, for the cryogenic force sensor, Raytheon could proceed by awarding to University of Maryland a subcontract for the construction of a large-size rotating chopper, complete with sapphire crystals. However, DAPRA authorization for this procurement has not yet been received by Raytheon at the time of this report.

An alternative way of proceeding would be to have LANL-WX-5 construct (under a MIPR from DARPA) the 2000 RPM rotating table. A preliminary design has been defined at SAO, as part of Raytheon's subcontract to the Observatory.

(j) A computer simulation of the response of all sensors to the rotating source/dummies, has been initiated at SAO, taking into account the dynamic properties of the torsion balance, the tuning fork and the cryogenic force sensor. This simulation is expected to provide vital data concerning manufacturing tolerances (total mass and position of the center of mass) required for constructing sources and dummies, to minimize the spurious signal due to newtonian gravity forces.

Raytheon is planning a visit to LANL in early June 1988, to illustrate to WX-5 the status of the project, to survey the laboratory area that could be assigned to the tests (using a 100 Kilocurie tritium source in a 3.5" sphere, or in a similar container) and to outline the measurement plan that Raytheon has formulated. In order to prepare for this important visit, Raytheon has worked out an updated presentation, that constitutes the majority of this report.

DEVELOPMENT AND TESTING OF DETECTORS OF LOW-ENERGY NEUTRINOS
(DARPA/AFOSR CONTRACT # F49620-87-C-0050)

A PRESENTATION TO
LOS ALAMOS NATIONAL LABORATORY (LANL)
LOS ALAMOS, N.M.
87545

(SCHEDULED FOR EARLY JUNE 1988)

RAYTHEON COMPANY
SUBMARINE SIGNAL DIVISION
PORTSMOUTH, R.I. 02871

OUTLINE OF PRESENTATION

PRESENTORS : DENNIS J. KRETZSCHMAR, PROGRAM MANAGER, RAYTHEON Co.
MARIO D. GROSSI, DR. ENG., PRINCIPAL INVESTIGATOR, RAYTHEON Co.

1. PROGRAMMATIC ASPECTS - RAYTHEON NEUTRINO DETECTORS PROGRAM
2. THE INSTRUMENTS- STATUS OF THEIR DEVELOPMENT
3. MEASUREMENT PLAN
4. WAYS OF COPING WITH MEASUREMENT DIFFICULTIES
5. THE CONDUCT OF A VERIFICATION EXPERIMENT ON PROF. J. WEBER'S CLAIM THAT HE HAS DETECTED LOW-ENERGY NEUTRINOS WITH A ROOM-TEMPERATURE TORSION BALANCE AND A ROOM-TEMPERATURE TUNING FORK
6. MEASUREMENTS WITH A RAYTHEON/SAO CRYOGENIC FORCE SENSOR (IN A 4⁰K CRYOSTAT)
7. THE REQUIRED TRITIUM SOURCES
8. THE REQUIRED LABORATORY SPACE
9. DESIRABLE PROGRAM EXPANSION (NOT YET FUNDED BY DARPA/AFOSR)
10. CONCLUSIONS

The Initial Investigation Performed Under the First DARPA Contract No. F49620-85-C-0030 (1985-1987) – Neutrino Detection

Theoretical study of expected signal intensity based on promising detection schemes, such as:

1. Cryogenic sensor of Neutrino Radiation Pressure
2. Magnetic interaction sensor
3. Superconducting Superheated Colloid (SSC) calorimeter
4. Sensor of the neutrino interaction with superconducting electrons
5. Bolometric sensor with silicon interaction target

Approaches 1 and 3 were the subject of Raytheon proposal to DARPA of October 1983, while approach 2 was the subject of proposal addendum of May 1984. These three approaches were investigated in detail, while only a minor effort was devoted to approaches 4 and 5.

**The Initial Investigation Performed Under the First DARPA Contract
No. F49620-85-C-0030 (1985-1987) – Neutrino Detection (Cont)**

Approaches 1, 2 and 3 were found deserving of experimental verification, and Raytheon recommended to DARPA that three sensors, for approaches 1, 2 and 3, be built and tested with neutrino sources.

4

In the meantime, DARPA's programmatic interest moved in the direction of providing a rigorous verification of Prof. Weber's claim that he had detected the radiation pressure of low-energy neutrinos with room-temperature instrumentation.

Consequently, the follow-on contract that was awarded to Raytheon in 1987 (F49620-87-C-0050) had as its main objective to perform tests with radiation pressure sensors, with only a minor effort devoted to the magnetic interaction approach, and no effort for the remaining approaches.

**Follow-on Contract DARPA No. F49620-87-C-0050 (1987-to-date) Main
Objective of the Raytheon Investigation – Neutrino Detection**

Raytheon has been tasked by DARPA to attempt to independently reproduce the experimental results reported by Prof. Joseph Weber: i.e., that he has detected the radiation pressure of neutrinos with room-temperature instrumentation.

This assignment will be fulfilled by using a room-temperature torsion balance and a neutrino chopper-and-tuning fork constructed under Prof. Weber's guidance by University of Maryland.

Current plans call for repeating Weber's measurements by using a 100 kilocurie tritium source contained in a 3.5" sphere, made available to Raytheon by DARPA.

Further measurements will be performed by using a Raytheon cryogenic force sensor at 4°K with a better expected sensitivity than Weber's two room-temperature instruments.

Follow-on Contract DARPA No. F49620-87-C-0050 (1987-to-date) Main Objective of the Raytheon Investigation - Neutrino Detection

Raytheon has been tasked by DARPA to attempt to independently reproduce the experimental results reported by Prof. Joseph Weber: i.e., that he has detected the radiation pressure of neutrinos with room-temperature instrumentation.

This assignment will be fulfilled by using a room-temperature torsion balance and a neutrino chopper-and-tuning fork constructed under Prof. Weber's guidance by University of Maryland.

Current plans call for repeating Weber's measurements by using a 100 kilocurie tritium source contained in a 3.5" sphere, made available to Raytheon by DARPA.

Further measurements will be performed by using a Raytheon cryogenic force sensor at 4°K with a better expected sensitivity than Weber's two room-temperature instruments.

Fundamental Guidelines for the Conduct of Weber Verification Tests (JASON/DARPA Formulation) – Neutrino Detection

Raytheon will identify and reduce, as much as practical, possible causes (other than neutrino radiation pressure) of Weber's experimental results, if these are confirmed by the verification tests.

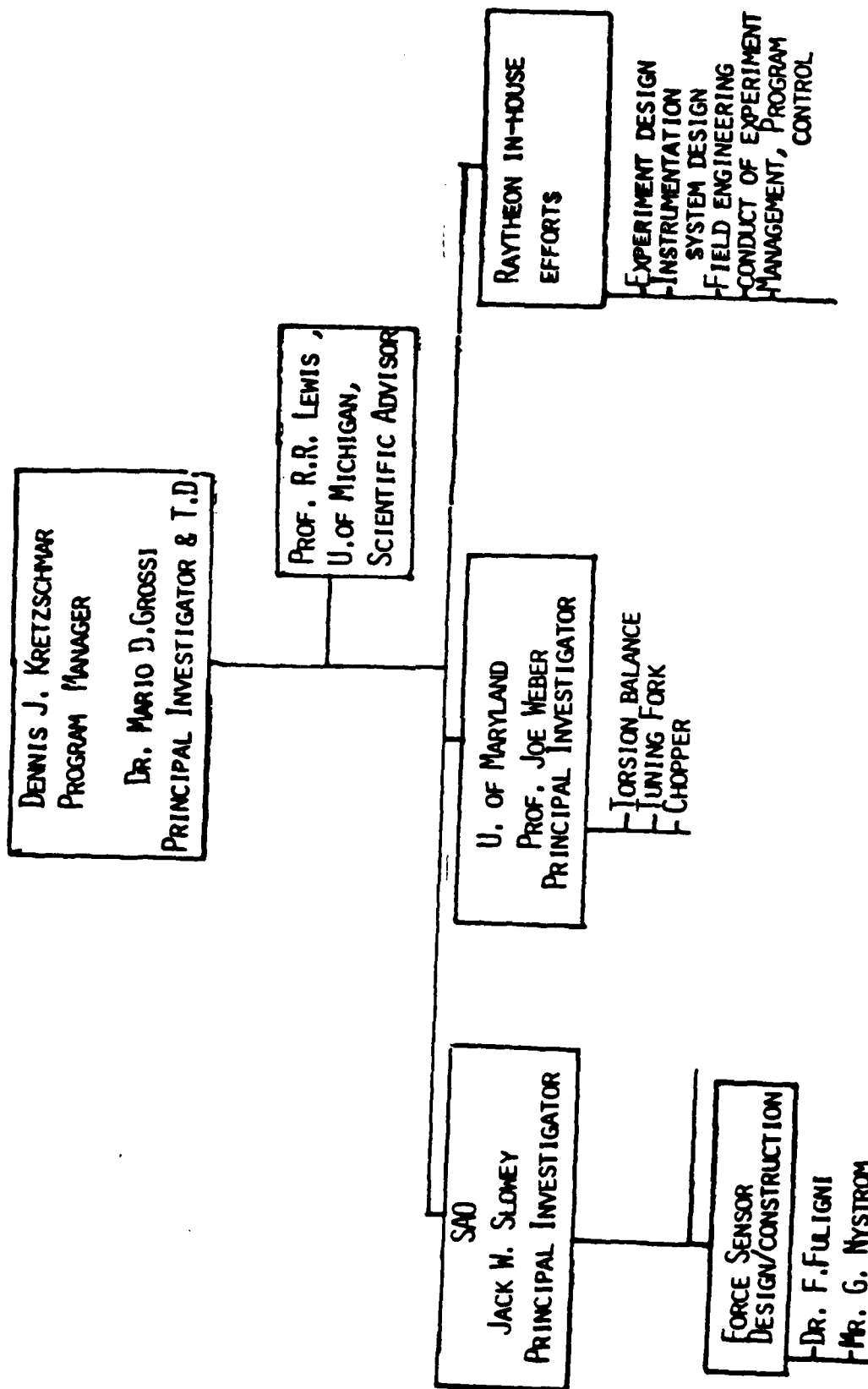
In particular, Raytheon will investigate the following mechanisms as potential sources of signals that might mimic the neutrino radiation pressure:

- Time variable Newtonian gradients produced by the rotating table that holds the source(s)
- As above, for the fifth force
- Time variable thermal radiation (and related radiation pressure) also associated with rotating source
- Time variable magnetic fields and electrostatic fields, of possible external as well as internal origin
- Effects of mechanical vibrations, inclusive of motion of instrument operators in the experiment room

Raytheon will remove, as much as practical, the above effects and will measure the residuals after correction in order to establish unambiguously the origin of candidate signals at the output of the sensors.

RAYTHEON NEUTRINO DETECTORS PROGRAM ORGANIZATION

WEBER VERIFICATION EFFORT



MEASUREMENTS TO BE PERFORMED TO SATISFY REQUIREMENTS
OF CONTRACT F49620-87-C-0050

AT LOS ALAMOS NATIONAL LABORATORY (LANL)

(a) Start as soon as possible tests with Prof. Weber's Torsion Balance.
Required instrumentation :

1. Torsion Balance (already available from U. of Maryland)
 2. Rotating Table, 1 RPM (expected to be available mid July 1988)
 3. Data acquisition system (expected to be available mid July 1988)
 4. 100 Kilocurie tritium source and one dummy (already available at LANL)
- (b) Start as soon as possible tests with Prof. Weber's Tuning Fork.
Required instrumentation (built under direct contract from DARPA/AFOSR to U. of Maryland):
5. Tuning Fork (already available from U. of Maryland)
 6. Small-size rotating shutter (already available from U. of Maryland)

(c) Tests with Cryogenic Force sensor will start in September 1988.
Required instrumentation :

7. Cryogenic Force Sensor in 4°K cryostat
8. Large-size rotating shutter (to be built by U. of Maryland)
9. Tripod with vibration-abatement provisions (under construction at SAO)

MEASUREMENTS TO BE PERFORMED TO SATISFY REQUIREMENTS

OF CONTRACT F49620-87-C-0050

(Continued)

AT RAYTHEON PORT: UTH LABORATORIES

- (a) Tests with SQUID magnetometer on fundamental performance parameters affecting feasibility of magnetic interaction sensor will be performed starting late August 1988.

Specific measurements: (a) highest achievable relative permeability in permalloy target (about 1 Kg material) when operating on the steepest side of the hysteresis cycle;

(b) minimum achievable intrinsic noise density with SQUID magnetometer, when this is loaded by a large-mass, high-permeability target;

(c) maximum achievable pick-up area by pick-up coil of SQUID.

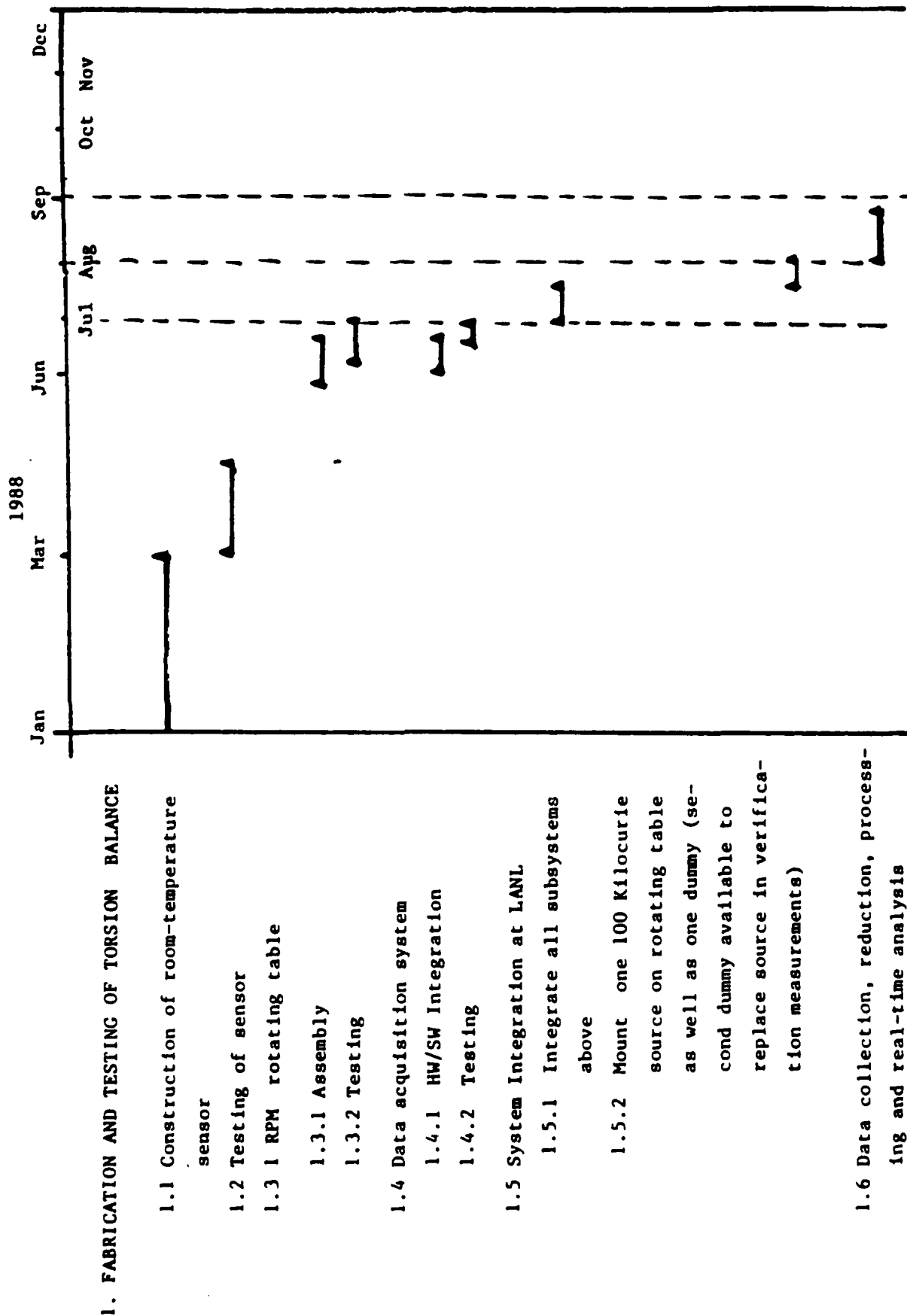
Required instrumentation:

1. SQUID magnetometer in 4°K cryostat (IESS-CNR)
2. Tripod with vibration abatement provisions(SAO)
3. Data acquisition system (already available at Raytheon)

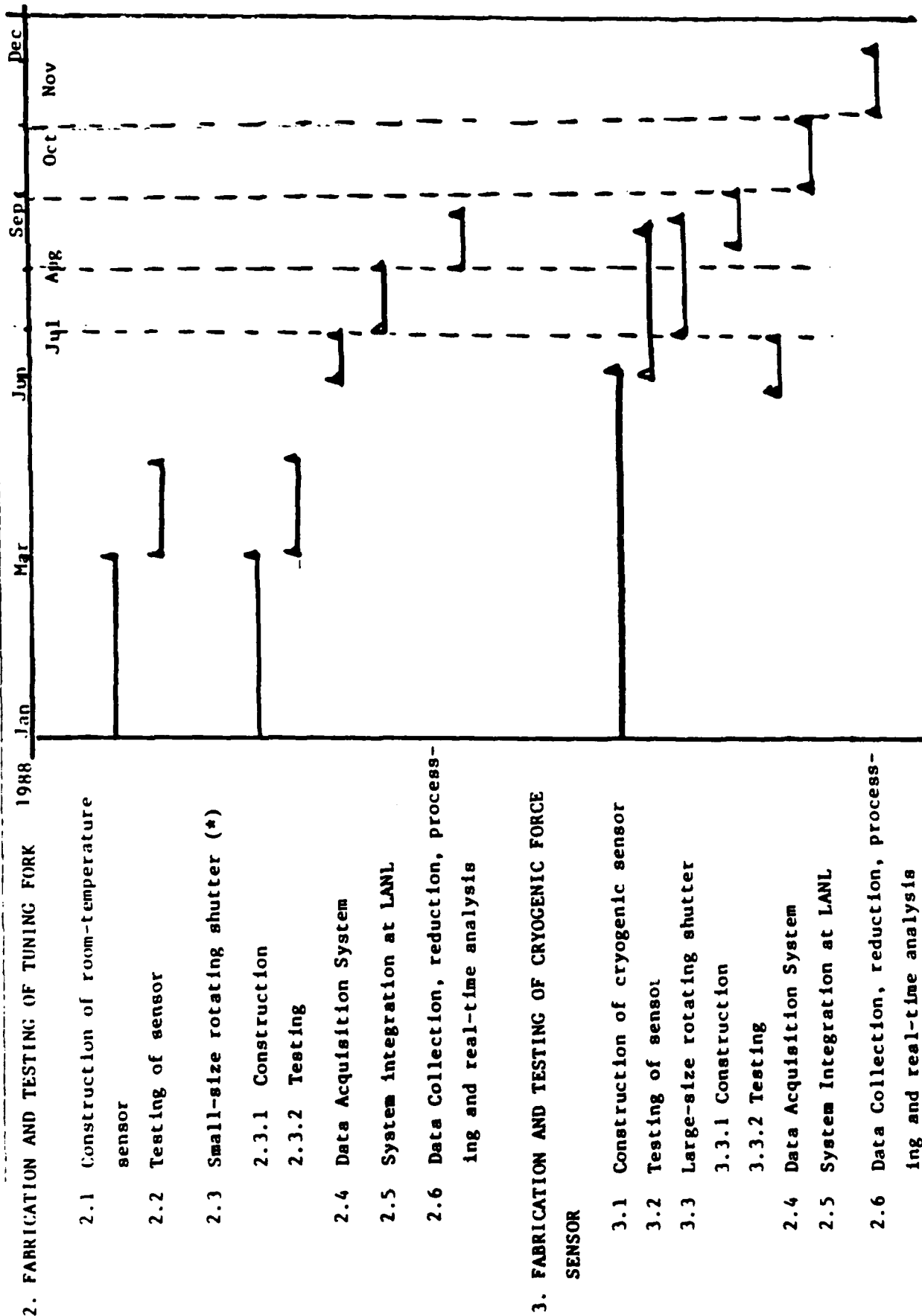
Tritium Sources

Not required for the measurements above

RAYTHEON NEUTRINO DETECTORS PROGRAM - TASK DESCRIPTION AND SCHEDULE



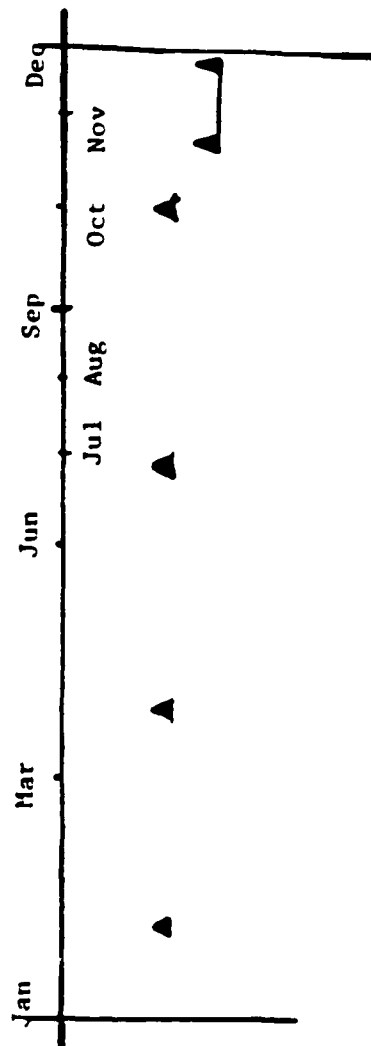
RAYTHEON NEUTRINO DETECTORS PROGRAM - TASK DESCRIPTION AND SCHEDULE (Continued)



(*) This is constructed and tested at U. of Maryland under a direct contract awarded to the University by DARPA/AFOSR

RAYTHEON NEUTRINO DETECTORS PROGRAM - TASK DESCRIPTION AND SCHEDULE (Continued)

1988



4. REPORTING ACTIVITY

- 4.1 Quarterly Reports
- 4.2 Final Report

REQUIRED TRITIUM SOURCES

(FOR USE IN TESTING DETECTORS OF LOW-ENERGY NEUTRINOS)

- | | |
|-------------------------------|--|
| 0 SOURCE INTENSITY | EQUAL OR LARGER THAN 100 KILOCURIE
(1 CURIE \rightarrow 3.4 $10^{10} \bar{\nu}$ sec ⁻¹) |
| 0 FLUX AT A DISTANCE OF 25 CM | $\geq 4.3 \cdot 10^{11} \bar{\nu}$ cm ⁻² sec ⁻¹ |
| 0 SHAPE AND SIZE OF CONTAINER | A SPHERE OF 3.5" DIAMETER OR SMALLER

A CYLINDER WITH DIAMETER SMALLER THAN 6" AND WITH LENGTH SHORTER THAN 15" (WITH THE TRITIUM CONFINED TO A SEGMENT OF THE CYLINDER NOT LONGER THAN 3", AT ONE OF THE BASES OF THE CYLINDER) |
| 0 NUMBER OF SOURCES REQUIRED | AT LEAST THREE, TO CARRY-OUT SIMULTANEOUS MEASUREMENTS WITH THE 1 RPM ROTARY TABLE AND WITH EACH OF THE TWO CHOPPERS |
| 0 NUMBER OF DUMMIES REQUIRED | AT LEAST FOUR (TWO ON THE 1 RPM ROTATING TABLE, MOUNTED RADIALLY, HEAD-TO-HEAD; ALSO, ONE EACH FOR THE TWO CHOPPERS) |

MAXIMUM

EXPECTED INTENSITY OF FORCE SIGNAL GENERATED BY A

100 KILOCURIE TRITIUM SOURCE

- 0 F_{SIG} CANNOT EXCEED THE FORCE THAT WOULD RESULT FROM THE TRANSFER TO THE TARGET ,
OF THE TOTAL MOMENTUM OF THE NEUTRINOS INTERSECTED BY THE TARGET'S AREA.

- 0 THEREFORE, WE HAVE :

$$F_{SIG} \leq j \left(\frac{E_{\nu}}{c} \right) \cdot A$$

WHERE

$$j = \text{FLUX} = 1.2 \cdot 10^{12} \nu \text{ CM}^{-2} \text{ SEC}^{-1} \quad (\text{THIS IS THE FLUX FROM A 100 KILO- CURIE SOURCE AT A DISTANCE OF 15 CM} \rightarrow 3.4 \cdot 10^{10} \nu \text{ SEC}^{-1})$$

$$E_{\nu} \approx 10 \text{ KeV } (= 10^4 \cdot 1.6 \cdot 10^{-12} \text{ ERG})$$

$$A \approx 50 \text{ CM}^2 \text{ (AREA OF THE TARGET, A SAPPHIRE CRYSTAL)}$$

$$c = \text{VELOCITY OF LIGHT} = 3 \cdot 10^{10} \text{ CM SEC}^{-1}$$

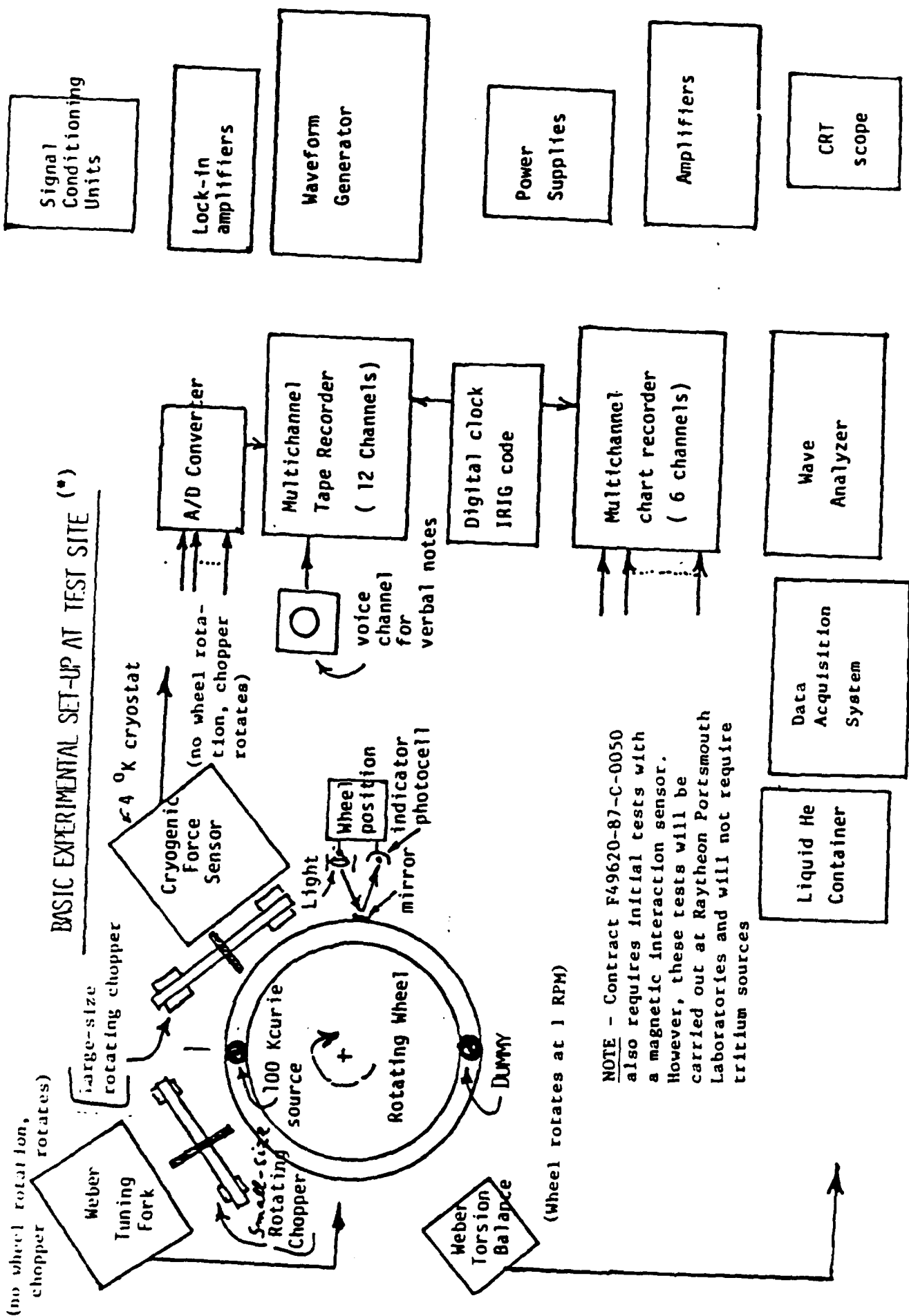
AND , NUMERICALLY:

$$F_{SIG} \leq 3.2 \cdot 10^{-5} \text{ DYNES}$$

- 0 IT IS PRUDENT TO DESIGN A SENSOR WITH A SENSITIVITY MARGIN OF 10^3 . UNDER THESE CIRCUMSTANCES, THE THRESHOLD SENSITIVITY OF THE INSTRUMENT SHOULD BE $3.2 \cdot 10^{-8}$ DYNES.

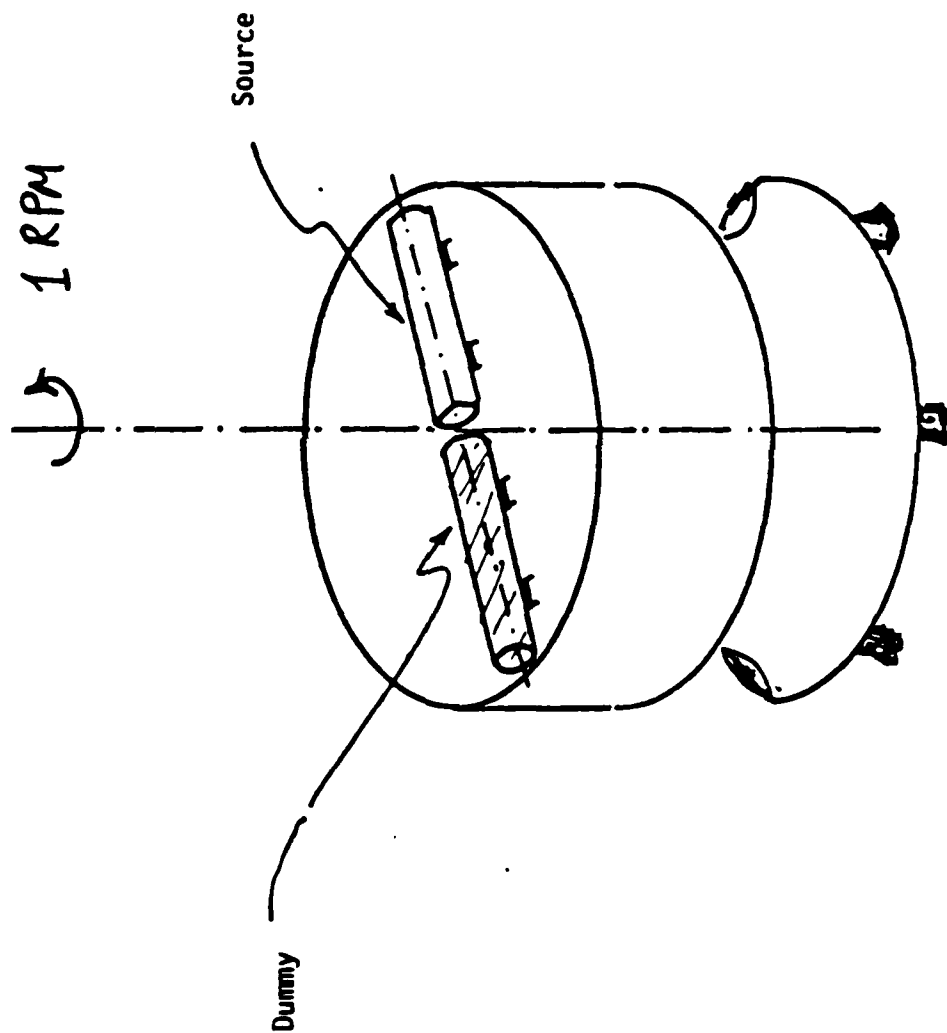
POSSIBLE SOURCES OF MEASUREMENT ERRORS THAT HAVE BEEN IDENTIFIED
AND THAT REQUIRE SPECIAL ATTENTION

1. ISOLATION OF INSTRUMENTS FROM MECHANICAL VIBRATIONS, SEISMIC OSCILLATIONS,
GRAVITY GRADIENT NOISE, TO A DEGREE COMPATIBLE WITH REQUIRED SENSITIVITY
2. ABATEMENT OF VIBRATIONS PRODUCED BY ROTATING SOURCE ASSEMBLY AND CHOICE OF
SIGNAL FREQUENCY TO MINIMIZE EFFECTS OF RESIDUAL VIBRATIONS THAT REACH SENSORS
3. OTHER SOURCES OF SPURIOUS SIGNALS THAT HAVE BEEN IDENTIFIED : TIME-VARIABLE
GRAVITY GRADIENTS, MAGNETIC FIELDS, THERMAL SOURCES- SPECIAL ATTENTION REQUIRED
TO MINIMIZE THEIR EFFECTS ON SENSORS, TO ISOLATE SENSORS FROM RESIDUAL EFFECTS,
TO ASSESS QUANTITATIVELY THEIR REMAINING INFLUENCE



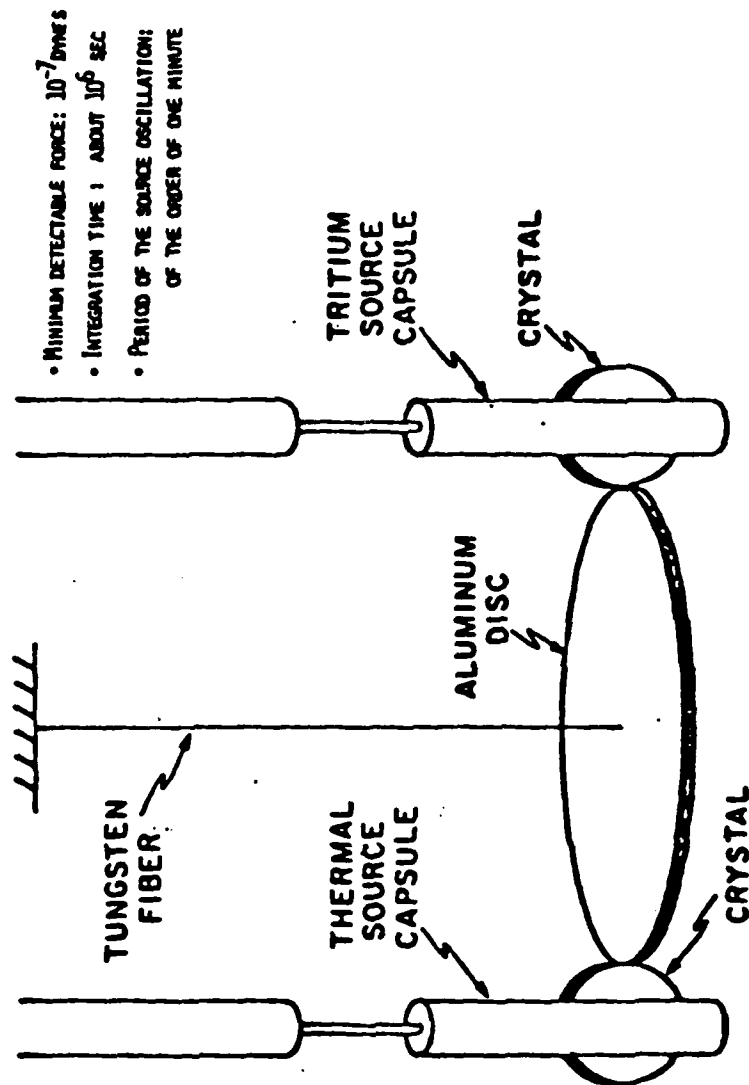
(*) As required by Contract F49620-87-C-0050

1 RPM ROTATING TABLE FOR USE WITH WEBER'S TORSION BALANCE



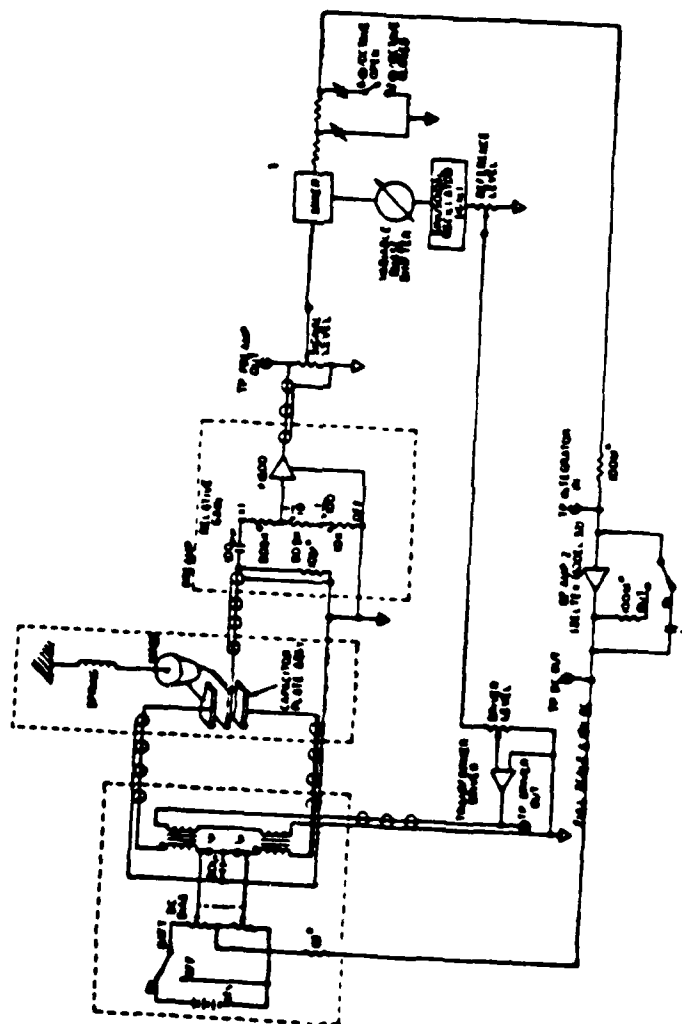
TORSION BALANCE WITH 3 KILOCURIE SOURCE INITIALLY USED

BY PROF. JOE WEBER



- MINIMUM DETECTABLE FORCE: 10^{-7} DYNES
- INTEGRATION TIME : ABOUT 10^6 SEC
- PERIOD OF THE SOURCE OSCILLATION: OF THE ORDER OF ONE MINUTE

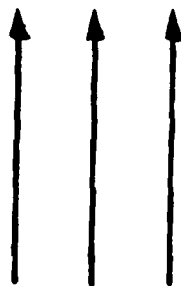
WEBER TORSION BALANCE - ELECTRONICS



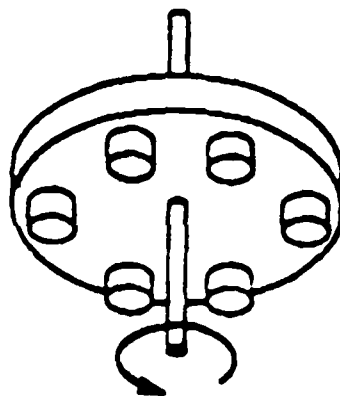
SCHEMATIC DIAGRAM OF OVERALL INSTRUMENT

MEIER TUNING FORK AND ROTATING CHOPPER

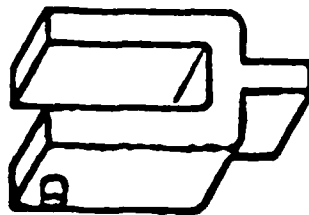
Neutrinos
From
Reactor



Wheel
With
Crystals



Tuning Fork
With
Crystal

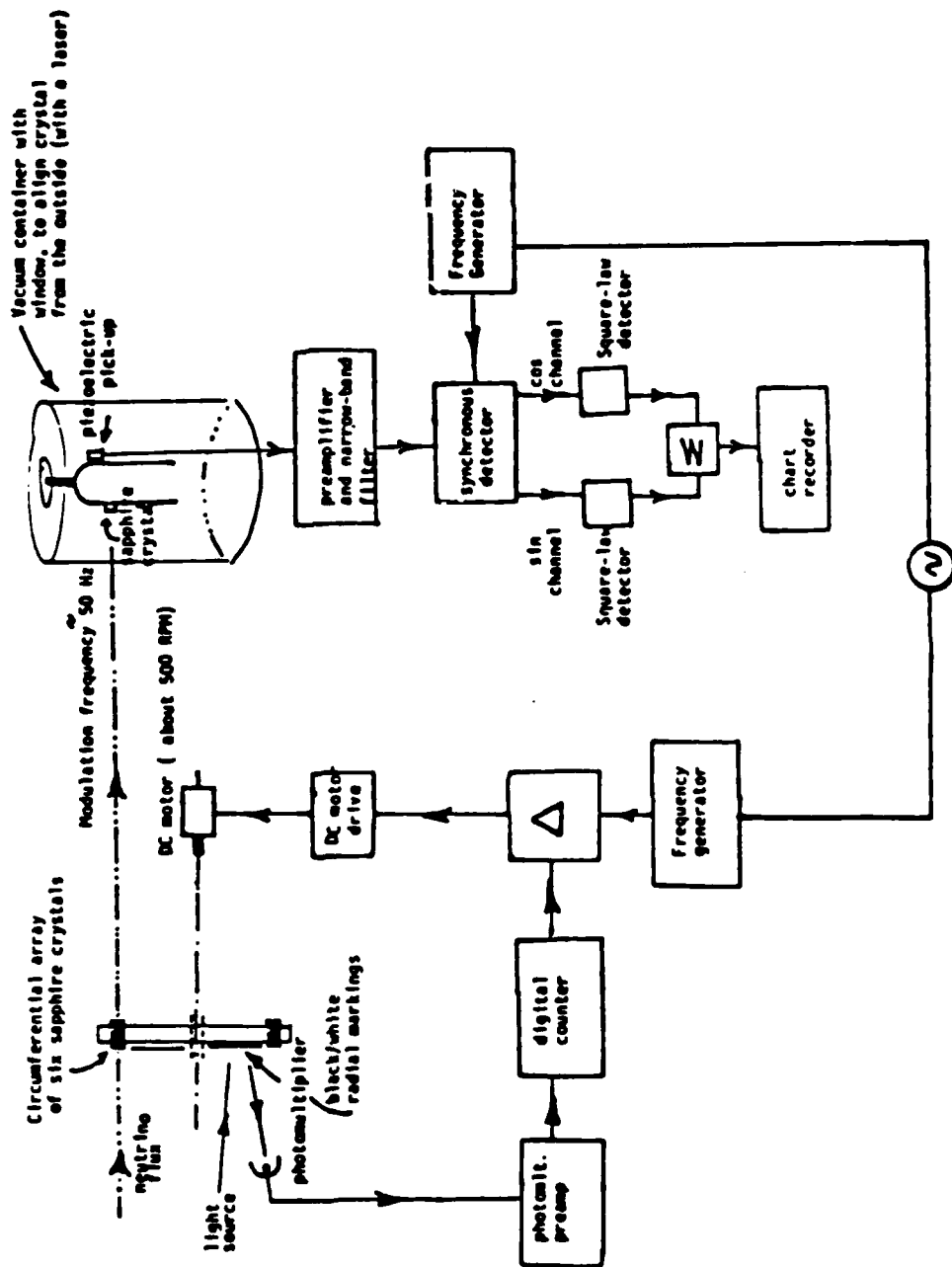


Tuning Fork Vibrates at Resonance Due to
Chopper-Modulated Neutrino Flux

- MINIMUM DETECTABLE FORCE 10^{-7} DYNES
- INTEGRATION TIME $\sim 10^2$ SEC

WEBER'S TUNING FORK INSTRUMENTATION SYSTEM

SIMPLIFIED BLOCK DIAGRAM

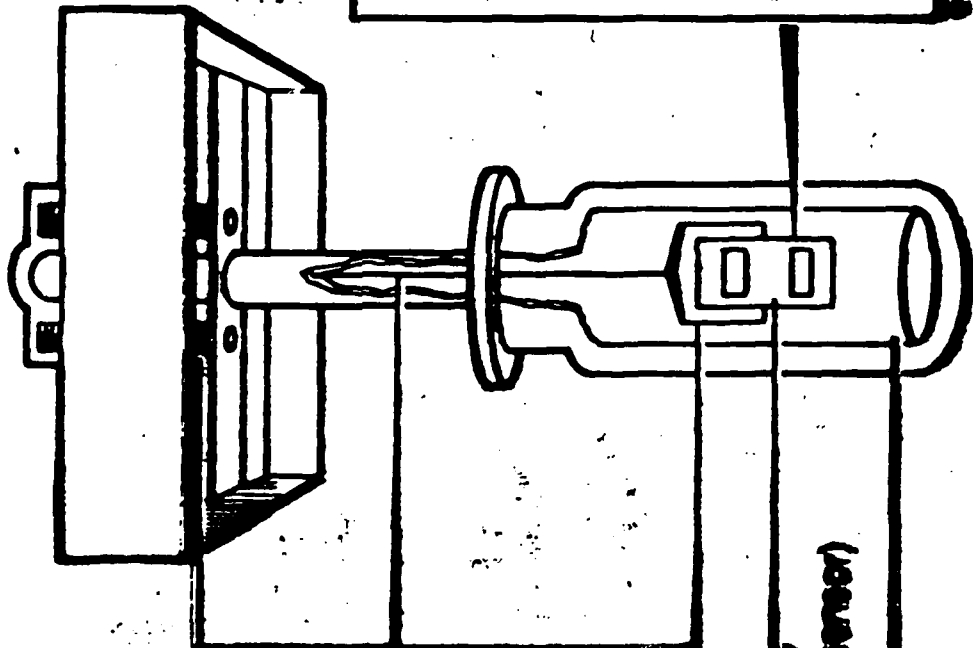


Neutrino Detector. . .Cryogenic Force Sensor

Laboratory tests

- Tritium source
- Neutrino flux
- Force (assuming total momentum transfer)
- Instrument sensitivity

10^5 curie
 4.5×10^{11} cm⁻² sec⁻¹
 (at 20 cm)
 1.18×10^{-8} dynes
 10^{-8} dynes (in 10^4 sec
 integration time)

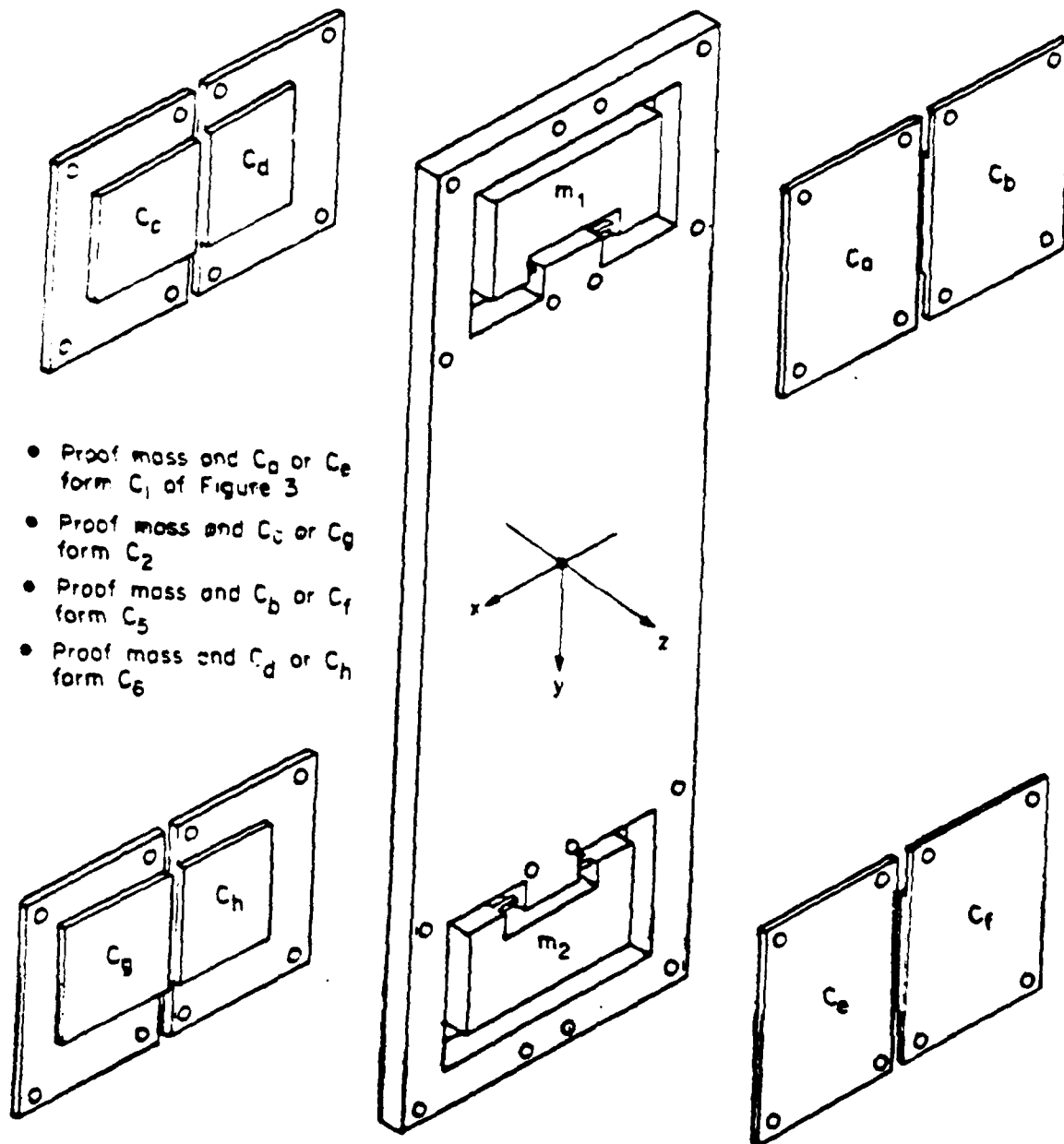


Suspension with
Vibration Isolation

Gravity Gradient
(single-axis, 2-sat sensor)

4°K Cryostat

MECHANICAL STRUCTURE OF GRAVITY GRADIOMETER



THE CRYOGENIC FORCE SENSOR (IN A 4°K CRYOSTAT)

BASIC PERFORMANCE PARAMETERS

- MASS 250 GR
- TEMPERATURE 4° K
- RESONANCE FREQUENCY 100 Hz
- Q FACTOR 10^4
- REQUIRED INTEGRATION TIME 10^4 SECONDS
- MINIMUM DETECTABLE FORCE 10^{-8} DYNES
- OSCILLATION DECAY TIME 32 SECONDS
- REQUIRED ABATEMENT OF VIBRATION NOISE ≥ 150 DB

Numerical Estimate of Minimum Detectable Force Signal (Neutrino Radiation Pressure)

Minimum detectable force signal, at resonance, by each one of the sensing cells, in absence of vibrations.

$$F \geq \sqrt{\frac{2kTm\omega_0}{Q t_{INT}}}$$

Where:

$k = 1.38 \cdot 10^{-23}$ Joules (deg K)⁻¹

$m = 0.250$ kg

$T = 4^\circ\text{K}$

$\omega_0 = 2 \pi \cdot 10^2$

$Q = 10^4$; $t_{INT} = 10^4$ seconds

Therefore:

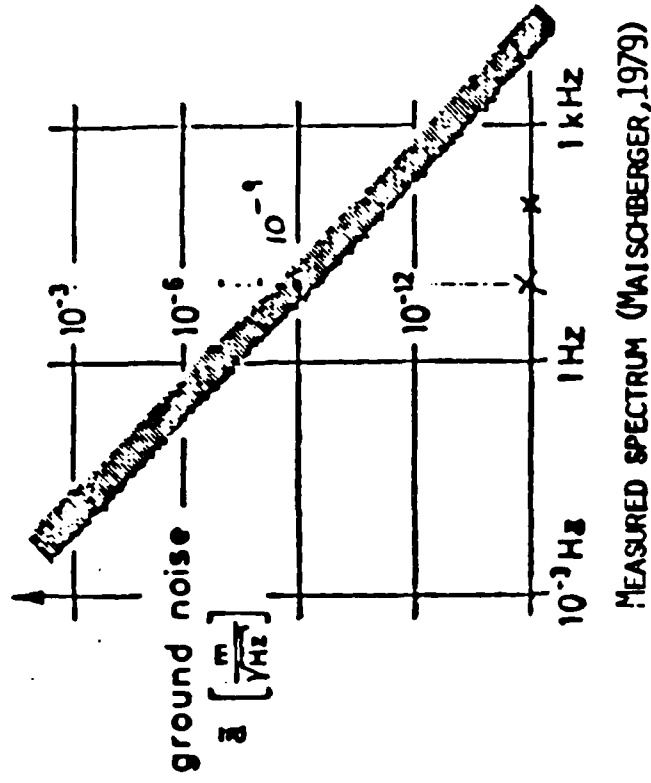
$F \geq 1.3 \cdot 10^{-14}$ Newton =
1.3 10^{-9} dynes

Adopted Sensitivity Specification: 10^{-8} dynes

Minimum detectable gradient (baseline = 20 cm): 2.83×10^{-3} Eötvös units

ESTIMATE OF VIBRATION NOISE

0 DISPLACEMENT NOISE DENSITY (MAX PLANCK INSTITUTE)



0 ADOPTED VALUES , IN OUR SYSTEM STUDIES (CONSERVATIVE ASSUMPTION)

AN ORDER OF MAGNITUDE WORSE THAN ABOVE SPECTRUM
(AT 100 Hz, $\ddot{a} = 10^{-8} \text{ cm}/\sqrt{\text{Hz}}$)

0 ACCELERATION NOISE AT 100 Hz

ACCELERATION NOISE DENSITY :

$$(2\pi 100)^2 \cdot 10^{-8} \approx 4 \cdot 10^{-3} \text{ gal}/\sqrt{\text{Hz}}$$

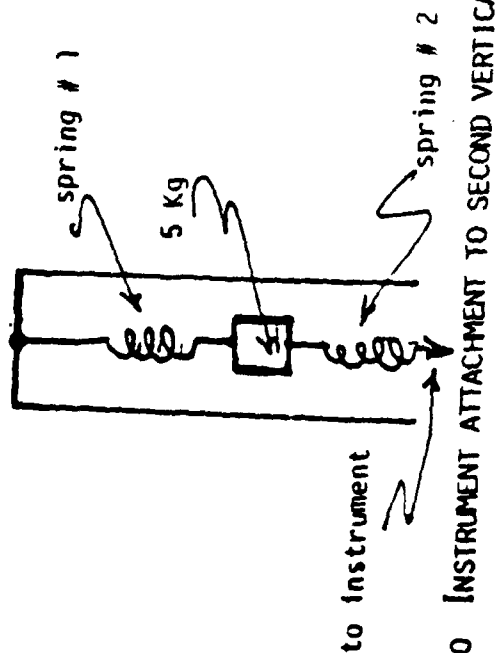
WITH A 10^4 SECONDS INTEGRATION TIME, ACCELERATION
NOISE AT EACH CELL IS $4 \cdot 10^{-5}$ GAL

AN APPROACH TO ABATE MECHANICAL VIBRATIONS AND SEISMIC OSCILLATIONS

0 REQUIRED OVERALL VIBRATION ATTENUATION

150 DB

0 PASSIVE, SIMPLE, TWO-SPRING, SYSTEM



0 CHECKING THE ANGULAR POSITION OF THE INSTRUMENT INSIDE THE CRYOSTAT

EACH VERTICAL SPRING RESONATES AT 1 Hz
AND PROVIDES AN ATTENUATION OF 80 DB AT
THE FREQUENCY OF THE SIGNAL (100 Hz).

TOTAL ATTENUATION PROVIDED BY THE SPRING
PAIR 160 DB

BY ADDING THE CONTRIBUTION TO THE ATTENUATION
DUE TO THE COMMON-MODE REJECTION (80 DB), WE
ACHIEVE A GRAND TOTAL ATTENUATION OF....240 DB
(WITH A 90 DB MARGIN WITH RESPECT TO REQUIREMENT

BY FRICTION-LESS GIMBALS, THE CENTER OF MASS OF
THE INSTRUMENT BEING THE ACTUAL SUSPENSION POINT

BY FIBER OPTICS VISUAL OBSERVATIONS FROM THE
OUTSIDE

A BACK-OF-AN ENVELOPE ESTIMATE OF SIGNAL-TO-NOISE RATIO

0 ACCELERATION SIGNAL INTENSITY

A MINIMUM DETECTABLE FORCE OF 10^{-8} DYNES
APPLIED TO A 250 GR MASS PRODUCES AN ACCELERATION
OF $10^{-8} / 250 = 4 \cdot 10^{-11}$ GAL.

0 REQUIRED EXTENT OF VIBRATION ABATEMENT

BECAUSE THE ACCELERATION NOISE IN THE LABORATORY
IS $4 \cdot 10^{-5}$ GAL (SEE PREVIOUS SLIDE), WE REQUIRE
AN ABATEMENT OF AT LEAST

$$\frac{4 \cdot 10^{-5}}{4 \cdot 10^{-11}} = 10^{-6} \text{ OR } -120 \text{ DB}$$

0 ADOPTED VALUE FOR MINIMUM ACCEPTABLE VIBRATION ABATEMENT (CONSERVATIVE)

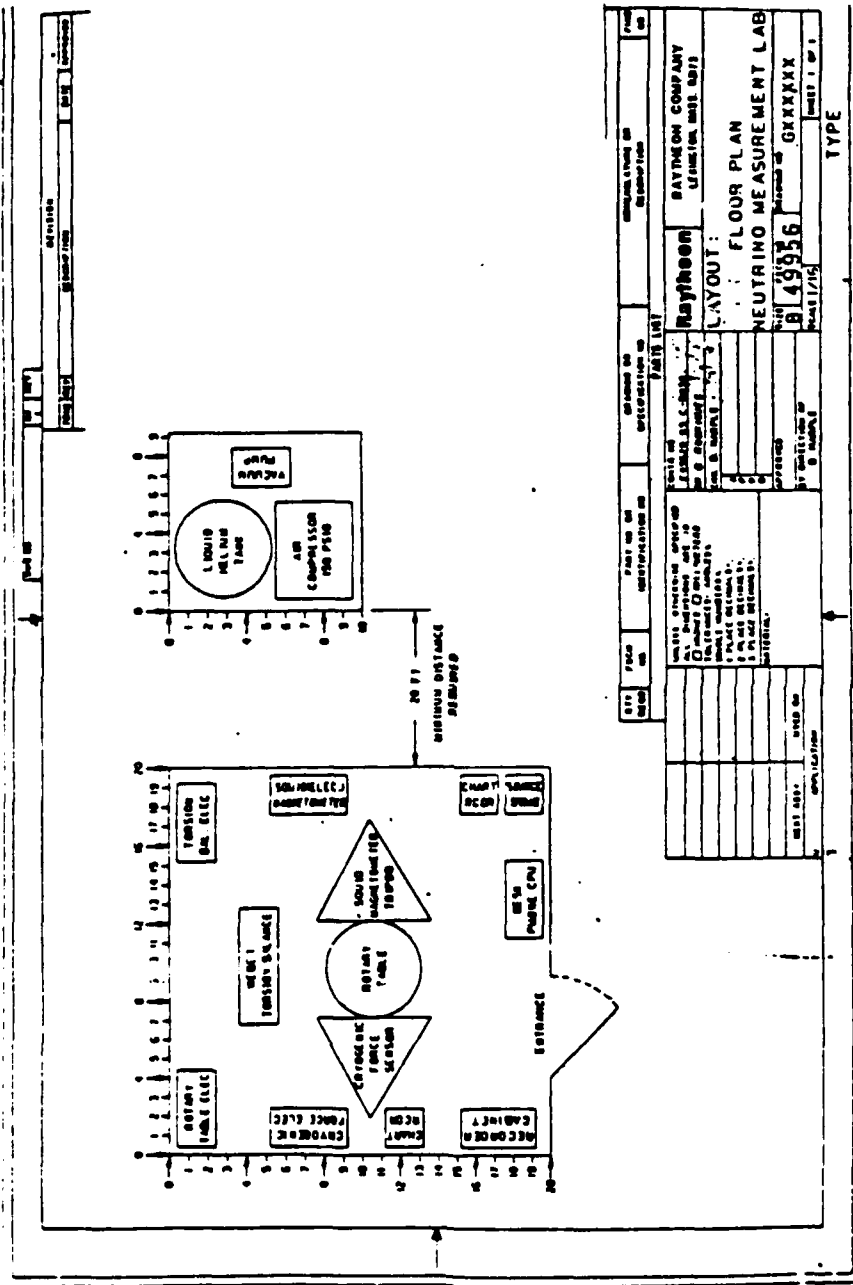
- 150 DB

0 WHAT DO WE EXPECT TO ACHIEVE ?

COMMON MODE REJECTION WILL PROVIDE AN ISOLATION
OF AT LEAST 10^{-4} OR 80 DB.

BY USING A SUSPENSION WITH RESONANCE FREQUENCY
OF 1 HZ, EASY TO MECHANIZE, WE ACHIEVE AN ISOLATION
(AT 100 HZ) OF 10^{-4} OR 80 DB. THIS PROVIDES A
TOTAL ISOLATION OF -160 DB, 10 DB MORE THAN
REQUIRED.

.....



BASIC PLAN OF MEASUREMENTS AT LANL

(A) MEASUREMENTS TO BE CARRIED-OUT WITHOUT THE USE OF A TRITIUM SOURCE

A.1 TRITIUM SOURCE IS REPLACED BY A DUMMY THAT HAS THE SAME MASS, SHAPE AND SIZE OF THE TRITIUM SOURCE

A.1.1 WEBER TORSION BALANCE

- 0 MEASUREMENT OF SENSOR OUTPUT WITH ROTATING WHEEL TURNED OFF 168 HOURS
- 0 MEASUREMENTS AS ABOVE, WITH WHEEL TURNED ON 168

A.1.2 WEBER TUNING FORK

- 0 MEASUREMENTS WITH SMALL-SIZE CHOPPER TURNED OFF 168
- 0 MEASUREMENTS WITH CHOPPER TURNED ON 168

A.1.3 CRYOGENIC FORCE SENSOR

- 0 MEASUREMENTS WITH LARGE-SIZE CHOPPER TURNED OFF 168
- 0 MEASUREMENTS WITH CHOPPER TURNED ON 168

(B) MEASUREMENTS TO BE CARRIED-OUT WITH THE TRITIUM SOURCE IN USE

B.1 TRITIUM SOURCE IS MOUNTED ON THE 1 RPM ROTATING TABLE

B.1.1 WEBER TORSION BALANCE

- 0 MEASUREMENTS WITH ROTATING TABLE TURNED ON 168

B.1.2 WEBER TUNING FORK

- 0 MEASUREMENTS WITH SMALL-SIZE CHOPPER TURNED ON 168

B.1.3 CRYOGENIC FORCE SENSOR

- 0 MEASUREMENTS WITH LARGE-SIZE CHOPPER TURNED ON 168

TOTAL MEASUREMENT TIME 1,512 HOURS

ADDITIONAL MEASUREMENTS

(TO BE CARRIED-OUT IF WARRANTED BY THE RESULTS OF THE BASIC MEASUREMENT CAMPAIGN)

(C) TRITIUM SOURCE IS REPLACED BY A DUMMY WITH EQUAL MASS, SIZE AND SHAPE, CONTAINING A BATTERY OPERATED HEATER

C.1	WEBER TORSION BALANCE, 1 RPM TABLE IS TURNED ON	168 HOURS
C.2	WEBER TUNING FORK, SMALL-SIZE CHOPPER IS TURNED ON	168
C.3	CRYOGENIC FORCE SENSOR, LARGE-SIZE CHOPPER IS TURNED ON	168

(D) TRITIUM SOURCE IS REPLACED BY A DUMMY WITH EQUAL MASS, SIZE AND SHAPE, CONTAINING A PERMANENT MAGNET

D.1	WEBER TORSION BALANCE, 1 RPM TABLE IS TURNED ON	168
D.2	WEBER TUNING FORK, SMALL-SIZE CHOPPER IS TURNED ON	168
D.3	CRYOGENIC FORCE SENSOR, LARGE-SIZE CHOPPER IS TURNED ON	168

TOTAL TIME REQUIRED FOR ADDITIONAL MEASUREMENTS	1,008 HOURS
---	-------------

DESIRABLE EXPANSION OF PRESENTLY FUNDED AND PLANNED MEASUREMENT CAMPAIGN AT LANL

1. Construct and use with Cryogenic Force Sensor a 2000 RPM rotating table.
Rationale : achieve intensity modulation of neutrino beam reaching sensor by periodically changing the distance source-to-sensor (signal frequency 100 Hz, with three sources mounted on the rim of the wheel)
At present, beam modulation for use with cryogenic force sensor is attempted by using Weber's large-size rotating shutter.

Status of this initiative : Added-scope proposal for the 2000 RPM rotating table, complete with vacuum system and air spindle has been submitted by Raytheon to DARPA in April 1988. Proposal still under review.

2. Complete development of magnetic interaction sensor for tests at LANL with tritium sources, under the assumption that present tests scheduled at Raytheon Portsmouth for Summer 1988 are successful.

Required instrumentation: Large Cryostat at 4°K (initial design was performed under a Raytheon subcontract by Meyer Tool Mfg. Co., Inc.).
Approximate cost 40 K .

250-Kg ,high-permeability interaction target. Approximate cost 150 K.

3. Construct dilution refrigeration cryostats for tests at 4 millioK of the Cryogenic Force Sensor and of the Magnetic Interaction Sensor.

CONCLUSIONS AND RECOMMENDATIONS

- 0 RAYTHEON WOULD WELCOME THE POSSIBILITY THAT THE FEASIBILITY TESTS REQUIRED TO PROVE/DISPROVE THE DETECTABILITY OF LOW-ENERGY NEUTRINOS WITH SENSORS THAT THE COMPANY AND ITS SUBCONTRACTORS HAVE BUILT OR ARE ABOUT TO COMPLETE, BE CARRIED OUT AT LOS ALAMOS NATIONAL LABORATORY (LANL)
- 0 CONDUCTING THE TESTS AT LANL WOULD MAKE IT POSSIBLE, IN PRINCIPLE, TO USE IN THE EXPERIMENTS TRITIUM SOURCES THAT WOULD MAXIMIZE THE CHANCES OF SUCCESS, AND HELP DISCRIMINATING THE RESULTS FROM SPURIOUS CAUSES THAT MIGHT MIMIC THE NEUTRINO RADIATION PRESSURE EFFECTS (FOR INSTANCE, IT WOULD BE POSSIBLE TO OBTAIN DUMMIES DESIGNED AND BUILT AT LANL, TO IDENTIFY THE EFFECTS OF NEWTONIAN GRADIENTS, GENERATION OF HEAT, OR MAGNETIC FIELDS)
- 0 THE VERIFICATION OF PROF. WEBER'S CLAIM THAT HE HAS OBSERVED WITH ROOM-TEMPERATURE INSTRUMENTATION THE RADIATION PRESSURE OF LOW-ENERGY NEUTRINOS CAN BE PERFORMED AT LANL MOST EFFECTIVELY, USING MUCH LARGER TRITIUM SOURCES THAN HE WAS ABLE TO EXPERIMENT-WITH AT UNIVERSITY OF MARYLAND.
- 0 ABOVE AND BEYOND THE VERIFICATION TASK ABOVE, RAYTHEON'S OPINION IS THAT CONDUCTING THE FEASIBILITY EXPERIMENTS AT LANL WILL MAKE IT POSSIBLE TO TEST APPROACHES, SUCH AS THE CRYOGENIC FORCE SENSOR, AND LATER-ON, THE MAGNETIC INTERACTION SENSOR, THAT REPRESENT A MASSIVE ATTACK ON THE PROBLEM OF DETECTING LOW-ENERGY NEUTRINOS- AN EXPANSION OF THE PRESENTLY FUNDED MEASUREMENT CAMPAIGN TO INCLUDE A 2000 RPM ROTATING TABLE, THE MAGNETIC INTERACTION SENSOR AND DILUTION REFRIGERATION CRYOSTATS MIGHT COME WITHIN REACH.


SECOND CONTRACT
FIFTH QUARTERLY REPORT
15 AUGUST 1988
EXPERIMENTAL TESTING OF CORPUSCULAR RADIATION DETECTORS

SUBMITTED TO
DEFENSE ADVANCED RESEARCH PROJECT AGENCY (DARPA)
DARPA ORDER #5271
CONTRACT #F49620-87-C-0050

MONITORED BY AIR FORCE OFFICE OF SCIENTIFIC RESEARCH
(AFOSR)

DARPA PROGRAM DIRECTOR: US ARMY LT. COLONEL G. P. LASCHE', PH.D.

The views and conclusions contained in this document are those of the authors and should not be interpreted as necessarily representing the official policies, either expressed or implied, of the Defense Advanced Research Projects Agency or the U.S. Government.

Approved: 
Dennis J. Kretzschmar
Program Manager, Raytheon Co.

RAYTHEON COMPANY
SUBMARINE SIGNAL DIVISION
PORTSMOUTH, RHODE ISLAND 02871

TABLE OF CONTENTS

<u>SECTION</u>	<u>PAGE</u>
o ACKNOWLEDGEMENTS	ii
o EXECUTIVE SUMMARY	iii
o STATUS OF READINESS FOR THE INSTRUMENTATION TO BE USED AT LANL, LOS ALAMOS, N.M.	1
o CONCLUSIONS AND RECOMMENDATIONS	7

ACKNOWLEDGEMENTS

This quarterly report has been prepared by Mario D. Grossi, Principal Investigator, with inputs from all members of the program team.

EXECUTIVE SUMMARY

In this quarter, a substantial milestone was achieved: Raytheon established a laboratory base at LANL, Los Alamos, N.M. and received from LANL three dummies, for installation on the 1 RPM rotating table. Specific accomplishments were as follows.

1. Raytheon 1 RPM rotating table and U. of Maryland room-temperature Torsion Balance were installed in the LANL lab area assigned to the project. The area is in Building 86, Technical Area TA-33.

2. The two pieces of equipment that LANL is constructing for our project under a direct DARPA contract, (the support-stand for the 1 RPM rotating table, and the 40" table-top, where neutrino sources and dummies will be mounted), are scheduled for delivery to TA-33, Bldg. 86 in early September 88.

3. The low-speed, PC-controlled, data acquisition system (based on a Lab/Tech Notebook approach) is expected to be ready for shipment by Raytheon to LANL no later than September 9, 1988.

4. If the LANL neutrino sources are available, Prof. Weber's torsion balance experiment (with real-time presentation of the experiment results) could start around September 12, 1988.

5. Raytheon's cryogenic force sensor, based on the room-temperature gravity gradiometer developed at SAO/IFSI-CNR by Co-Investigator Dr. Fuligni is expected to be ready for 4°K laboratory tests in Portsmouth, RI in the last week of September 1988. According to the DARPA contract, these tests will not require neutrino sources and will be based on the measurement of instrument sensitivity to electrostatically generated "force signals". High-speed data collection (the cryogenic force sensor resonates at 100 Hz, while Weber's torsion balance has a resonance period of 16 seconds) will be performed with the Diabase approach. The software for Diabase does not function yet and will require, most probably, the assistance of the software developers, Morra Inc.

The above instrumentation will be shipped to Los Alamos and tested there with neutrino sources when the 2000 RPM rotating table is available. DARPA has not yet funded the related development effort. A possible date of availability of this table is January 1989, at the earliest.

6. The SQUID magnetometer (built under a 1988 Raytheon in-house IDP project) was successfully assembled and tested in Portsmouth. Based on DARPA's contract, we are scheduling tests at Raytheon on basic feasibility issues concerning the potential use of the SQUID in detecting neutrinos, for the second half of September 1988. As contractually specified, these tests will not require neutrino sources and will consist of the following tasks: (a) measurement of minimum-achievable SQUID intrinsic noise, when the SQUID is loaded by a large-mass, high-permeability interaction target; (b) measurement of maximum-achievable collecting area, using superconducting transformer; (c) measurement of maximum-achievable relative permeability for interaction target.

As can be seen from items 1 through 6 above, Raytheon effort concentrated in getting ready for the verification of the results that Prof. Weber claimed he has obtained with his room-temperature torsion balance. This was the focus of project activity in the past quarter. Progress was, however, also made in the area of the cryogenic force sensor. This will become the next focus of activity, once the tests on the torsion balance have been carried out. Also, we have moved further in another area: the development of the magnetic interaction sensor. For this last instrument, DARPA has only authorized laboratory tests on basic (and controversial), feasibility issues pertaining to magnetic material properties and high-sensitivity SQUID development, with the proviso that Raytheon construct with its own IDP funds, as an in-house effort, the SQUID itself (which Raytheon did).

By the time the next quarterly report is submitted (15 November 1988), we expect that final conclusions will be available concerning Weber's torsion balance, thus completing the most immediate and urgent assignment that Raytheon received from DARPA.

STATUS OF READINESS FOR INSTRUMENTATION TO BE USED AT LANL, LOS ALAMOS, N.M.

1. Room-temperature Torsion Balance

The room-temperature torsion balance, that Prof. Weber has constructed at U. of Maryland under the terms of a Raytheon subcontract, was installed in late July 1988 at LANL. Figures 1, 2 and 3 show the mounting of the instrument. The figures depict a Vac-Ion cryogenic pump which allows torsion balance measurements in vacuum. At this point, the torsion balance has been operated at LANL without vacuum by Prof. Weber and his assistants. With the system addition of an electronic damper, the balance exhibited a damping time of about 39 seconds, and a resonance period of about 16 seconds. The torsion balance was tested by Prof. Weber, after installation at TA-33, LANL and it was found to meet pre-shipment performance. Weber made a crude evaluation of sensitivity by moving two lead bricks near the balance's disk and seeing that the response was identical to what he obtained in Maryland with a similar arrangement. There was also no change in the tendency of the balance to drift away from a mean position. Because of this drift, Raytheon designed its data collection system with the ability to search for a signal, smaller than 1 millivolt, on an overall output that might be as large as ± 10 volts. As requested by Prof. Weber, Raytheon Analog-to-Digital converter will have a resolution of 16 bits (instead of the 12 bits used by Prof. Weber in his tests at U. of Maryland). As a consequence, the overall instrumentation system that Raytheon is assembling at LANL, TA-33, will have superior performance than that achieved in Prof. Weber's torsion balance tests at U. of Maryland.

2. 1 RPM Rotating Table

Figure 4 and 5 show the rotating table that Raytheon has installed at TA-33. There are still two pieces missing from the table: the support-stand and the table-top. LANL will construct these under the terms of a direct DARPA contract. The performance characteristics of the table are given in Table 1. The addition of the two missing subsystem will not affect this performance. The table is controlled from a H-P computer master control, visible in Figure 4.

Figure 1-
Front view of
Torsion Balance

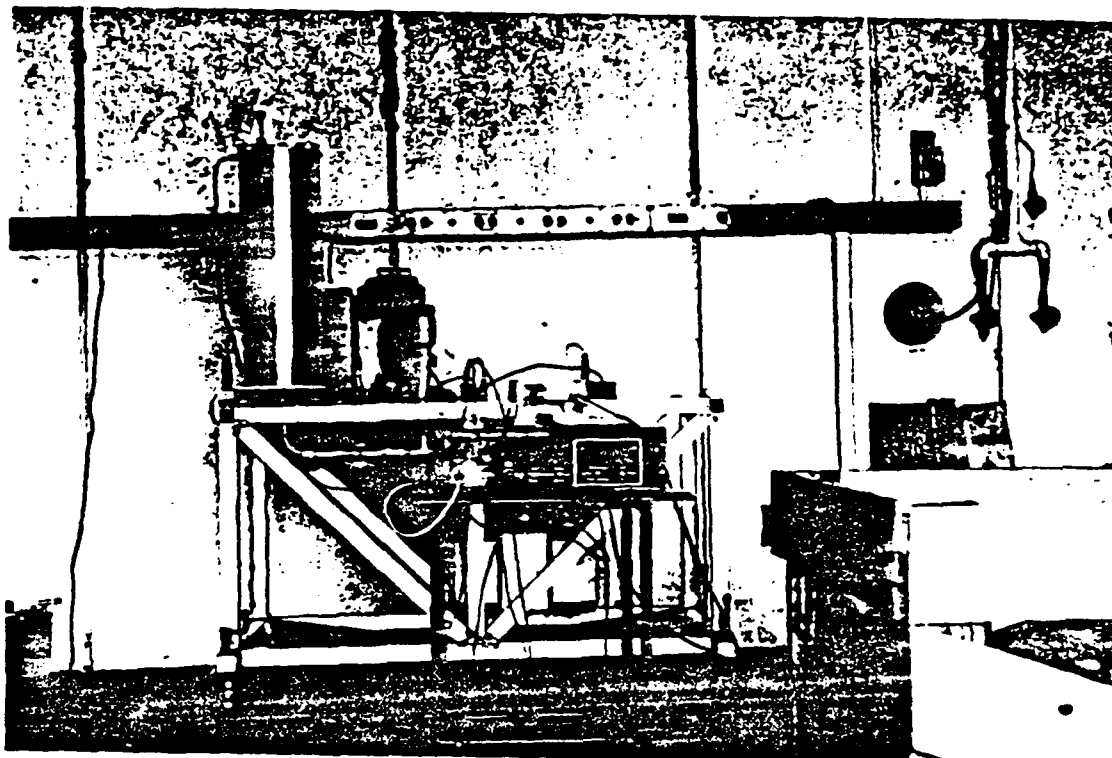


Figure 2 -
Another front
view of the
torsion balance

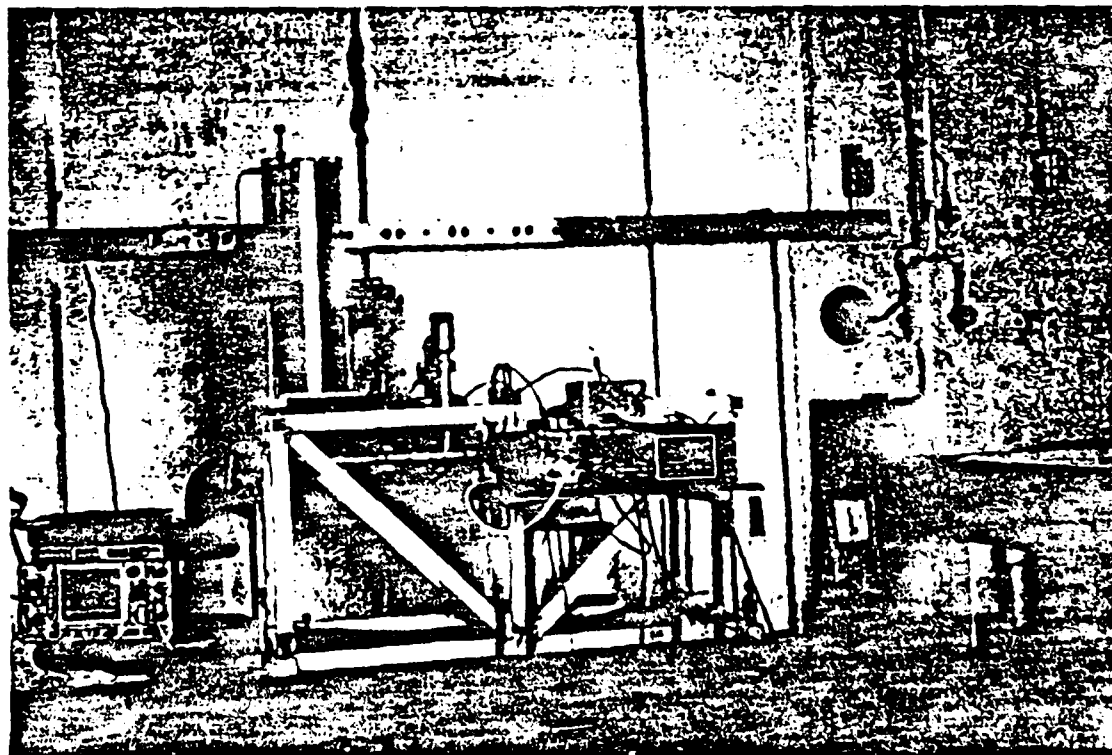


Figure 3-

Side view of the
torsion balance

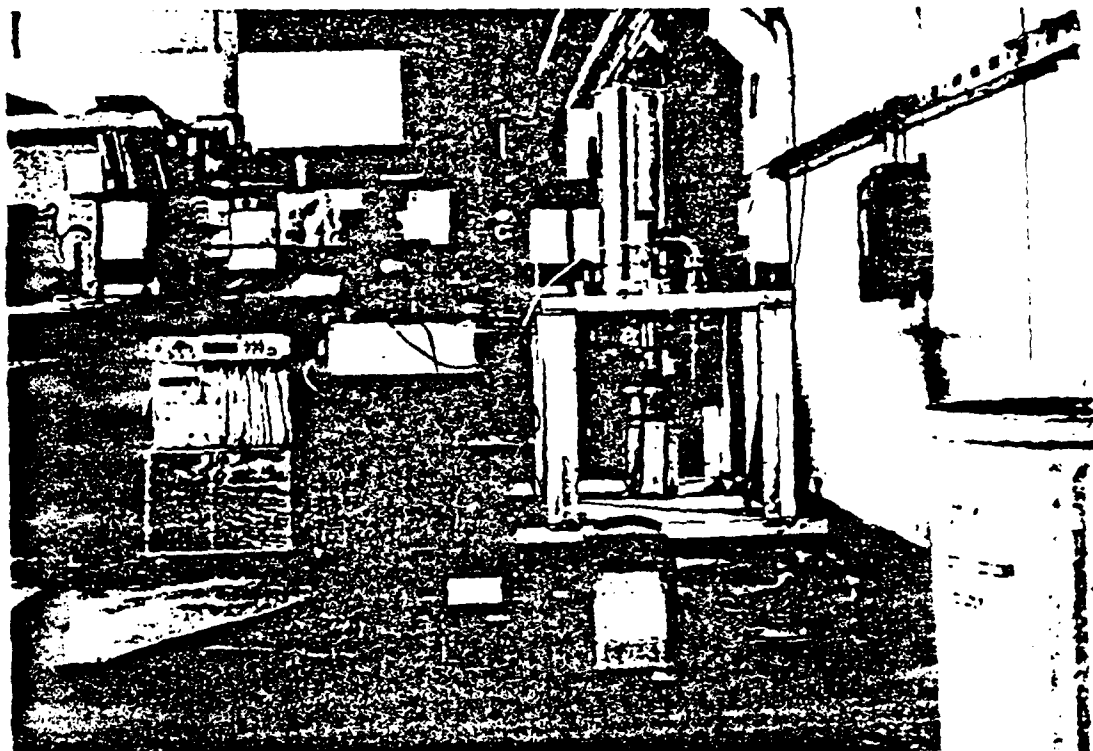


Figure 4 -

The control
unit of the
1 RPM rotating
table.

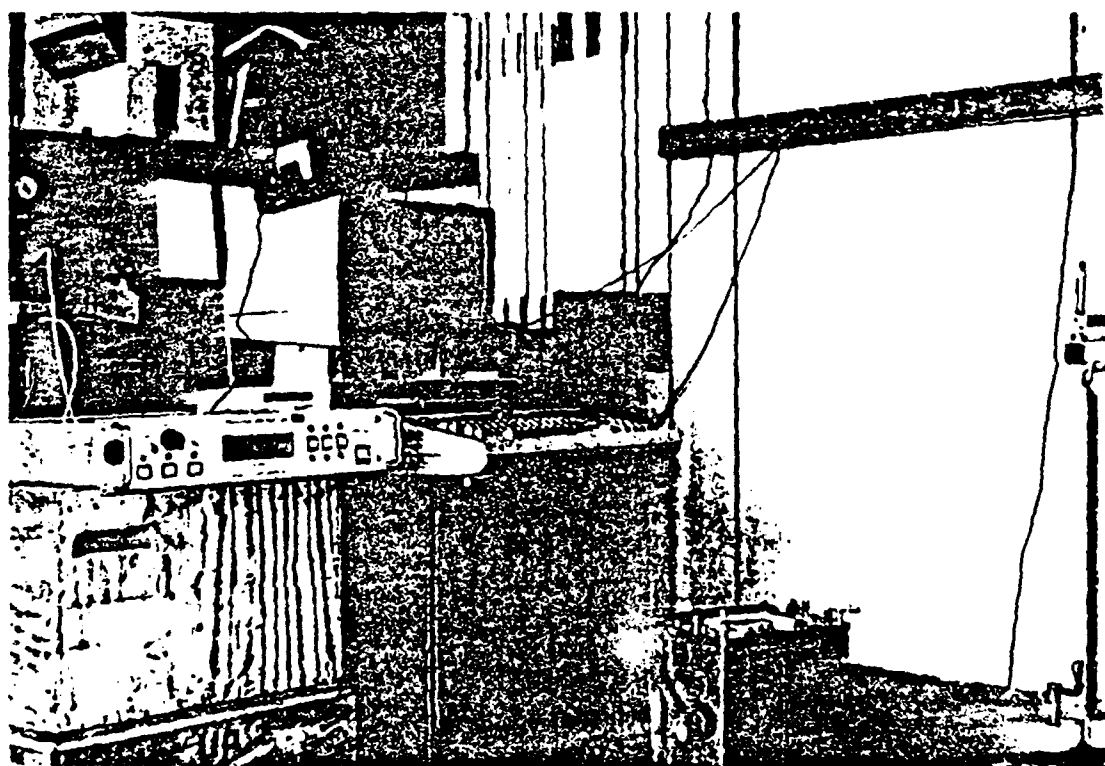


Figure 5 -
The 1 RPM
rotating table



TABLE 1
PERFORMANCE SPECIFICATIONS OF ROTATING TABLE
MODEL SA 5115B-3

1. Table out of Roundness0.015" $3.81 \cdot 10^{-1}$ mm	(w/dial meter)
2. Caliper out of Roundness0.010" $2.54 \cdot 10^{-1}$ mm	
3. _____ Axis0.005" $1.27 \cdot 10^{-1}$ mm	
4. Flatness of Top0.0005" $1.27 \cdot 10^{-2}$ mm	
5. Rocking0.003" $7.62 \cdot 10^{-2}$ mm	(*) Outside Diameter

(*) This could increase with addition of table-top

3. SQUID Magnetometer at Raytheon, Portsmouth, RI for Tests on Magnetic Interaction Targets

During this past quarter, Raytheon has assembled and tested a SQUID magnetometer, as a part of the company's 1988 IDP Program. Next quarter, we plan to use this SQUID in critical feasibility tests of direct interest to DARPA's neutrino detectors program, funded by the DARPA/AFOSR contract. The magnetometer consists of basically four units: the SQUID proper, the cryogenic descendent, the preamplifier head with filters, and finally the control unit. The preamplifier head is connected to the cryogenic descendent. At the other (lower) end of the descendent, inside a superconducting magnetic shield, is the SQUID proper. The control unit is energized by rechargeable batteries with about a 10 hour lifetime. We have conducted lab tests to measure the intrinsic noise of the system and found it to be about $1.8 \cdot 10^{-6} \phi_0/\text{Hz}^{1/2}$, where $\phi_0 = 2.07 \cdot 10^{-15}$ Weber, for frequencies above 10 Hz. Commercial SQUIDs are characterized by an intrinsic noise of $1.5 \cdot 10^{-5} \phi_0/\text{Hz}^{1/2}$, in comparable conditions.

As far as the energy sensitivity is concerned, our SQUID is characterized by a value of $8.5 \cdot 10^{-31}$ J/Hz, against a value of $3 \cdot 10^{-30}$ J/Hz typical of commercial SQUIDs. There is therefore an improvement of about 18 db in intrinsic noise and of about 6 db in energy sensitivity, when compared to commercial units. We are now in a position to perform the

three sets of measurements to address the feasibility of the magnetic interaction sensor: (a) measurement of minimum achievable intrinsic noise, when loading the SQUID with a heavy, high-permeability magnetic interaction target; (b) measurement of maximum achievable collecting area, using a superconducting transformer; (c) measurement of maximum-achievable relative permeability of the target materials. We plan to perform these measurements in the forthcoming quarter of contract performance.

4. The Cryogenic Force Sensor

The fundamental subsystem of this instrument is the room-temperature gravity gradiometer nearing completion at IFSI-CNR, Frascati, Italy. This subsystem is expected to reach Raytheon Portsmouth, RI in the third week of September 1988. The 4°K cryostat will reach Raytheon in the same time period, so that by the end of FY 88, the cryogenic force sensor will be undergoing system tests by the use of electrostatically-generated "force-signals". Transfer of this instrument to LANL, TA-33 and testing it with neutrino sources must wait for DARPA's decision concerning the construction of the 2000 RPM rotating table. As contractually allowed, Raytheon will keep this instrument here in Portsmouth, RI, until the high speed table is available.

CONCLUSIONS AND RECOMMENDATIONS

No major obstacles are expected to arise in Raytheon's feasibility testing of detecting low-energy neutrinos with Prof. Weber's room-temperature torsion balance. Concerning possible tests with the cryogenic force sensor, developed by SAO/IFSI-CNR under a Raytheon subcontract, everything has proceeded according to plans, apart from a few weeks delay. However, final neutrino tests cannot be scheduled and performed until the 2000 RPM rotating table is available at LANL. Since April 88, DARPA has had necessary information to make a decision to fund this effort. We recommend that this decision be made without further delay. Finally, as far as the magnetic sensor is concerned, we have to perform the basic feasibility tests on the SQUID system and magnetic materials, before we can hope to receive DARPA authorization to proceed on the procurement of the large-size interaction target and the large 4°K cryostat required by this instrument. Any decision on this must wait for the results of the on-going tests.

$$-m_1\omega_2^2 = 10^4 k_1 \quad (91)$$

Therefore from equation (88) the motion of mass m_1 is still given by equation (89) to an accuracy of about 1 part in 10^4 . This provides a qualitative explanation of the factor of 10^4 seen between cases 1 and 3.

In case 4, the high Q of system 2 is somewhat degraded by the low Q of system 1. Since there is a factor of 10^2 between the resonant frequencies, there is not a large damping effect on system 2 because of the low Q in system 1.

The calculations in cases 1 to 4 were all done at the ω_2 resonance computed by setting equation (56) equal to zero. For cases 1, 2, and 3, we have

$$\omega_2 = 638.7493909 \text{ rad/sec} \quad (92)$$

For case 4 we have

$$\omega_2 = 638.7494069 \quad (93)$$

In the presence of damping the maximum amplitude may not coincide exactly with ω_2 calculated from equation (56). In order to determine the actual positions of the maximum amplitude, resonance curves have been computed using the full solutions given by equations (76) and (77). For case 1, the actual position of the maximum of A_1 is $\omega_2 = 638.7493893$ rad/sec and for case 4, $\omega_2 = 638.7493874$ rad/sec. For case 1 the frequency shift is $-.0000016$ rad/sec. For case 4 it is $-.0000195$ rad/sec. Plots of Δ_R show it to be zero at exactly the values given in equations (92) and (93). In both cases the frequency shift is negligible compared